

# Brain-Body Interactions in Perception and Action

Inaugural-Dissertation

zur Erlangung des Doktorgrades der Philosophie  
der Ludwig-Maximilians-Universität München



vorgelegt von

Qiaoyue Ren

aus

Chongqing, China

2024

Referent/in: Prof. Dr. Simone Schütz-Bosbach

Korreferent/in: Prof. Dr. Thomas Schenk

Tag der mündlichen Prüfung: 22 February 2024

# Table of Contents

List of Abbreviations.....	iii
1 General Introduction .....	1
1.1 Cardiac Interoception .....	2
1.2 The Influence of Cardiac Interoception on Visual Perception .....	5
1.3 The Influence of Cardiac Interoception on Action.....	7
1.4 The Influence of Sense of Agency on Action.....	8
1.5 Objectives.....	10
2 Cumulative Thesis .....	11
2.1 Study I: Multisensory Integration of Anticipated Cardiac Signals with Visual Targets Affects Their Detection Among Multiple Visual Stimuli .....	13
2.2 Study II: Listen to Your Heart: Attentional Trade-off Between Cardiac and Visual Domains.....	41
2.3 Study III: Response Inhibition is Disrupted by Interoceptive Processing at Cardiac Systole .....	93
2.4 Study IV: Ready to Go: Higher Sense of Agency Enhances Action Readiness and Reduces Response Inhibition .....	111
2.5 Study V: Prepared to Stop: How Sense of Agency in a Preceding Trial Modulates Inhibitory Control in the Current Trial .....	141
3 General Discussion .....	163
3.1 How Do Cardiac Signals Influence Visual Perception? .....	163
3.2 How Do Cardiac Signals Influence Action Regulation? .....	165

3.3 How Does Sense of Agency Influence Action Regulation? .....	166
3.4 General Conclusions.....	168
3.5 Limitations and Future Directions.....	168
References (General Introduction and General Discussion).....	171
Summary .....	185
Zusammenfassung.....	189
Acknowledgments.....	195
Curriculum Vitae.....	197
List of Publications .....	199

## **List of Abbreviations**

ECG Electrocardiography

EEG Electroencephalography

ERP Event-Related Potential

fMRI Functional Magnetic Resonance Imaging

HEP Heartbeat-Evoked Potential

MEG Magnetoencephalography

SSVEP Steady State Visual Evoked Potential



# 1 General Introduction

How we perceive and react to the environment is not fixed; it changes dynamically. For example, at different moments, we may experience varying intensities of the same sensory stimulus and have diverse tendencies toward performing the same action. This variability is shaped by many factors. While many studies have focused on factors that we can consciously process or easily become aware of, such as the impact of emotions on perception (Zadra & Clore, 2011) and the influence of rewards on action (Chen et al., 2018), some factors have a lesser presence in our conscious awareness but still have a significant impact on our perception and action.

One of these factors is the internal bodily signals. The brain does not exist in isolation but resides within the body, which means it receives signals not only from the external environment (e.g., visual, auditory, and somatosensory signals) but also from within the body (e.g., cardiac and respiratory signals). However, the vast majority of research in cognitive neuroscience focuses on how we sense and interact with the external world while disregarding the role of internal bodily signals (Tallon-Baudry, 2023). The predictive coding framework proposes that the brain not just passively receives inputs but actively generates predictions and adjusts its internal models to minimize discrepancies or errors between these predictions and incoming inputs (Clark, 2013; Friston, 2009). This continuous process of refining predictions and minimizing errors is thought to underlie various cognitive functions, including perception and action (Friston, 2010). Given that this framework does not just consider external stimuli but also incorporates internal inputs, it is posited that internal bodily signals also play a role in brain functions (Barrett & Simmons, 2015; Seth & Friston, 2016). This perspective has recently gained support from empirical studies, which indicate that internal bodily signals, such as cardiac signals, can influence perception (e.g., Al et al., 2020; Grund et al., 2022; Motyka et al., 2019; van Elk et al., 2014) and action (e.g., Makowski et al., 2020; Marshall et al., 2019; Rae et al., 2018). Nevertheless, the findings are partly inconsistent, and the underlying neural mechanisms remain largely unclear.

Another factor is the sense of agency, which refers to the feeling of control over our actions and their outcomes (Haggard, 2017). The brain constantly monitors and

compares our intended actions with their actual outcomes, even if we are not fully aware of this process (Friston, 2012). A sense of agency emerges if the predicted outcomes of the motor command match the actual sensory inputs, and the sense of agency diminishes if they mismatch. Notably, the sense of agency is not merely a byproduct of motor behavior; it also exerts an influence on motor behavior itself (Wen & Imamizu, 2022). While several studies have demonstrated the influence of sense of agency on action selection and execution (e.g., Eitam et al., 2013; Karsh & Eitam, 2015), whether and how changes in the sense of agency influence our ability to regulate behavior flexibly are largely unknown.

This thesis focuses on how these two mostly unconscious factors (internal bodily signals and the sense of agency) affect two critical aspects of human perception and action: visual perception and action regulation. After a brief introduction to cardiac interoception (Chapter 1.1) and the empirical evidence regarding its influence on visual perception (Chapter 1.2) and action (Chapter 1.3), as well as the influence of the sense of agency on action (Chapter 1.4), this dissertation comprises a total of five studies. Initially, we examine the multisensory integration of cardiac signals and visual inputs (Chapter 2.1), followed by an exploration of the spontaneous shifts of attention between cardiac signals and visual information across the cardiac cycle (Chapter 2.2) through two separate EEG studies. The third EEG study demonstrates how cardiac signals influence response inhibition in a stop-signal task (Chapter 2.3). The last two studies explore the influence of the sense of agency on subsequent response inhibition (Chapter 2.4) and the associated electrophysiological responses in go/no-go tasks (Chapter 2.5).

## **1.1 Cardiac Interoception**

Interoception refers to the physiological and cognitive processes involved in sensing, interpreting, integrating, and regulating signals that arise within the body (Chen et al., 2021). It can be distinguished from exteroception (the sensation of the environment) and proprioception (the sensation of the body in space). Interoceptive signals originate from diverse physiological systems inside the body, encompassing the cardiovascular, respiratory, gastrointestinal, and other systems (Khalsa et al., 2018; Quigley et al., 2021). Cardiovascular interoception is the most studied of these systems, probably due

to the relative ease of measuring discrete rhythmic events (i.e., heartbeats) with noninvasive tools such as ECG, pulse oximeters, and wearable heart rate monitors.

Cardiac activity occurs in a cycle of two phases: systole and diastole (see **Figure 1**). At ventricular systole, the ventricles of the heart contract, pumping blood to the body, while at ventricular diastole, the ventricles relax and refill with blood (DeSaix et al., 2013). The onset of a new cardiac cycle is indicated by the R-peak in the ECG signal. The duration between the ECG R-peak and the T wave roughly corresponds to the ventricular systole, and the duration between the T wave and the next R-peak roughly corresponds to the ventricular diastole (DeSaix et al., 2013). Baroreceptors in the walls of arterial vessels are the main way that information about the strength and timing of individual heartbeats is sent to the brain (Azzalini et al., 2019; Garfinkel, 2016). In a cardiac cycle, these baroreceptors fire intensely at systole and minimally at diastole, responding to fluctuations in arterial blood pressure. In other words, cardiac signals are strong at systole and relatively weaker at diastole.

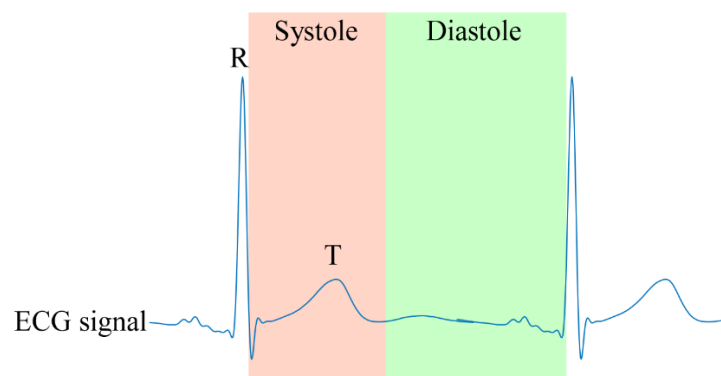


**Figure 1.** Systole and diastole phases in a cardiac cycle.

Cardiac activity can evoke HEP in electrophysiological signals (e.g., scalp EEG, intracranial EEG, and MEG), just like visual stimulation can evoke visual-evoked potentials (Park & Blanke, 2019). The HEP is time-locked to participants' heartbeats, typically to the R-peak in the ECG signal. Several studies have demonstrated that HEP amplitudes are affected by cardiac physiological factors, such as the amount of blood pumped by the heart every minute and heart rate (Gray et al., 2007; Schandry &

Montoya, 1996). Furthermore, a recent meta-analysis shows that there is a moderate to large relationship between HEP amplitude and various measurements and manipulations of cardiac interoception (Coll et al., 2021). More specifically, directing one's attention on the heart has been found to evoke heightened HEP responses (Petzschner et al., 2019). Additionally, it has been observed that heightened arousal induced by emotional cues or painful stimuli is accompanied by changes in HEP amplitude (Marshall et al., 2017; Shao et al., 2011). Moreover, the amplitude of the HEP has been found to correlate with participants' performance on tasks assessing interoceptive ability, such as the heartbeat counting task (Pollatos & Schandry, 2004) and the heartbeat detection task (Fittipaldi et al., 2020). Furthermore, differential HEPs have been observed between healthy participants and clinical groups with atypical interoception (Salamone et al., 2018; Schulz et al., 2015). Drawing from the evidence above, the HEP is regarded as a reliable neurophysiological indicator of cardiac processing (Park et al., 2018).

Studies using scalp EEG or MEG have observed HEP modulations in widely distributed sensors, including frontal, central, and parietal channels, and across a wide time window, i.e., 0-700 ms after the ECG R-peak (Coll et al., 2021). Studies recording intracranial EEG during the resting state have demonstrated that the cortical sources of the HEP include not only the somatosensory cortex (Kern et al., 2013) but also the insula, opercular cortex, inferior frontal gyrus, and amygdala (Park et al., 2018). Nevertheless, it should be noted that intracranial EEG has the limitation that its electrodes are unlikely to cover the entire cortex (Parvizi & Kastner, 2018). Other studies investigated the neural origins of HEP by analyzing the source localization of scalp EEG or MEG data. For instance, studies have reported distinct HEP patterns between conditions in the viscerosensory cortices, including the insula opercular regions, the anterior-posterior cingulate regions, and the inferior parietal lobe, in various cognitive tasks (Babo-Rebelo et al., 2016; Park et al., 2014, 2016). Interestingly, some of these regions overlap with the default mode network, a network involved in several critical cognitive functions (Fox & Raichle, 2007). This finding implies that the neural responses to heartbeats, as measured by the HEP, may influence cognitive functions by regulating the neural

activity in the default mode network (Park & Tallon-Baudry, 2014; Winston & Rees, 2014).

Notably, in addition to the cortical processing of cardiac activities as reflected by the HEP, heartbeats also give rise to "mechanical noise" in the brain (Skora et al., 2022). Firstly, the periodic beating of the heart induces pulsation in the blood vessels, cerebrospinal fluid, and brain tissue, which can be called pulse-related artifacts (Kern et al., 2013). Secondly, the muscle contractions occurring during ventricular systole generate notable electrical artifacts, termed cardiac field artifacts (Kern et al., 2013). Thirdly, heartbeats can prompt minuscule movements in the eyeballs and even the entire body (Kim et al., 2016). These kinds of "noise" may introduce confounding factors and thus should be carefully considered when assessing the impact of cardiac processing on brain functions.

## **1.2 The Influence of Cardiac Interoception on Visual Perception**

Many studies have investigated the influence of cardiac activity on the perception of visual stimuli by presenting them during systolic or diastolic phases. While earlier research failed to find any cardiac cycle effect on the detection of flashes (Elliott & Graf, 1972), the majority of existing literature has highlighted a modulation effect of the cardiac phase on both behavioral and neural responses to visual stimuli. For example, presenting visual stimuli during systole, in contrast to diastole, resulted in prolonged reaction times (McIntyre et al., 2007; Sandman et al., 1977; but see Makowski et al., 2020), reduced interference from visual distractors (Pramme et al., 2014, 2016), and smaller visual evoked potentials (Walker & Sandman, 1982). Additionally, these effects of the cardiac cycle were found to be modulated by the emotional valence of the visual stimuli. In a rapid serial presentation task, Garfinkel et al. (2014) found that fearful faces were detected more easily and rated as more intense when presented at systole compared to diastole, while the detection of neutral, disgust or happy faces remained comparable across both cardiac phases. In another study that employed an emotional visual search task where five neutral distractors surrounded a target emotional face, Leganes-Fonteneau et al. (2021) observed that accuracy in the visual search was higher for happy and disgust faces presented during systole.

Conversely, the opposite effect was found for fearful faces. Furthermore, participants perceived fearful and happy faces as more intense when presented at systole. Considering that cardiac activity differs significantly during systole and diastole (Azzalini et al., 2019; Garfinkel, 2016), these findings strongly suggest that cardiac processing impacts concurrent visual processing.

This view is further supported by evidence from studies manipulating the synchronization between visual stimuli and participants' heartbeats. For example, near-threshold visual stimuli presented at participants' cardiac frequencies took longer to enter visual awareness and induced smaller activation in the insular cortex (Salomon et al., 2016), a region involved in the integration of internal cardiac signals and external visual inputs (Salomon et al., 2018). Conversely, supra-threshold visual stimuli (i.e., images of the body) evoked larger visual evoked potentials when synchronized with participants' heartbeats compared to when presented out of synchrony (Ronchi et al., 2017). The inconsistent findings may be attributed to whether the visual stimuli were presented at near- or supra-threshold perceptual levels.

Moreover, other studies have contributed to this body of evidence by exploring how pre-stimulus cardiac processing influences subsequent visual processing. For instance, Park et al. (2014) found that the amplitude of the pre-stimulus HEP positively predicted subsequent visual detection of near-threshold visual stimuli. On the contrary, our lab's previous studies showed that larger pre-stimulus HEPs predicted lower detection rates of near-threshold visual stimuli (Marshall et al., 2020), smaller P3 responses to visual action outcomes (Marshall et al., 2019), as well as smaller visual evoked potentials in response to repeated neutral faces (Marshall et al., 2022). The variation in results can be attributed to the diverse methodologies employed in measuring HEP. In our case, the HEP was locked to the R-peak in the ECG signal, which aligns with most previous studies, such as Petzschnner et al. (2019) and Al et al. (2020). However, Park and colleagues extracted the HEP time-locked to the T wave in the ECG signal, approximately 350 ms after the R-peak. This difference in measurement could represent distinct aspects of heartbeat-related brain activity, which might lead to the observed discrepancy in the results.

Overall, the existing evidence indicates that the processing of internal cardiac signals can moderate the processing of external visual information. However, whether it facilitates or inhibits this processing depends on the task and stimuli, such as emotional valence and perceptual level.

### **1.3 The Influence of Cardiac Interoception on Action**

Empirical evidence regarding the influence of cardiac interoception on action remains relatively scarce compared to the evidence available for its impact on perception. There is, however, preliminary evidence suggesting that the cardiac cycle does influence spontaneous actions. For example, more eye movements (saccades, microsaccades, and blinks) were generated at systole, while more ocular fixations were observed at diastole (Galvez-Pol et al., 2020; Ohl et al., 2016). In a memory task, the freely generated keypress that can lead to the presentation of images occurs more frequently during systole than diastole (Kunzendorf et al., 2019). Similarly, self-initiated movements were less likely to occur during heartbeats (i.e., around ECG R-peak) and more likely to occur between heartbeats (Palser et al., 2021; but see Herman & Tsakiris, 2020). Moreover, systole is associated with stronger hand muscle activity (Al, Stephani, et al., 2021) and enhanced rifle shooting performance (Kontinen et al., 2003). These findings suggest that the systolic phase has a facilitatory effect on spontaneous or self-paced motor behavior.

Another line of research focuses on action regulation, which involves higher-level cognitive control. Action regulation refers to adjusting ongoing behavior to enhance one's chances of successfully achieving a goal (Kaiser et al., 2021). In a stop-signal task, Rae et al. (2018) observed enhanced response inhibition during systole when the stop signal was presented, in contrast to diastole. Conversely, Makowski et al. (2020) found contrasting results in a go/no-go task, with the probability of stop failure being highest, indicating that response inhibition was at its worst when the no-go cue occurred in the middle of systole. Moreover, Rae et al. (2020) conducted a second study using a modified go/no-go task, but they did not find any significant effect of the cardiac cycle on inhibitory performance. Specifically, the cardiac cycle failed to influence accuracy in no-go trials and had no impact on the probability of withholding actions in voluntary

inhibition trials. The inconsistency in findings may stem from divergences in task design. Firstly, stop-signal and go/no-go tasks may recruit different motor and cognitive processes (Raud et al., 2020). Secondly, Rae and colleagues time-locked the onset of action stimuli to different cardiac phases. In contrast, Makowski and colleagues presented stimuli randomly in the cardiac cycle but categorized them into different cardiac-coupling conditions during later data analysis. These disparities could perhaps explain the noted inconsistency in the findings.

Overall, the existing evidence indicates that motor behavior concurrent with the systolic phase of the cardiac cycle appears to be facilitated. However, the impact of cardiac signaling on action regulation exhibits inconsistent findings, requiring further research for a better understanding.

#### **1.4 The Influence of Sense of Agency on Action**

Our motor behavior is not only influenced by internal bodily signals but is typically also associated with the sense of agency, which refers to the subjective feeling of controlling one's own actions and their effects (Haggard, 2017; Haggard & Eitam, 2015). The sense of agency, also called the sense of control, is shaped by three critical components: intention, action, and effect (Wen & Imamizu, 2022). Intention refers to the desired state one hopes to achieve through actions; action refers to the awareness of one's own actions; and effect refers to the perception of the action outcomes (Wen & Imamizu, 2022).

In recent decades, the impact of a sense of agency on action has attracted substantial attention. An increasing number of studies have demonstrated the impact of a sense of agency on action selection and execution (Wen & Imamizu, 2022). For example, infants as young as two months old moved their limbs more frequently when they could trigger the movements of an attached mobile (Watanabe & Taga, 2006, 2011). Also, they applied pressure to a pacifier around the threshold more frequently, which produced congruent auditory feedback (Rochat & Striano, 1999). Similarly, adult participants responded faster when their actions consistently led to an immediate effect compared to conditions when no effect appeared or when the effect was delayed (Eitam et al.,

2013). Moreover, buttons that had a high probability of causing a visual outcome were more likely to be selected and pressed faster than buttons associated with no perceivable effect, despite these outcomes being task-irrelevant and valence-neutral (Karsh et al., 2020; Karsh & Eitam, 2015; Penton et al., 2018). Recent studies have further indicated that this facilitation effect was sensitive to the effectiveness of the motor response, specifically, how likely the response was to evoke a perceivable effect (Hemed et al., 2020; Tanaka et al., 2021). These findings suggest that actions associated with a strong sense of agency are frequently selected and executed more fluently.

There is also evidence that the sense of agency modulates goal-directed behavior. For instance, in a study where participants had to determine the dot over which they had control from among multiple dots whose motion was triggered by their voluntary actions, they exhibited fewer exploratory movements before making a decision when their actual control over the specific dot was high (Wen et al., 2017; Wen & Haggard, 2020). This finding implies a heightened sense of control or agency associated with fewer exploratory actions. In a similar task with dots on a screen moving according to participants' actions, participants were asked to identify a single dot with a distinct degree of control compared to the others (Wen et al., 2020). Results showed that participants initially had a higher frequency of movements when the average control over all stimuli was high, and the detection of the target resulted in a subsequent decrease in the frequency of movement (Wen et al., 2020). These findings indicate a strong link between goal-directed behavior and the sense of agency. This perspective is also supported by evidence from learning tasks. For example, a high versus low sense of control during the training phase of motor learning tasks resulted in enhanced training success, i.e., more performance improvements (Lewthwaite et al., 2015; Matsumiya, 2021). Conversely, learned helplessness, i.e., a lack of control, has been associated with diminished performance in learning tasks (Maier & Seligman, 2016). These findings suggest that a strong sense of agency can facilitate goal-directed behavior.

Overall, the existing evidence indicates that our sense of agency over actions and their outcomes can modulate action selection, action execution, and goal-directed behavior. Nevertheless, how the sense of agency impacts action regulation, including aspects like

action readiness and response inhibition, remains relatively uncharted. Furthermore, previous research has predominantly centered around behavioral effects, leaving the underlying neural mechanisms largely unexplored.

## **1.5 Objectives**

The general aims of this thesis are to investigate (i) how cardiac signals influence visual perception, (ii) how cardiac signals influence action regulation, and (iii) how the sense of agency influences action regulation.

The specific objectives of the five studies included in this thesis are as follows:

- Study I (Chapter 2.1) aims to (i) explore whether the co-occurrence of an external visual target and internal cardiac signals impacts the detection of this target among multiple visual distractors, and (ii) uncover the electrophysiological modulations underlying this cardio-visual integration.
- Study II (Chapter 2.2) aims to (i) compare selective attention toward visual stimuli that were presented concurrently and spatially overlapping but coincided with strong or weak cardiac signals, and (ii) reveal the dynamic shifts of attention between internal cardiac signals and external visual information across the cardiac cycle.
- Study III (Chapter 2.3) aims to explore the influence of cardiac signals on response inhibition and its electrophysiological brain mechanisms.
- Study IV (Chapter 2.4) aims to explore the effect of a sense of agency on subsequent action readiness and response inhibition at the behavioral level.
- Study V (Chapter 2.5) aims to (i) replicate the findings obtained in Study IV, and (ii) investigate the influence of the sense of agency on subsequent response inhibition at the electrophysiological level.

## **2 Cumulative Thesis**

The following section consists of five original quantitative studies, four of which have already been peer-reviewed and published (Chapters 2.1, 2.3, 2.4, and 2.5), and one has been submitted to a scientific journal (Chapter 2.2).



## **2.1 Study I: Multisensory Integration of Anticipated Cardiac Signals with Visual Targets Affects Their Detection Among Multiple Visual Stimuli**

**This article was published in *NeuroImage*:**

Ren, Q., Marshall, A. C., Kaiser, J., & Schütz-Bosbach, S. (2022). Multisensory integration of anticipated cardiac signals with visual targets affects their detection among multiple visual stimuli. *NeuroImage*, 262, 119549. <https://doi.org/10.1016/j.neuroimage.2022.119549>

Copyright © 2022 The Authors. Published by Elsevier Inc. This is an open access article under the CC BY-NC-ND license (<http://creativecommons.org/licenses/by-nc-nd/4.0/>). The main manuscript and supplements here are the published version.

### **Contributions:**

Qiaoyue Ren: Conceptualization, Methodology, Investigation, Data curation, Formal analysis, Visualization, Writing – original draft.

Amanda C. Marshall: Methodology, Writing – review& editing.

Jakob Kaiser: Methodology, Writing – review& editing.

Simone Schütz-Bosbach: Conceptualization, Methodology, Writing – review& editing, Supervision, Funding acquisition.





# Multisensory integration of anticipated cardiac signals with visual targets affects their detection among multiple visual stimuli

Qiaoyue Ren, Amanda C. Marshall, Jakob Kaiser, Simone Schütz-Bosbach\*

Department of Psychology, General and Experimental Psychology Unit, LMU Munich, Germany

## ARTICLE INFO

### Keywords:

Multisensory integration  
Interoception  
Visual search  
Cardiac signals  
Cardiac systole  
Cardiac diastole

## ABSTRACT

Many studies have elucidated the multisensory processing of different exteroceptive signals (e.g., auditory-visual stimuli), but less is known about the multisensory integration of interoceptive signals with exteroceptive information. Here, we investigated the perceptual outcomes and electrophysiological brain mechanisms of cardio-visual integration by using participants' electrocardiogram signals to control the color change of a visual target in dynamically changing displays. Reaction times increased when the target change coincided with strong cardiac signals concerning the state of cardiovascular arousal (i.e., presented at the end of ventricular systole), compared to when the target change occurred at a time when cardiac arousal was relatively low (i.e., presented at the end of ventricular diastole). Moreover, the concurrence of the target change and cardiac arousal signals modulated the event-related potentials and the beta power in an early period (~100 ms after stimulus onset), and decreased the N2pc and the beta lateralization in a later period (~200 ms after stimulus onset). Our results suggest that the multisensory integration of anticipated cardiac signals with a visual target negatively affects its detection among multiple visual stimuli, potentially by suppressing sensory processing and reducing attention toward the visual target. This finding highlights the role of cardiac information in visual processing and furthers our understanding of the brain dynamics underlying multisensory perception involving both interoception and exteroception.

## 1. Introduction

At any given moment, we receive inputs from various sensory modalities. The processes involved in integrating these multisensory inputs are fundamental to effective perception and cognitive functioning (Wallace et al., 2020). Past work on multisensory/cross-modal integration has largely focused on sensory inputs from the external world, i.e., exteroceptive signals such as visual and auditory stimuli (Tang et al., 2016; van Atteveldt et al., 2014). For example, an auditory signal co-occurring with a visual stimulus has been shown to facilitate visual detection (Leo et al., 2008), visual discrimination (Noesselt et al., 2008), and visual target search (Van der Burg et al., 2008, 2011). Auditory-visual integration starts as early as about 50 ms after stimulus onset (Giard and Peronnet, 1999; Molholm et al., 2002; Senkowski et al., 2011) and appears to modulate the activation of sensory cortices (Kayser et al., 2017; Martuzzi et al., 2007).

Recent neuroscientific research is progressively targeting interoceptive information from internal visceral organs (especially the heart) as an important source of sensory input for perceptual and cognitive processes in the brain (Chen et al., 2021; Park and Blanke, 2019; Quigley et al., 2021). Cardiac activity occurs in a cycle of two phases. During the ventricular systole, the muscles in the ventricle contract,

pumping blood from the heart to the body. During the ventricular diastole, the heart muscle is relaxed as it refills with blood (DeSaix et al., 2018). It has been proposed that cardiac interoceptive information is conveyed to brain regions (e.g., the insula, cingulate cortex, amygdala, and somatosensory cortex) mainly by arterial baroreceptors located in the aortic arch and the carotid arteries (Azzalini et al., 2019; Garfinkel and Critchley, 2016; Park and Blanke, 2019). Within a cardiac cycle, these baroreceptors fire maximally at the end of ventricular systole and minimally at the end of ventricular diastole in response to the fluctuations of arterial blood pressure. In other words, cardiac signals are strongest at the end of the ventricular systole while relatively weak at the end of the ventricular diastole. In addition, heartbeats can evoke heartbeat evoked potentials (HEP) on the cortex, just like visual stimuli can evoke visually evoked potentials (Park and Blanke, 2019). Abundant work has suggested that the HEP reflects the cortical processing of cardiac afferent signals and is therefore a reliable neurophysiological marker of cardiac interoception (Coll et al., 2021; Park et al., 2018; Petzschner et al., 2019).

Up to now, there is only limited evidence about the multisensory processing of exteroceptive visual signals in combination with interoceptive cardiac signals. Previous investigations mainly focused on the cardiac cycle effect on visual perception, i.e., whether participants' re-

\* Corresponding author.

E-mail address: [S.Schuetz-Bosbach@psy.lmu.de](mailto:S.Schuetz-Bosbach@psy.lmu.de) (S. Schütz-Bosbach).

<https://doi.org/10.1016/j.neuroimage.2022.119549>.

Received 16 February 2022; Received in revised form 29 July 2022; Accepted 4 August 2022

Available online 5 August 2022.

1053-8119/© 2022 The Authors. Published by Elsevier Inc. This is an open access article under the CC BY-NC-ND license (<http://creativecommons.org/licenses/by-nc-nd/4.0/>)

sponses to a visual stimulus were modulated by the timing of the stimulus with respect to their cardiac cycle. While past work failed to find any cardiac cycle effect on the detection of flashes (Elliott and Graf, 1972), the majority of previous studies highlighted a significant impact of cardiac phase on visual processing. For example, the presentation of visual stimuli at systole compared to diastole has been shown to influence reaction times towards these stimuli, with most studies finding prolonged reaction times during the systole (McIntyre et al., 2007; Sandman et al., 1977, but see also: Makowski et al. (2021)). Processing visual stimuli presented at cardiac systole compared to diastole evoked smaller visual evoked potentials (Walker and Sandman, 1982) and resulted in reduced interference of visually distracting stimuli (Pramme et al., 2014, 2016). In addition, cardiac cycle effects have been found to be modulated by the emotional valence of the visual stimuli: while fearful faces were detected more easily and rated as more intense if presented at systole compared with diastole, the detection of neutral, disgusted, or happy faces was comparable across the two cardiac phases (Garfinkel et al., 2014). Given that cardiac signals are conveyed to the brain mainly during the cardiac systole rather than the diastole (Azzalini et al., 2019; Garfinkel and Critchley, 2016), it can be assumed that cardiac signals may influence the perception and neural processing of a simultaneous visual stimulus. This assumption is also supported by the finding that visual evoked potentials are enhanced when these images are synchronized with participants' heartbeats compared to when they are presented out of synchrony to participants' heartbeats (Ronchi et al., 2017). By measuring neural markers of cardiac processing such as the HEP and insula activity (Coll et al., 2021; Salomon et al., 2018), recent studies have further provided evidence about the interplay between cardiac processing and visual processing. For example, the amplitude of the pre-stimulus heartbeat-evoked potential positively predicts subsequent visual detection (Park et al., 2014). Additionally, contrary to the finding reported by Ronchi et al. (2017), Salomon et al. (2016) observed that visual stimuli presented at participants' cardiac frequency take longer to enter visual awareness and induce smaller activation in the insular cortex. Up to now, it is still unclear how simultaneously encountered cardiac signals and visual information are integrated into the brain. Moreover, previous studies mainly examined the influence of cardiac signals on the perception of a single visual stimulus, leaving out the question how cardio-visual integration can affect the competition among multiple visual stimuli.

Here, we employed a novel adaptation of the dynamic visual search task (Van der Burg et al., 2008, 2011) to investigate the multisensory integration of cardiac signals with a visual target in a dynamic cluttered environment, while recording the electrocardiogram (ECG) and electroencephalogram (EEG). Critically, the visual target changed its color either at a time when cardiac arousal signals were strongly present (i.e., at the end of ventricular systole) or when cardiac arousal was relatively low and thus did not provide a strong signal (i.e., at the end of ventricular diastole). Consistent with both recent reviews (Azzalini et al., 2019; Quigley et al., 2021) and empirical studies (Ronchi et al., 2017; Sel et al., 2017), we treated visual and cardiac signals as sensory input signals of equal relevance. At the behavioral level, we measured reaction times and accuracy rates. At the electrophysiological level, we explored the brain dynamics of cardio-visual integration from two different perspectives. The first perspective was to compare the electrophysiological responses to the bimodal cardio-visual stimulus (i.e., the concurrence of cardiac arousal signals and the target change) with the sum of the electrophysiological responses to the unimodal cardiac arousal signals and the unimodal visual stimulus (i.e., the target change). This comparison approach (i.e., the additive model) has been widely used in previous EEG studies to reveal early multisensory processes underlying auditory-visual integration (Senkowski et al., 2011; Talsma and Woldorff, 2005; Van der Burg et al., 2011; Zhao et al., 2020, 2018). In the present study, this approach was applied in analyses of both event-related potentials (ERPs) and neural oscillations. According to the additive model (Cappe et al., 2010; Senkowski et al., 2011; Talsma and

Woldorff, 2005), electrophysiological responses to the simultaneous cardiac and visual input would be different from the sum of the cardiac and visual responses alone if multisensory integration occurred across cardiac processing and visual processing in the brain. Second, the lateralized presentation of the visual target in the visual field made it possible to compare the lateralized electrophysiological responses to the bimodal cardio-visual stimulus and the unimodal visual stimulus. We mainly focused on the lateralized N2pc component and alpha/beta oscillations, which are well-validated measures of the allocation of attention to lateralized visual stimuli (Bacigalupo and Luck, 2019; Bauer et al., 2012).

## 2. Materials and methods

### 2.1. Participants

Twenty-six participants (12 females; mean age:  $25.46 \pm 0.87$  years; range: 20–38 years) took part in the present study for payment (9 € per h) or student credits. All participants reported normal or corrected-to-normal vision, no color blindness, no diagnosed heart-rhythm abnormalities, no present or past psychiatric or neurological disorders, and no current use of medication. Consent was obtained from all participants, and the procedures were approved by the local ethics committee at the Department of Psychology of LMU Munich in accordance with the Declaration of Helsinki. To the best of our knowledge, no previous studies have explored cardio-visual integration in a similar task. Therefore, we could not compute the required sample size a priori. However, our sample size is comparable with relevant previous studies (e.g., Adelhöfer et al. 2020; Marshall et al. 2022; Pramme et al. 2016).

### 2.2. Experiment design

Participants completed a dynamic visual search task in which a display of randomly oriented line segments changed color dynamically (Van der Burg et al., 2008). Each display consisted of several oblique lines (the distractors), and only one line which was perfectly horizontal or vertical (the target). The participants had to identify the target as quickly as possible by indicating if it was horizontal or vertical via button press. To investigate the cardio-visual integration, the experiment contained two conditions in which the visual target changed color when cardiac arousal signals were relatively low (i.e., when arterial baroreceptors are relatively quiescent; corresponding to the end of ventricular diastole) or strong (i.e., when arterial baroreceptors fire strongly; corresponding to the end of ventricular systole; see Fig. 1A). The ventricular systole refers to the period from approximately the ECG R-peak to the T wave, and the ventricular diastole refers to the period from approximately the T wave to the next upcoming R-peak (DeSaix et al., 2018). In the diastole coupling condition, the color change of the visual target was designed to always occur at the R-peak to coincide with the end of ventricular diastole. In the systole coupling condition, the color change of the visual target was designed to always occur at 290 ms after the R-peak (approximately at the T wave) to coincide with the end of ventricular systole (Rae et al., 2020, 2018). Participants completed 10 diastole coupling blocks and 10 systole coupling blocks presented in counterbalanced, alternating order and preceded by 1 practice block. Each block consisted of 24 trials. In addition to the 20 blocks for the visual search task, one resting block (duration: 2.5 min) was performed before the task. During the resting block, participants were asked to look at the fixation dot centrally presented on the monitor while no other visual stimuli were presented. The EEG signal obtained from this type of resting condition has been used to correct for cardiac cycle-related artifacts present in the EEG signal of task conditions in previous studies (Ronchi et al., 2017; van Elk et al., 2014).

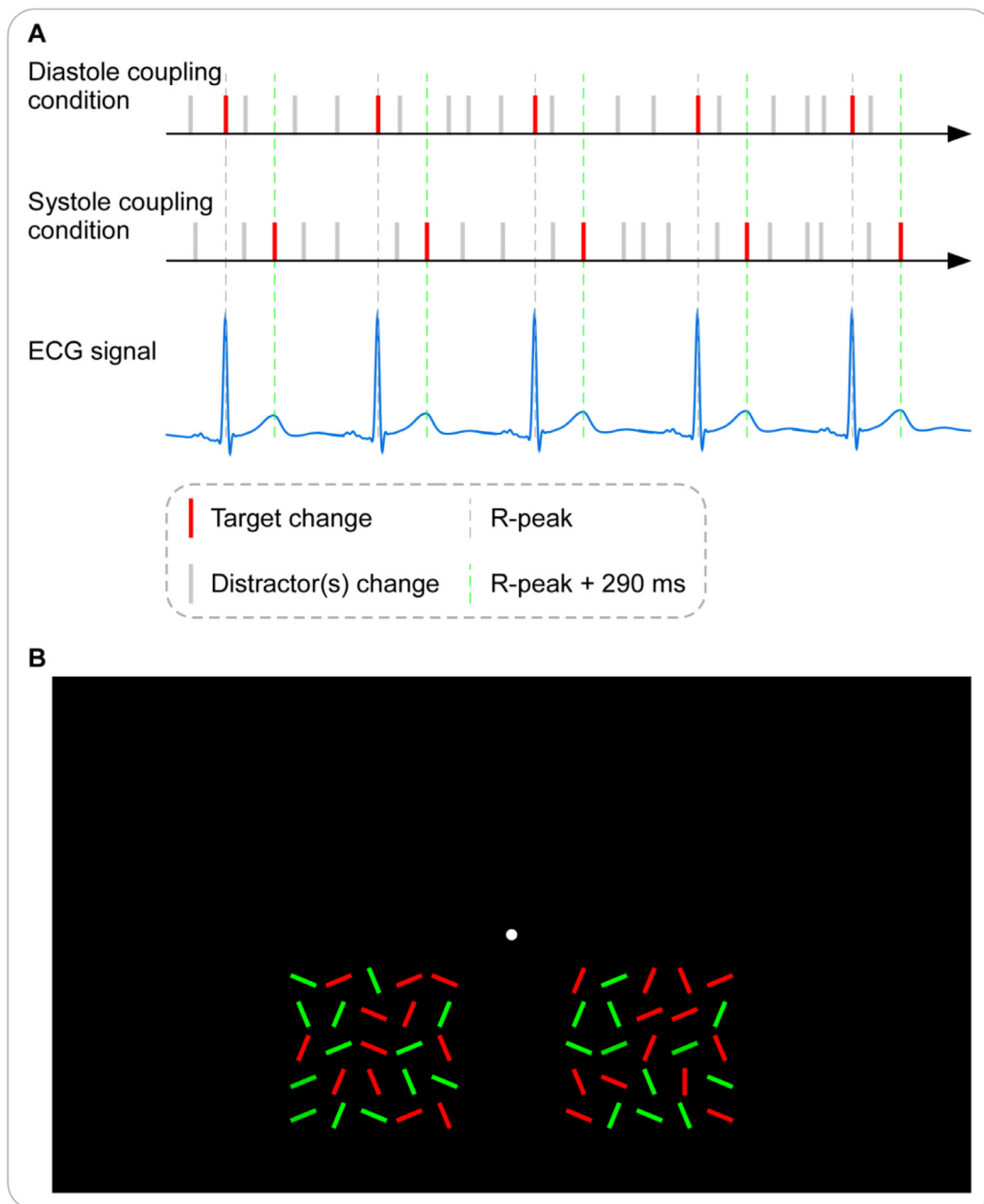


**Fig. 1.** The dynamic visual search task. (A) Schematic illustration of the experimental conditions. In the diastole coupling condition, the color change of the visual target always occurred at the R-peak to coincide with the end of ventricular diastole (i.e., when cardiac arousal signals were relatively low). In the systole coupling condition, the color change of the visual target always occurred at 290 ms after the R-peak to coincide with the end of ventricular systole (i.e., when cardiac arousal signals were strong). (B) An example visual search display. The search display consisted of 1 target (horizontal or vertical) and 49 distractors (oblique). In the example display, the target consists of the vertical red line on the right side. The colors of the target and the distractors (green or red) were randomly assigned and changed randomly over time. Participants were required to indicate the orientation of the visual target as fast and accurately as possible.

### 2.3. Stimuli and procedure

Participants were seated in a dimly lit room at 70 cm from the monitor (24 inches; refresh rate: 60 Hz; resolution: 1920 × 1080 pixels) with their heads on a chin rest. The visual search displays were generated and displayed using the Presentation software (Neurobehavioral Systems, Inc.).

Each search display consisted of 50 red (luminance: 49.5 cd/m<sup>2</sup>) or green (49.5 cd/m<sup>2</sup>) line segments on a black (0.30 cd/m<sup>2</sup>) background (Fig. 1B). One of the line segments was the target, while the remaining ones acted as distractors. The color of each line segment was randomly determined. The target was either horizontal (visual angle:

0.60° × 0.10°) or vertical (0.10° × 0.60°). Each distractor was the same size as the target, but its orientation deviated randomly by either plus or minus 22.5° from horizontal or vertical. Given that target-elicited lateralized effects (e.g., N2pc component) are largely absent for upper-field visual targets (Bacigalupo and Luck, 2019), we presented the search display only in the lower visual field. Specifically, half of the line segments were placed on an invisible 5 × 5 grid (3.40° × 3.40°) in the lower left visual field, and the other half were placed on an identical grid in the lower right visual field. Both grids were 2.83° horizontally away from and 2.13° below the center of the screen marked with a white (245.00 cd/m<sup>2</sup>) fixation dot. To avoid immediate target detection after the search display appeared, the target never appeared on the outer ring

of each grid (Van der Burg et al., 2011). Target orientation (horizontal or vertical) and location (left or right visual field) were balanced and randomly mixed within blocks.

In order to time-lock the target rather than the distractors to specific time points in each cardiac cycle, the search display changed continuously by switching the color of a random number of line segments between red and green (i.e., either from red to green or from green to red). Color changes of either the target or the distractors never occurred at the same time. That is, at a given moment either the target changed its color while the color of the distractors remained unchanged, or some of the distractors changed their color while the target's color remained constant. During each distractor change, we switched the color of either one, four, or seven randomly selected line segments. The interval between two successive color changes in the visual display varied randomly from 50 to 250 ms. However, there were two constraints with respect to the timings of the color changes. First, the visual target could change its color only once in each cardiac cycle, either at the R-peak (in the diastole coupling condition) or 290 ms after the R-peak (in the systole coupling condition). Second, the distractors could never change within the time window from -150 to 100 ms relative to the two aforementioned timings specific for the target change, to promote unambiguous binding of the target change and cardiac signals (Van der Burg et al., 2008, 2011). In other words, the distractors could change color within the time window from 100 to 140 ms after the R-peak and within the time window from 390 ms after the R-peak to 150 ms before the next R-peak in both coupling conditions. In this way, we ensured that the timings of distractor color changes were comparable across the two cardiac coupling conditions and thus would not lead to any confounding effect. The onset of an upcoming R-peak was estimated by calculating a median inter-beat interval based on the timings of the previous six R-peaks.

Each trial started with a central fixation dot, followed by a dynamic visual search display. The onset of the search display was randomly set from 0 to 600 ms after the R-peak to avoid it coinciding with specific time points in the cardiac cycle. Notably, it was the first R-peak detected 800 ms after the onset of the fixation dot that was used to calculate the onset of the search display. This ensured that the presentation of the fixation dot was not too short, i.e., at least 800 ms. The search display remained on the screen until the participant responded or the visual target had changed five times (i.e., 5 heartbeats, about 4000 ms). Note that in the latter case, the search display would not disappear immediately but disappear 300 ms after the fifth target change to ensure that the fifth target change was perceivable. Participants were asked to indicate the visual target orientation as fast and accurately as possible by a button press ("F" and "J" corresponding to horizontal and vertical, respectively). At the end of each trial, there was a blank presented for 1000 ms. Participants were required to maintain fixation of the central dot during the trial and try to blink only during the breaks. Accuracy rate and mean reaction time were presented as visual feedback after each block during the self-paced inter-block rest.

#### 2.4. Recordings

For EEG recording, we used 65 active electrodes (BrainProducts ActiSnap) and 1 additional ground electrode positioned following the international 10–20 system. The FCz functioned as the online reference for these scalp electrodes. Horizontal and vertical electrooculograms (EOGs) were also recorded via electrodes at the left and right outer canthi, and electrodes above and below the left eye, respectively. For recording ECG, we used 3 electrodes placed below the left clavicle (reference electrode), the right clavicle (ground electrode), and the left pectoral muscle (active electrode) respectively. All impedances were kept below 20 k $\Omega$ . Both EEG and ECG were recorded using a 1000 Hz sampling rate and a 0.1–1000 Hz online bandpass filter. Signal acquisition and amplification were implemented using the BrainVision Recorder software (Brain Products, Inc.). Online detection of the ECG R-peaks

was achieved using the BrainVision RecView software (Brain Products, Inc.). ECG R-peaks were defined as the first decreasing voltage sample after exceeding a constant threshold. The threshold was individually set after the experimenter visually inspected the 2.5 min ECG signal during the resting block. Each detection of the R-peak added a marker to the online ECG signals and sent a pulse to the experimental PC. During the experiment, the pulse-related markers were visually inspected by the experimenter to ensure that R-peaks were detected with high precision. Furthermore, a post hoc analysis was performed to check the precision of the R-peak detection and the latencies between the ECG R-peaks and the visual stimuli (i.e., the color changes of the visual target) across the experiment. Specifically, we used the NeuroKit2 toolbox (Makowski et al., 2021) in Python to identify the timings of the R-peaks in the offline ECG data, and then compared them with the timings of the target changes. The results suggest that we detected the R-peaks in real-time ECG signal with high precision (in the diastole coupling condition: hit rate:  $92.35 \pm 1.48\%$ ; missing rate:  $7.65 \pm 1.48\%$ ; false alarm rate:  $4.13 \pm 1.02\%$ ; in the systole coupling condition: hit rate:  $90.09 \pm 2.11\%$ ; missing rate:  $9.91 \pm 2.11\%$ ; false alarm rate:  $3.37 \pm 0.78\%$ ), and that the target changes were time-locked to R-peaks (in the diastole coupling condition:  $120.78 \pm 8.51$  ms after R-peaks) or 290 ms after R-peaks (in the systole coupling condition:  $403.25 \pm 6.57$  ms after R-peaks) accordingly in close temporal proximity.

#### 2.5. Behavioral analysis

Behavioral performance was assessed by reaction times for correct responses and accuracy rates in the diastole coupling and the systole coupling condition. Notably, although the number of distractors per display (i.e., 49) was relatively large to avoid immediate visual target detection, in a minority of trials ( $8.12 \pm 1.96\%$  and  $2.50 \pm 0.75\%$  of diastole coupling and systole coupling trials per participant, respectively), participants found the visual target very fast and responded before the first color change of the visual target. These trials were excluded in the behavioral analysis as the experimental manipulation could not be effective (i.e., coupling the color change of the visual target to the presence of strong or weak cardiac signals).

#### 2.6. EEG Preprocessing

EEG data were preprocessed using MATLAB toolbox FieldTrip (Oostenveld et al., 2011). EEG data were re-referenced to the common average, filtered using a 40 Hz low-pass filter, and down-sampled to 500 Hz. No bad electrodes were found. Then, EEG epochs were extracted between -800 and 900 ms around the color change of the visual target. Independent component analysis (ICA) was conducted to identify stereotypical components reflecting eye movements, blinks, and the cardiac field artifact (CFA) which is produced by the movement of the heart muscle. The eye-related artifactual components were manually identified and removed based on scalp topography and time course ( $2.42 \pm 0.32$  components per participant), while CFA-related components were identified using a custom algorithm. More specifically, we first redefined EEG trials around the ECG R-peaks. Then, we computed the coherence of the time-frequency data between each independent component and the ECG signal, and elected four components with the highest coherence. Finally, we decided which of the four components should be removed ( $1.50 \pm 0.21$  components per participant) based on additional characteristics which were commonly associated with CFA, e.g., a bimodal topography, a frequency peak around 5 Hz, and a rhythmically repeating time course (Viola et al., 2009). Furthermore, epochs contaminated by artifacts (e.g., eye movements and muscle activity) were automatically rejected based on a threshold of four times the standard deviation in the horizontal EOG channel and a threshold of  $\pm 100 \mu\text{V}$  in EEG channels.

In total,  $14.12 \pm 2.25\%$  of trials per participant were rejected due to (i) lack of target change before the participant responded, and (ii)

the contamination of artifacts. Additionally, only trials with correct responses were included in further EEG analysis. These procedures left on average  $168.42 \pm 7.97$  trials for the diastole coupling condition and  $155.04 \pm 5.76$  trials for the systole coupling condition per participant.

## 2.7. ERP analysis

EEG epochs were further segmented into periods ranging from -100 to 600 ms relative to four events of interest, with baseline correction using the first 100 ms period. Specifically, in the diastole coupling condition (i.e., time-locking the target change to the R-peak), we assumed that the epochs time-locked to the target change (i.e., about at the R-peak) mainly reflected the responses to the visual stimulus (i.e., unimodal visual input as in this situation the cardiac arousal was low and the visual stimulus therefore was assumed to provide the dominant sensory input). Whereas, the epochs time-locked to 290 ms after the target change (i.e., about at 290 ms after the R-peak) were assumed to mainly reflect the responses to cardiac signals (i.e., unimodal cardiac input as in this situation no visual stimulus was changing color but the cardiac signals were strong and therefore were assumed to provide the dominant sensory input). In the systole coupling condition (i.e., time-locking the target change to 290 ms after the R-peak), we assumed that the epochs time-locked to the target change (i.e., about at 290 ms after the R-peak) reflected the responses to not only the visual stimulus but also the concurrent cardiac signals (i.e., bimodal input as the sensory input was a combined cardio-visual stimulus). Whereas, the epochs time-locked to 290 ms before the target change (i.e., about at the R-peak) were assumed to reflect the responses to “no stimulus” (i.e., at this moment the cardiac arousal was low and no visual stimulus was changing color). We referred to this condition as “no stimulus” as it did not include any stimulus-evoked EEG responses of interest (i.e., EEG responses evoked by the cardiac signals, the visual target, or the cardio-visual stimulus), which helps to distinguish it from the other three conditions including the EEG responses of interest.

Altogether, this procedure yielded four kinds of epochs time-locked to the unimodal visual stimulus, the unimodal cardiac signals, the bimodal cardio-visual stimulus, and the “no stimulus”, respectively (Supplementary Fig. 1). Please note that we used the term “unimodal” to empathize that the brain receives relevant sensory input mainly from a single modality (i.e., the cardiac modality or the visual modality) at a given moment, and that we use “bimodal” to empathize that the brain simultaneously receives relevant sensory information from two different modalities (i.e., the cardiac modality and the visual modality) at a given moment. In addition, as visual-evoked responses could generally last over 500 ms (Fong et al., 2020), all four kinds of epochs also included residual distractor evoked responses. However, any residual distractor evoked responses had been removed prior to comparisons of the relevant experimental conditions and could thus not affect the results in the present study (see detailed explanation in Section 2.9).

## 2.8. Time-frequency analysis

EEG epochs were decomposed into their time-frequency representations using Morlet wavelets (Tallon-Baudry and Bertrand, 1999) from 2 to 40 Hz in steps of 1 Hz (Kaiser and Schütz-Bosbach, 2021). The number of wavelet cycles increased from 3 to 10 cycles in linearly spaced steps to have a good balance between time and frequency resolution. Consistent with the ERP analysis, time-frequency data were further segmented into periods ranging from -300 to 500 ms relative to the four events of interest (i.e., the unimodal visual stimulus, the unimodal cardiac signals, the bimodal cardio-visual stimulus, and the “no stimulus”), with baseline correction via decibel conversion using the period from -300 to -100 ms. This baseline interval was chosen to avoid the adverse influence of spectral estimates biased by windowing post-stimulus activity and padding values (Hu and Zhang, 2019; Zhang et al., 2020).

## 2.9. Statistical analysis

For behavioral data, separate paired samples *t*-tests were performed to compare reaction times and accuracy rates between the diastole coupling and the systole coupling condition. The effect size was estimated by Cohen's *d*.

For ERP data, to investigate the cardio-visual integration in early sensory processing, the ERP elicited by the bimodal cardio-visual stimulus was compared with the summed ERP elicited by the unimodal cardiac signals and visual stimulus. Consistent with previous studies (Senkowski et al., 2011; Talsma and Woldorff, 2005; Van der Burg et al., 2011), the average waveform time-locked to the “no stimulus” was subtracted from the original waveforms elicited by the bimodal cardio-visual stimulus, the unimodal cardiac signals, and the unimodal visual stimulus, respectively, to correct for any residual distractor evoked responses. While we expect an early cardio-visual interaction (< 200 ms; Giard and Peronnet, 1999; Van der Burg et al., 2011; Zhao et al., 2020), we did not have a clear prediction regarding the morphology (latency and topography) of this effect. Therefore, a nonparametric cluster-based permutation *t*-test (the responses to the bimodal cardio-visual stimulus versus the summed responses to the unimodal cardiac signals and visual stimulus) was applied for the ERP amplitudes in the time window from 0 to 200 ms relative to the stimulus onset.

In addition, to investigate the cardio-visual integration in visuospatial selective attention, we compared the N2pc components elicited by the bimodal cardio-visual stimulus and by the unimodal visual stimulus. The N2pc components were measured by the contralateral-minus-ipsilateral difference waveforms relative to the side of the visual target (left or right visual field). Please note that a correction of residual distractor evoked responses prior to this analysis was not required, as the color change of distractors randomly occurred in both visual fields and thus, contralateral-minus-ipsilateral EEG responses were not affected by any residual distractor evoked responses. Previous studies consistently found the maximum N2pc amplitude in the time window from 200 to 300 ms relative to the stimulus onset and around the lateral posterior electrodes (Arslanova et al., 2019; Luck and Hillyard, 1994; Van der Burg et al., 2011). Therefore, a nonparametric cluster-based permutation *t*-test was applied for N2pc amplitudes in this time window and electrode region (left hemisphere: P3, P7, O1, P1, P5, PO7, and PO3; right hemisphere: P4, P8, O2, P2, P6, PO8, and PO4).

For time-frequency data, to investigate the cardio-visual integration in neural oscillations related to early sensory processing, the oscillation power elicited by the bimodal cardio-visual stimulus was compared with the summed oscillation power elicited by the unimodal cardiac signals and visual stimulus. Notably, the time-frequency maps time-locked to the bimodal cardio-visual stimulus, the unimodal cardiac signals, the unimodal visual stimulus, and the “no stimulus” were first averaged over a cluster of posterior electrodes (CP5, P7, P5, P3, P1, PO7, POz, PO4, P4, Oz), respectively. These electrodes were chosen to match the electrodes revealing a prominent early cardio-visual interaction in the ERP analysis. Then, consistent with the ERP analysis, the average oscillation power time-locked to the “no stimulus” was subtracted from the original oscillation power elicited by the bimodal cardio-visual stimulus, the unimodal cardiac signals, and the unimodal visual stimulus, respectively, to correct for potential residual distractor evoked responses. Finally, a nonparametric cluster-based permutation *t*-test (responses to the bimodal cardio-visual stimulus versus the summed responses to the unimodal cardiac signals and visual stimulus) was applied to determine oscillatory power in the time window from 0 to 300 ms relative to the stimulus onset and in frequencies from 2 to 40 Hz.

In addition, to investigate the cardio-visual integration in neural oscillations related to visuospatial selective attention, we compared the lateralized oscillation power elicited by the bimodal cardio-visual stimulus and by the unimodal visual stimulus. The lateralized oscillation power was measured by the contralateral-minus-ipsilateral difference time-frequency maps relative to the side of the visual target (left or

right visual field). A correction of residual distractor evoked responses prior to this analysis was again not required, as the color change of distractors randomly occurred in both visual fields and thus, contralateral-minus-ipsilateral EEG responses were not affected by any residual distractor evoked responses. Notably, the contralateral-minus-ipsilateral difference time-frequency maps time-locked to the cardio-visual stimulus and the visual stimulus were first averaged over a cluster of lateral posterior electrodes (left hemisphere: P5, PO7, P3; right hemisphere: P6, PO8, P4), respectively. These electrodes were chosen to match the electrodes revealing a prominent cardio-visual interaction in the N2pc analysis. Then, a nonparametric cluster-based permutation  $t$ -test was applied for the lateralized oscillation power in the time window from 100 to 400 ms relative to the stimulus onset and in frequencies from 2 to 40 Hz.

Nonparametric cluster-based permutation  $t$ -tests were performed using the FieldTrip toolbox (Oostenveld et al., 2011). Permutation analysis allows for statistical tests over whole time series or time-frequency maps, while still controlling for multiple comparisons (Maris and Oostenveld, 2007). More specifically, for each permutation test used in the present study, adjacent spatio-temporal or spatio-spectro-temporal points for which  $t$ -values exceed a threshold were clustered (dependent  $t$ -test; cluster-defining threshold  $p = .05$ , two-tailed; iterations = 5000). Then, the cluster-level statistics were calculated by taking the sum of the  $t$ -values of all points within each cluster. Last, the observed cluster-level statistic was compared against the permutation distribution to test the null hypothesis of no difference between conditions (two-tailed test). Clusters with  $p < .05$  were considered significant.

Unlike the  $p$ -value in frequentist hypothesis testing, the Bayes Factors (e.g., the  $BF_{10}$  value) in Bayesian hypothesis testing can indicate how much more likely the alternative hypothesis is than the null hypothesis (Wagenmakers et al., 2018). Therefore, for all the tests in behavioral and EEG analyses, we also reported  $BF_{10}$  values from the corresponding Bayesian tests performed in the JASP software (JASP Team, 2022). For the  $t$ -tests, in the absence of previous evidence on cardio-visual integration, we used the default priors, which assume a medium effect size on a Cauchy distribution of 0.707. A  $BF_{10}$  between 1.00 and 3.00 was interpreted as an anecdotal effect, a  $BF_{10}$  between 3.00 and 10.00 as a moderate effect, and a  $BF_{10}$  greater than 10.00 as a strong effect (Wagenmakers et al., 2018).

### 2.10. Control analyzes to exclude possible effects of cardiovascular artifacts

Cardiac cycle-related EEG responses include not only neural responses evoked by cardiac signals but also cardiac field artifact and pulse-related artifact (Kern et al., 2013). Any potential effects of cardiac cycle-related artifacts on our results should thus be carefully considered. We therefore conducted two sets of control analyses to ensure that the observed effects in the present study are caused by neural responses rather than cardiac cycle-related artifacts.

The first set of control analyses was inspired by Petzschner et al. (2019). To rule out any impact of cardiac cycle-related artifacts on the effect in early ERP amplitude, firstly, we compared the mean ECG amplitudes and the mean heart rates within the time window (46–142 ms) of this effect between the bimodal cardio-visual stimulus condition and the unimodal cardiac signals + unimodal visual stimulus condition, using separate paired samples  $t$ -tests. Secondly, we tested if there was any relationship between the differences in early ERP amplitude and the differences in ECG amplitude as well as the differences in heart rate across the aforementioned two conditions using separate linear regressions, i.e., predict the differences in early ERP amplitude from the differences in ECG amplitude or from the differences in heart rate across participants. Furthermore, we also compared the heart rates at R-peak between the systole coupling condition and the diastole coupling condition, and we tested if there was any relationship between the differences in early ERP amplitude across the

bimodal cardio-visual stimulus condition and the unimodal cardiac signals + unimodal visual stimulus condition and the differences in the heart rate at R-peak across the two coupling conditions, using linear regression. The heart rate at each R-peak and the heart rate at each time point were calculated based on ECG signal using the NeuroKit2 toolbox (Makowski et al., 2021).

Similarly, to rule out any impact of cardiac cycle-related artifacts on the effect in early upper-alpha/beta power, firstly, we compared the mean ECG power and the mean heart rates within the time window (60–300 ms) and frequency window (11–24 Hz) of this effect between the bimodal cardio-visual stimulus condition and the unimodal cardiac signals + unimodal visual stimulus condition, using separate paired samples  $t$ -tests. Secondly, we tested if there was any relationship between the differences in early EEG power and the differences in ECG power as well as the differences in heart rate across the aforementioned two conditions using separate linear regressions, i.e., predict the differences in EEG power from the differences in ECG power or from the differences in heart rate across participants. We also tested if there was any relationship between the differences in early EEG power across the bimodal cardio-visual stimulus condition and the unimodal cardiac signals + unimodal visual stimulus condition and the differences in the heart rate at R-peak across the two coupling conditions, using linear regression.

However, this approach does not allow exploring the impact of cardiac cycle-related artifacts on the effects in lateralized N2pc amplitude and lateralized beta power, because it is impossible to extract lateralized ECG response from a single ECG channel. Moreover, the linear regression analysis can detect only potential linear but not nonlinear effects of cardiac cycle-related artifacts, and it does not consider any trial-by-trial variability.

We therefore performed another set of control analyses as suggested by some previous studies (Al et al., 2020; Gray et al., 2010; Ronchi et al., 2017; van Elk et al., 2014). Specifically, for each EEG epoch of our task conditions, we first calculated the latency between the event of interest and the previous ECG R-peak. Then we extracted EEG epochs time-locked to the time point having identical latency after the R-peak during the resting condition, in which no visual stimulus was presented. Next, we averaged the epochs of the resting condition for each EEG electrode. Lastly, we subtracted the mean signal of the resting condition from the aforementioned epoch of the task conditions for each EEG electrode. The corrected EEG data was analyzed using the same statistical methods as the uncorrected data. That is, by using separate nonparametric cluster-based permutation  $t$ -tests, we (1) compared the ERP amplitude elicited by the bimodal cardio-visual stimulus with the summed ERP amplitude elicited by the unimodal cardiac signals and visual stimulus; (2) compared the N2pc amplitudes elicited by the bimodal cardio-visual stimulus and by the unimodal visual stimulus; (3) compared the oscillation power elicited by the bimodal cardio-visual stimulus with the summed oscillation power elicited by the unimodal cardiac signals and visual stimulus; (4) compared the lateralized oscillation power elicited by the bimodal cardio-visual stimulus and by the unimodal visual stimulus.

Please note that there is a caveat to this artifact correction approach. The epochs of the resting condition not only include cardiac cycle-related artifacts, but also neural responses evoked by cardiac signals, as they were time-locked to one specific time point within the cardiac cycle. Hence, this correction procedure not only removes cardiac cycle-related artifacts that we aimed to control for, but also (at least in part) cardiac cycle-related brain responses, that is, the EEG measures of interest in the present study. We therefore report both the uncorrected (see Section 3.2 and 3.3) and corrected data (see Section 3.4.3 and 3.4.4).

## 3. Results

### 3.1. Behavioural results

The paired samples  $t$ -tests showed that reaction times were prolonged in the systole coupling condition ( $2034.70 \pm 108.40$  ms), i.e.,

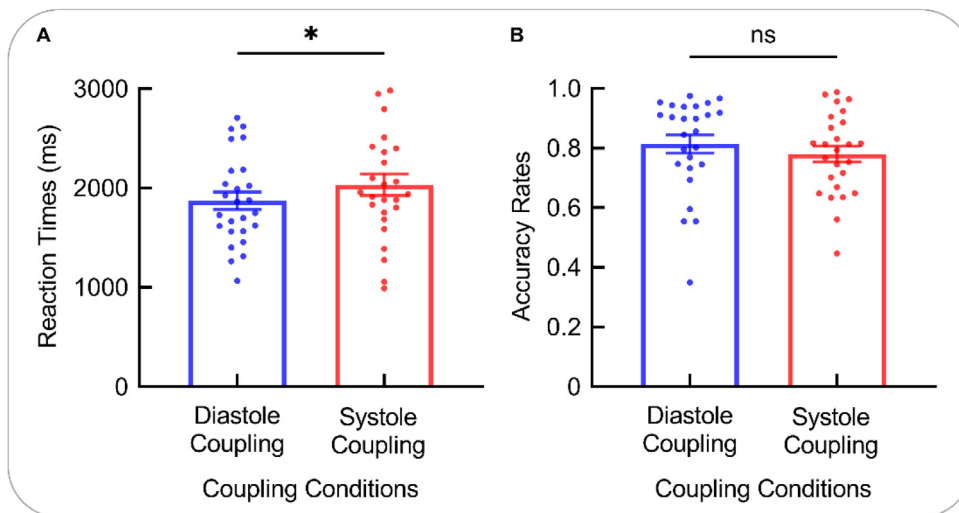


**Fig. 2.** Reaction times and accuracy rates. The reaction times were prolonged in the systole coupling condition, i.e., when the color change of the visual target coincided with strong cardiac signals concerning the state of cardiovascular arousal, compared to the diastole coupling condition, i.e., when the color change of the visual target occurred at a time when cardiac arousal was relatively low. However, the accuracy rates did not significantly differ between the two conditions. Data are expressed as  $M \pm SEM$ . ns: not significant; \*:  $p < .05$ .

when the color change of the visual target coincided with strong cardiac signals concerning the state of cardiovascular arousal, compared to the diastole coupling condition ( $1874.36 \pm 87.61$  ms), i.e., when the color change of the visual target occurred at a time when cardiac arousal was relatively low ( $t(25) = 2.54$ ,  $p = .017$ , Cohen's  $d = 0.50$ ,  $BF_{10} = 2.96$ ). However, the accuracy rates did not significantly differ between the diastole coupling ( $0.81 \pm 0.03$ ) and the systole coupling condition ( $0.78 \pm 0.03$ ;  $t(25) = -1.37$ ,  $p = .182$ , Cohen's  $d = -0.27$ ,  $BF_{10} = 0.48$ ). Fig. 2 represents the reaction times and accuracy rates in the diastole coupling and the systole coupling condition.

### 3.2. ERP results

#### 3.2.1. Early cardio-visual integration in ERPs

The nonparametric cluster-based permutation  $t$ -test for ERP amplitudes revealed a significant cluster over posterior electrodes (CP5, P7, P5, P3, P1, PO7, POz, PO4, P4, and Oz;  $\sim 46$ – $142$  ms;  $p = .023$ , Cohen's  $d = -0.77$ ). The ERP amplitude elicited by the bimodal cardio-visual stimulus ( $-1.22 \pm 0.17 \mu V$ ) was larger than the summed ERP amplitude elicited by the unimodal cardiac signals and visual stimulus ( $-0.87 \pm 0.17 \mu V$ ;  $BF_{10} = 53.64$ ; see Fig. 3).

#### 3.3. The effect of cardio-visual integration in lateralized N2pc components

The nonparametric cluster-based permutation  $t$ -test for contralateral-minus-ipsilateral N2pc amplitudes revealed a significant cluster over lateral posterior electrodes (left hemisphere: P5, PO7, and P3; right hemisphere: P6, PO8, and P4;  $\sim 220$ – $246$  ms;  $p = .016$ , Cohen's  $d = 0.56$ ). Compared to the unimodal visual stimulus ( $-0.60 \pm 0.10 \mu V$ ), the bimodal cardio-visual stimulus elicited a lower N2pc amplitude ( $-0.26 \pm 0.07 \mu V$ ;  $BF_{10} = 5.30$ ; see Fig. 4).

### 3.4. Time-frequency results

#### 3.4.1. Early cardio-visual integration in oscillation power

The nonparametric cluster-based permutation  $t$ -test for oscillation power revealed a significant cluster within the upper-alpha/beta range (11–24 Hz; CP5, P7, P5, P3, P1, PO7, POz, PO4, P4, and Oz;  $\sim 60$ – $300$  ms;  $p < .001$ , Cohen's  $d = -0.67$ ). The upper-alpha/beta power elicited by the bimodal cardio-visual stimulus ( $0.49 \pm 0.12$  dB) was lower than the summed upper-alpha/beta power elicited by the unimodal cardiac signals and visual stimulus ( $0.78 \pm 0.17$  dB;  $BF_{10} = 16.75$ ; see Fig. 5).

#### 3.4.2. The effect of cardio-visual integration in lateralized oscillation power

The nonparametric cluster-based permutation  $t$ -test for lateralized oscillation power revealed a significant cluster within the beta range (16–26 Hz; left hemisphere: P5, PO7, and P3; right hemisphere: P6, PO8, and P4;  $\sim 180$ – $340$  ms;  $p = .006$ , Cohen's  $d = 0.93$ ). Compared to the unimodal visual stimulus ( $-0.20 \pm 0.05$  dB), the bimodal cardio-visual stimulus elicited weaker beta lateralization ( $0.07 \pm 0.05$  dB;  $BF_{10} = 354.15$ ; see Fig. 6).

### 3.5. Results of control analyses to exclude possible effects of cardiovascular artifacts

#### 3.5.1. No impact of ECG amplitude and heart rate on the effect in early ERP amplitude

Within the time window (46–142 ms) of the effect in early ERP amplitude, we did not find any relationship between the differences in early ERP amplitude and the differences in ECG amplitude across the bimodal cardio-visual stimulus condition and the unimodal cardiac signals + unimodal visual stimulus condition (linear regression:  $F(1,25) = 1.97$ ,  $p = .173$ ,  $R^2 = .08$ ,  $BF_{10} = 0.74$ ), although there was a significant difference between the ECG amplitude in response to the bimodal cardio-visual stimulus ( $96.42 \pm 19.06 \mu V$ ) and the summed ECG amplitude in response to the unimodal cardiac signals and visual stimulus ( $51.69 \pm 22.09 \mu V$ ;  $t(25) = 6.49$ ,  $p < .001$ , Cohen's  $d = 1.27$ ,  $BF_{10} = 20736.45$ ; see Supplementary Fig. 1).

In addition, within the time window (46–142 ms) of the effect in early ERP amplitude, there was no difference between the heart rate in response to the bimodal cardio-visual stimulus ( $-0.08 \pm 0.02$  bpm) and the summed heart rate in response to the unimodal cardiac signals and visual stimulus ( $-0.05 \pm 0.04$  bpm;  $t(25) = -0.77$ ,  $p = .447$ , Cohen's  $d = -0.15$ ,  $BF_{10} = 0.27$ ). We did not find any relationship between the differences in early ERP amplitude and the differences in heart rate across the bimodal cardio-visual stimulus condition and the unimodal cardiac signals + unimodal visual stimulus condition, either (linear regression:  $F(1,25) = 3.23$ ,  $p = .085$ ,  $R^2 = .12$ ,  $BF_{10} = 0.87$ ).

Furthermore, we did not find any relationship between the differences in early ERP amplitude across the bimodal cardio-visual stimulus condition and the unimodal cardiac signals + unimodal visual stimulus condition and the differences in heart rate at R-peak across the systole coupling condition and the diastole coupling condition (linear regression:  $F(1,25) = 2.55$ ,  $p = .123$ ,  $R^2 = .10$ ,  $BF_{10} = 0.91$ ), although there was a significant difference in heart rate between the systole coupling ( $74.82 \pm 2.15$  bpm) and the diastole coupling condition ( $73.76 \pm 2.13$  bpm;  $t(25) = 2.43$ ,  $p = .022$ , Cohen's  $d = 0.48$ ,  $BF_{10} = 2.41$ ).

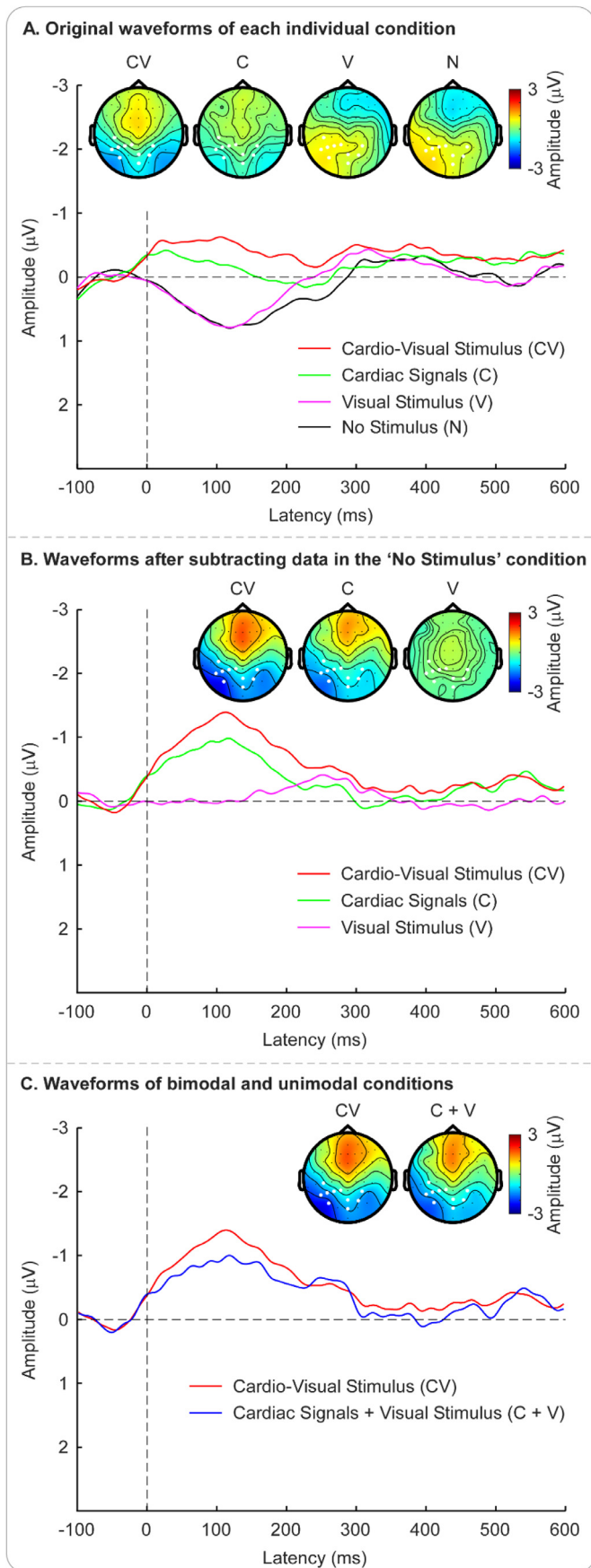


**Fig. 3.** Early cardio-visual integration in ERPs. (A) The original grand-average waveforms elicited by the bimodal cardio-visual stimulus, the unimodal cardiac

**3.5.2. No impact of ECG power and heart rate on the effect in early EEG power**

Within the time window (60–300 ms) and frequency window (11–24 Hz) of the effect in early EEG power, we did not find any relationship between the differences in early EEG power and the differences in ECG power across the bimodal cardio-visual stimulus condition and the unimodal cardiac signals + unimodal visual stimulus condition (linear regression:  $F(1,25) = 2.47, p = .129, R^2 = .09, BF_{10} = 0.88$ ), although there was a significant difference between the ECG power in response to the bimodal cardio-visual stimulus ( $25.27 \pm 2.09 \mu\text{V}$ ) and the summed ECG power in response to the unimodal cardiac signals and visual stimulus ( $27.56 \pm 2.49 \mu\text{V}; t(25) = -2.70, p = .012, \text{Cohen's } d = -0.53, BF_{10} = 4.01$ ; see Supplementary Fig. 2).

In addition, within the time window (60–300 ms) and frequency window (11–24 Hz) of the effect in early EEG power, we did not find any relationship between the differences in early EEG power and the differences in heart rate across the bimodal cardio-visual stimulus condition and the unimodal cardiac signals + unimodal visual stimulus condition (linear regression:  $F(1,25) = 1.81, p = .191, R^2 = .07, BF_{10} = 0.70$ ), although there was a significant difference between the heart rate in response to the bimodal cardio-visual stimulus ( $-0.63 \pm 0.11 \text{ bpm}$ ) and the summed heart rate in response to the unimodal cardiac signals and visual stimulus ( $-2.65 \pm 0.92 \text{ bpm}; t(25) = 2.27, p = .032, \text{Cohen's } d = 0.45, BF_{10} = 1.81$ ).

Furthermore, we did not find any relationship between the differences in early EEG power across the bimodal cardio-visual stimulus condition and the differences in heart rate at R-peak across the systole coupling condition and the diastole coupling condition (linear regression:  $F(1,25) = 3.09, p = .092, R^2 = .11, BF_{10} = 0.91$ ). The scatter plots of linear regression are displayed in Supplementary Fig. 3.

**3.5.3. ERP results based on corrected data**

The nonparametric cluster-based permutation *t*-test for ERP amplitudes revealed a significant cluster over posterior electrodes (CP5, P7, P5, PO7, and P4;  $\sim 90\text{--}136 \text{ ms}; p = .046, \text{Cohen's } d = -0.78$ ). The ERP amplitude elicited by the bimodal cardio-visual stimulus ( $-0.51 \pm 0.29 \mu\text{V}$ ) was larger than the summed ERP amplitude elicited by the unimodal cardiac signals and visual stimulus ( $-0.08 \pm 0.28 \mu\text{V}; BF_{10} = 63.41$ ; see Supplementary Fig. 4).

The nonparametric cluster-based permutation *t*-test for contralateral-minus-ipsilateral N2pc amplitudes revealed a significant cluster over lateral posterior electrodes (left hemisphere: P5, PO7, and P3; right hemisphere: P6, PO8, and P4;  $\sim 220\text{--}250 \text{ ms}; p = .016, \text{Cohen's } d = 0.57$ ). Compared to the unimodal visual stimulus ( $-0.59 \pm 0.10 \mu\text{V}$ ), the

signals, the unimodal visual stimulus, and the “no stimulus”, respectively. Notably, the waveform elicited by the cardio-visual stimulus was time-locked to the target change in the systole coupling condition (about at 290 ms after the R-peak); the waveform elicited by the cardiac signals was time-locked to 290 ms after the target change in the diastole coupling condition (about at 290 ms after the R-peak); the waveform elicited by the visual stimulus was time-locked to the target change in the diastole coupling condition (about at the R-peak); the waveform elicited by the “no stimulus” was time-locked to 290 ms before the target change in the systole coupling condition (about at the R-peak). (B) The grand-average waveforms elicited by the bimodal cardio-visual stimulus, the unimodal cardiac signals, and the unimodal visual stimulus after subtraction of the waveform elicited by the “no stimulus”, respectively. (C) The grand-average waveform elicited by the bimodal cardio-visual stimulus and the summed waveform elicited by the unimodal cardiac signals and visual stimulus. Permutation analysis indicated that the ERP amplitude elicited by the bimodal cardio-visual stimulus was larger than the summed ERP amplitude elicited by the unimodal cardiac signals and visual stimulus. This corresponded to a cluster extended from 46 to 142 ms after stimulus onset over posterior electrodes. Electrodes with high contribution to the cluster (i.e., with a total number of significant samples at or above the mean; CP5, P7, P5, P3, P1, PO7, POz, PO4, P4, and Oz) are highlighted with enlarged white dots in the scalp topographies.

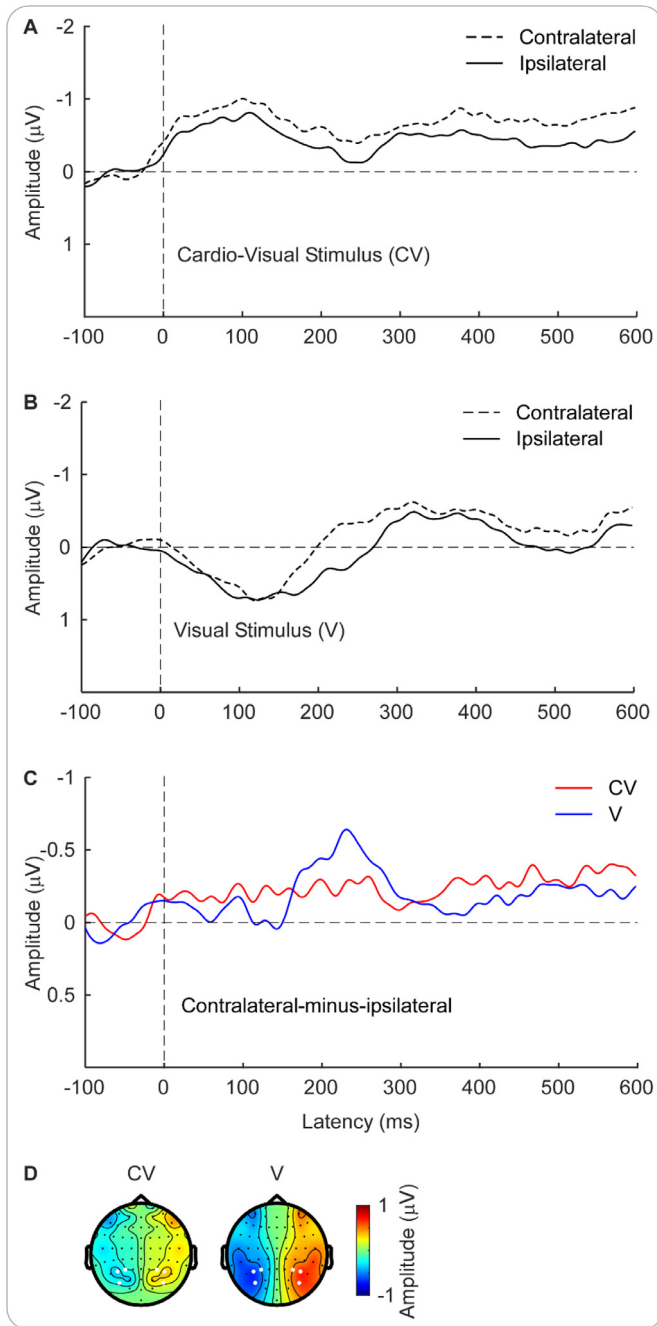


**Fig. 4.** The effect of cardio-visual integration in lateralized N2pc components. Grand-average waveforms elicited contralateral and ipsilateral to the location of the bimodal cardio-visual stimulus (A) or the unimodal visual stimulus (B). (C) Grand-average contralateral-minus-ipsilateral difference waveforms elicited by the bimodal cardio-visual stimulus and by the unimodal visual stimulus, respectively. Permutation analysis indicated that compared to the unimodal visual stimulus, the bimodal cardio-visual stimulus elicited a lower N2pc amplitude. This corresponded to a cluster extended from 220 to 246 ms after stimulus onset over lateral posterior electrodes. Electrodes with high contribution to the cluster (left hemisphere: P5, PO7, and P3; right hemisphere: P6, PO8, and P4) are highlighted with enlarged white dots in the scalp topographies in (D). The scalp topographies show amplitude differences at homologous electrodes over the hemisphere contralateral and ipsilateral to the target location, with electrodes on the midline artificially set to zero.

bimodal cardio-visual stimulus elicited a lower N2pc amplitude ( $-0.26 \pm 0.07 \mu\text{V}$ ;  $\text{BF}_{10} = 6.06$ ; see Supplementary Fig. 5).

#### 3.5.4. Time-frequency results based on corrected data

The nonparametric cluster-based permutation  $t$ -test for oscillation power revealed a significant cluster within the beta range (13–22 Hz; CP5, P7, P5, PO7, and P4;  $\sim 120$ –300 ms;  $p = .007$ , Cohen's  $d = -0.71$ ). The beta power elicited by the bimodal cardio-visual stimulus ( $0.49 \pm 0.15 \text{ dB}$ ) was lower than the summed beta power elicited by the unimodal cardiac signals and visual stimulus ( $0.79 \pm 0.17 \text{ dB}$ ;  $\text{BF}_{10} = 26.71$ ; see Supplementary Fig. 6).

The nonparametric cluster-based permutation  $t$ -test for lateralized oscillation power revealed a significant cluster within the beta range (16–26 Hz; left hemisphere: P5, PO7, and P3; right hemisphere: P6, PO8, and P4;  $\sim 170$ –360 ms;  $p = .003$ , Cohen's  $d = 1.03$ ). Compared to the unimodal visual stimulus ( $-0.21 \pm 0.04 \text{ dB}$ ), the bimodal cardio-visual stimulus elicited weaker beta lateralization ( $0.05 \pm 0.04 \text{ dB}$ ;  $\text{BF}_{10} = 1166.22$ ; see Supplementary Fig. 7).

In summary, our linear regression analyses did not return any linear relationship between the changes in cardiac activity (as measured by ECG amplitude, ECG power, and heart rate) and the effects in early ERP amplitude and early EEG power. More importantly, after correcting for cardiac cycle-related artifacts by subtracting the EEG signal of the resting condition from the EEG signal of task conditions, we observed similar effects based on corrected EEG data as those based on uncorrected EEG data. These results indicate that the observed effects are reflective of neural responses rather than cardiac cycle-related artifacts.

## 4. Discussion

In this study, we explored the multisensory integration of cardiac signals with a visual target in a dynamic cluttered environment by pairing a dynamic visual search task with an ECG recording. We further recorded EEG to explore brain mechanisms associated with this phenomenon. We observed prolonged reaction times when the color change of the visual target occurred simultaneously with the presence of strong cardiac signals concerning the state of cardiovascular arousal (i.e., presented at the end of ventricular systole), compared to when the color change of the visual target occurred at a time when cardiac arousal was relatively low (i.e., presented at the end of ventricular diastole). This result indicates that the co-occurrence of the target change together with cardiac afferent signals makes it harder to detect the visual target among multiple visual stimuli. Moreover, the co-occurrence of the target change with cardiac signals modulated the ERP responses and the beta power at an early stage ( $\sim 100$  ms after stimulus onset) and suppressed lateralization effects of the N2pc component and the beta-band activity at a later stage ( $\sim 200$  ms after stimulus onset). EEG results hereby reveal distinct periods of electrophysiological modulations that reflect the cardio-visual integration.

The results of the present study are – to the best of our knowledge – the first to demonstrate that multisensory integration of cardiac signals with a visual target negatively affects its detection among multiple visual stimuli. Findings hereby extend earlier reports that simultaneous cardiac signals suppress the perception of a single visual event (McIntyre et al., 2007; Sandman et al., 1977; Walker and Sandman, 1982). Specifically, we observed that searching for the visual target in a dynamically changing visual display took longer when the color change of the visual target coincided with strong cardiac arousal signals compared to when cardiac arousal was relatively weak. Similar perceptual attenuation effects have been reported in other exteroceptive modalities, although based on single events only. For example, auditory stimuli presented at cardiac systole compared with diastole led to prolonged reaction times (Yang et al., 2017) and lower likelihood to be judged as louder (Cohen et al., 1980), indicating that cardiac signals can suppress auditory perception. In addition, in the field of pain and somatosensory perception, participants exhibited higher pain thresholds

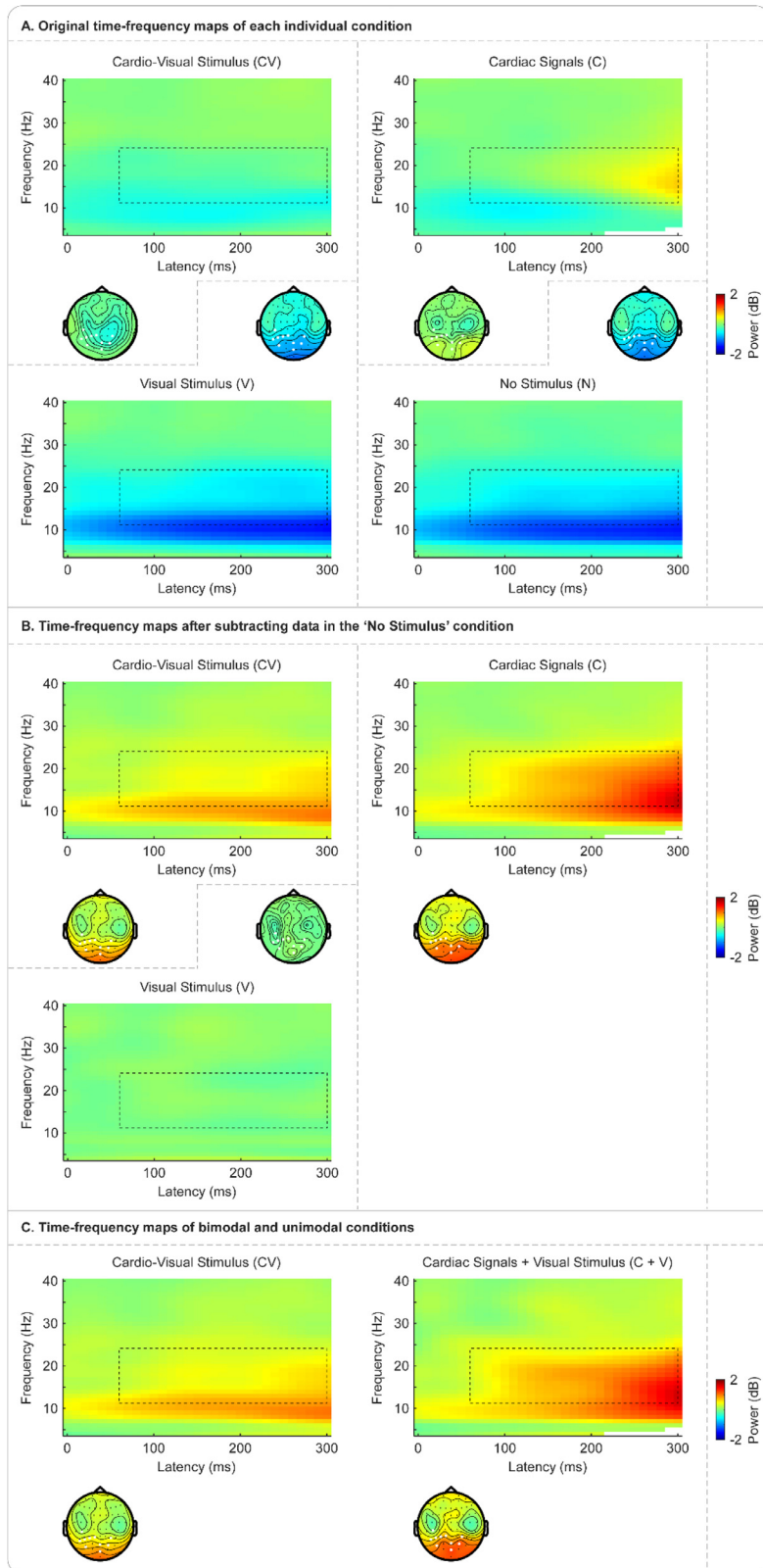


**Fig. 5.** Early cardio-visual integration in oscillatory power. (A) The original grand-average time-frequency maps elicited by the bimodal cardio-visual stimulus, the unimodal cardiac signals, the unimodal visual stimulus, and the “no stimulus”, respectively. (B) The grand-average time-frequency maps elicited by the bimodal cardio-visual stimulus after subtraction of the time-frequency map elicited by the “no stimulus”, respectively. (C) The grand-average time-frequency map elicited by the bimodal cardio-visual stimulus and the summed time-frequency map elicited by the unimodal cardiac signals and visual stimulus. All time-frequency maps were averaged over the posterior electrodes (CP5, P7, P5, P3, P1, PO7, POz, PO4, P4, and Oz) to match the electrodes used in Fig. 3. These electrodes are highlighted with enlarged white dots in the scalp topographies. Permutation analysis indicated that the upper-alpha/beta power elicited by the bimodal cardio-visual stimulus was lower than the summed upper-alpha/beta power elicited by the unimodal cardiac signals and visual stimulus. This corresponded to a cluster extended from 60 to 300 ms after stimulus onset in frequencies from 11 to 24 Hz, marked using dashed rectangles in the time-frequency maps.

(Wilkinson et al., 2013) and worse performance in detecting and localizing somatosensory stimuli during cardiac systole compared to diastole (Al et al., 2020, 2021; Motyka et al., 2019). These studies also support the inhibitory effect of systolic cardiac signals on exteroceptive perception.

More importantly, the present study reveals the brain dynamics underlying this perceptual attenuation phenomenon, which is characterized by electrophysiological modulations during two time periods. First, we observed early modulations in both ERP responses and oscillation power for correctly reported cardio-visual targets. Specifically,

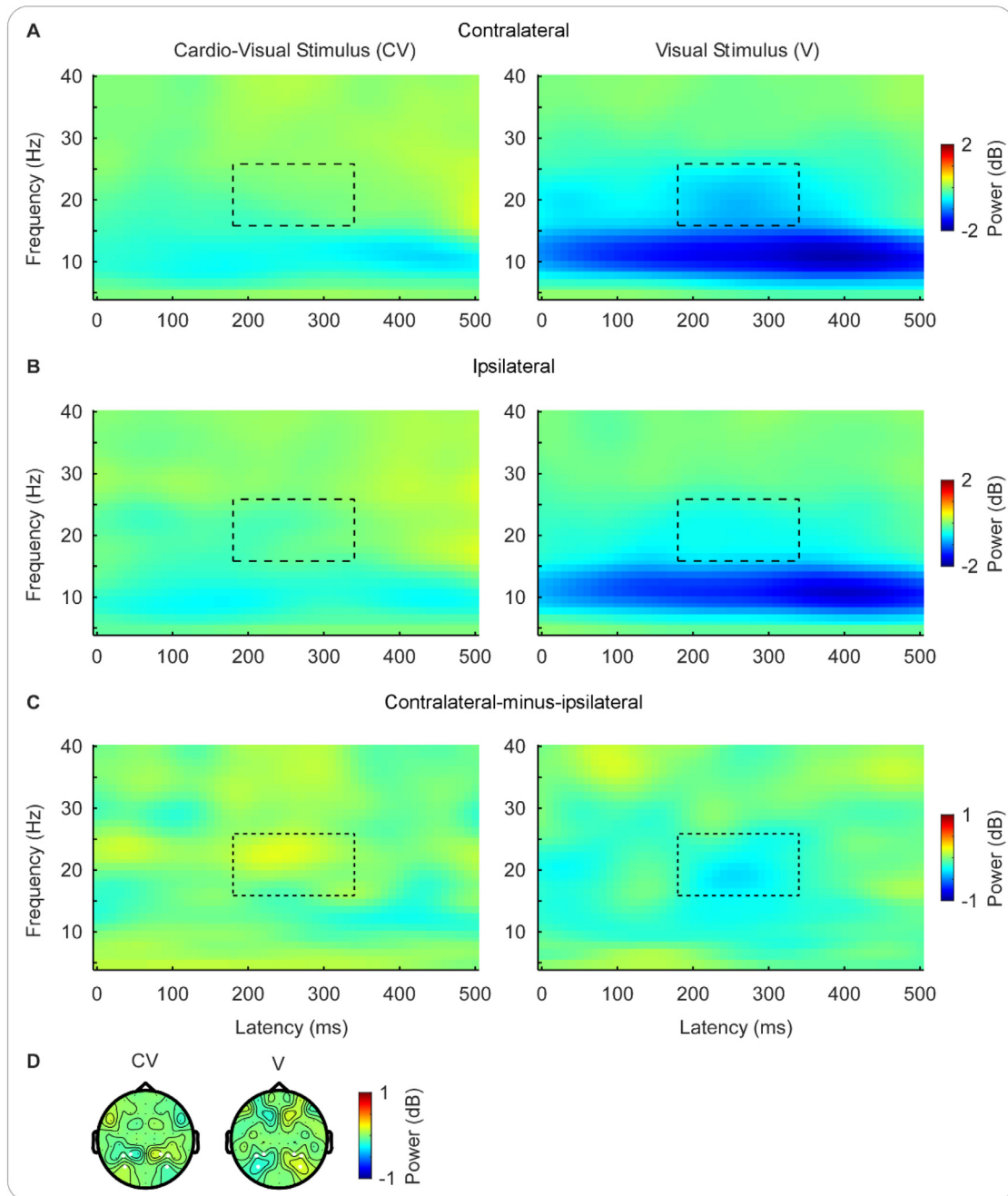


**Fig. 6.** The effect of cardio-visual integration in lateralized oscillation power. Grand-average time-frequency maps for oscillation power elicited contralateral (A) or ipsilateral (B) to the target location. (C) Grand-average time-frequency maps for contralateral-minus-ipsilateral difference oscillation power. Time-frequency maps elicited by the bimodal cardio-visual stimulus (left panel) and the unimodal visual stimulus (right panel) were averaged over lateral posterior electrodes (left hemisphere: P5, PO7, and P3; right hemisphere: P6, PO8, and P4) respectively to match the electrodes used in Fig. 4. These electrodes are highlighted with enlarged white dots in the scalp topographies in (D). Permutation analysis indicated that compared to the bimodal visual stimulus, the bimodal cardio-visual stimulus elicited weaker beta-band lateralization. This corresponded to a cluster extended from 180 to 340 ms after stimulus onset in frequencies from 16 to 26 Hz, marked using dashed rectangles in the time-frequency maps. The scalp topographies show power differences at homologous electrodes over the hemisphere contralateral and ipsilateral to the target location, with electrodes on the midline artificially set to zero.

the modulation of ERP amplitudes and beta power started at  $\sim 90$  and  $\sim 120$  ms respectively, suggesting a rapid interplay between cardiac processing and visual processing. The latencies of these early multisensory responses are consistent with earlier studies reporting cross-modal interactions between different exteroceptive senses. For example, prior studies on auditory-visual (Giard and Peronnet, 1999; Molholm et al., 2002; Senkowski et al., 2011; Van der Burg et al., 2011) and auditory-somatosensory integration (Foxe et al., 2000; Murray et al., 2004) have

reported early ERP modulations starting at around 50 ms after stimulus onset. Early modulations in the alpha-/beta-band activity have also been observed to start at around 100 ms after the presentation of the auditory-visual stimulus (Gleiss and Kayser, 2014; Michail et al., 2021). In addition, the parietal-occipital distribution of these early electrophysiological modulations observed in the current study corresponds to claims that the parietal cortex (e.g., inferior parietal lobule) and primary cortices (e.g., primary visual cortex) are involved

in early multisensory integration (Gentile et al., 2010; Murray et al., 2016).

The early ERP modulation seems to be super-additive, i.e., the ERP amplitude elicited by the bimodal cardio-visual stimulus showed increased negativity relative to the summed ERP amplitude elicited by the unimodal cardiac signals and visual stimulus. However, it is difficult to determine the directionality of the cardio-visual interaction simply according to this result, as the polarity of ERP waveforms recorded at scalp surface does not necessarily reflect the directionality of underlying neural activity (Cappe et al., 2010). Interestingly, the association between behavioral improvement and the sub-additive ERP modulation has been well established in the field of auditory-visual integration. For example, studies using animal models have repeatedly reported sub-additive neural response interactions that enhanced sensory processing (Angelaki et al., 2009; Bizley et al., 2007; Kayser et al., 2009). Likewise, many human studies have shown that the behavioral benefits of multisensory stimuli are related to sub-additive ERP responses (Mercier et al., 2013; Stekelenburg and Vroomen, 2012; Van der Burg et al., 2011). Therefore, it is reasonable to speculate that super-additive ERP responses observed in the present study reflect decreased neural responses to the bimodal cardio-visual stimulus. This view was also supported by our finding in oscillation power, i.e., the power elicited by the bimodal cardio-visual stimulus was lower than the summed power elicited by the unimodal cardiac signals and visual stimulus within the upper-alpha/beta range. Specifically, decreased posterior alpha/beta power may suggest that the participants had to deploy increased attentional resources in the bimodal cardio-visual condition in order to detect the target (Kaiser et al., 2022; Sadaghiani and Kleinschmidt, 2016). Therefore, this could represent further evidence that the presence of cardiac signals in combination with visual information inhibited the processing of such sensory input, which participants needed to compensate for probably by increasing their attentional effort. Altogether, these early modulations in ERP responses and oscillation power suggest an inhibitory cardio-visual integration in early sensory processing.

In addition, we also observed reduced ERP responses and oscillation power in a later time window. Specifically, the bimodal cardio-visual compared with the unimodal visual stimulus elicited lower N2pc amplitude (~220–250 ms) and weaker beta lateralization (~170–360 ms). Both lateralized N2pc component and beta activity are known to be modulated by visuospatial selective attention (Bacigalupo and Luck, 2019; Bauer et al., 2012). Larger lateralization effects in N2pc amplitudes and beta power may reflect more attention to the lateralized visual target. Therefore, our findings may indicate that participants paid less attention to external visual information when it coincided with strong cardiac arousal signals compared to when cardiac arousal was relatively weak. However, future studies are needed to clarify the exact mechanisms underlying the effects reported here. The modulation of attentional resources has been repeatedly proposed as the potential mechanism underlying the cardiac cycle effects on exteroception (Al et al., 2020, 2021). Interestingly, a recent study found that participants had more fixations at diastole and more saccades at systole in a free visual search task (Galvez-Pol et al., 2020). Given that people obtain visual information during fixations rather than during saccades (Pertzov et al., 2009), this result suggests that people especially tend to sample task-relevant visual information in the external environment when cardiac signals are relatively weak and in this way may release attentional resources.

Our attentional modulation account may be further explained within the larger framework of predictive coding. Predictive coding implies that perceptual content is determined by knowledge-driven active inference on the causes of sensory signals (Clark, 2013; Friston, 2009), which is applied not only to exteroception but probably also to interoception such as cardiac signals (Seth, 2013). The goal of this active inference is to minimize prediction error (Friston et al., 2017). Cardiac interoceptive information is conveyed to the brain mainly via the firing of arterial baroreceptors during the systolic phase of each cardiac cycle

(Azzalini et al., 2019; Garfinkel and Critchley, 2016). This periodical transmission of cardiac signals is predictable and therefore attenuated by the brain to reduce the possibility of mistaking these internal spontaneous signals as external input (Barrett and Simmons, 2015; Seth and Friston, 2016). In the present study, the external target change occurring at cardiac systole compared with diastole may be more likely to be regarded as heartbeat-related, task-irrelevant “internal noise”, and thus obtain less attentional and representational resources, finally leading to impaired visual search. Such a predictive coding mechanism has also been proposed to explain the suppression of somatosensory-evoked potentials and pain-evoked potentials during cardiac systole compared to diastole (Al et al., 2020, 2021; Gray et al., 2010), as well as the attenuation of auditory-evoked potentials for heartbeat-related sounds relative to externally generated sounds (van Elk et al., 2014).

In conclusion, multisensory integration of systolic cardiac signals with visual stimulation disrupted the detection of a goal-relevant target among multiple visual distractors, as reflected by prolonged reaction times as well as inhibitory modulations in ERP amplitudes and oscillation power during both early and late time periods. The possible mechanisms underlying this heart-brain interaction are the attenuation of early sensory processing and the reduction of attentional resources deployed toward the outer visual target. Our findings highlight the role of cardiac information in visual processing and further our understanding of the brain dynamics underlying multisensory perception involving both interoception and exteroception.

## Funding

This work was supported by Deutsche Forschungsgemeinschaft [SCHU 2471/5-1 to S.S-B.] and China Scholarship Council [grant number 202004910347 to Q.R.].

## Declaration of Competing Interest

None.

## Credit authorship contribution statement

**Qiaoyue Ren:** Conceptualization, Methodology, Investigation, Data curation, Formal analysis, Visualization, Writing – original draft. **Amanda C. Marshall:** Methodology, Writing – review & editing. **Jakob Kaiser:** Methodology, Writing – review & editing. **Simone Schütz-Bosbach:** Conceptualization, Methodology, Writing – review & editing, Supervision, Funding acquisition.

## Data Availability

I have shared the link to my data/code at the attach file step.

## Acknowledgments

We thank Elsa Sangaran and Sara-Estelle Gößwein for their assistance in data collection.

## Supplementary materials

Supplementary material associated with this article can be found, in the online version, at doi:10.1016/j.neuroimage.2022.119549.

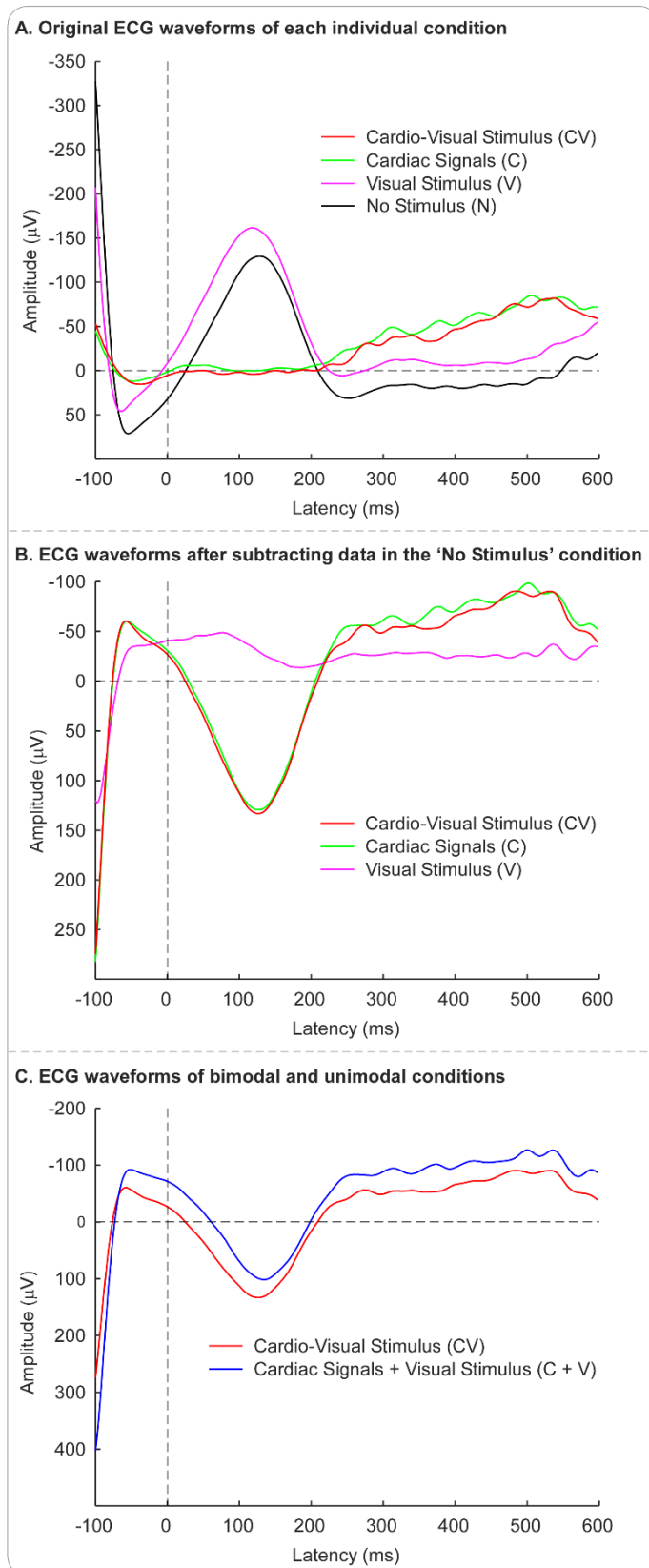
## References

- Adelhoefer, N., Schreiter, M.L., Beste, C., 2020. Cardiac cycle gated cognitive-emotional control in superior frontal cortices. *NeuroImage* 222, 117275. doi:10.1016/j.neuroimage.2020.117275.
- Al, E., Iliopoulos, F., Forschack, N., Nierhaus, T., Grund, M., Motyka, P., Villringer, A., 2020. Heart-brain interactions shape somatosensory perception and evoked potentials. *Proc. Natl. Acad. Sci. U. S. A.* 117 (19), 10575–10584. doi:10.1073/pnas.1915629117.

- Al, E., Iliopoulos, F., Nikulin, V.V., Villringer, A., 2021. Heartbeat and somatosensory perception. *NeuroImage* 238, 118247. doi:10.1016/j.neuroimage.2021.118247.
- Angelaki, D.E., Gu, Y., DeAngelis, G.C., 2009. Multisensory integration: psychophysics, neurophysiology, and computation. *Curr. Opin. Neurobiol.* 19 (4), 452–458. doi:10.1016/j.conb.2009.06.008.
- Arslanova, I., Galvez-Pol, A., Calvo-Merino, B., Forster, B., 2019. Searching for bodies: ERP evidence for independent somatosensory processing during visual search for body-related information. *NeuroImage* 195, 140–149. doi:10.1016/j.neuroimage.2019.03.037.
- Azzalini, D., Rebollo, L., Tallon-Baudry, C., 2019. Visceral signals shape brain dynamics and cognition. *Trends Cogn. Sci.* 23 (6), 488–509. doi:10.1016/j.tics.2019.03.007.
- Bacigalupo, F., Luck, S.J., 2019. Lateralized suppression of alpha-band EEG activity as a mechanism of target processing. *J. Neurosci.* 39 (5), 900–917. doi:10.1523/JNEUROSCI.0183-18.2018.
- Barrett, L.F., Simmons, W.K., 2015. Interoceptive predictions in the brain. *Nat. Rev. Neurosci.* 16 (7), 419–429. doi:10.1038/nrn3950.
- Bauer, M., Kluge, C., Bach, D., Bradbury, D., Heinze, H.J., Dolan, R.J., Driver, J., 2012. Cholinergic enhancement of visual attention and neural oscillations in the human brain. *Curr. Biol.* 22 (5), 397–402. doi:10.1016/j.cub.2012.01.022.
- Bizley, J.K., Nodal, F.R., Bajo, V.M., Nelken, I., King, A.J., 2007. Physiological and anatomical evidence for multisensory interactions in auditory cortex. *Cereb. Cortex* 17 (9), 2172–2189. doi:10.1093/cercor/bhl128.
- Cappe, C., Thut, G., Romei, V., Murray, M.M., 2010. Auditory–visual multisensory interactions in humans: timing, topography, directionality, and sources. *J. Neurosci.* 30 (38), 12572–12580. doi:10.1523/JNEUROSCI.1099-10.2010.
- Chen, W.G., Schloesser, D., Arendsdorf, A.M., Simmons, J.M., Cui, C., Valentino, R., Langevin, H.M., 2021. The emerging science of interoception: sensing, integrating, interpreting, and regulating signals within the self. *Trends Neurosci.* 44 (1), 3–16. doi:10.1016/j.tins.2020.10.007.
- Clark, A., 2013. Whatever next? Predictive brains, situated agents, and the future of cognitive science. *Behav. Brain Sci.* 36 (3), 181–204. doi:10.1017/S0140525X12000477.
- Cohen, R., Lieb, H., Rist, F., 1980. Loudness judgments, evoked potentials, and reaction time to acoustic stimuli early and late in the cardiac cycle in chronic schizophrenics. *Psychiatry Res.* 3 (1), 23–29. doi:10.1016/0165-1781(80)90044-X.
- Coll, M.P., Hobson, H., Bird, G., Murphy, J., 2021. Systematic review and meta-analysis of the relationship between the heartbeat-evoked potential and interoception. *Neurosci. Biobehav. Rev.* 122, 190–200. doi:10.1016/j.neubiorev.2020.12.012.
- DeSaix, P., Betts, J.G., Johnson, E., Johnson, J.E., Korol, O., Kruse, D.H., Poe, B., Wise, J.A., Young, K.A., 2018. *Anatomy & Physiology: OpenStax*. 12th Media Services (18 May 2016).
- Elliott, R., Graf, V., 1972. Visual sensitivity as a function of phase of cardiac cycle. *Psychophysiology* 9 (3), 357–361. doi:10.1111/j.1469-8986.1972.tb03219.x.
- Fong, C.Y., Law, W.H.C., Braithwaite, J.J., Mazaheri, A., 2020. Differences in early and late pattern-onset visual-evoked potentials between self-reported migraineurs and controls. *NeuroImage Clin.* 25, 102122. doi:10.1016/j.nicl.2019.102122.
- Foxe, J.J., Morocz, I.A., Murray, M.M., Higgins, B.A., Javitt, D.C., Schroeder, C.E., 2000. Multisensory auditory–somatosensory interactions in early cortical processing revealed by high-density electrical mapping. *Cogn. Brain Res.* 10 (1), 77–83. doi:10.1016/S0926-6410(00)00024-0.
- Friston, K., 2009. The free-energy principle: a rough guide to the brain? *Trends Cogn. Sci.* 13 (7), 293–301. doi:10.1016/j.tics.2009.04.005.
- Friston, K., FitzGerald, T., Rigoli, F., Schwartenbeck, P., Pezzulo, G., 2017. Active inference: a process theory. *Neural Comput.* 29 (1), 1–49. doi:10.1162/NECO\_a\_00912.
- Galvez-Pol, A., McConnell, R., Kilner, J.M., 2020. Active sampling in visual search is coupled to the cardiac cycle. *Cognition* 196, 104149. doi:10.1016/j.cognition.2019.104149.
- Garfinkel, S.N., Critchley, H.D., 2016. Threat and the body: how the heart supports fear processing. *Trends Cogn. Sci.* 20 (1), 34–46. doi:10.1016/j.tics.2015.10.005.
- Garfinkel, S.N., Minati, L., Gray, M.A., Seth, A.K., Dolan, R.J., Critchley, H.D., 2014. Fear from the heart: sensitivity to fear stimuli depends on individual heartbeats. *J. Neurosci.* 34 (19), 6573–6582. doi:10.1523/JNEUROSCI.3507-13.2014.
- Gentile, G., Petkova, V.I., Ehrsson, H.H., 2010. Integration of visual and tactile signals from the hand in the human brain: an fMRI study. *J. Neurophysiol.* 105 (2), 910–922. doi:10.1152/jn.00840.2010.
- Giard, M.H., Peronnet, F., 1999. Auditory–visual integration during multimodal object recognition in humans: a behavioral and electrophysiological study. *J. Cogn. Neurosci.* 11 (5), 473–490. doi:10.1162/0899892999563544.
- Gleiss, S., Kayser, C., 2014. Oscillatory mechanisms underlying the enhancement of visual motion perception by multisensory congruency. *Neuropsychologia* 53, 84–93. doi:10.1016/j.neuropsychologia.2013.11.005.
- Gray, M.A., Minati, L., Paoletti, G., Critchley, H.D., 2010. Baroreceptor activation attenuates attentional effects on pain-evoked potentials. *Pain* 151 (3), 853–861. doi:10.1016/j.pain.2010.09.028.
- Hu, L., Zhang, Z., 2019. *EEG Signal Processing and Feature Extraction*. Springer.
- JASP Team, 2022. *JASP (Version 0.16.3)* [Computer software]. <https://jasp-stats.org/>.
- Kaiser, J., Iliopoulos, P., Steinmassl, K., Schütz-Bosbach, S., 2022. Preparing for success: neural frontal theta and posterior alpha dynamics during action preparation predict flexible resolution of cognitive conflicts. *J. Cogn. Neurosci.* 34 (6), 1070–1089. doi:10.1162/jocn\_a\_01846.
- Kaiser, J., Schütz-Bosbach, S., 2021. Motor interference, but not sensory interference, increases midfrontal theta activity and brain synchronization during reactive control. *J. Cogn. Neurosci.* 41 (8), 1788–1801. doi:10.1523/JNEUROSCI.1682-20.2020.
- Kayser, C., Petkov, C.I., Logothetis, N.K., 2009. Multisensory interactions in primate auditory cortex: fMRI and electrophysiology. *Hear. Res.* 258 (1), 80–88. doi:10.1016/j.heares.2009.02.011.
- Kayser, S.J., Philiastides, M.G., Kayser, C., 2017. Sounds facilitate visual motion discrimination via the enhancement of late occipital visual representations. *NeuroImage* 148, 31–41. doi:10.1016/j.neuroimage.2017.01.010.
- Kern, M., Aertsen, A., Schulze-Bonhage, A., Ball, T., 2013. Heart cycle-related effects on event-related potentials, spectral power changes, and connectivity patterns in the human ECoG. *NeuroImage* 81, 178–190. doi:10.1016/j.neuroimage.2013.05.042.
- Leo, F., Bertini, C., di Pellegrino, G., Làdavas, E., 2008. Multisensory integration for orienting responses in humans requires the activation of the superior colliculus. *Exp. Brain Res.* 186 (1), 67–77. doi:10.1007/s00221-007-1204-9.
- Luck, S.J., Hillyard, S.A., 1994. Electrophysiological correlates of feature analysis during visual search. *J. Exp. Psychol. Hum. Percept. Perform.* 31 (3), 291–308. doi:10.1111/j.1469-8986.1994.tb02218.x.
- Makowski, D., Pham, T., Lau, Z.J., Brammer, J.C., Lespinaise, F., Pham, H., Chen, S.H.A., 2021. NeuroKit2: a Python toolbox for neurophysiological signal processing. *Behav. Res. Methods* 53 (4), 1689–1696. doi:10.3758/s13428-020-01516-y.
- Maris, E., Oostenveld, R., 2007. Nonparametric statistical testing of EEG and MEG data. *J. Neurosci. Methods* 164 (1), 177–190. doi:10.1016/j.jneumeth.2007.03.024.
- Marshall, A.C., Gentsch-Ebrahimzadeh, A., Schütz-Bosbach, S., 2022. From the inside out: interoceptive feedback facilitates the integration of visceral signals for efficient sensory processing. *NeuroImage* 251, 119011. doi:10.1016/j.neuroimage.2022.119011.
- Martuzzi, R., Murray, M.M., Michel, C.M., Thiran, J.P., Maeder, P.P., Clarke, S., Meuli, R.A., 2007. Multisensory interactions within human primary cortices revealed by BOLD dynamics. *Cereb. Cortex* 17 (7), 1672–1679. doi:10.1093/cercor/bhl077.
- McIntyre, D., Ring, C., Hamer, M., Carroll, D., 2007. Effects of arterial and cardiopulmonary baroreceptor activation on simple and choice reaction times. *Psychophysiology* 44 (6), 874–879. doi:10.1111/j.1469-8986.2007.00547.x.
- Mercier, M.R., Foxe, J.J., Fiebelkorn, I.C., Butler, J.S., Schwartz, T.H., Molholm, S., 2013. Auditory-driven phase reset in visual cortex: human electrocorticography reveals mechanisms of early multisensory integration. *NeuroImage* 79, 19–29. doi:10.1016/j.neuroimage.2013.04.060.
- Michail, G., Senkowski, D., Holtkamp, M., Wächter, B., Schroeder, C.E., Keil, J., 2021. Early beta oscillations in multisensory association areas underlie crossmodal performance enhancement. *bioRxiv*. [doi:10.1101/2022.11.9307](https://doi.org/10.1101/2022.11.9307).
- Molholm, S., Ritter, W., Murray, M.M., Javitt, D.C., Schroeder, C.E., Foxe, J.J., 2002. Multisensory auditory–visual interactions during early sensory processing in humans: a high-density electrical mapping study. *Cogn. Brain Res.* 14 (1), 115–128. doi:10.1016/S0926-6410(02)00066-6.
- Motyka, P., Grund, M., Forschack, N., Al, E., Villringer, A., Gaebler, M., 2019. Interactions between cardiac activity and conscious somatosensory perception. *Psychophysiology* 56 (10), e13424. doi:10.1111/psyp.13424.
- Murray, M.M., Molholm, S., Michel, C.M., Heslenfeld, D.J., Ritter, W., Javitt, D.C., Foxe, J.J., 2004. Grabbing your ear: rapid auditory–somatosensory multisensory interactions in low-level sensory cortices are not constrained by stimulus alignment. *Cereb. Cortex* 15 (7), 963–974. doi:10.1093/cercor/bbh197.
- Murray, M.M., Thelen, A., Thut, G., Romei, V., Martuzzi, R., Matusz, P.J., 2016. The multisensory function of the human primary visual cortex. *Neuropsychologia* 83, 161–169. doi:10.1016/j.neuropsychologia.2015.08.011.
- Noesselt, T., Bergmann, D., Hake, M., Heinze, H.J., Fendrich, R., 2008. Sound increases the saliency of visual events. *Brain Res.* 1220, 157–163. doi:10.1016/j.brainres.2007.12.060.
- Oostenveld, R., Fries, P., Maris, E., Schoffelen, J.M., 2011. FieldTrip: open source software for advanced analysis of MEG, EEG, and invasive electrophysiological data. *Comput. Intell. Neurosci.* 2011, 156869. doi:10.1155/2011/156869.
- Park, H.D., Bernasconi, F., Salomon, R., Tallon-Baudry, C., Spinelli, L., Seeck, M., Blanke, O., 2018. Neural sources and underlying mechanisms of neural responses to heartbeats, and their role in bodily self-consciousness: an intracranial EEG study. *Cereb. Cortex* 28 (7), 2351–2364. doi:10.1093/cercor/bhx136.
- Park, H.D., Blanke, O., 2019. Heartbeat-evoked cortical responses: underlying mechanisms, functional roles, and methodological considerations. *NeuroImage* 197, 502–511. doi:10.1016/j.neuroimage.2019.04.081.
- Park, H.D., Correia, S., Ducorps, A., Tallon-Baudry, C., 2014. Spontaneous fluctuations in neural responses to heartbeats predict visual detection. *Nat. Neurosci.* 17 (4), 612–618. doi:10.1038/nn.3671.
- Pertsov, Y., Avidan, G., Zohary, E., 2009. Accumulation of visual information across multiple fixations. *J. Vis.* 9 (10), 2. doi:10.1167/9.10.2.
- Petzschner, F.H., Weber, L.A., Wellstein, K.V., Paolini, G., Do, C.T., Stephan, K.E., 2019. Focus of attention modulates the heartbeat evoked potential. *NeuroImage* 186, 595–606. doi:10.1016/j.neuroimage.2018.11.037.
- Pramme, L., Larra, M.F., Schächinger, H., Frings, C., 2014. Cardiac cycle time effects on mask inhibition. *Biol. Psychol.* 100, 115–121. doi:10.1016/j.biopsycho.2014.05.008.
- Pramme, L., Larra, M.F., Schächinger, H., Frings, C., 2016. Cardiac cycle time effects on selection efficiency in vision. *Psychophysiology* 53 (11), 1702–1711. doi:10.1111/psyp.12728.
- Quigley, K.S., Kanoski, S., Grill, W.M., Barrett, L.F., Tsakiris, M., 2021. Functions of interoception: from energy regulation to experience of the self. *Trends Neurosci.* 44 (1), 29–38. doi:10.1016/j.tins.2020.09.008.
- Rae, C.L., Ahmad, A., Larsson, D.E.O., Silva, M., Praag, C.D.G.V., Garfinkel, S.N., Critchley, H.D., 2020. Impact of cardiac interoception cues and confidence on voluntary decisions to make or withhold action in an intentional inhibition task. *Sci. Rep.* 10, 4184. doi:10.1038/s41598-020-60405-8.
- Rae, C.L., Botan, V.E., Gould van Praag, C.D., Herman, A.M., Nyssönen, J.A., Watson, D.R., Critchley, H.D., 2018. Response inhibition on the stop signal task improves during cardiac contraction. *Sci. Rep.* 8, 9136. doi:10.1038/s41598-018-27513-y.
- Ronchi, R., Bernasconi, F., Pfeiffer, C., Bello-Ruiz, J., Kaliuzhna, M., Blanke, O., 2017. Interoceptive signals impact visual processing: cardiac modulation of visual body perception. *NeuroImage* 158, 176–185. doi:10.1016/j.neuroimage.2017.06.064.

- Sadaghiani, S., Kleinschmidt, A., 2016. Brain networks and  $\alpha$ -oscillations: structural and functional foundations of cognitive control. *Trends Cogn. Sci.* 20 (11), 805–817. doi:[10.1016/j.tics.2016.09.004](https://doi.org/10.1016/j.tics.2016.09.004).
- Salomon, R., Ronchi, R., Dönz, J., Bello-Ruiz, J., Herbelin, B., Faivre, N., Blanke, O., 2018. Insula mediates heartbeat related effects on visual consciousness. *Cortex* 101, 87–95. doi:[10.1016/j.cortex.2018.01.005](https://doi.org/10.1016/j.cortex.2018.01.005).
- Salomon, R., Ronchi, R., Dönz, J., Bello-Ruiz, J., Herbelin, B., Martet, R., Blanke, O., 2016. The insula mediates access to awareness of visual stimuli presented synchronously to the heartbeat. *J. Neurosci.* 36 (18), 5115–5127. doi:[10.1523/JNEUROSCI.4262-15.2016](https://doi.org/10.1523/JNEUROSCI.4262-15.2016).
- Sandman, C.A., McCanne, T.R., Kaiser, D.N., Diamond, B., 1977. Heart rate and cardiac phase influences on visual perception. *J. Comp. Physiol. Psychol.* 91 (1), 189–202. doi:[10.1037/h0077302](https://doi.org/10.1037/h0077302).
- Sel, A., Azevedo, R.T., Tsakiris, M., 2017. Heartfelt self: cardio-visual integration affects self-face recognition and interoceptive cortical processing. *Cereb. Cortex* 27 (11), 5144–5155. doi:[10.1093/cercor/bhw296](https://doi.org/10.1093/cercor/bhw296). *J. Cerebral Cortex*.
- Senkowski, D., Saint-Amour, D., Höfle, M., Foxe, J.J., 2011. Multisensory interactions in early evoked brain activity follow the principle of inverse effectiveness. *NeuroImage* 56 (4), 2200–2208. doi:[10.1016/j.neuroimage.2011.03.075](https://doi.org/10.1016/j.neuroimage.2011.03.075).
- Seth, A.K., 2013. Interoceptive inference, emotion, and the embodied self. *Trends Cogn. Sci.* 17 (11), 565–573. doi:[10.1016/j.tics.2013.09.007](https://doi.org/10.1016/j.tics.2013.09.007).
- Seth, A.K., Friston, K.J., 2016. Active interoceptive inference and the emotional brain. *Philos. Trans. R. Soc. B Biol. Sci.* 371 (1708), 20160007. doi:[10.1098/rstb.2016.0007](https://doi.org/10.1098/rstb.2016.0007).
- Stekelenburg, J.J., Vroomen, J., 2012. Electrophysiological correlates of predictive coding of auditory location in the perception of natural audiovisual events. *Front. Integr. Neurosci.* 6, 26. doi:[10.3389/fnint.2012.00026](https://doi.org/10.3389/fnint.2012.00026).
- Tallon-Baudry, C., Bertrand, O., 1999. Oscillatory gamma activity in humans and its role in object representation. *Trends Cogn. Sci.* 3 (4), 151–162. doi:[10.1016/S1364-6613\(99\)01299-1](https://doi.org/10.1016/S1364-6613(99)01299-1).
- Talsma, D., Woldorff, M.G., 2005. Selective attention and multisensory integration: multiple phases of effects on the evoked brain activity. *J. Cogn. Neurosci.* 17 (7), 1098–1114. doi:[10.1162/0898929054475172](https://doi.org/10.1162/0898929054475172).
- Tang, X., Wu, J., Shen, Y., 2016. The interactions of multisensory integration with endogenous and exogenous attention. *Neurosci. Biobehav. Rev.* 61, 208–224. doi:[10.1016/j.neubiorev.2015.11.002](https://doi.org/10.1016/j.neubiorev.2015.11.002).
- van Atteveldt, N., Murray, M.M., Thut, G., Schroeder, C.E., 2014. Multisensory integration: flexible use of general operations. *Neuron* 81 (6), 1240–1253. doi:[10.1016/j.neuron.2014.02.044](https://doi.org/10.1016/j.neuron.2014.02.044).
- Van der Burg, E., Olivers, C.N., Bronkhorst, A.W., Theeuwes, J., 2008. Pip and pop: non-spatial auditory signals improve spatial visual search. *J. Exp. Psychol. Hum. Percept. Perform.* 34 (5), 1053. doi:[10.1037/0096-1523.34.5.1053](https://doi.org/10.1037/0096-1523.34.5.1053).
- Van der Burg, E., Talsma, D., Olivers, C.N., Hickey, C., Theeuwes, J., 2011. Early multisensory interactions affect the competition among multiple visual objects. *NeuroImage* 55 (3), 1208–1218. doi:[10.1016/j.neuroimage.2010.12.068](https://doi.org/10.1016/j.neuroimage.2010.12.068).
- van Elk, M., Lenggenhager, B., Heydrich, L., Blanke, O., 2014. Suppression of the auditory N1-component for heartbeat-related sounds reflects interoceptive predictive coding. *Biol. Psychol.* 99, 172–182. doi:[10.1016/j.biopsycho.2014.03.004](https://doi.org/10.1016/j.biopsycho.2014.03.004).
- Viola, F.C., Thorne, J., Edmonds, B., Schneider, T., Eichele, T., Debener, S., 2009. Semi-automatic identification of independent components representing EEG artifact. *Clin. Neurophysiol.* 120 (5), 868–877. doi:[10.1016/j.clinph.2009.01.015](https://doi.org/10.1016/j.clinph.2009.01.015).
- Wagenmakers, E.J., Love, J., Marsman, M., Jamil, T., Ly, A., Verhagen, J., Morey, R.D., 2018. Bayesian inference for psychology. Part II: example applications with JASP. *Psychon. Bull. Rev.* 25 (1), 58–76. doi:[10.3758/s13423-017-1323-7](https://doi.org/10.3758/s13423-017-1323-7).
- Wagenmakers, E.J., Marsman, M., Jamil, T., Ly, A., Verhagen, J., Love, J., Morey, R.D., 2018. Bayesian inference for psychology. Part I: theoretical advantages and practical ramifications. *Psychon. Bull. Rev.* 25 (1), 35–57. doi:[10.3758/s13423-017-1343-3](https://doi.org/10.3758/s13423-017-1343-3).
- Walker, B.B., Sandman, C.A., 1982. Visual evoked potentials change as heart rate and carotid pressure change. *Psychophysiology* 19 (5), 520–527. doi:[10.1111/j.1469-8986.1982.tb02579.x](https://doi.org/10.1111/j.1469-8986.1982.tb02579.x).
- Wallace, M.T., Woynarowski, T.G., Stevenson, R.A., 2020. Multisensory integration as a window into orderly and disrupted cognition and communication. *Annu. Rev. Psychol.* 71 (1), 193–219. doi:[10.1146/annurev-psych-010419-051112](https://doi.org/10.1146/annurev-psych-010419-051112).
- Wilkinson, M., McIntyre, D., Edwards, L., 2013. Electrocutaneous pain thresholds are higher during systole than diastole. *Biol. Psychol.* 94 (1), 71–73. doi:[10.1016/j.biopsycho.2013.05.002](https://doi.org/10.1016/j.biopsycho.2013.05.002).
- Yang, X., Jennings, J.R., Friedman, B.H., 2017. Exteroceptive stimuli override interoceptive state in reaction time control. *Psychophysiology* 54 (12), 1940–1950. doi:[10.1111/psyp.12958](https://doi.org/10.1111/psyp.12958).
- Zhang, L., Li, Z., Zhang, F., Gu, R., Peng, W., Hu, L., 2020. Demystifying signal processing techniques to extract task-related EEG responses for psychologists. *Brain Sci. Adv.* 6 (3), 171–188. doi:[10.26599/BSA.2020.9050018](https://doi.org/10.26599/BSA.2020.9050018).
- Zhao, S., Wang, Y., Feng, C., Feng, W., 2020. Multiple phases of cross-sensory interactions associated with the audiovisual bounce-inducing effect. *Biol. Psychol.* 149, 107805. doi:[10.1016/j.biopsycho.2019.107805](https://doi.org/10.1016/j.biopsycho.2019.107805).
- Zhao, S., Wang, Y., Xu, H., Feng, C., Feng, W., 2018. Early cross-modal interactions underlie the audiovisual bounce-inducing effect. *NeuroImage* 174, 208–218. doi:[10.1016/j.neuroimage.2018.03.036](https://doi.org/10.1016/j.neuroimage.2018.03.036).

## Supplementary Materials



### Supplementary Figure 1.

Waveforms in the ECG electrode. (A) The original grand-average ECG waveforms time-locked to the bimodal cardio-visual stimulus, the unimodal cardiac signals, the unimodal visual stimulus, and the “no stimulus”, respectively. (B)

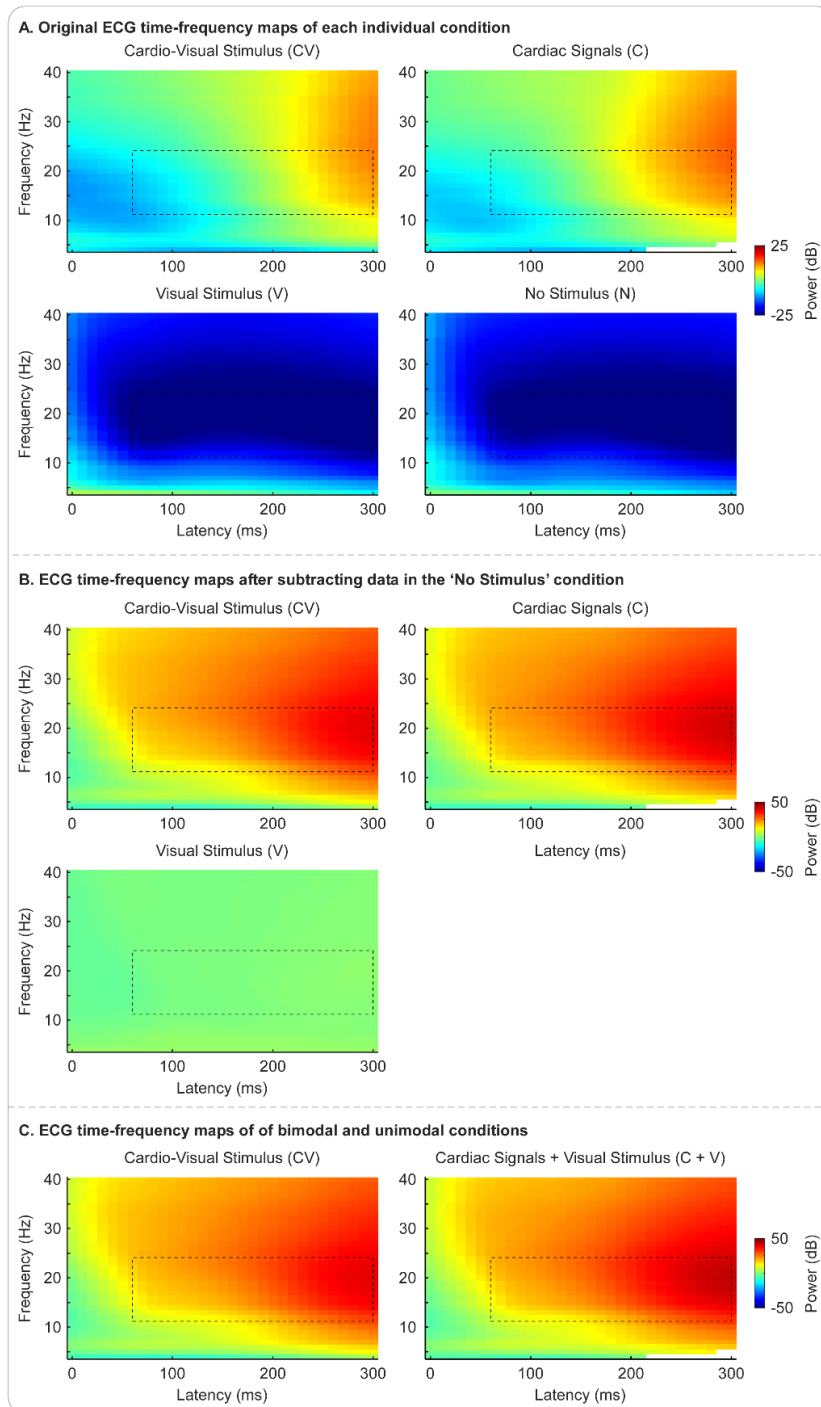
The grand-average ECG waveforms time-locked to the bimodal cardio-visual stimulus, the unimodal cardiac signals, and the unimodal visual stimulus after subtraction of the ECG waveform time-locked to the “no stimulus”, respectively. (C)

The grand-average ECG waveform time-locked to the bimodal cardio-visual stimulus and the summed ECG waveform time-locked to the unimodal cardiac signals and visual stimulus.

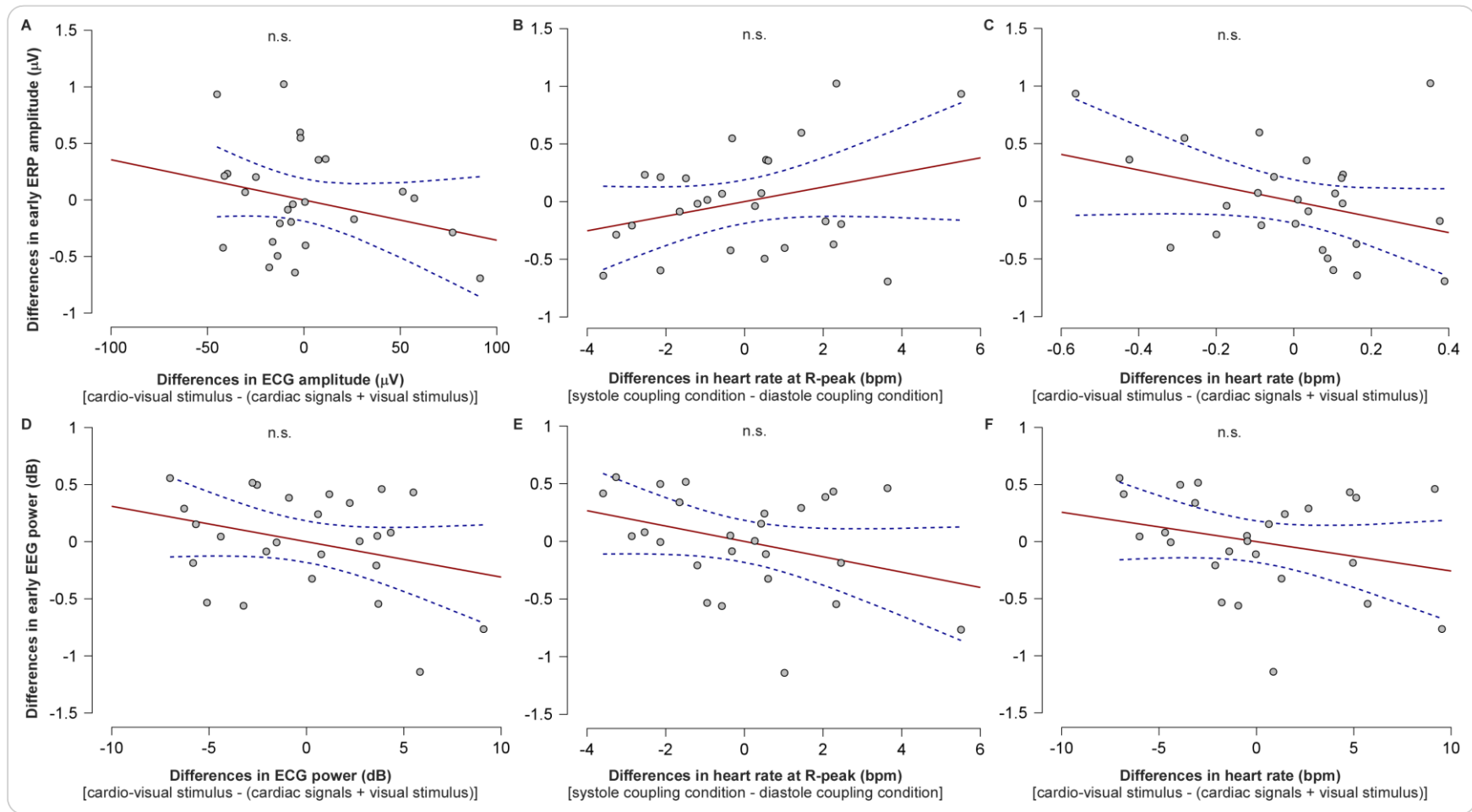
## Supplementary

### Figure 2.

Oscillatory power in the ECG electrode. (A) The original grand-average ECG time-frequency maps time-locked to the bimodal cardio-visual stimulus, the unimodal cardiac signals, the unimodal visual stimulus, and the “no stimulus”, respectively. (B) The grand-average ECG time-frequency maps time-locked to the bimodal cardio-visual stimulus, the unimodal cardiac signals, and the unimodal visual stimulus after subtraction of the ECG time-frequency map time-locked to the “no stimulus”, respectively. (C) The grand-average ECG time-frequency map time-locked to the bimodal cardio-visual stimulus and the summed ECG time-frequency map time-locked to the unimodal cardiac signals and visual stimulus. The same time window (60–300 ms) and frequency window (11–24 Hz) as in Figure 5 were marked using dashed rectangles in the time-frequency maps.

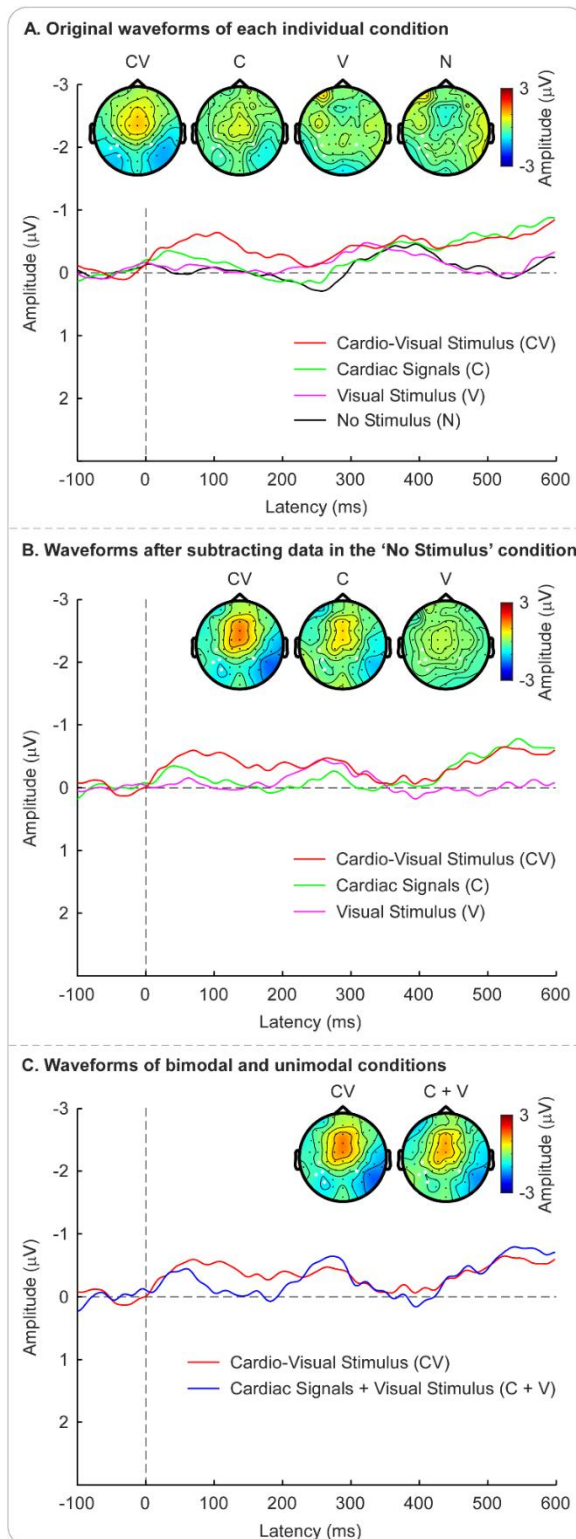


and the unimodal visual stimulus after subtraction of the ECG time-frequency map time-locked to the “no stimulus”, respectively. (C) The grand-average ECG time-frequency map time-locked to the bimodal cardio-visual stimulus and the summed ECG time-frequency map time-locked to the unimodal cardiac signals and visual stimulus. The same time window (60–300 ms) and frequency window (11–24 Hz) as in Figure 5 were marked using dashed rectangles in the time-frequency maps.



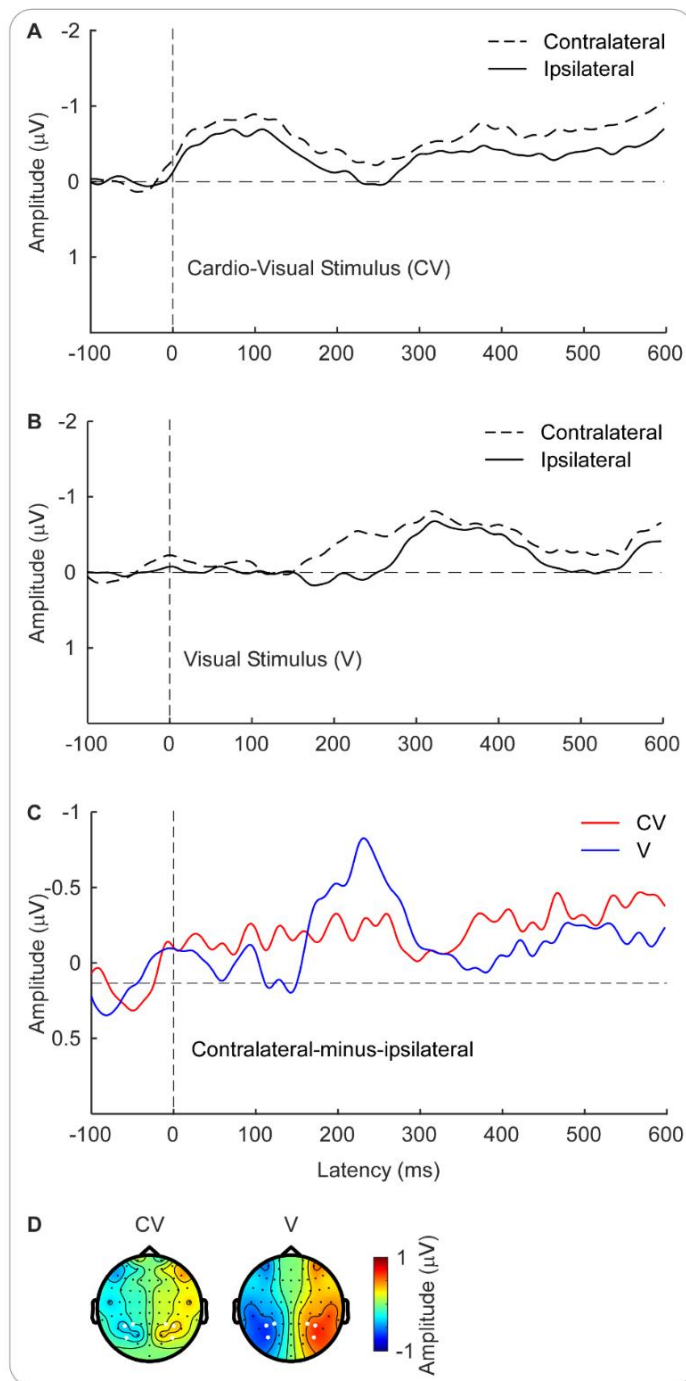
**Supplementary Figure 3.** Linear regressions between the changes in cardiac activity and the effects in EEG responses. Upper panel: scatter plot of the differences in early ERP amplitude with the differences between the ECG amplitude in response to the bimodal cardio-

visual stimulus and the summed ECG amplitude in response to the unimodal cardiac signals and visual stimulus **(A)**, the differences in heart rate at R-peak between the systole coupling and the diastole coupling condition **(B)**, and the differences between the heart rate in response to the bimodal cardio-visual stimulus and the summed heart rate in response to the unimodal cardiac signals and visual stimulus **(C)**. Lower panel: scatter plot of the differences in early EEG power with the differences between the ECG power in response to the bimodal cardio-visual stimulus and the summed ECG power in response to the unimodal cardiac signals and visual stimulus **(D)**, the differences in heart rate at R-peak between the systole coupling and the diastole coupling condition **(E)**, and the differences between the heart rate in response to the bimodal cardio-visual stimulus and the summed heart rate in response to the unimodal cardiac signals and visual stimulus **(F)**. Notably, for plot A, C, D, and F, the ECG amplitude, ECG power, and heart rate were extracted from the time window (and the frequency window) of the corresponding effect. The red line indicates the linear fit, and the dotted blue lines indicate the 95% confidence bounds. The effects in early ERP amplitude and EEG power did not have any linear relationship with the physiological changes of heart activity (as measured by the amplitude, oscillation power, and heart rate in ECG signal) across conditions. n.s.: not significant.



**Supplementary Figure 4.** Early cardio-visual integration in ERPs (after subtracting cardiac cycle-related EEG responses in the resting condition). **(A)** The original grand-average waveforms elicited by the bimodal cardio-visual stimulus, the unimodal cardiac signals, the unimodal visual stimulus, and the “no stimulus”, respectively. **(B)** The grand-average waveforms elicited by the bimodal cardio-visual stimulus, the unimodal cardiac signals, and the unimodal visual stimulus after subtraction of the waveform elicited by the “no stimulus”, respectively. **(C)** The grand-average waveform elicited by the bimodal cardio-visual stimulus and the summed waveform elicited by the unimodal cardiac signals and visual stimulus. Permutation analysis indicated that the ERP amplitude elicited by the bimodal cardio-visual stimulus was larger than the summed ERP amplitude elicited by the unimodal cardiac signals and visual stimulus. This corresponded to a cluster extended from 90 to 136 ms after

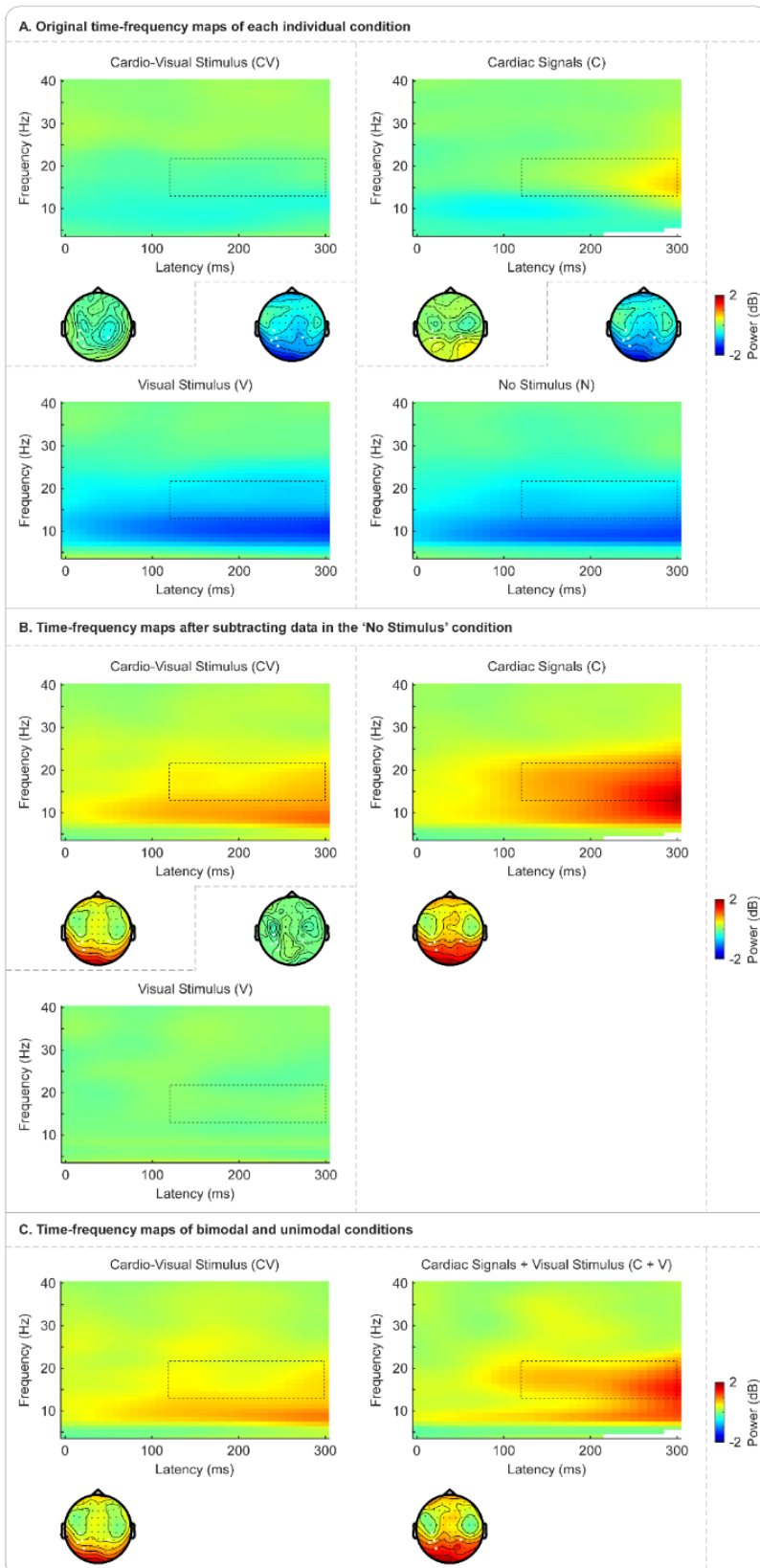
stimulus onset over posterior electrodes. Electrodes with high contribution to the cluster (i.e., with a total number of significant samples at or above the mean; CP5, P7, P5, PO7, and P4) are highlighted with enlarged white dots in the scalp topographies.



### Supplementary Figure 5.

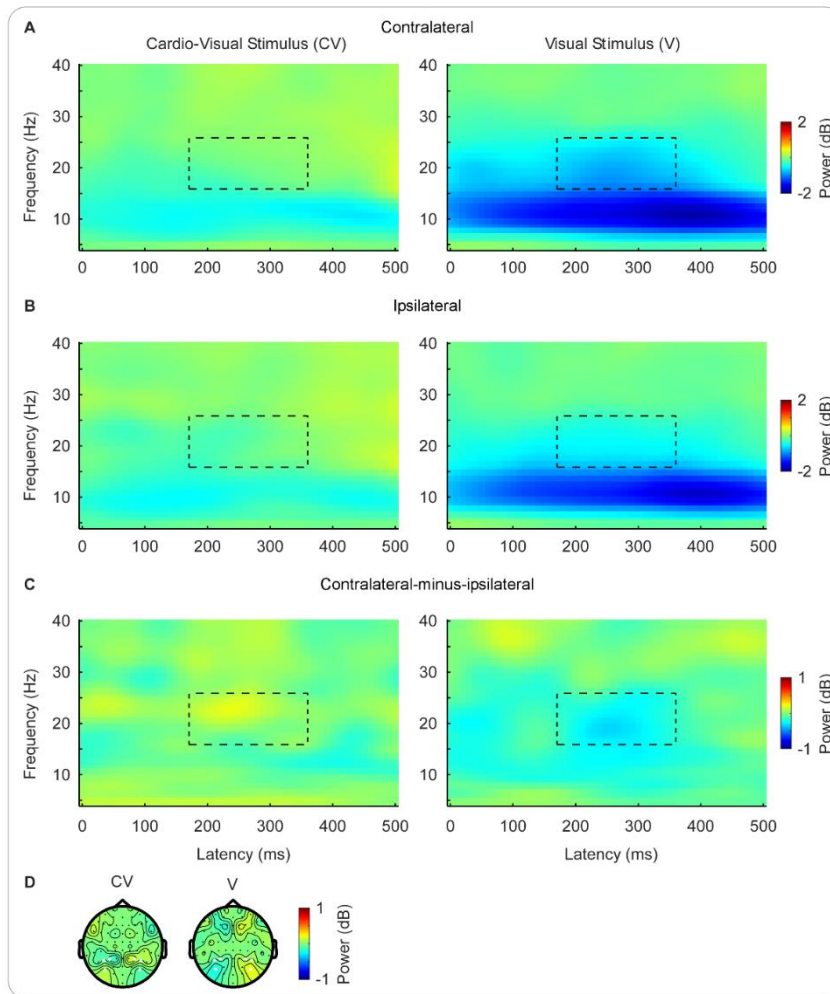
The effect of cardio-visual integration in lateralized N2pc components (after subtracting cardiac cycle-related EEG responses in the resting condition). Grand-average waveforms elicited contralateral and ipsilateral to the location of the bimodal cardio-visual stimulus (**A**) or the unimodal visual stimulus (**B**). (**C**) Grand-average contralateral-minus-ipsilateral difference waveforms elicited by the bimodal cardio-visual stimulus and by the unimodal visual stimulus, respectively. Permutation analysis indicated that compared to the unimodal visual stimulus, the bimodal cardio-visual stimulus elicited a lower N2pc amplitude. This corresponded to a cluster

extended from 220 to 250 ms after stimulus onset over lateral posterior electrodes. Electrodes with high contribution to the cluster (left hemisphere: P5, PO7, and P3; right hemisphere: P6, PO8, and P4) are highlighted with enlarged white dots in the scalp topographies in (**D**). The scalp topographies show amplitude differences at homologous electrodes over the hemisphere contralateral and ipsilateral to the target location, with electrodes on the midline artificially set to zero.



**Supplementary Figure 6.** Early cardio-visual integration in oscillatory power (after subtracting cardiac cycle-related EEG responses in the resting condition). **(A)** The

original grand-average time-frequency maps elicited by the bimodal cardio-visual stimulus, the unimodal cardiac signals, the unimodal visual stimulus, and the “no stimulus”, respectively. **(B)** The grand-average time-frequency maps elicited by the bimodal cardio-visual stimulus, the unimodal cardiac signals, and the unimodal visual stimulus after subtraction of the time-frequency map elicited by the “no stimulus”, respectively. **(C)** The grand-average time-frequency map elicited by the bimodal cardio-visual stimulus and the summed time-frequency map elicited by the unimodal cardiac signals and visual stimulus. All time-frequency maps were averaged over the posterior electrodes (CP5, P7, P5, PO7, and P4) to match the electrodes used in Supplementary Figure 4. These electrodes are highlighted with enlarged white dots in the scalp topographies. Permutation analysis indicated that the beta power elicited by the bimodal cardio-visual stimulus was lower than the summed beta power elicited by the unimodal cardiac signals and visual stimulus. This corresponded to a cluster extended from 120 to 300 ms after stimulus onset in frequencies from 13 to 22 Hz, marked using dashed rectangles in the time-frequency maps.



**Supplementary Figure 7.** The effect of cardio-visual integration in lateralized oscillation power (after subtracting cardiac cycle-related EEG responses in the resting condition). Grand-average time-frequency maps for oscillation power elicited contralateral (**A**) or ipsilateral (**B**)

to the target location. (**C**) Grand-average time-frequency maps for contralateral-minus-ipsilateral difference oscillation power. Time-frequency maps elicited by the bimodal cardio-visual stimulus (left panel) and the unimodal visual stimulus (right panel) were averaged over lateral posterior electrodes (left hemisphere: P5, PO7, and P3; right hemisphere: P6, PO8, and P4) respectively to match the electrodes used in Supplementary Figure 5. These electrodes are highlighted with enlarged white dots in the scalp topographies in (**D**). Permutation analysis indicated that compared to the bimodal visual stimulus, the bimodal cardio-visual stimulus elicited weaker beta-band lateralization. This corresponded to a cluster extended from 170 to 360 ms after stimulus onset in frequencies from 16 to 26 Hz, marked using dashed rectangles in the time-frequency maps. The scalp topographies show power differences at homologous electrodes over the hemisphere contralateral and ipsilateral to the target location, with electrodes on the midline artificially set to zero.

To investigate whether the behavioral effect (i.e., prolonged reaction times in the systole coupling condition compared to the diastole coupling condition) was related to the effects at the electrophysiological level, we conducted correlation analyses between the differences in reaction times and the differences in early ERP amplitude, in lateralized N2pc amplitude, in early upper-alpha/beta power, as well as in lateralized beta power across conditions, respectively. The correlation analyses were performed based on both uncorrected and corrected EEG data. We first used a Shapiro-Wilk Test to check the bivariate normality. If it was normally distributed, we ran a Pearson correlation analysis, otherwise a Spearman correlation analysis. We corrected  $p$ -values for multiple comparisons using a false discovery rate procedure (Benjamini & Hochberg, 1995).

The correlation analysis showed that the differences in reaction times between the systole coupling condition and the diastole coupling condition were positively correlated with the differences in lateralized N2pc amplitude between the bimodal cardio-visual stimulus condition and the unimodal visual stimulus condition (based on uncorrected EEG data:  $r = .43$ ,  $p = .031$ ,  $BF_{10} = 1.22$ ; based on corrected EEG data:  $r = .44$ ,  $p = .026$ ,  $BF_{10} = 1.11$ ). The lateralized N2pc component is known to be modulated by visuospatial selective attention (Bacigalupo & Luck, 2019; Bauer et al., 2012). Therefore, this correlation supports the interpretation that the inhibitory modulation of visual attention caused by the cardio-visual integration increased participants' search time for the visual target. However, this correlation did not survive the correction for multiple comparisons (based on uncorrected EEG data: corrected  $p = .124$ ; based on corrected EEG data: corrected  $p = .104$ ), and therefore any conclusion from this should be regarded with caution. In addition, there were no significant correlations between the differences in reaction times and the differences in early ERP amplitude, in early amplitude, as well as in lateralized beta power (all  $p > .05$ ; see **Supplementary Table 1**). The lack of significant correlations between these variables is most probably due to the limited sample size of our study, which underlines the need for further exploration based on a larger sample.

**Supplementary Table 1.** Correlations between the effect at the behavioral level and the effects at the electrophysiological level.

	Differences in early ERP amplitude	Differences in lateralized N2pc amplitude	Differences in early upper-alpha/beta power	Differences in lateralized beta power	
<i>Based on uncorrected EEG data</i>					
	<i>r</i>	.13	.43	.22	-.004
	<i>p</i>	.518	.031	.288	.984
	<b>corrected <i>p</i></b>	.691	.124	.576	.984
Differences in reaction times	<i>Based on corrected EEG data</i>				
	<i>r</i>	.27	.44	.03	.04
	<i>p</i>	.191	.026	.903	.855
	<b>corrected <i>p</i></b>	.382	.104	.903	.903

Corrected *p*: corrected *p*-values for multiple comparisons using a false discovery rate procedure.

## References:

- Bacigalupo, F., & Luck, S. J. (2019). Lateralized suppression of alpha-band EEG activity as a mechanism of target processing. *Journal of Neuroscience*, *39*(5), 900–917. doi:10.1523/JNEUROSCI.0183-18.2018
- Bauer, M., Kluge, C., Bach, D., Bradbury, D., Heinze, H. J., Dolan, R. J., & Driver, J. (2012). Cholinergic enhancement of visual attention and neural oscillations in the human brain. *Current Biology*, *22*(5), 397–402. doi:10.1016/j.cub.2012.01.022
- Benjamini, Y., & Hochberg, Y. (1995). Controlling the false discovery rate: a practical and powerful approach to multiple testing. *Journal of the Royal Statistical Society Series B (Statistical Methodology)*, *57*(1), 289–300. 752 doi:10.1111/j.2517-6161.1995.tb02031.x

## Data and Code Availability Statement

All data and code are publicly available via the Open Science Framework repository under the following link:

[https://osf.io/p7gs9/?view\\_only=b0abb6b59f62428e98ba0d32b356b459](https://osf.io/p7gs9/?view_only=b0abb6b59f62428e98ba0d32b356b459)

## **2.2 Study II: Listen to Your Heart: Attentional Trade-off Between Cardiac and Visual Domains**

### **Contributions:**

Qiaoyue Ren: Conceptualization, Methodology, Investigation, Data curation, Formal analysis, Visualization, Writing – original draft.

Amanda C. Marshall: Writing – review& editing.

Junhui Liu: Data curation, Writing – review& editing.

Simone Schütz-Bosbach: Conceptualization, Writing – review& editing, Supervision, Funding acquisition.



## **Listen to Your Heart: Attentional Trade-Off between Cardiac and Visual Domains**

Qiaoyue Ren<sup>1</sup>, Amanda C. Marshall<sup>1</sup>, Junhui Liu<sup>1</sup>, Simone Schütz-Bosbach<sup>1\*</sup>

<sup>1</sup>General and Experimental Psychology Unit, Department of Psychology, LMU Munich, 80802 Munich, Germany

### **\* Corresponding author:**

Simone Schütz-Bosbach

Department of Psychology, LMU Munich, Leopoldstr. 13, 80802 Munich, Germany

Email: S.Schuetz-Bosbach@psy.lmu.de

**Running title:** Cardiac Arousal Redirects Attention

**Author contributions:** Q.R. designed and performed the experiment, analyzed the data and wrote the paper. A.M. edited the paper. J.L. helped performed the experiment and edited the paper. S-S.B. supervised the project and edited the paper.

**Acknowledgments:** This work was supported by Deutsche Forschungsgemeinschaft [SCHU 24716-1 to S.S-B.] and China Scholarship Council. We thank Yannick Janvier for his assistance in data collection.

**The authors declare no competing financial interests.**

### **Data accessibility**

The data generated in this study have been deposited in the OSF database under the link: [https://osf.io/xkpvu/?view\\_only=fd28e7cea8f04b4dad5d9b0c5d7fd753](https://osf.io/xkpvu/?view_only=fd28e7cea8f04b4dad5d9b0c5d7fd753).

## **Abstract**

Internal bodily signals, such as heartbeats, can influence conscious perception of external sensory information. Spontaneous shifts of attention between interoception and exteroception have been proposed as the underlying mechanism, but direct evidence is lacking. Here, we used steady-state visual evoked potential (SSVEP) frequency tagging to independently measure the neural processing of visual stimuli that were concurrently presented but varied in heartbeat coupling. Although heartbeat coupling was irrelevant to participants' task of detecting brief color changes, we found decreased SSVEP power for systole-coupled stimuli and increased SSVEP phase synchronization for diastole-coupled stimuli, compared to non-coupled stimuli. Furthermore, the coupling of visual stimuli to the systole led to a larger heartbeat evoked potential (HEP) but a smaller N2 component evoked by the color change. The increase in HEP amplitude was related to the decrease in N2 amplitude. These findings suggest that cardiac arousal automatically redirects attention from external to internal domains. Our study highlights the dynamic reallocation of limited processing resources between interoception and exteroception across the cardiac cycle.

## **Keywords**

Cardiac signals, Cardiac systole, Cardiac diastole, EEG, Heartbeat-evoked potential, Steady-state visual evoked potential

### **Significance Statement**

Our brain continuously processes signals from both our body and the surrounding environment. The ability to flexibly allocate attention to internal and external cues is crucial for adaptive cognitive functioning. We use a novel paradigm to detect spontaneous shifts of attention along the internal-external axis throughout the cardiac cycle. Results show that visual stimuli coinciding with strong cardiac signals receive less attention compared to concurrently presented stimuli coinciding with weaker cardiac signals. Additionally, the cardiac-visual coupling directs more attention to internal cardiac signals, leading to reduced sensitivity to external visual targets. These findings shed light on the dynamic interplay between physiological processes and attentional allocation, suggesting that our attentional focus naturally adjusts in response to internal bodily signals.

## 1 Introduction

Our brain receives signals from both the external environment and inside our body. Internal bodily processes can impact our processing of external information (Tallon-Baudry, 2023). For instance, the timing of external stimuli with respect to the cardiac cycle can affect their perception, with reduced perceptual sensitivity and neural responses most often observed during systole compared to diastole (van Elk et al., 2014; Al et al., 2020, 2021; Grund et al., 2022; Ren et al., 2022a; but see Garfinkel et al., 2014).

This phenomenon has been explained by an attentional trade-off framework (e.g., Al et al., 2020; Ren et al., 2022a). It posits that attentional resources are shared between exteroceptive and interoceptive processing, with some attention being automatically redirected from the exteroceptive to interoceptive domain in the face of internal bodily signals like heartbeats. Within a cardiac cycle, cardiac signals are strongly presented during systole but relatively weak during diastole (Skora et al., 2022). Therefore, attentional demands from the cardiac system are higher during systole, leading to reduced attentional resources for exteroceptive processing. This results in attenuated perception of external stimuli during systole compared to diastole.

So far, direct evidence on the spontaneous shifts of attention between interoception and exteroception is still lacking. Here, we employed a dynamic visual detection task with simultaneous electrocardiogram (ECG) and electroencephalogram (EEG) recordings. Critically, participants' real-time heartbeats were used to control the direction change of two groups of moving dots on a screen. One group changed direction randomly within each cardiac cycle, while the other group changed direction either during strong (at systole) or weak cardiac signals (at diastole). Participants' task was to detect a brief color change within one group of dots. In other words, the coupling between the dots' movements and the participants' heartbeats was irrelevant to their task goal. This allows us to explore the *spontaneous* shifts of attention along the internal-external axis, which complements earlier studies focusing on *intentional* shifts between interoception and exteroception (Villena-González et al., 2017; Petzschner et al., 2019; Kritzman et al., 2022).

We used frequency tagging to measure the distinct steady-state visual evoked potentials (SSVEP) for each group of dots, which were presented concurrently but differed in heartbeat coupling. SSVEPs are continuous neurophysiological responses elicited by a visual stimulus with periodic luminance or contrast modulation, producing oscillatory activity at the driving frequency as well as its higher harmonics (Norcia et al., 2015). This technique allows us to independently quantify selective attention to multiple stimuli, even when presented concurrently and overlapping spatially (Müller et al., 2006). By using this approach, we can directly compare and provide stronger evidence compared to previous studies that examined responses to heartbeat-coupled versus non-coupled stimuli separately in different trials (Salomon et al., 2016; Ronchi et al., 2017).

We also quantified the heartbeat evoked potential (HEP) and the visual evoked potential (VEP) evoked by the color change. These measures enable us to explore the mechanisms associated with attentional shifts between exteroception and interoception. The HEP reflects cardiac processing in the brain (Park et al., 2018; Coll et al., 2021) and has been shown to be modulated by attention directed towards cardiac signals (Petzschner et al., 2019; Kritzman et al., 2022). For the VEP evoked by the color change, we specifically focused on the N2 component, which is widely believed to reflect visual awareness (Koivisto and Grassini, 2016; Eiserbeck et al., 2022).

According to the attentional trade-off theory, we hypothesized that systole-coupled visual stimuli would receive less attention (lower SSVEP responses), while diastole-coupled visual stimuli would receive more attention (larger SSVEP responses), compared to concurrently-presented, non-coupled visual stimuli. Furthermore, coupling visual stimuli with systole would direct more attention to internal cardiac signals (increased HEP amplitude), leading to a decreased sensitivity to external visual stimuli (decreased N2 amplitude), compared to coupling with diastole or no heartbeat coupling. Additionally, the increase in HEP amplitude was expected to be associated with the decrease in N2 amplitude.

## **2 Materials and Methods**

### **2.1 Participants**

Thirty-two participants (20 females; age:  $25.69 \pm 6.28$  years [mean  $\pm$  SD], range: 19–44 years) were recruited from the university participant database. To the best of our knowledge, no previous studies had explored the cardiac cycle effect on SSVEPs in a similar task. Therefore, we could not compute the required sample size a priori. However, our sample size is comparable with relevant previous studies (Gjorgieva et al., 2022; Kritzman et al., 2022; Ren et al., 2022a). Furthermore, a post-hoc power analysis, conducted using the MorePower software (Campbell and Thompson, 2012), indicates that our sample size is sufficient for detecting effects with an  $\eta_p^2$  of 0.14 in a one-way (3 levels) repeated measures ANOVA, as well as effects with an  $\eta_p^2$  of 0.21 in a three-way ( $2 \times 2 \times 2$ ) repeated measures ANOVA, both with a power of 0.80 and  $\alpha$  of 0.05. All the participants reported normal or corrected-to-normal visual acuity, no color blindness, no diagnosed heart-rhythm abnormalities, no present or past psychiatric or neurological disorders, and no current use of medication. The study was approved by the local ethics committee at the Department of Psychology of LMU Munich in accordance with the Declaration of Helsinki. All participants provided written informed consent and received either financial compensation (9 euros per hour) or course credit for their participation.

## 2.2 Experimental design

The study employed a dynamic visual detection task, in which a display of two groups of moving dots changed their direction of motion dynamically. Participants were required to detect a brief color change of one group of dots' frame. To investigate the effect of cardiac signals on visual processing, the experiment contained three different trial types (see **Figure 1A**). In the “systole-coupled vs non-coupled” trials, the direction change of one group of dots was designed to always occur at 290 ms after the R-peak, to coincide with the end of ventricular systole, i.e., when cardiac arousal signals were relatively strong (Rae et al., 2018; Marshall et al., 2022; Ren et al., 2022b), while the direction change of the other group of dots occurred at a random time within 0–600 ms after the R-peak, to be out of sync with cardiac cycle. This condition was designed to compare the SSVEPs of the systole-coupled versus non-coupled motion. In the “diastole-coupled vs non-coupled” trials, the direction change of one group of dots was designed to always occur at the R-peak, to coincide with the end of ventricular diastole,

i.e., when cardiac arousal signals were relatively low (DeSaix et al., 2013; Garfinkel et al., 2014; Ren et al., 2022a), while the direction change of the other group of dots occurred at a random time within 0–600 ms after the R-peak. This condition was designed to compare the SSVEPs of the diastole-coupled versus non-coupled motion. Finally, in the “non-coupled vs non-coupled” trials, the direction changes of both groups of dots occurred at random times within 0–600 ms after the R-peak, which served as the control condition.

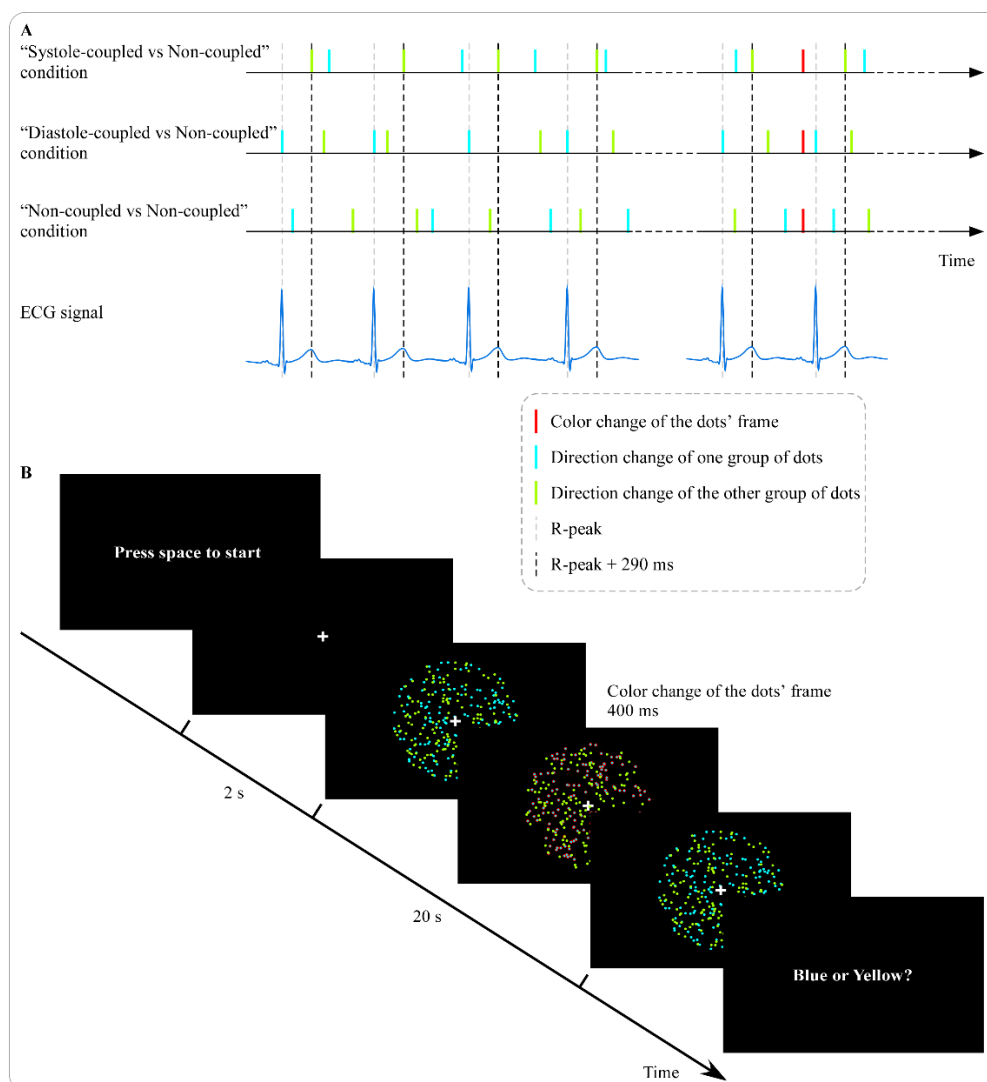


**Figure 1. The dynamic visual detection task.** (A) Experimental conditions. In the “systole-coupled vs non-coupled” condition, the direction change of one group of dots always occurred at 290 ms after the R-peak (i.e., when cardiac signals were strong), while the direction change of the other group of dots occurred at a random time within

0–600 ms after the R-peak (i.e., out of sync with cardiac cycle). In the “diastole-coupled vs non-coupled” condition, the direction change of one group of dots always occurred at the R-peak (i.e., when cardiac signals were low), while the direction change of the other group of dots occurred at a random time within 0–600 ms after the R-peak. In the “non-coupled vs non-coupled” condition, the direction changes of both groups of dots occurred at random times within 0–600 ms after the R-peak. **(B)** Timeline of each trial. Participants pressed the space key to start the trial, and observed two groups of random dots that differed in color (blue or yellow), direction of motion, and flickering frequency (7.5 or 10 Hz). They then reported the color of the dots whose frame briefly flashed to red during the trial.

### 2.3 Stimuli and procedure

Participants were seated in a dimly lit room at 70 cm from a monitor (24 inches; refresh rate: 60 Hz; resolution:  $1920 \times 1080$  pixels) with their heads on a chin rest. The visual displays were generated and displayed using the Presentation software (Neurobehavioral Systems, Inc.).

Each visual display consisted of 300 blue (luminance:  $203 \text{ cd/m}^2$ ) and yellow ( $203 \text{ cd/m}^2$ ) dots (150 of each; diameter:  $0.23^\circ$  of visual angle). These dots were randomly distributed within an invisible circle (radius:  $5.00^\circ$ ) at the center of the screen that was marked with a white ( $245 \text{ cd/m}^2$ ) fixation cross. The background was black ( $0.3 \text{ cd/m}^2$ ). The order of drawing the dots was randomized, to prevent the perception of depth. All dots were continuously in motion throughout the trial, with a velocity of  $0.08^\circ$ . Dots that moved out of the invisible circle immediately disappeared but reappeared on the opposite side of the circle. Specifically, their location shifted from  $[x, y]$  to  $[-x, -y]$ , given that the center of the screen was located at  $[0, 0]$ . Therefore, participants always saw 300 dots. The motion of the dots with the same color was the same, but differed from the dots of the other color. Participants were therefore able to perceive two distinct groups of moving dots using color and coherent movements. The two groups of dots changed their direction of motion dynamically (deviated randomly by plus  $60\text{--}300^\circ$  from the original direction) while keeping the directions different at any time (the absolute difference between the two motion directions was always greater than  $60^\circ$ ).

The two groups of dots flickered at different frequencies, either 7.5 or 10 Hz (Wen et al., 2018). The on/off duty cycles were 50/50 for both frequencies. While in motion, the two groups of dots might partially and briefly overlap, but their visibility was maintained due to their flickering at different frequencies. In short, the two groups of dots differed in color, direction of motion, and flickering frequency.

The timeline of the experimental trial is depicted in **Figure 1B**. Participants pressed the space key on the keyboard to start the trial when they felt ready, and waited for the visual stimuli to appear. After 2 s, a dynamic visual display appeared, lasting for 20 s. Participants were instructed to pay equal attention to both groups of dots, and to detect a brief (400 ms) red flashing frame (frame width:  $0.02^\circ$ ; luminance:  $60 \text{ cd/m}^2$ ) on one group of dots. The red frame flickered at the same frequency as the dots. The color change of the dots' frame and the experience of having already detected it (successfully finding the target) can potentially influence participants' attention towards the dots during the remaining time of the trial, which may interfere with the anticipated effect of heartbeat coupling on SSVEPs. Therefore, in a majority of trials, the color change was designed to appear at the end of each trial ( $> 15$  s after display onset), and the data of the last 5 s in these trials were excluded for SSVEP analysis (see **Section 2.5.3.1**). In addition, if the color change always appeared at the end of each trial, participants might have become aware of this pattern at the cost of paying full attention at the very beginning of each trial. Therefore, we also added few trials presenting the color change early ( $< 15$  s after display onset), while these trials were excluded for SSVEP analysis. Specifically, the color change occurred between 5 and 10 s after display onset with a probability of 1/12, between 10 and 15 s with a probability of 1/12, between 15 and 17 s with a probability of 5/12, and between 17 and 19 s with a probability of 5/12. Participants were instructed to continue observing the visual display until it disappeared from the screen, even after having seen the color change. Participants then pressed either the "F" key for blue dots or the "J" key for yellow dots to indicate which group of dots' frame briefly flashed to red during the trial. They were not given any feedback about their response. After their response, a blank screen was displayed on the screen for 1.5 s, followed by the start screen of the next trial. Participants were instructed to keep their gaze fixed on the central cross throughout the trial and to avoid intentionally

focusing on a specific or partial area of the moving dots or actively shifting their gaze between different parts of the visual stimuli.

To get familiar with the experimental procedure, participants completed a practice session consisting of three trials (one trial for each trial type in a random order), with accuracy feedback provided. The experiment comprised 5 blocks, with 24 trials per block. Each block included 10 “systole-coupled vs non-coupled” trials, 10 “diastole-coupled vs non-coupled” trials, and 4 “non-coupled vs non-coupled” trials, presented in a random order. Participants took self-paced breaks between blocks. Additionally, a resting block (duration: 2.5 min) was conducted before the visual detection task, during which participants were asked to focus on the centrally presented fixation cross with no other visual stimuli. The study lasted approximately 1 hour, preceded by about 1 hour of preparation.

## **2.4 Data acquisition**

For EEG recording, we used 65 active electrodes (BrainProducts ActiSnap) and one additional ground electrode positioned following the international 10-20 system. The FCz functioned as the online reference for these scalp electrodes. For ECG recording, we used 3 electrodes placed below the left clavicle (reference electrode), the right clavicle (ground electrode), and the left pectoral muscle (active electrode). All electrophysiological signals were recorded with a 1000-Hz sampling rate and a 0.1–1000 Hz online bandpass filter. All impedances were kept below 20 k $\Omega$ . The BrainVision Recorder software (Brain Products, Inc.) was used for signal acquisition and amplification. The BrainVision RecView software (Brain Products, Inc.) was employed to achieve online detection of ECG R-peaks. R-peaks were identified as the first sample of decreasing voltage after surpassing a predetermined threshold. The threshold for detecting R-peaks was individually set by the experimenter after visually examining the 2.5-minute ECG signal during the resting block. Each time an R-peak was detected, a pulse was sent to the experimental PC.

## **2.5 Data quantification**

### 2.5.1 EEG and ECG pre-processing

EEG pre-processing was performed using the FieldTrip toolbox (Oostenveld et al., 2011) in Matlab (Mathworks Inc., Natick, MA; version R2019b). The EEG data were re-referenced to the average of the left and right-mastoids, filtered using a 60-Hz low-pass filter, and segmented into epochs ranging from -2 to 20 s relative to the onset of the visual display. No bad electrodes were found during the analysis. Independent component analysis was employed to identify and remove components caused by eye blinks or other artifacts that were clearly unrelated to neural activity. On average,  $2.22 \pm 1.04$  components per participant were removed, and artifact-free EEG data were obtained by back-projecting the remaining components onto the scalp electrodes.

### 2.5.2 Stimulus timing and heartbeat coupling

A post hoc analysis was performed to check the precision of the R-peak detection and the intervals between the R-peaks and the direction changes of the dots throughout the experiment. Specifically, we used *findpeaks* function in Matlab to identify the timings of the R-peaks in the offline ECG data in each trial, and then compared them with the timings of the direction changes of each group of dots. Trials with imprecise R-peak detection (hit rate  $< 0.80$  or false alarm rate  $> 0.20$ ;  $4.75 \pm 7.40$  trials per participant) were excluded in further analysis as the experimental manipulation (coupling the direction changes of the dots with heartbeats) could not be effective. In the remaining trials, the R-peaks in real-time ECG signal were detected with high precision (hit rate:  $0.99 \pm 0.02$ ; missing rate:  $0.01 \pm 0.02$ ; false alarm rate:  $0.02 \pm 0.02$ ). Moreover, the direction changes of the coupled dots were time-locked to R-peaks (diastole-coupled dots:  $120.64 \pm 28.12$  ms after R-peaks) or 290 ms after R-peaks (systole-coupled dots:  $405.98 \pm 24.84$  ms after R-peaks) accordingly in close temporal proximity. In contrast, the direction changes of the non-coupled dots were out of sync with any cardiac phase ( $396.87 \pm 170.54$  ms after R-peaks).

### 2.5.3 SSVEP pre-processing and analysis

#### 2.5.3.1 SSVEP pre-processing

The EEG data segments were first filtered using a 1-Hz high-pass filter to remove slow drifts. Subsequently, the filtered data were down-sampled to 900 Hz, which is a common multiple of both stimulation frequencies, to ensure that the data segments contained full cycles of SSVEP at integer numbers of sample points (Figueira et al., 2022). The data segment of each trial was then baseline corrected using the period ranging from -1.5 to 0 s relative to the display onset. Trials containing large artifacts were discarded ( $3.03 \pm 5.72$  trials per participant) based on a threshold of  $\pm 200 \mu\text{V}$  in EEG channels. The number of remaining trials per participant did not differ significantly across conditions ( $F_{4,124} = 1.60$ ,  $p = .202$ ,  $\eta_p^2 = .05$ ; see **Supplementary Table 1**). To attenuate the influence of display onset-evoked activity on EEG spectral decomposition, the initial 1 s of stimulation was excluded for further analysis (Müller et al., 2006; Keitel et al., 2019). In addition, to exclude the influence of color change-evoked responses and potential attentional adjustment after the detection of color change, the last 5 s of stimulation was also discarded (as mentioned in **section 2.3**). In other words, the time of interest (TOI) for analysis was from 1 to 15 s after display onset, with a TOI of 14 s ensuring that each TOI contained full cycles of SSVEP (7.5 Hz: 105 cycles; 10 Hz: 140 cycles).

#### 2.5.3.2 SSVEP quantification

The Fourier components of the stimulus frequency (either 7.5 or 10 Hz), which represent the stimulus-locked oscillations, were extracted using the FreqTag toolbox (Figueira et al., 2022) in Matlab. Specifically, a window containing ten cycles of SSVEP (1333.33 or 1000 ms, i.e., 1200 or 900 time points, for 7.5 and 10 Hz, respectively) was shifted across each segment in steps of one cycle (133.33 or 100 ms, i.e., 120 or 90 time points), and the potential within the shifting windows was averaged in the time domain. This resulted in a single segment containing ten cycles of SSVEP, which was then transformed into the frequency domain using the Fast Fourier Transform (FFT). The sliding window approach was adopted to enhance the signal-to-

noise ratio of SSVEP (Figueira et al., 2022). To avoid unexpected interaction between 7.5-Hz and 10-Hz signal, ten cycles of the stimulation frequency were contained in sliding windows, resulting in a frequency resolution of 0.75 Hz for 7.5-Hz stimuli and 1 Hz for 10-Hz stimuli.

We focused on both the power and the phase synchronization of the SSVEP response at the driving frequency. The power refers to the amplitude of the SSVEP response, while the phase synchronization provides an amplitude-independent measure of the degree to which stimulus-evoked EEG responses are phase-locked to stimulus dynamics (Kim et al., 2007; Eidelman-Rothman et al., 2019). Many studies have found that compared with unattended stimuli, attended stimuli result in higher SSVEP power (Müller et al., 1998; Kim et al., 2007; Andersen et al., 2011) as well as higher phase synchronization (Ding et al., 2006; Kashiwase et al., 2012).

**Power analysis.** The signal-to-noise ratio (SNR) was computed to enhance the comparability between stimulation frequencies (Mora-Cortes et al., 2018; Wen et al., 2018), taking into account differences in background (induced) activity. Specifically, we extracted the power in the stimulation frequency and divided it by the average power of neighboring frequencies ( $\pm 0.75$  or  $\pm 1$  Hz for 7.5 and 10 Hz, respectively). The resulting SNR value was then log-transformed to produce SNR in dB. Next, we averaged the SNR values across trials in each condition for each participant.

**Phase stability analysis.** Single-trial phase stability was calculated to evaluate the temporal synchronization of the SSVEP response with the stimulus dynamics (Wieser et al., 2016; Ji et al., 2018; Keitel et al., 2019; Kritzman et al., 2022). Specifically, we computed the FFT of the signal for each window in the aforementioned sliding window procedure and then used it to calculate phase stability across windows for each trial. The resulting phase stability value ranges from 0 (indicating high phase variability and thus low phase stability between windows) to 1 (indicating complete phase stability between windows). Next, we averaged the single-trial phase stability values across trials in each condition for each participant.

Finally, SNR and phase stability were averaged across conditions and participants, and the electrode with the maximal value of each measure (Oz) was chosen for further analysis. This electrode has been commonly used to quantify SSVEP in previous studies (Kastner-Dorn et al., 2018; Panitz et al., 2023), which is consistent with the functional localization of visual processing in the occipital area (Luck and Gaspelin, 2017).

## **2.5.4 HEP pre-processing and analysis**

### **2.5.4.1 HEP pre-processing**

The EEG data segments were first filtered using a 30-Hz low-pass filter to remove high-frequency noises. Subsequently, the EEG signal within TOI of each trial (1 – 15 s relative to display onset) was segmented into HEP epochs from -100 to 600 ms relative to the R-peak. The end point of epoch window was chosen to eliminate possible contamination by subsequent R-peaks. Furthermore, R-peaks for which the subsequent R-peak appeared within 650 ms were discarded to avoid the early components of the cardiac field artifact of the next heartbeat (Petzschner et al., 2019; Kritzman et al., 2022). Notably, to exclude artefactual biases from preceding heartbeats, we did not perform baseline correction on these epochs (Petzschner et al., 2019). It is highly likely that any selected time window before the R-peak, which is usually utilized for baseline correction, would be confounded by cardiac field artifact such as those from P and Q waves preceding the R-peak. Additionally, in periods of high heart rates (small R-to-R intervals), the time window before the R-peak could also potentially overlap with the late components of the HEP, which have been reported to persist for up to 595 ms after the R-peak (Schulz et al., 2013, 2015). Moreover, to exclude potential confounding effects resulting from differential overlap between the direction change-evoked responses and the HEP under different conditions, we removed the direction change-evoked responses from the HEP epochs. More specifically, in the 'diastole-coupled vs non-coupled' condition, the HEP epochs included not only neural responses evoked by heartbeats but also those evoked by the direction change of the diastole-coupled dots, as the direction change of the diastole-coupled dots was also time-locked to the R-peak. However, in the 'systole-coupled vs non-coupled' condition, the direction change of the systole-coupled dots was time-locked to 290 ms after each R-peak, thus mainly

contaminating the late part of the HEP. To remove these confounding responses, we extracted the direction change-evoked responses in the 'non-coupled vs non-coupled' condition, and then subtracted these responses from each HEP epoch in the other two conditions according to the actual interval between the R-peak and the direction change of the diastole-/systole-coupled dots (see **Supplementary Analysis** for further details). Lastly, epochs containing large artifacts were excluded based on a threshold of  $\pm 100$   $\mu\text{V}$  in EEG channels. The HEP in each trial was calculated by averaging across all epochs of that trial. Notably, trials in which over 50% of HEP epochs were excluded due to high heart rates (R-to-R interval  $< 650$  ms) or excessive noise were discarded ( $2.87 \pm 6.63$  trials per participant). This resulted in the exclusion of two participants from further HEP analysis due to an insufficient number of remaining trials ( $< 10$  trials in one condition), leaving 30 datasets for analysis. The number of remaining trials per participant did not differ significantly across conditions ( $F_{4,116} = 0.27$ ,  $p = .833$ ,  $\eta_p^2 = .01$ ; see **Supplementary Table 1**).

#### **2.5.4.2 HEP quantification**

We used a nonparametric cluster-based permutation test in the FieldTrip toolbox (Oostenveld et al., 2011) to determine the HEP morphology and time windows of interest. This type of analysis allows for statistical tests over entire time series while still controlling for multiple comparisons (Maris and Oostenveld, 2007). Specifically, we submitted EEG data in the time window from 300 to 600 ms relative to the R-peak and over all electrodes to a repeated-measures permutation  $F$ -test. This specific time window was chosen to prevent the analysis of potential cardiac field artifact (Kritzman et al., 2022). Adjacent spatio-temporal electrodes with  $F$ -values exceeding a threshold were clustered (cluster-defining threshold  $p = .05$ ; iterations = 5000). Then, the cluster-level statistics were calculated by taking the sum of the  $F$ -values of all points within each cluster. Last, the observed cluster-level statistic was compared against the permutation distribution to test the null hypothesis of no difference between conditions (two-tailed test). Clusters with  $p < .05$  were considered significant. Finally, the mean HEP amplitude per condition and participant was calculated over the cluster that revealed a significant effect of Trial Type (“systole-coupled vs non-coupled,” “diastole-coupled vs non-coupled,” and “non-coupled vs non-coupled”) in the permutation test

for further analysis. Additionally, we extracted the HEP amplitude during the 2.5-minute resting-state condition from the same cluster and compared it with the HEP amplitude during the task (across all task trials). We found no significant difference between the two conditions, which suggests comparable cardiac processing during both the task and the resting state in the present study (see **Supplementary Analysis** for further details).

#### **2.5.4.3 Control analysis to exclude possible effects of cardiovascular artifacts**

Cardiac cycle-related EEG responses (as measured by HEP in the present study) comprise not only neural responses evoked by cardiac signals but also cardiac field artifact and pulse-related artifact (Kern et al., 2013). Any potential effects of cardiac cycle-related artifacts on our results should thus be carefully considered. To ensure that the observed effect in HEP amplitude was not a result of cardiac cycle-related artifacts, we conducted a control analysis by comparing the mean ECG amplitudes within the time window (480–540 ms after the R peak) of the observed effect. This approach has been recommended and utilized in recent studies (Petzschner et al., 2019; Kritzman et al., 2022).

Another approach used in prior studies to remove cardiac field artifact is independent component analysis. However, this approach has received criticism for its limited ability to fully eliminate the cardiac field artifact and the potential risk of removing task-related signals (Petzschner et al., 2019). For transparency, we analyzed the HEP data after applying this correction approach (see **Supplementary Analysis**). Importantly, the effects observed in the corrected HEP data were consistent with the effects observed in the uncorrected HEP data.

#### **2.5.5 VEP pre-processing and analysis**

The EEG signal in each trial was segmented into an epoch from -100 to 600 ms relative to the onset of color change. Epochs were baseline corrected using the period from -100 to 0 ms prior to the onset of color change, and those containing large artifacts were discarded ( $1.53 \pm 2.27$  trials per participant) based on a threshold of  $\pm 100 \mu\text{V}$  in EEG channels. No participants were excluded due to insufficient number of remaining trials

(> 10 trials in any condition). Furthermore, the number of remaining trials per participant did not differ significantly across conditions ( $F_{4,124} = 0.63$ ,  $p = .584$ ,  $\eta_p^2 = .02$ ; see **Supplementary Table 1**). On the basis of earlier related research (Koivisto and Grassini, 2016; Eiserbeck et al., 2022) and inspection of the grand-averaged waveform, we extracted the peak amplitude of N2 per condition and participant within 200–300 ms after the onset of color change and at electrode Oz for further analysis.

### **2.5.6 Relationship between HEP and VEP**

The relationship between changes in HEP and VEP across conditions was evaluated using the Correspondence-tradeoff index (CTI; Boylan et al., 2019; Kritzman et al., 2022). For each participant, we calculated the difference in HEP and VEP between any two of the three conditions ("systole-coupled vs. non-coupled", "diastole-coupled vs. non-coupled", and "non-coupled vs. non-coupled"), resulting in a single difference value for each measure. We then multiplied the difference value in HEP by the difference value in VEP, yielding one CTI between "systole-coupled vs. non-coupled" and "diastole-coupled vs. non-coupled" conditions, one CTI between "systole-coupled vs. non-coupled" and "non-coupled vs. non-coupled" conditions, and one CTI between "diastole-coupled vs. non-coupled" and "non-coupled vs. non-coupled" conditions. The CTI reflects the relationship between the two measures and is negative when an increase in HEP corresponds to a decrease in VEP, and vice versa, and positive when both measures increase or decrease together.

## **2.6 Statistical analysis**

**Detection accuracy.** Behavioral performance was evaluated by the accuracy of detecting the color change. To explore differences across trial types, we conducted a one-way repeated-measures ANOVA (Trial Type: "systole-coupled vs non-coupled", "diastole-coupled vs non-coupled", and "non-coupled vs non-coupled") on the detection accuracy. Post hoc pairwise comparisons were conducted, and Holm correction was applied for multiple comparisons when there was a significant effect of Trial Type. Additionally, we conducted separate paired samples *t*-tests between the target dots (the group of dots that changed color) that were coupled with the cardiac

cycle and those that were not coupled with the cardiac cycle. These tests were performed separately for "systole-coupled vs. non-coupled" trials and "diastole-coupled vs. non-coupled" trials.

**SSVEP.** We conducted separate three-way repeated-measures ANOVAs to explore the effects of Trial Type ("systole-coupled vs non-coupled" or "diastole-coupled vs non-coupled"), Heartbeat Coupling (coupled or non-coupled), and Flicker Frequency (7.5 or 10 Hz) on the power and the phase stability of the SSVEP response. The justification for including these three factors in the analysis is explained in detail in **section 3.2**. To investigate the difference in SSVEP triggered by coupled versus non-coupled dots, we also performed planned pairwise comparisons between the two levels of Heartbeat Coupling for each Trial Type. Specifically, we compared the SSVEP triggered by systole-coupled and non-coupled dots in the "systole-coupled vs non-coupled" trials, and compared the SSVEP triggered by diastole-coupled and non-coupled dots in the "diastole-coupled vs non-coupled" trials.

**HEP and VEP.** We conducted separate one-way repeated-measures ANOVA (Trial Type: "systole-coupled vs non-coupled", "diastole-coupled vs non-coupled", and "non-coupled vs non-coupled") on HEP amplitude and the N2 amplitude evoked by the color change. Post hoc pairwise comparisons were conducted, and Holm correction was applied for multiple comparisons when there was a significant effect of Trial Type. For the N2 amplitude, we also conducted separate paired samples *t*-tests between the target dots (the group of dots that changed color) that were coupled with the cardiac cycle and those that were not coupled with the cardiac cycle. These tests were performed separately for "systole-coupled vs. non-coupled" trials and "diastole-coupled vs. non-coupled" trials.

**The CTI between HEP and VEP.** To test the significance of the CTI, we conducted separate one-sample *t*-tests on the CTI values between "systole-coupled vs. non-coupled" and "diastole-coupled vs. non-coupled" conditions, the CTI values between "systole-coupled vs. non-coupled" and "non-coupled vs. non-coupled" conditions, and the CTI values between "diastole-coupled vs. non-coupled" and "non-coupled vs. non-coupled" conditions.

All statistical analyses were performed using the JASP software (JASP Team, 2023). Partial eta-squared ( $\eta_p^2$ ) was calculated as the effect size for  $F$ -tests, and Cohen's  $d$  was calculated as the effect size for  $t$ -tests. The Greenhouse-Geisser correction was applied in case of violations of the sphericity assumption. For the sake of brevity, the uncorrected degrees of freedom were reported.

### 3 Results

#### 3.1 Detection accuracy

In the “systole-coupled vs non-coupled” trials, when the direction changes of the target dots (the group of dots that changed color) were coupled with cardiac systole and when they were not coupled with any phase of the cardiac cycle, the accuracy of detecting the color change was  $0.98 \pm 0.05$  and  $0.98 \pm 0.05$ , respectively. In the “diastole-coupled vs non-coupled” trials, when the direction changes of the target dots were coupled with cardiac diastole and when they were not coupled with the cardiac cycle, the detection accuracy was  $0.98 \pm 0.05$  and  $0.98 \pm 0.04$ , respectively. In the “non-coupled vs non-coupled” trials, the detection accuracy was  $0.97 \pm 0.07$ .

To compare the detection accuracy among trial types, we conducted a one-way repeated-measures ANOVA (Trial Type: “systole-coupled vs non-coupled”, “diastole-coupled vs non-coupled”, and “non-coupled vs non-coupled”). The analysis showed no significant difference in detection accuracy among trial types ( $F_{2,62} = 1.10$ ,  $p = .339$ ,  $\eta_p^2 = .03$ ).

Additionally, to compare the detection accuracy between the target dots that were coupled with the cardiac cycle and those that were not coupled with the cardiac cycle, we conducted separate paired samples  $t$ -tests for the "systole-coupled vs non-coupled" trials and the "diastole-coupled vs non-coupled" trials. The analyses did not show any significant effects in the "systole-coupled vs non-coupled" trials ( $t_{31} = -0.14$ ,  $p = .887$ , Cohen's  $d = -0.03$ ) and "diastole-coupled vs non-coupled" trials ( $t_{31} = 0.57$ ,  $p = .576$ , Cohen's  $d = 0.10$ ). That is, the coupling status of the target dots with the cardiac cycle did not have a significant impact on participants' accuracy in detecting their color

change. This is likely attributed to the ceiling effect in detection accuracy resulting from the relatively long duration of the color change (400 ms).

### **3.2 SSVEP measures**

EEG signals have varying background activities across frequencies, and different peak amplitudes of SSVEP have been observed for the same stimuli presented at different frequencies (Srinivasan et al., 2006; Wen et al., 2018). Therefore, we compared the SSVEP of the same frequency between different trials in which the frequency was coupled versus non-coupled with the cardiac cycle. We divided each trial type into two subtypes. In one subtype, the 7.5-Hz dots were coupled with the cardiac cycle (systole or diastole) while the 10-Hz dots were not coupled with the cardiac cycle. In the other subtype, this was reversed. Therefore, our analysis had three independent factors: Trial Type (“systole-coupled vs non-coupled” or “diastole-coupled vs non-coupled”), Heartbeat Coupling (coupled or non-coupled), and Flicker Frequency (7.5 or 10 Hz). Notably, we excluded the “non-coupled vs non-coupled” trial type in this analysis as neither frequency was coupled with the cardiac cycle. We conducted separate three-way repeated-measures ANOVAs on the power (indexed by signal-to-noise ratio; SNR) and the phase stability of the SSVEP response. The analysis results are presented in **Table 1**.

**Table 1. Analysis results of the ANOVAs conducted on SSVEP power and phase stability.**

<b>Factor</b>	<b><math>F_{(df = 1,31)}</math></b>	<b><math>p</math></b>	<b><math>\eta_p^2</math></b>
<b><i>Power</i></b>			
Trial Type*	4.94	.034	.14
Heartbeat Coupling	0.30	.586	.01
Flicker Frequency***	22.67	< .001	.42
Trial Type $\times$ Heartbeat Coupling*	6.07	.020	.16
Trial Type $\times$ Flicker Frequency	0.86	.361	.03
Heartbeat Coupling $\times$ Flicker Frequency	2.12	.155	.06
Trial Type $\times$ Heartbeat Coupling $\times$ Flicker Frequency	0.09	.766	<.01
<b><i>Phase Stability</i></b>			
Trial Type	0.15	.706	.01
Heartbeat Coupling*	6.34	.017	.17
Flicker Frequency***	47.56	< .001	.61
Trial Type $\times$ Heartbeat Coupling	0.81	.374	.03
Trial Type $\times$ Flicker Frequency	0.50	.487	.02
Heartbeat Coupling $\times$ Flicker Frequency	0.54	.468	.02
Trial Type $\times$ Heartbeat Coupling $\times$ Flicker Frequency	1.89	.179	.06

\*:  $p < .05$ ; \*\*\*:  $p < .001$ .

### 3.2.1 Power

The main effect of Trial Type was significant, showing that the SNR of SSVEP was smaller when part of the visual stimuli (the direction change of one group of dots) were coupled with cardiac systole ( $19.49 \pm 1.97$  dB), compared to when part of the visual stimuli were coupled with cardiac diastole ( $19.94 \pm 1.77$  dB). The main effect of Flicker Frequency was also significant, showing that the SNR of 7.5-Hz visual stimuli ( $20.97 \pm 2.18$  dB) was larger than that of 10-Hz visual stimuli ( $18.46 \pm 2.47$  dB). This effect was probably due to large activation and noise in the alpha band. Furthermore, the two-

way interaction between Trial Type and Heartbeat Coupling was significant. To further explore the interaction effect, we conducted post hoc pairwise comparisons between the two levels of Heartbeat Coupling for each Trial Type. In the "systole-coupled vs non-coupled" trials, systole-coupled dots triggered smaller SNR ( $19.19 \pm 2.39$  dB) compared to non-coupled dots ( $19.80 \pm 1.83$  dB;  $p = .035$ ; see **Figure 2**), despite being presented concurrently in the same visual field. However, no significant difference in SNR was observed between diastole-coupled dots ( $20.13 \pm 1.72$  dB) and non-coupled dots ( $19.74 \pm 2.14$  dB) in the "diastole-coupled vs non-coupled" trials ( $p = .170$ ).

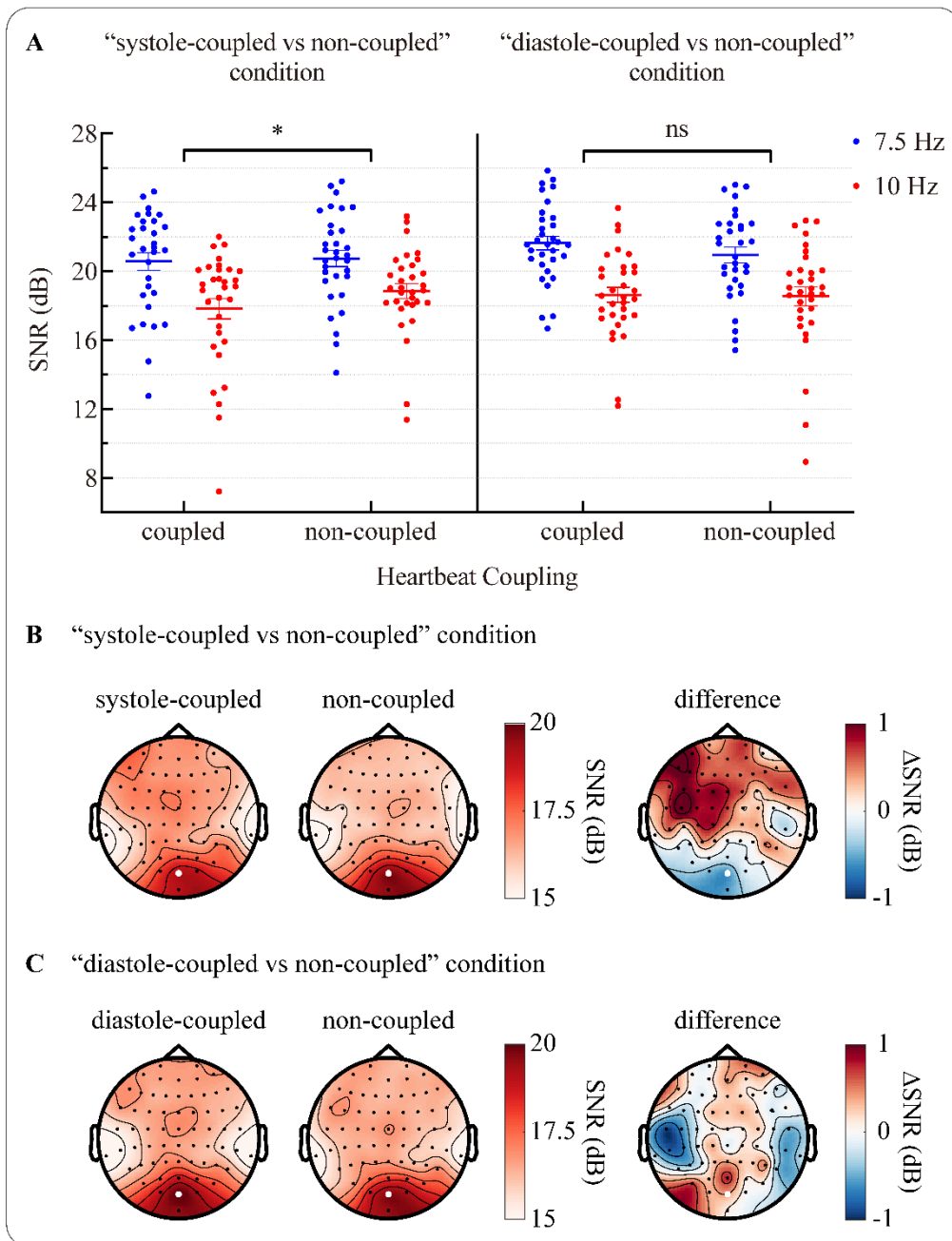


**Figure 2. Power of the SSVEP response.** (A) Individual (circles) and group averaged (bars) power (indexed by signal-to-noise ratio; SNR) values in different conditions. Error bars represent standard errors. ns: not significant; \*:  $p < .05$ . (B) Topographies of SNR averaged across participants for the systole-coupled and the non-coupled dots, as well as their difference in the “systole-coupled vs non-coupled” condition. (C) Topographies of SNR averaged across participants for the diastole-coupled and the non-

coupled dots, as well as their difference in the “diastole-coupled vs non-coupled” condition. The electrode Oz used for SNR analysis is marked in white.

### 3.2.2 Phase stability

The main effect of Heartbeat Coupling was significant, showing that the phase stability of SSVEP was higher when the visual stimuli were coupled with cardiac cycle (systole or diastole;  $0.63 \pm 0.14$ ), compared to when they were not coupled with cardiac cycle ( $0.62 \pm 0.14$ ). The main effect of Flicker Frequency was also significant, showing that the phase stability of 7.5-Hz visual stimuli ( $0.72 \pm 0.16$ ) was higher than that of 10-Hz visual stimuli ( $0.53 \pm 0.15$ ). Again, this effect was probably due to large activation and noise in the alpha band. Although the two-way interaction between Trial Type and Heartbeat Coupling was not significant, to further explore differences in phase stability between the group of dots that were coupled with the cardiac cycle and the group of dots that were not coupled with the cardiac cycle, we conducted pairwise comparisons between the two levels of Heartbeat Coupling for each Trial Type. In the “diastole-coupled vs non-coupled” trials, diastole-coupled dots triggered higher phase stability ( $0.63 \pm 0.14$ ) compared to non-coupled dots ( $0.62 \pm 0.13$ ;  $p = .034$ ; see **Figure 3**), despite being presented concurrently in the same visual field. However, no significant difference in phase stability was observed between systole-coupled dots ( $0.63 \pm 0.14$ ) and non-coupled dots ( $0.62 \pm 0.14$ ) in the "systole-coupled vs non-coupled" trials ( $p = .494$ ).

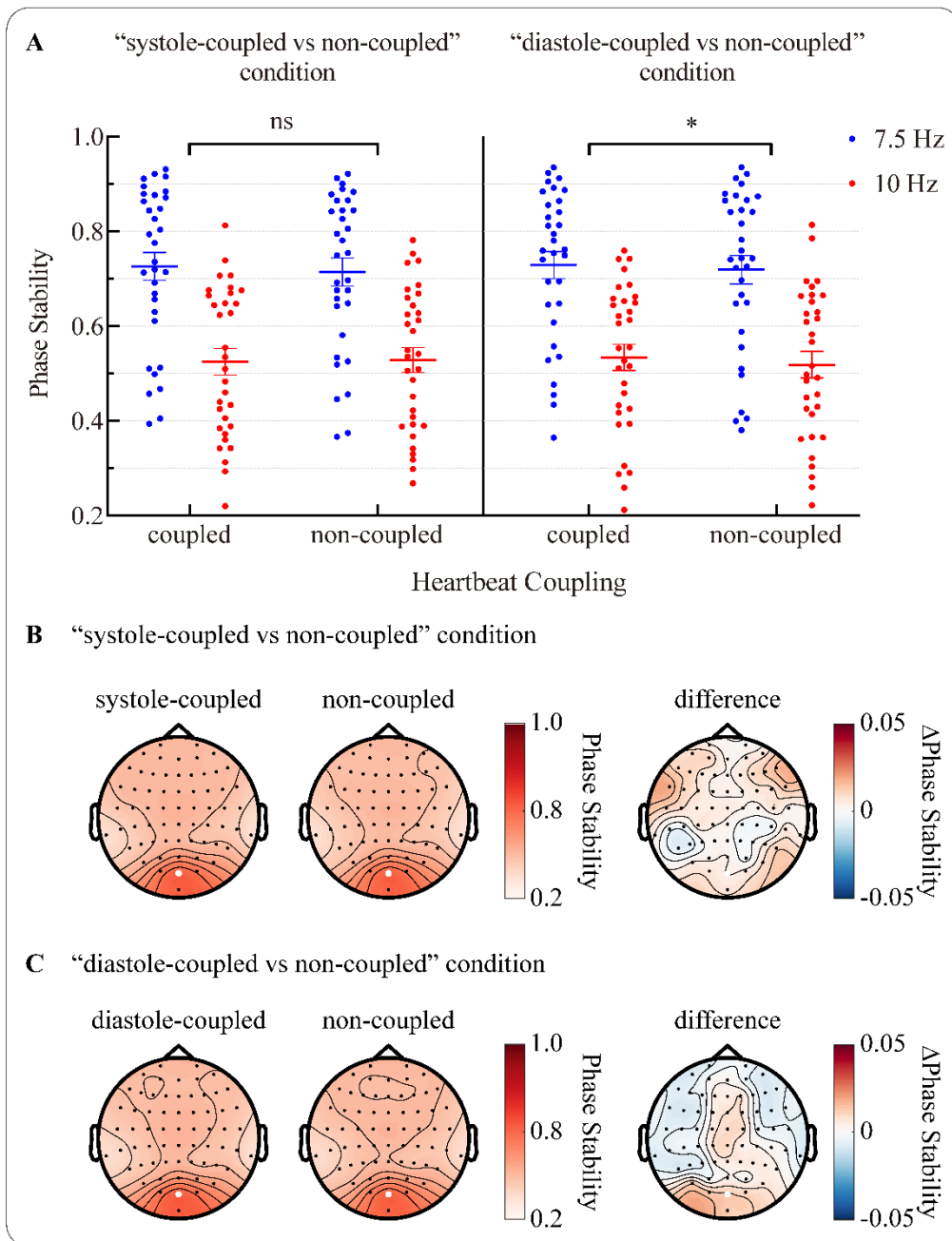


**Figure 3. Phase stability of the SSVEP response.** (A) Individual (circles) and group averaged (bars) phase stability values in different conditions. Error bars represent standard errors. ns: not significant; \*:  $p < .05$ . (B) Topographies of phase stability averaged across participants for the systole-coupled and the non-coupled dots, as well as their difference in the “systole-coupled vs non-coupled” condition. (C) Topographies of phase stability averaged across participants for the diastole-coupled and the non-

coupled dots, as well as their difference in the “diastole-coupled vs non-coupled” condition. The electrode Oz used for phase stability analysis is marked in white.

### 3.3 HEP amplitude

Consistent with previous studies (Al et al., 2020; Marshall et al., 2022), we used a nonparametric cluster-based permutation test to determine the HEP morphology and time windows of interest. The permutation analysis revealed a significant effect of Trial Type (“systole-coupled vs non-coupled”, “diastole-coupled vs non-coupled”, and “non-coupled vs non-coupled”) over fronto-central electrodes (AFz, AF4, AF7, Cz, C1, C2, C4, CP1, CP2, CP6, Fz, F1, F2, F3, F4, FCz, FC2, FC4, FP1, FT8, FT10, T8, and TP10) in a time window of 480–540 ms after the R peak ( $p = .042$ ). Based on the HEP amplitude averaged over this cluster, the one-way repeated-measures ANOVA also showed significant difference in HEP amplitude among trial types ( $F_{2,58} = 4.69$ ,  $p = .021$ ,  $\eta_p^2 = .14$ ; see **Figure 4**). Post hoc pairwise comparisons showed significant differences between “systole-coupled vs non-coupled” trials and “diastole-coupled vs non-coupled” trials ( $p = .010$ ). That is, the HEP was larger when part of the visual stimuli (the direction change of one group of dots) were coupled with cardiac systole, compared to when part of them were coupled with cardiac diastole. However, neither the differences between “systole-coupled vs non-coupled” and “non-coupled vs non-coupled” trials ( $p = .252$ ) nor the differences between “diastole-coupled vs non-coupled” and “non-coupled vs non-coupled” trials were significant ( $p = .252$ ). That is, HEP amplitudes were comparable when part of the visual stimuli were coupled with cardiac systole or diastole, compared to when neither group of dots was coupled with heartbeats.

As recommended in recent studies (Petzschner et al., 2019; Kritzman et al., 2022), to rule out the possibility that differences in cardiac activity between conditions may have contributed to the observed effect in HEP amplitude, we conducted a one-way repeated-measures ANOVA on the ECG amplitude averaged across the identical time window (see **Supplementary Figure 1**). This analysis revealed that the ECG amplitude did not significantly differ among trial types ( $F_{2,58} = 2.00$ ,  $p = .144$ ,  $\eta_p^2 = .07$ ). That is, the

cardiovascular artifacts are constant across conditions in the present task and would not have affected the observed effects in HEP amplitude.

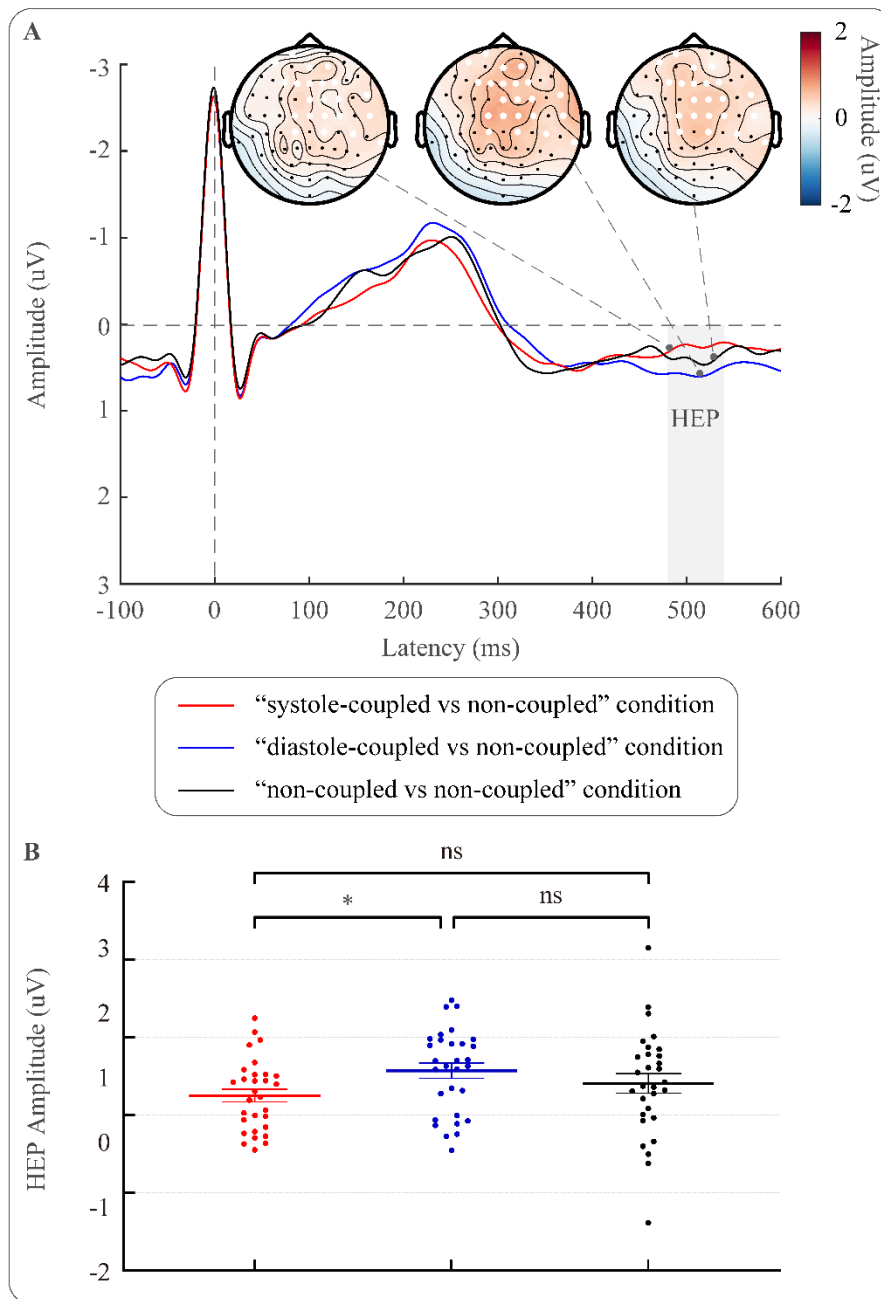


**Figure 4. Heartbeat-evoked potential (HEP).** (A) Grand average HEP waveforms and topographies in different conditions. Time “0” corresponds to the time of the R-peak. Permutation analysis revealed a significant cluster extended from 480 to 540 ms after R-peak (marked using a gray rectangle) over fronto-central electrodes (marked in

white). **(B)** Individual (circles) and group averaged (bars) HEP amplitudes in different conditions. Error bars represent standard errors. ns: not significant; \*:  $p < .05$ .

### 3.4 N2 amplitude evoked by the color change

In the “systole-coupled vs non-coupled” trials, when the direction changes of the target dots (the group of dots that changed color) were coupled with cardiac systole and when they were not coupled with any phase of the cardiac cycle, the N2 amplitude evoked by the color change was  $-4.59 \pm 2.90$  and  $-3.96 \pm 2.65$   $\mu\text{V}$ , respectively. In the “diastole-coupled vs non-coupled” trials, when the direction changes of the target dots were coupled with cardiac diastole and when they were not coupled with cardiac cycle, the N2 amplitude was  $-5.35 \pm 3.33$  and  $-4.98 \pm 3.57$   $\mu\text{V}$ , respectively. In the “non-coupled vs non-coupled” trial type, the N2 amplitude was  $-4.72 \pm 3.36$   $\mu\text{V}$ .

To compare the N2 amplitude evoked by the color change among trial types, we conducted a one-way repeated-measures ANOVA (Trial Type: “systole-coupled vs non-coupled”, “diastole-coupled vs non-coupled”, and “non-coupled vs non-coupled”). The analysis showed significant difference in N2 amplitude among trial types ( $F_{2,62} = 4.95, p = .010, \eta_p^2 = .14$ ). Post hoc pairwise comparisons showed significant differences between “systole-coupled vs non-coupled” and “diastole-coupled vs non-coupled” trials ( $p = .015$ ), as well as between “systole-coupled vs non-coupled” and “non-coupled vs non-coupled” trials ( $p = .031$ ; see **Figure 5**). That is, the color change evoked smaller N2 when part of the visual stimuli (the direction change of one group of dots) were coupled with cardiac systole, compared to when part of them were coupled with cardiac diastole and when neither group of dots was coupled with cardiac cycle. However, there were no significant differences between “diastole-coupled vs non-coupled” and “non-coupled vs non-coupled” trials ( $p = .671$ ). That is, N2 amplitudes were comparable when part of the visual stimuli were coupled with cardiac diastole, compared to when neither group of dots was coupled with heartbeats.

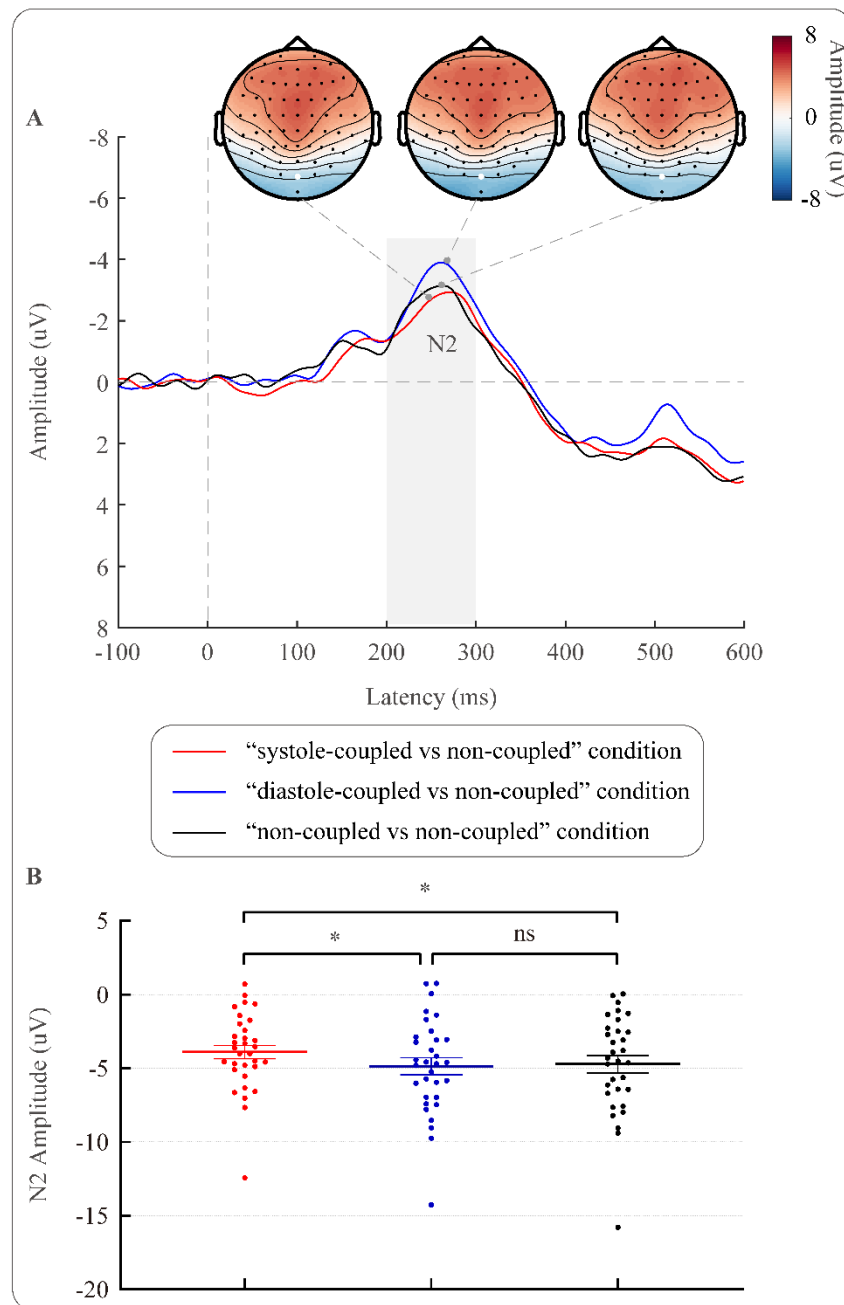


**Figure 5. N2 component evoked by the color change. (A)** Grand average waveforms and topographies in different conditions. Time “0” corresponds to onset of the color change. Peak amplitudes of N2 component were extracted within the time window from 200 to 300 ms after the onset of the color change (marked using a gray rectangle) and at electrode Oz (marked in white). **(B)** Individual (circles) and group averaged (bars) N2 amplitudes in different conditions. Error bars represent standard errors. ns: not significant; \*:  $p < .05$ .

Additionally, to compare the N2 amplitude evoked by the color change between the target dots that were coupled with the cardiac cycle and those that were not coupled with the cardiac cycle, we conducted separate paired samples *t*-tests for the "systole-coupled vs non-coupled" trials and the "diastole-coupled vs non-coupled" trials. However, the analyses did not show any significant effects in the "systole-coupled vs non-coupled" trials ( $t_{31} = -1.71, p = .097$ , Cohen's  $d = -0.30$ ) and the "diastole-coupled vs non-coupled" trials ( $t_{31} = -0.81, p = .424$ , Cohen's  $d = -0.14$ ). That is, the coupling status of the target dots with the cardiac cycle did not have a significant impact on N2 amplitude evoked by the color change.

### **3.5 The relationship between HEP and VEP**

To explore the relationship between changes in HEP and VEP across conditions, we calculated the Correspondence-tradeoff index (CTI) according to previously established procedures (Boylan et al., 2019; Kritzman et al., 2022). We found significantly negative CTI values between "systole-coupled vs. non-coupled" and "diastole-coupled vs. non-coupled" conditions ( $-0.44 \pm 0.88; t_{29} = -2.73, p = .011$ , Cohen's  $d = -0.50$ ), indicating that an increase in HEP is accompanied by a decrease in VEP. However, neither the CTI values between "systole-coupled vs. non-coupled" and "non-coupled vs. non-coupled" conditions ( $0.47 \pm 1.64; t_{29} = 1.56, p = .130$ , Cohen's  $d = 0.29$ ) nor the CTI values between "diastole-coupled vs. non-coupled" and "non-coupled vs. non-coupled" conditions reach significance ( $0.34 \pm 1.28; t_{29} = 1.47, p = .151$ , Cohen's  $d = 0.27$ ).

## **4 Discussion**

The present study investigated spontaneous shifts of attention between interoception and exteroception. Using EEG frequency tagging, we measured the neural processing of two groups of moving dots. The first group changed direction either when cardiac signals were strong (systole-coupled) or when they were relatively weak (diastole-coupled). These were compared to a second group of dots that were presented simultaneously and spatially overlapping but whose direction change was not synchronized with the cardiac cycle (non-coupled stimuli). Importantly, participants'

task (detecting brief color changes) did not require any intentional attention to the heartbeat coupling. We observed decreased SSVEP power for systole-coupled stimuli and increased SSVEP phase synchronization for diastole-coupled stimuli, compared to non-coupled stimuli. Additionally, coupling one group of dots with cardiac systole, compared with diastole, led to a larger HEP but a smaller N2 evoked by the color change. Moreover, the increase in HEP amplitude was associated with the decrease in N2 amplitude. Our findings suggest that interoceptive cardiac signals automatically shift some of our attention from the external to the internal milieu, supporting an attentional trade-off between interoception and exteroception.

The present study introduces three contributions. Firstly, it examines the attentional shifts between internal cardiac signals and external sensory stimuli *across the cardiac cycle*. Previous investigations primarily focused on how pre-stimulus cardiac processing affects subsequent exteroceptive processing. For example, larger pre-stimulus HEPs were followed by lower detection rates and electrophysiological response for near-threshold somatosensory stimuli (Al et al., 2020, 2021). Our lab's past research also showed that larger pre-stimulus HEPs predicted lower detection rates of near-threshold visual stimuli (Marshall et al., 2020), smaller P3 in response to visual action outcomes (Marshall et al., 2019), and reduced visual and auditory evoked potentials to repeated neutral face and auditory feedback of heartbeats (Marshall et al., 2022). As larger HEPs are regarded as reflecting stronger internally directed attention (Villena-González et al., 2017; Petzschner et al., 2019), these findings suggest that paying more attention to cardiac signals attenuates the perception of upcoming external stimuli. In contrast, by coupling visual stimuli with cardiac systole or diastole, the present study reveals how attention allocation across the internal-external axis fluctuates in response to intrinsic periodic changes in the strength of cardiac signals. Decreased SSVEP power is consistently associated with reduced visual attention (Morgan et al., 1996; Müller et al., 1998; Kim et al., 2007; Andersen et al., 2011). Thus, our result showing smaller SSVEP power for systole-coupled stimuli than concurrently-presented, non-coupled stimuli suggests that participants pay less attention to visual information coinciding with strong cardiac signals. Increased SSVEP phase synchronization is linked to heightened visual attention (Ding et al., 2006; Kashiwase

et al., 2012). Therefore, our finding of larger SSVEP phase synchronization for diastole-coupled stimuli compared to concurrently-presented, non-coupled stimuli suggests increased attention to visual information during the brief pause between cardiac signaling.

Overall, we speculate that during each cardiac cycle, attention towards the external world may decrease at systole due to interference from strong cardiac signals, while more attention can be directed to the external environment at diastole when interference is minimal. Notably, we did not observe a significant difference in SSVEP magnitude between diastole-coupled and non-coupled stimuli, nor in SSVEP phase synchronization between systole-coupled and non-coupled stimuli. This lack of significant effects may be due to the overall relatively *small* impact of changes in cardiac signals on SSVEP responses across the cardiac cycle. The subtle rather than pronounced effect appears to be adaptive, ensuring that our attentional and representational resources are not overly consumed by cardiac activities. If every heartbeat significantly influenced attentional allocation, it could potentially impair our cognitive functions. Therefore, the modest impact of cardiac activity on cognition seems to strike a balance, allowing us to maintain a stable focus while remaining responsive to our bodily signals. Additionally, in the present study, non-coupled stimuli changed direction randomly within each cardiac cycle, which means that they were also influenced by cardiac processing, albeit to a lesser extent than systole-coupled stimuli and to a greater extent than diastole-coupled stimuli. For future research, presenting systole-coupled and diastole-coupled stimuli simultaneously on the screen and directly comparing their SSVEP responses could potentially reveal stronger effects.

Secondly, the present study provides insights into the mechanisms underlying *spontaneous* shifts of attention along the internal-external axis. Prior studies instructed participants to either count visual targets (external attention condition) or their heartbeats (internal attention condition; Villena-González et al., 2017; Petzschner et al., 2019; Kritzman et al., 2022). In the external attention condition, visual information was task-relevant, while cardiac information was considered irrelevant, and vice versa in the internal attention condition. However, our present study diverges from this paradigm as participants were asked to detect color changes, making visual information

task-relevant while cardiac activity remained irrelevant in all conditions. Previous research showed that the internal attention condition resulted in larger HEPs but smaller VEPs/SSVEPs compared to the external attention condition (Villena-González et al., 2017; Petzschner et al., 2019; Kritzman et al., 2022), indicating prioritization of task-relevant cardiac information over processing irrelevant visual information. Similarly, we observed a larger HEP but a smaller VEP (the N2 component evoked by the color change) when one group of dots coupled with systole compared to diastole. These results suggest an enhanced representation of cardiac activity and a reduced representation of visual stimulus when the continuous, dynamic visual stimuli partially coincide with strong cardiac signals. Importantly, this effect is probably driven by an *automatic* process rather than a strategic allocation of attention or explicit judgment regarding heartbeat coupling.

Moreover, we found a trade-off pattern between increased HEP and decreased VEP, similar to the patterns observed in intentional shifts of attention between cardiac and visual modalities (Kritzman et al., 2022), auditory and visual modalities (Saupe et al., 2009), and tactile and visual modalities (Porcu et al., 2013). This suggests that visual and cardiac processing share a limited pool of resources (Kritzman et al., 2022). An increase in cardiac processing can lead to a reduction in visual processing. It also indicates that our brain automatically allocates more attentional and representational resources to internal cardiac signals when visual and cardiac inputs repeatedly coincide. One possible explanation for this phenomenon is that visual inputs occurring simultaneously with cardiac signals might be misinterpreted as signals associated with heartbeats (Al et al., 2020), thus amplifying the perceived intensity of the cardiac signals. The resulting stronger-than-expected "cardiac signals" may attract greater attention, consistent with the recent view that our brain carefully monitors internal bodily signals and is highly responsive to their changes (Tallon-Baudry, 2023).

Last but not least, the present study directly contrasts selective attention to heartbeat-coupled and non-coupled visual stimuli that are *concurrently presented* and *spatially overlapping*. Previous studies typically examined the effect of the cardiac cycle on visual processing by comparing brief events with varying heartbeat couplings across separate trials (Walker and Sandman, 1982; Pramme et al., 2014, 2016). For instance,

our recent study demonstrated that coupling a visual target's color change with cardiac systole, as opposed to diastole, disrupted its detection among multiple distractors that randomly changed color within each cardiac cycle (Ren et al., 2022a). This disruption was evident through prolonged reaction times, reduced N2pc amplitude, and reduced beta lateralization (Ren et al., 2022a). These findings imply a decrease in attentional resources directed towards external visual information when it coincides with strong cardiac signals. However, potential confounding factors, such as differences in general attentional resources or variations in spatial attention across trials, may contaminate the effects. The present study minimizes these potential confounds by presenting visual stimuli with varying heartbeat coupling simultaneously and at the same spatial location. Thus, compared to previous evidence, our findings provide more robust and direct evidence that systole-coupled visual stimuli receive less attention, while diastole-coupled stimuli receive more attention, compared to non-coupled stimuli. Furthermore, our findings suggest that the brain automatically and flexibly allocates varying degrees of attention to different visual information based on its coupling with the heartbeats. In other words, when external sensory inputs coincide with strong internal cardiac signals, the brain appears to selectively and specifically attenuate attentional and representational resources allocated to these specific external sensory signals, rather than uniformly suppressing all external inputs.

In conclusion, this study provides compelling evidence that the presence of interoceptive cardiac signals automatically redirects a portion of our attention from the external to the internal environment. This is demonstrated by the modulation effect observed in SSVEP responses, HEP amplitude, and visual target-evoked N2 amplitude when task-irrelevant visual information is coupled with specific cardiac phases. Our findings highlight the dynamic reallocation of limited processing resources between interoception and exteroception across the cardiac cycle, supporting the attentional trade-off mechanism between these two processes. Furthermore, our study introduces a novel paradigm that incorporates the SSVEP frequency tagging, which holds great potential as a crucial tool for exploring the interplay between internal and external processing in both healthy individuals and those affected by interoceptive

abnormalities, such as anxiety disorders, eating disorders, addictive disorders, and autism (Khalsa et al., 2018; Bonaz et al., 2021).

## References

- Al E, Iliopoulos F, Forschack N, Nierhaus T, Grund M, Motyka P, Gaebler M, Nikulin VV, Villringer A (2020) Heart–brain interactions shape somatosensory perception and evoked potentials. *Proc Natl Acad Sci* 117:10575–10584.
- Al E, Iliopoulos F, Nikulin VV, Villringer A (2021) Heartbeat and somatosensory perception. *NeuroImage* 238:118247.
- Andersen SK, Fuchs S, Müller MM (2011) Effects of feature-selective and spatial attention at different stages of visual processing. *J Cogn Neurosci* 23:238–246.
- Bonaz B, Lane RD, Oshinsky ML, Kenny PJ, Sinha R, Mayer EA, Critchley HD (2021) Diseases, disorders, and comorbidities of interoception. *Trends Neurosci* 44:39–51.
- Boylan MR, Kelly MN, Thigpen NN, Keil A (2019) Attention to a threat-related feature does not interfere with concurrent attentive feature selection. *Psychophysiology* 56:e13332.
- Campbell JID, Thompson VA (2012) MorePower 6.0 for ANOVA with relational confidence intervals and Bayesian analysis. *Behav Res Methods* 44:1255–1265.
- Coll M-P, Hobson H, Bird G, Murphy J (2021) Systematic review and meta-analysis of the relationship between the heartbeat-evoked potential and interoception. *Neurosci Biobehav Rev* 122:190–200.
- DeSaix P, Betts, Gordon J., Johnson, Eddie, Johnson, Jody E., Oksana, Korol, Kruse, Dean H., Poe, Brandon, Wise, James A., Young, Kelly A. (2013) *Anatomy & Physiology*. openStax.

- Ding J, Sperling G, Srinivasan R (2006) Attentional modulation of SSVEP power depends on the network tagged by the flicker frequency. *Cereb Cortex* 16:1016–1029.
- Eidelman-Rothman M, Ben-Simon E, Freche D, Keil A, Hendler T, Levit-Binnun N (2019) Sleepless and desynchronized: Impaired inter trial phase coherence of steady-state potentials following sleep deprivation. *NeuroImage* 202:116055.
- Eiserbeck A, Enge A, Rabovsky M, Abdel Rahman R (2022) Electrophysiological chronometry of graded consciousness during the attentional blink. *Cereb Cortex* 32:1244–1259.
- Figueira JSB, Kutlu E, Scott LS, Keil A (2022) The FreqTag toolbox: A principled approach to analyzing electrophysiological time series in frequency tagging paradigms. *Dev Cogn Neurosci* 54:101066.
- Garfinkel SN, Minati L, Gray MA, Seth AK, Dolan RJ, Critchley HD (2014) Fear from the heart: Sensitivity to fear stimuli depends on individual heartbeats. *J Neurosci* 34:6573–6582.
- Gjorgieva E, Geib BR, Cabeza R, Woldorff MG (2022) The influence of imagery vividness and internally-directed attention on the neural mechanisms underlying the encoding of visual mental images into episodic memory. *Cereb Cortex*:bhac270.
- Grund M, Al E, Pabst M, Dabbagh A, Stephani T, Nierhaus T, Gaebler M, Villringer A (2022) Respiration, heartbeat, and conscious tactile perception. *J Neurosci* 42:643–656.
- JASP Team (2023) JASP (Version 0.17.0.0)[Computer software].
- Ji H, Petro NM, Chen B, Yuan Z, Wang J, Zheng N, Keil A (2018) Cross multivariate correlation coefficients as screening tool for analysis of concurrent EEG-fMRI recordings. *J Neurosci Res* 96:1159–1175.

- Kashiwase Y, Matsumiya K, Kuriki I, Shioiri S (2012) Time courses of attentional modulation in neural amplification and synchronization measured with steady-state visual-evoked potentials. *J Cogn Neurosci* 24:1779–1793.
- Kastner-Dorn AK, Andreatta M, Pauli P, Wieser MJ (2018) Hypervigilance during anxiety and selective attention during fear: Using steady-state visual evoked potentials (ssVEPs) to disentangle attention mechanisms during predictable and unpredictable threat. *Cortex* 106:120–131.
- Keitel C, Keitel A, Benwell CSY, Daube C, Thut G, Gross J (2019) Stimulus-driven brain rhythms within the alpha band: The attentional-modulation conundrum. *J Neurosci* 39:3119–3129.
- Kern M, Aertsen A, Schulze-Bonhage A, Ball T (2013) Heart cycle-related effects on event-related potentials, spectral power changes, and connectivity patterns in the human ECoG. *NeuroImage* 81:178–190.
- Khalsa SS et al. (2018) Interoception and mental health: A roadmap. *Biol Psychiatry Cogn Neurosci Neuroimaging* 3:501–513.
- Kim YJ, Grabowecy M, Paller KA, Muthu K, Suzuki S (2007) Attention induces synchronization-based response gain in steady-state visual evoked potentials. *Nat Neurosci* 10:117–125.
- Koivisto M, Grassini S (2016) Neural processing around 200 ms after stimulus-onset correlates with subjective visual awareness. *Neuropsychologia* 84:235–243.
- Kritzman L, Eidelman-Rothman M, Keil A, Freche D, Sheppes G, Levit-Binnun N (2022) Steady-state visual evoked potentials differentiate between internally and externally directed attention. *NeuroImage* 254:119133.
- Luck SJ, Gaspelin N (2017) How to get statistically significant effects in any ERP experiment (and why you shouldn't). *Psychophysiology* 54:146–157.
- Maris E, Oostenveld R (2007) Nonparametric statistical testing of EEG- and MEG-data. *J Neurosci Methods* 164:177–190.

- Marshall AC, Gentsch A, Blum A-L, Broering C, Schütz-Bosbach S (2019) I feel what I do: Relating interoceptive processes and reward-related behavior. *NeuroImage* 191:315–324.
- Marshall AC, Gentsch A, Schütz-Bosbach S (2020) Interoceptive cardiac expectations to emotional stimuli predict visual perception. *Emotion* 20:1113–1126.
- Marshall AC, Gentsch-Ebrahimzadeh A, Schütz-Bosbach S (2022) From the inside out: Interoceptive feedback facilitates the integration of visceral signals for efficient sensory processing. *NeuroImage* 251:119011.
- Mora-Cortes A, Ridderinkhof KR, Cohen MX (2018) Evaluating the feasibility of the steady-state visual evoked potential (SSVEP) to study temporal attention. *Psychophysiology* 55:e13029.
- Morgan ST, Hansen JC, Hillyard SA (1996) Selective attention to stimulus location modulates the steady-state visual evoked potential. *Proc Natl Acad Sci* 93:4770–4774.
- Müller MM, Andersen S, Trujillo NJ, Valdés-Sosa P, Malinowski P, Hillyard SA (2006) Feature-selective attention enhances color signals in early visual areas of the human brain. *Proc Natl Acad Sci* 103:14250–14254.
- Müller MM, Picton TW, Valdes-Sosa P, Riera J, Teder-Sälejärvi WA, Hillyard SA (1998) Effects of spatial selective attention on the steady-state visual evoked potential in the 20–28 Hz range. *Cogn Brain Res* 6:249–261.
- Norcia AM, Appelbaum LG, Ales JM, Cottareau BR, Rossion B (2015) The steady-state visual evoked potential in vision research: A review. *J Vis* 15:4.
- Oostenveld R, Fries P, Maris E, Schoffelen J-M (2011) FieldTrip: Open source software for advanced analysis of MEG, EEG, and invasive electrophysiological data. *Comput Intell Neurosci* 2011:156869.

- Panitz C, Gundlach C, Boylan MR, Keil A, Müller MM (2023) Higher amplitudes in steady-state visual evoked potentials driven by square-wave versus sine-wave contrast modulation – A dual-laboratory study. *Psychophysiology*:e14287.
- Park H-D, Bernasconi F, Salomon R, Tallon-Baudry C, Spinelli L, Seeck M, Schaller K, Blanke O (2018) Neural sources and underlying mechanisms of neural responses to heartbeats, and their role in bodily self-consciousness: An intracranial EEG study. *Cereb Cortex* 28:2351–2364.
- Petzschner FH, Weber LA, Wellstein KV, Paolini G, Do CT, Stephan KE (2019) Focus of attention modulates the heartbeat evoked potential. *NeuroImage* 186:595–606.
- Porcu E, Keitel C, Müller MM (2013) Concurrent visual and tactile steady-state evoked potentials index allocation of inter-modal attention: A frequency-tagging study. *Neurosci Lett* 556:113–117.
- Pramme L, Larra MF, Schächinger H, Frings C (2014) Cardiac cycle time effects on mask inhibition. *Biol Psychol* 100:115–121.
- Pramme L, Larra MF, Schächinger H, Frings C (2016) Cardiac cycle time effects on selection efficiency in vision: Baroreceptor activity and visual attention. *Psychophysiology* 53:1702–1711.
- Rae CL, Botan VE, Gould van Praag CD, Herman AM, Nyssönen JAK, Watson DR, Duka T, Garfinkel SN, Critchley HD (2018) Response inhibition on the stop signal task improves during cardiac contraction. *Sci Rep* 8:9136.
- Ren Q, Marshall AC, Kaiser J, Schütz-Bosbach S (2022a) Multisensory integration of anticipated cardiac signals with visual targets affects their detection among multiple visual stimuli. *NeuroImage* 262:119549.
- Ren Q, Marshall AC, Kaiser J, Schütz-Bosbach S (2022b) Response inhibition is disrupted by interoceptive processing at cardiac systole. *Biol Psychol* 170:108323.

- Ronchi R, Bernasconi F, Pfeiffer C, Bello-Ruiz J, Kaliuzhna M, Blanke O (2017) Interoceptive signals impact visual processing: Cardiac modulation of visual body perception. *NeuroImage* 158:176–185.
- Salomon R, Ronchi R, Dönz J, Bello-Ruiz J, Herbelin B, Martet R, Faivre N, Schaller K, Blanke O (2016) The insula mediates access to awareness of visual stimuli presented synchronously to the heartbeat. *J Neurosci* 36:5115–5127.
- Saupe K, Schröger E, Andersen S, Müller M (2009) Neural mechanisms of intermodal sustained selective attention with concurrently presented auditory and visual stimuli. *Front Hum Neurosci* 3 Available at: <https://www.frontiersin.org/articles/10.3389/neuro.09.058.2009> [Accessed May 22, 2023].
- Schulz A, Köster S, Beutel ME, Schächinger H, Vögele C, Rost S, Rauh M, Michal M (2015) Altered patterns of heartbeat-evoked potentials in depersonalization/derealization disorder: neurophysiological evidence for impaired cortical representation of bodily signals. *Psychosom Med* 77:506–516.
- Schulz A, Strelzyk F, Ferreira de Sá DS, Naumann E, Vögele C, Schächinger H (2013) Cortisol rapidly affects amplitudes of heartbeat-evoked brain potentials--implications for the contribution of stress to an altered perception of physical sensations? *Psychoneuroendocrinology* 38:2686–2693.
- Skora LI, Livermore JJA, Roelofs K (2022) The functional role of cardiac activity in perception and action. *Neurosci Biobehav Rev* 137:104655.
- Srinivasan R, Bibi FA, Nunez PL (2006) Steady-state visual evoked potentials: Distributed local sources and wave-like dynamics are sensitive to flicker frequency. *Brain Topogr* 18:167–187.
- Tallon-Baudry C (2023) Interoception: Probing internal state is inherent to perception and cognition. *Neuron*:S0896627323003045.

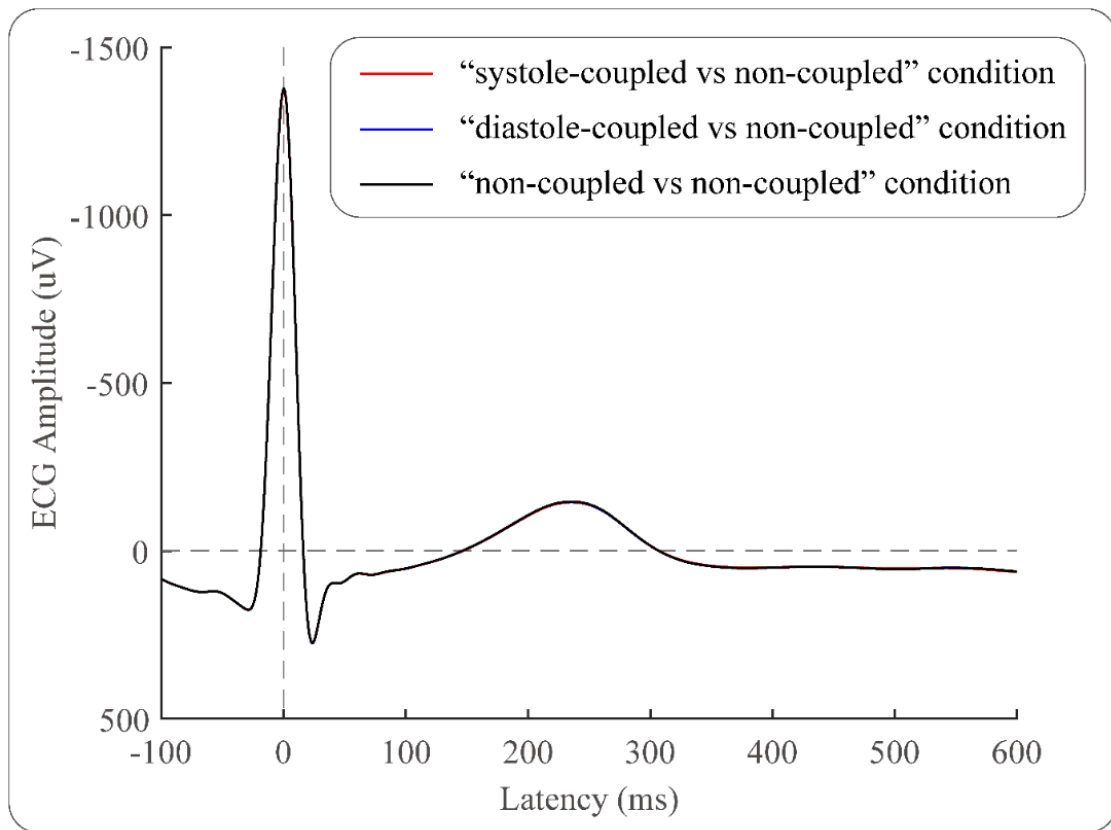
- van Elk M, Lenggenhager B, Heydrich L, Blanke O (2014) Suppression of the auditory N1-component for heartbeat-related sounds reflects interoceptive predictive coding. *Biol Psychol* 99:172–182.
- Villena-González M, Moëgne-Loccoz C, Lagos RA, Alliende LM, Billeke P, Aboitiz F, López V, Cosmelli D (2017) Attending to the heart is associated with posterior alpha band increase and a reduction in sensitivity to concurrent visual stimuli. *Psychophysiology* 54:1483–1497.
- Walker BB, Sandman CA (1982) Visual evoked potentials change as heart rate and carotid pressure change. *Psychophysiology* 19:520–527.
- Wen W, Brann E, Di Costa S, Haggard P (2018) Enhanced perceptual processing of self-generated motion: Evidence from steady-state visual evoked potentials. *NeuroImage* 175:438–448.
- Wieser MJ, Miskovic V, Keil A (2016) Steady-state visual evoked potentials as a research tool in social affective neuroscience. *Psychophysiology* 53:1763–1775.

### Supplementary Materials

**Supplementary Table 1.** Trial number ( $M \pm SD$ ) for each analysis.

	“systole-coupled target vs non-coupled non-target” condition	“systole-coupled non-target vs non-coupled target” condition	“diastole-coupled target vs non-coupled non-target” condition	“diastole-coupled non-target vs non-coupled target” condition	“non-coupled target vs non-coupled non-target” condition
Behavioural accuracy	19.19 $\pm$ 1.58	19.09 $\pm$ 1.55	18.91 $\pm$ 1.77	19.00 $\pm$ 1.76	18.75 $\pm$ 2.14
Visual evoked potential	18.94 $\pm$ 1.92	18.81 $\pm$ 1.86	18.59 $\pm$ 1.81	18.81 $\pm$ 1.87	18.56 $\pm$ 2.36
	“systole-coupled 7.5 Hz vs non-coupled 10 Hz” condition	“systole-coupled 10 Hz vs non-coupled 7.5 Hz” condition	“diastole-coupled 7.5 Hz vs non-coupled 10 Hz” condition	“diastole-coupled 10 Hz vs non-coupled 7.5 Hz” condition	“non-coupled 7.5 Hz vs non-coupled 10 Hz” condition
SSVEP	18.56 $\pm$ 1.81	18.66 $\pm$ 2.18	18.66 $\pm$ 2.01	18.13 $\pm$ 2.49	18.16 $\pm$ 2.63
Heartbeat evoked potential (uncorrected)	18.57 $\pm$ 2.13	18.57 $\pm$ 2.27	18.73 $\pm$ 1.93	18.47 $\pm$ 2.43	18.57 $\pm$ 2.10
Heartbeat evoked potential (CFA-corrected)	18.60 $\pm$ 2.14	18.60 $\pm$ 2.25	18.73 $\pm$ 1.93	18.50 $\pm$ 2.42	18.57 $\pm$ 2.10

CFA: cardiac field artefact.



**Supplementary Figure 1.** ECG waveforms. Time “0” corresponds to the time of the R-peak.

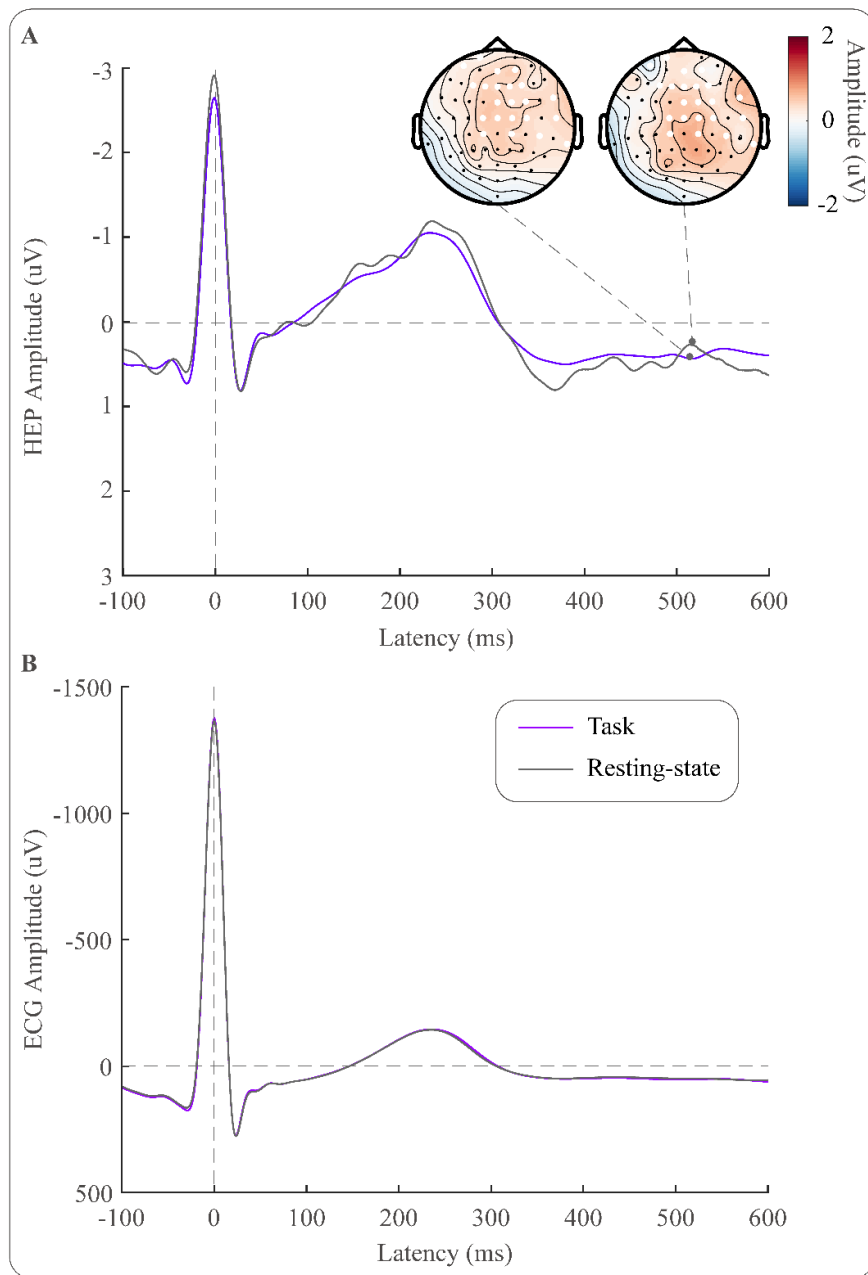
## **Supplementary Analysis 1: Removing confounding direction change-evoked responses from the HEP epochs**

For each HEP epoch in the 'diastole-coupled vs non-coupled' condition and the 'systole-coupled vs non-coupled' condition, we first calculated the latency between the ECG R-peak and the most recent subsequent direction change of the diastole-/systole-coupled dots. Then, we extracted EEG epochs time-locked to the time point having identical latency before each direction change of the non-coupled dots within the TOI of each trial (1 – 15 s relative to display onset) in the 'non-coupled vs non-coupled' condition. Epochs containing large artifacts were excluded based on a threshold of  $\pm 100 \mu\text{V}$  in EEG channels. Next, we averaged the epochs from the 'non-coupled vs non-coupled' condition for each EEG electrode. Lastly, we subtracted the mean signal of these epochs from the aforementioned HEP epoch in the 'diastole-coupled vs non-coupled' condition and the 'systole-coupled vs non-coupled' condition for each EEG electrode.

In other words, the direction change-evoked responses in the 'non-coupled vs non-coupled' condition were utilized to minimize the potential contamination of the responses evoked by the direction change of the coupled dots on HEP epochs in the 'diastole-coupled vs non-coupled' condition and the 'systole-coupled vs non-coupled' condition.

## **Supplementary Analysis 2: comparing HEP amplitudes during the task and the resting state.**

To explore any potential differences in cardiac processing between the dynamic visual detection task and the resting state, we compared the averaged HEP amplitude across all task trials with the HEP amplitude during the resting-state condition recorded prior to the task. The paired-sample *t*-test showed no significant difference between the HEP amplitudes during the task ( $0.40 \pm 0.46 \mu\text{V}$ ) and the resting-state condition ( $-0.40 \pm 1.19 \mu\text{V}$ ;  $t_{29} = -0.02$ ,  $p = .987$ , Cohen's  $d = -0.003$ ; see **Supplementary Figure 2A**). To exclude the potential influence of cardiac cycle-related artifacts on this finding, we also compared the ECG amplitude between the two conditions. The paired-sample *t*-test showed no significant difference in the ECG amplitudes during the task ( $54.42 \pm 39.08 \mu\text{V}$ ) and the resting-state condition ( $50.94 \pm 42.77 \mu\text{V}$ ;  $t_{29} = -1.58$ ,  $p = .126$ , Cohen's  $d = -0.29$ ; see **Supplementary Figure 2B**). These results suggest that there was comparable neural processing of cardiac activities when participants were engaged in the dynamic visual detection task and when they were in a resting state with their eyes open.



**Supplementary Figure 2.** Heartbeat-evoked potential (HEP) during the dynamic visual detection task and the resting state. **(A)** HEP waveforms and topographies. Time window and electrodes used to extract HEP amplitude were identical to those in Figure 4. **(B)** ECG waveforms. Time “0” corresponds to the time of the R-peak.

### **Supplementary Analysis 3: HEP analysis with removal of cardiac field artifact using independent component analysis**

#### **1 HEP analysis**

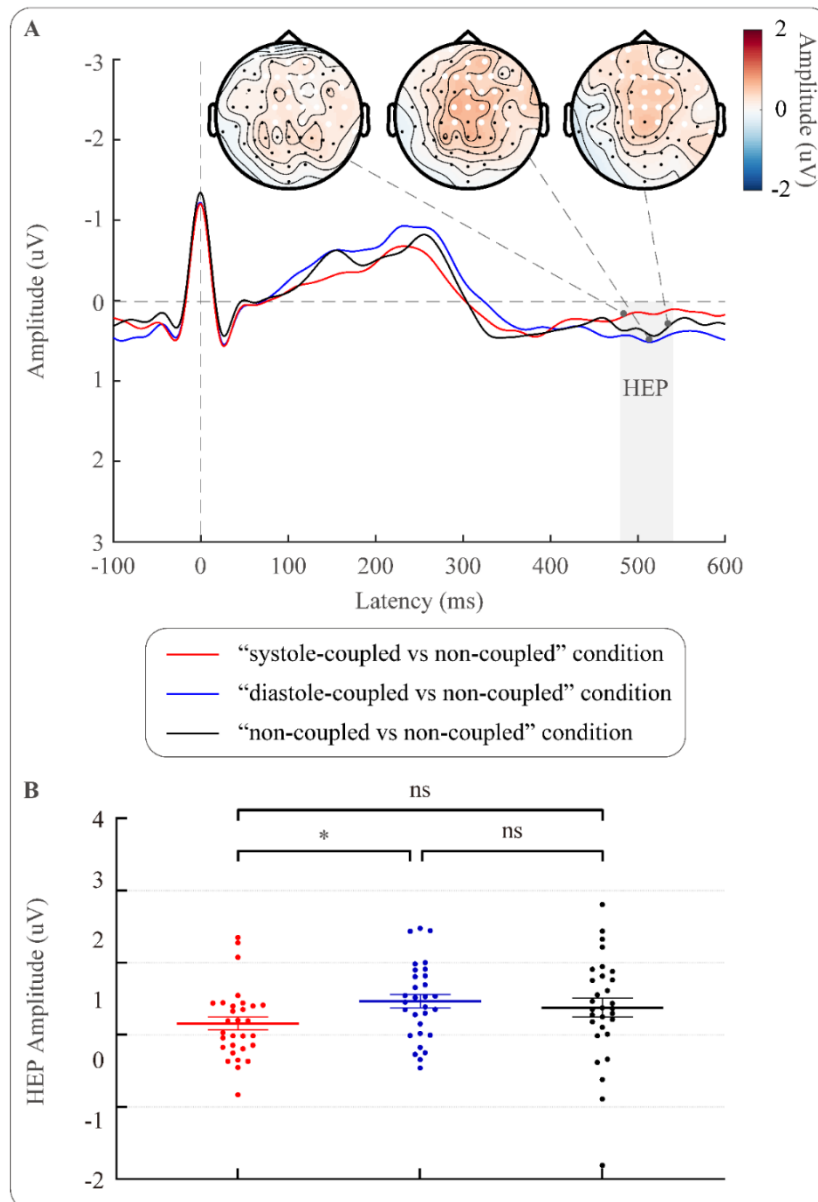
After conducting the analysis steps in **4.5.1 EEG and ECG pre-processing**, we removed the cardiac field artifact (CFA) in EEG data by means of independent component analysis (Marshall et al., 2019; Ren et al., 2022). Specifically, we first redefined EEG trials around the ECG R-peaks. Then, we computed the coherence of the time-frequency data between each independent component and the ECG signal, and elected four components with the highest coherence. Finally, we decided which of the four components should be removed based on additional characteristics which were commonly associated with CFA, e.g., a bimodal topography, a frequency peak around 5 Hz, and a rhythmically repeating time course (Viola et al., 2009). On average,  $1.53 \pm 1.16$  components per participant were removed. The CFA-corrected EEG data were further processed following the same procedure as the uncorrected data in the main manuscript. After excluding trials due to high heart rate or excessive noise, we were left with 30 datasets containing a sufficient number of remaining trials (> 10 trials in any condition) for further HEP analysis. The number of remaining trials per participant did not differ significantly across conditions ( $F_{4,116} = 0.21$ ,  $p = .877$ ,  $\eta_p^2 = .01$ ; see **Supplementary Table 1**).

The mean HEP amplitude per condition and participant were calculated over the same cluster (electrodes: AFz, AF4, AF7, Cz, C1, C2, C4, CP1, CP2, CP6, Fz, F1, F2, F3, F4, FCz, FC2, FC4, FP1, FT8, FT10, T8, and TP10; time window: 480–540 ms after the R peak) as the uncorrected data in the main manuscript.

## 2 HEP results

The one-way repeated-measures ANOVA showed significant difference in HEP amplitude among trial types ( $F_{2,58} = 3.31$ ,  $p = .044$ ,  $\eta_p^2 = .10$ ; see **Supplementary Figure 3**). Post hoc pairwise comparisons showed significant differences between “systole-coupled vs non-coupled” trials and “diastole-coupled vs non-coupled” trials ( $p = .046$ ). That is, the HEP was larger when part of the visual stimuli (i.e., the direction change of one group of dots) were coupled with cardiac systole, compared to when part of them were coupled with cardiac diastole. However, neither the differences between “systole-coupled vs non-coupled” and “non-coupled vs non-coupled” trials ( $p = .165$ ) nor the differences between “diastole-coupled vs non-coupled” and “non-coupled vs non-coupled” trials were significant ( $p = .466$ ). That is, HEP amplitudes were comparable when part of the visual stimuli were coupled with cardiac systole or diastole, compared to when neither group of dots was coupled with heartbeats.

In summary, the effects on HEP amplitude observed in the CFA-corrected EEG data were consistent with those observed in the uncorrected data.



**Supplementary Figure 3.** Heartbeat-evoked potential (HEP) after deleting cardiac field artifact. **(A)** Grand average HEP waveforms and topographies in different conditions. Time “0” corresponds to the time of the R-peak. Time window (marked using a gray rectangle) and electrodes (marked in white) used to extract HEP amplitude were identical to those in Figure 4. **(B)** Individual (circles) and group averaged (bars) HEP amplitudes in different conditions. Error bars represent standard errors. ns: not significant; \*:  $p < .05$ .

## References

- Marshall AC, Gentsch A, Blum A-L, Broering C, Schütz-Bosbach S (2019) I feel what I do: Relating interoceptive processes and reward-related behavior. *NeuroImage* 191:315–324.
- Ren Q, Marshall AC, Kaiser J, Schütz-Bosbach S (2022) Multisensory integration of anticipated cardiac signals with visual targets affects their detection among multiple visual stimuli. *NeuroImage* 262:119549.
- Viola FC, Thorne J, Edmonds B, Schneider T, Eichele T, Debener S (2009) Semi-automatic identification of independent components representing EEG artifact. *Clin Neurophysiol* 120:868–877.

## **2.3 Study III: Response Inhibition is Disrupted by Interoceptive Processing at Cardiac Systole**

**This article was published in *Biological Psychology*:**

Ren, Q., Marshall, A. C., Kaiser, J., & Schütz-Bosbach, S. (2022). Response inhibition is disrupted by interoceptive processing at cardiac systole. *Biological Psychology*, 170, 108323. <https://doi.org/10.1016/j.biopsycho.2022.108323>

Copyright © 2022 Elsevier B.V. All rights reserved. As the author of this article, I retain the right to include it in this dissertation. The main manuscript and supplements here are the published version.

### **Contributions:**

Qiaoyue Ren: Conceptualization, Methodology, Investigation, Data curation, Formal analysis, Visualization, Writing – original draft.

Amanda C. Marshall: Conceptualization, Methodology, Writing – review& editing.

Jakob Kaiser: Methodology, Writing – review& editing.

Simone Schütz-Bosbach: Conceptualization, Methodology, Writing – review& editing, Supervision, Funding acquisition.





# Response inhibition is disrupted by interoceptive processing at cardiac systole

Qiaoyue Ren, Amanda C. Marshall, Jakob Kaiser, Simone Schütz-Bosbach\*

General and Experimental Psychology Unit, Department of Psychology, LMU Munich, Germany

## ARTICLE INFO

### Keywords:

Response inhibition  
Interoception  
Cardiac cycle  
Systole  
Heartbeat evoked potential  
Emotion

## ABSTRACT

The present study investigated how cardiac signals influence response inhibition at both behavioral and electrophysiological levels by using participants' electrocardiogram signals to control the occurrence of events in a stop-signal task, in which the go cue was unpredictably followed by a stop signal requiring the cancellation of the prepotent response. We observed prolonged stop-signal reaction times, reduced stop-signal P3 amplitudes, and higher heartbeat evoked potential amplitudes when the stop signal was presented at cardiac systole, compared to presentation randomly within the cardiac cycle. These effects were independent of the emotional attribute of the stop signal (i.e., emotional facial expression change or non-emotional color change). Our results suggest that coupling stop signals to peripheral autonomic cardiac signals has an impeding effect on response inhibition, probably via shifting attention from exteroception to interoception. Our findings help clarify the precise impact of interoceptive signals on inhibitory control.

## 1. Introduction

Interoception refers to the sense of the internal physiological condition of the body (Bonaz et al., 2021; Craig, 2002). Recently, theoretical and experimental research studying interoception has markedly increased and suggests a prominent role of interoception in human perception (Al et al., 2020; Seth & Friston, 2016), cognition (Critchley & Garfinkel, 2018; Galvez-Pol, McConnell, & Kilner, 2020), and action (Makowski, Sperduti, Blonde, Nicolas, & Piolino, 2020; Marshall, Gentsch, & Schütz-Bosbach, 2018; Rae et al., 2018). Interoception therefore is highly relevant for studying brain-body interactions.

Systolic cardiac signals are thought to influence other cognitive processes by competing for the allocation of attentional resources (Al et al., 2020; Critchley & Garfinkel, 2018; Khalsa et al., 2018; Marshall, Gentsch, & Schütz-Bosbach, 2020). Systolic cardiac signals may shift people's attention from the external environment to internal physiological states, and thereby interfere with other upcoming or ongoing cognitive processes such as detecting the external stop signal and stopping the prepotent response. We therefore expected disrupted response inhibition when the stop signal was presented at systole compared with when the stop signal was presented randomly within the cardiac cycle (i.e., no-coupling condition), evidenced by prolonged SSRTs, reduced stop-signal P3 peak amplitudes, and/or delayed stop-signal P3 peak

latencies. Additionally, given that HEP amplitudes are higher during interoceptive compared with exteroceptive attention (Petzschner et al., 2019; Villena-González et al., 2017), we expected increased HEP amplitudes after the stop signal presented at systole compared with the no-coupling condition. Furthermore, considering that emotionally salient stimuli are more closely coupled to cardiac interoceptive processing than neutral stimuli (Garfinkel et al., 2014; Gentsch, Sel, Marshall, & Schütz-Bosbach, 2019; Gray et al., 2012; Marshall, Gentsch, Schröder, & Schütz-Bosbach, 2018), we expected a stronger cardiac cycle effect on response inhibition when the stop signal has emotional significance. Finally, inspired by a recent finding that HEP amplitudes decreased when participants engaged in a somatosensory task compared to a resting-state condition (Al, Iliopoulos, Nikulin, & Villringer, 2021), we expected differential HEP amplitudes in the stop-signal task as compared to the resting-state condition.

A major channel of interoceptive information comes from the heart, where cardiac afferent signals are continuously conveyed to the brain to indicate how fast and strong the heart is beating. Several studies have explored interoception by focusing on heartbeat perception as a means to quantify internal awareness (Al et al., 2020; Marshall et al. 2020; Rae et al., 2020). Cardiac interoceptive information is conveyed to the brain mainly by arterial baroreceptors located in the aortic arch and carotid sinuses (Critchley & Harrison, 2013). In a cardiac cycle, these

\* Correspondence to: Department of Psychology, LMU Munich, Leopoldstr. 13, D-80802 Munich, Germany.

E-mail address: [S.Schuetz-Bosbach@psy.lmu.de](mailto:S.Schuetz-Bosbach@psy.lmu.de) (S. Schütz-Bosbach).

<https://doi.org/10.1016/j.biopsycho.2022.108323>

Received 26 August 2021; Received in revised form 24 February 2022; Accepted 22 March 2022

Available online 25 March 2022

0301-0511/© 2022 Elsevier B.V. All rights reserved.

baroreceptors fire strongly in response to the increased arterial blood pressure when the heart contracts and ejects the blood, i.e., cardiac systole, and keep quiescent when the heart expands and is being filled, i.e., cardiac diastole (Azzalini, Rebollo, & Tallon-Baudry, 2019; Garfinkel & Critchley, 2016). There is converging evidence showing that people's responses to an external stimulus are modulated by the timing of the stimulus with respect to their cardiac cycles, i.e., whether the processing of the stimulus is accompanied by the processing of cardiac afferent signals (Adelhofer, Schreiter, & Beste, 2020; Al et al., 2020; Garfinkel et al., 2014). For example, in the sensorimotor domain, processing information at systole has been associated with reduced interference of visually distracting stimuli (Pramme, Larra, Schachinger, & Frings, 2014; Pramme, Larra, Schachinger, & Frings, 2016), prolonged simple and choice reaction times (RTs) towards visual, auditory and tactile stimuli (Birren, Cardon, & Phillips, 1963; McIntyre, Ring, Edwards, & Carroll, 2008; McIntyre, Ring, Hamer, & Carroll, 2007; Saari & Pappas, 1976; Yang, Jennings, & Friedman, 2017), and an attenuated acoustic startle reflex (Schulz, van Dyck, Lutz, Rost, & Voegelé, 2017).

Apart from modulating low-level sensorimotor processes such as signal detection and processing speed, the cardiac cycle has also been shown to influence response inhibition which requires high-level cognitive control. For instance, Rae et al. (2018) observed improved response inhibition in a stop-signal task when the stop signal was presented at systole compared to presentation at diastole. This effect was quantified as participants' tolerance to a longer stop-signal delay (SSD; the delay between the presentation of the go cue and the appearance of the stop signal) at a 50% chance of successfully inhibiting response, and a shorter stop-signal reaction time (SSRT). However, Makowski et al. (2020) found an opposite pattern in a go/no-go task. That is, the probability of stop failure was highest when the no-go cue was presented in the middle of the systole. Furthermore, in a second study using a modified go/no-go task, Rae et al. (2020) found no effect of the cardiac cycle on inhibitory performance, neither commission errors in no-go trials nor the probability of withholding actions in voluntary-inhibition trials were influenced by the cardiac cycle. In addition to the difference in paradigms, the ways these previous studies used to designate the systole-coupling and the diastole-coupling condition were also different. Rae et al. (2018, 2020) delivered stimuli either 290 ms after the electrocardiogram (ECG) R-wave peak or 10 ms before the R-wave peak to have the stimuli coincide with the systole or diastole respectively. In contrast, Makowski et al. (2020) did not time-lock stimuli to specific time points within the cardiac cycle during online data collection but classified trials into the systole-coupling and the diastole-coupling condition during later data analysis. Specifically, trials whose stimulus onset was within the interval between the ECG R-wave peak and the end of the following T wave were clarified into the systole-coupling condition, while trials whose stimulus onset was within the remaining interval (i.e., between the end of the T wave to the next R-wave peak) were clarified into the diastole-coupling condition. The paradigm, operationalization, and the choice of the cardiac parameter render comparison of these studies difficult, resulting in the absence of a simple and straightforward description about the cardiac cycle effect on response inhibition. Furthermore, so far studies have only focused on the contribution of peripheral autonomic markers such as cardiac timing and baroreceptor feedback to sensorimotor skills, while evidence regarding the central, cortical mechanisms underlying the effect is scarce.

The purpose of the current study was therefore to clarify the way the cardiac cycle influences response inhibition by taking both peripheral and central levels into account, which could help us to better understand the precise impact of interoceptive signals on other cognitive processes. The first question we aimed to explore is whether response inhibition is facilitated or disrupted by the cardiac activity at systole. Similar to Rae et al. (2018), the current study adopted a stop-signal task to measure response inhibition, in which some go stimuli were unpredictably followed by a stop signal requiring the cancellation of the prepotent

response. The stop signals were presented either only at systole or at random times within the cardiac cycle by utilizing the timings of the real-time R-wave peaks in the ECG signal. In addition, to capture central electrophysiological responses of response inhibition and cardiac interoceptive processing, we also paired the tasks with electroencephalography (EEG) recordings. The second research question is whether the emotional attribute of the stop signal (i.e., non-emotional or emotional) modulates the cardiac cycle effect on response inhibition. Compared with neutral stimuli, emotionally salient stimuli are more likely to be modulated by the cardiac cycle (Garfinkel et al., 2014; Gray et al., 2012). Our previous studies also showed stronger modulations on the cortical representations of cardiac signals in response to repeated emotional stimuli compared with repeated neutral stimuli (Gentsch et al., 2019; Marshall et al., 2018). These findings demonstrated that the emotional attribute of the stimulus represented a potential factor influencing the cardiac cycle effect. To address this issue, we presented both non-emotional (colored mask) and emotional stimuli (facial expression) in the stop-signal tasks and assigned either the color change (from blue to red) or the facial expression change (from neutral to angry) as the stop signal in separate tasks.

At the behavioral level, we primarily focused on stop-signal reaction times (SSRTs). According to the independent race model, response inhibition in the stop-signal task can be conceptualized as an independent race between go and stop processes, and whichever wins the race determines the response outcome (Logan & Cowan, 1984). While there is no overtly observable response on successful stop trials, the assumptions of this race model provide a method for estimating SSRT, i.e., subtracting the average SSD from the go RT distribution percentile corresponding to the probability of unsuccessful stopping (Logan & Cowan, 1984; Verbruggen et al., 2019). The SSRT estimate is most reliable when the accuracy rate in stop trials is relatively close to 0.50 (Band, van der Molen, & Logan, 2003). The SSRT is known to reflect the duration of the covert response inhibition process (Verbruggen et al., 2019). A shorter SSRT indicates a faster, more efficient response inhibition process. At the electrophysiological level, we assessed the stop-signal P3 component and heartbeat evoked potential (HEP). The stop-signal P3 component is the most common event-related potential (ERP) index of inhibitory control processes. The P3 peak is usually detected around 250–500 ms after the stop signal in the fronto-central brain region (Dimoska, Johnstone, & Barry, 2006; Wessel & Aron, 2015). Increased P3 peak amplitudes generally correlate with more efficient inhibitory processing or higher inhibitory load (Huster, Messel, Thunberg, & Raud, 2020), while decreased P3 peak amplitudes generally reflect impaired inhibitory control (Johnstone, Barry, & Clarke, 2007). In addition, on the basis of the positive correlation between P3 peak latency and SSRT (Kok, Ramautar, De Ruiter, Band, & Ridderinkhof, 2004; Wessel & Aron, 2015), increased P3 peak latency is typically associated with slower inhibition processing (Hughes, Fulham, Johnston, & Michie, 2012). We measured the HEP as an electrophysiological marker of cardiac interoceptive processing. The HEP is a scalp potential time-locked to people's heartbeats (Coll, Hobson, Bird, & Murphy, 2021; Pollatos & Schandry, 2004) and is usually observed across fronto-central electrodes around 200–400 ms after the R-wave peak in the ECG signal (Marshall, Gentsch, Blum, Broering, & Schütz-Bosbach, 2019; Schandry & Montoya, 1996). A recent meta-analysis reported moderate to large effects of attention, arousal, and clinical status on HEP amplitudes, and a moderate correlation between HEP amplitudes and behavioral measures of interoception (Coll et al., 2021), suggesting that the HEP can be considered an established marker of cardiac interoceptive processing. In addition, we also measured participants' interoceptive accuracy and resting heart rate variability (HRV), given that individual difference in these dimensions may potentially influence participants' performance in response inhibition (Baiano et al., 2021; Thayer, Hansen, Saus-Rose, & Johnsen, 2009).

## 2. Materials and methods

### 2.1. Participants

Forty right-handed participants with normal or corrected-to-normal vision and without color blindness, psychiatric or neurological history, diagnosed heart-rhythm abnormalities, as well as current use of medications affecting neural or peripheral physiological function, took part in this study. All participants were naive to the purpose of the study before participation and participated in the study for payment (9 € per hour) or student credit. Consent was obtained from all participants and the procedures were approved by the local ethics committee at the Department of Psychology of LMU Munich in accordance with the Declaration of Helsinki. One participant was excluded for unsuccessful synchronization between stimuli and the ECG signal. Another three were excluded for extremely high accuracy rates in stop trials ( $> 0.70$ ) because it is unreliable to estimate SSRT when the accuracy rate in stop trials deviates substantially from 0.50 (Band et al., 2003; Verbruggen et al., 2019). The final sample was 36 participants (18 females; age range: 19–37 years; mean age:  $24.81 \pm 3.78$  years).

### 2.2. Stimuli

Each visual stimulus for the main experiment was a facial expression covered with a transparent colored mask. The facial expression stimuli came from the validated NimStim database (Tottenham et al., 2009). Specifically, a set of 48 colored photographs were selected for this study either showing neutral or angry facial expressions of 24 actors (12 females, 12 males). The mask was in red (RGB: 255, 0, 0) or blue (RGB: 0, 0, 255) with the transparency value as 40 (0–255: full transparency–full opacity). The combined stimulus of the facial expression and the colored mask was centrally presented in the size of  $506 \times 650$  pixels (width  $\times$  height) on a 24-inch computer screen (refresh rate: 60 Hz; resolution:  $1920 \times 1080$  pixels) at a viewing distance of about 80 cm. A pilot study confirmed that participants could easily distinguish the mask color as well as the facial expression. In addition, none of the participants reported any color or emotion recognition difficulties after the experiment.

### 2.3. Procedure

To evaluate individual differences in interoceptive accuracy and ensure our sample corresponded to a normal cohort in this dimension, participants began the experimental session with a heartbeat tracking task (Marshall, Gentsch, Schröder, et al., 2018; Schandry & Montoya, 1996). In this task, participants reported the number of heartbeats they silently counted during three time periods (25, 35, 45 s) presented in random order, while the actual heartbeats were recorded by ECG. Guessing or manually checking the number of heartbeats was explicitly discouraged. The interoceptive accuracy was indexed by the heartbeat tracking score calculated using the following formula:

$$\frac{1}{3} \sum (1 - (\text{recorded heartbeats} - \text{counted heartbeats}) \div \text{recorded heartbeats})$$

Next, to index individual differences in baseline autonomic sympathetic-parasympathetic balance, resting-state ECG signal was recorded during a period of 2.5 min, while participants kept their eyes open (Rae et al., 2018).

After a short rest, participants completed two revised stop-signal tasks (i.e., the face response task and the color response task) presented using the Presentation software (Neurobehavioral Systems, Inc.).

We aimed to adopt a 2 (target type: face vs. color)  $\times$  3 (heartbeat coupling: no-coupling vs. couple the stop cue to systole vs. couple the distractor cue to systole) within-subject design. Please note that the experimental design was refined after checking the actual synchronization between stimuli and the ECG signal (see *Control Analysis*). Both

the face response task and the color response task consisted of 1 practice session (18 trials) and 9 experimental blocks (3 blocks for each heartbeat coupling condition). Each block consisted of 72 trials (i.e., 24 go trials, 24 go-control trials, and 24 stop trials) which were randomly presented. In other words, each condition included 72 go trials, 72 go-control trials, and 72 stop trials. The order of tasks and the order of heartbeat coupling conditions were counterbalanced across participants. The accuracy rate and mean RT (i.e., averaged RT of the correct go and go-control trials) were presented as visual feedback after each block during the self-paced inter-block rest.

Specifically, in both tasks, there were 3 trial types: go trials, go-control trials, and stop trials, accounting for about 33% of the total trials respectively (see Fig. 1). The go trial only included a go cue which indicated an 'L' button press to be made using the right index finger. The go-control trial included not only a go cue but also a distractor cue which should be ignored. The stop trial included a go cue, a distractor cue, and a stop cue which indicated to withhold the button-press response, i.e., response inhibition. Altogether, the correct response in a go trial and a go-control trial was to press the button, while the correct response in a stop trial was not to press the button. Importantly, to discourage a waiting strategy, participants were required to respond as quickly as possible to the go cue and not wait for the stop cue to occur. Notably, the traditional stop-signal task generally only includes 2 trial types, i.e., the go trials and the stop trials. By adding the go-control trials, we aimed to ensure that participants stopped their action in response to the stop cue rather than the distractor cue in our revised stop-signal tasks.

In addition to the trial types, the types of visual stimuli (i.e., a facial expression covered with a transparent colored mask) were also identical in both tasks. Nevertheless, participants were instructed to pay attention to and respond to either the facial expression or the mask color in different tasks. Specifically, in the face response task, participants should pay attention to the facial expression (target) and ignore the mask color (distractor). The neutral facial expression was the go cue. A color change (from blue to red) served as the distractor cue. A facial expression change (from neutral to angry) served as the stop cue. Conversely, in the color response task, participants should pay attention to the mask color (target) and ignore the facial expression (distractor). The blue mask was the go cue. A facial expression change (from neutral to angry) served as the distractor cue. A color change (from blue to red) served as the stop cue.

Additionally, we synchronized the stimuli onsets to specific time points within the cardiac cycle (more details are described in *Stimulus Timing and Heartbeat Coupling*). In the coupling condition, either the stop cue or the distractor cue was delivered 290 ms after the ECG R-wave peak to coincide with the T wave at cardiac systole, when baroreceptor activation is processed centrally (Edwards, Inui, Ring, Wang, & Kakigi, 2008; Edwards, Ring, McIntyre, Winer, & Martin, 2009; Gray, Rylander, Harrison, Wallin, & Critchley, 2009). This timing (i.e., 290 ms after the R-wave peak) is consistent with stimulus onset timing in the systole-coupling conditions of previous studies (Rae et al., 2020; Rae et al., 2018). In the no-coupling condition, both the stop cue and the distractor cue were presented at random times within the cardiac cycle, i.e., 120–900 ms after the ECG R-wave peak. Notably, inconsistent with previous behavioral studies (Rae et al., 2020; Rae et al., 2018), we did not time-lock the stimuli to the end of cardiac diastole (indexed by the ECG R-wave peak) in the no-coupling/control condition. This is because the concurrence of the heartbeat and the stop cue would make it impossible to disentangle the ERPs related to response inhibition and cardiac interoceptive processing (i.e., the stop-signal P3 component and the HEP respectively) and thus make it inappropriate to compare the ERPs between the coupling and no-coupling conditions in the present study.

(A) Time course and trial structure of the face response task. Participants were required to pay attention to the facial expression and ignore the mask color. The neutral facial expression was the go cue. A color change (from blue to red) served as the distractor cue. A facial

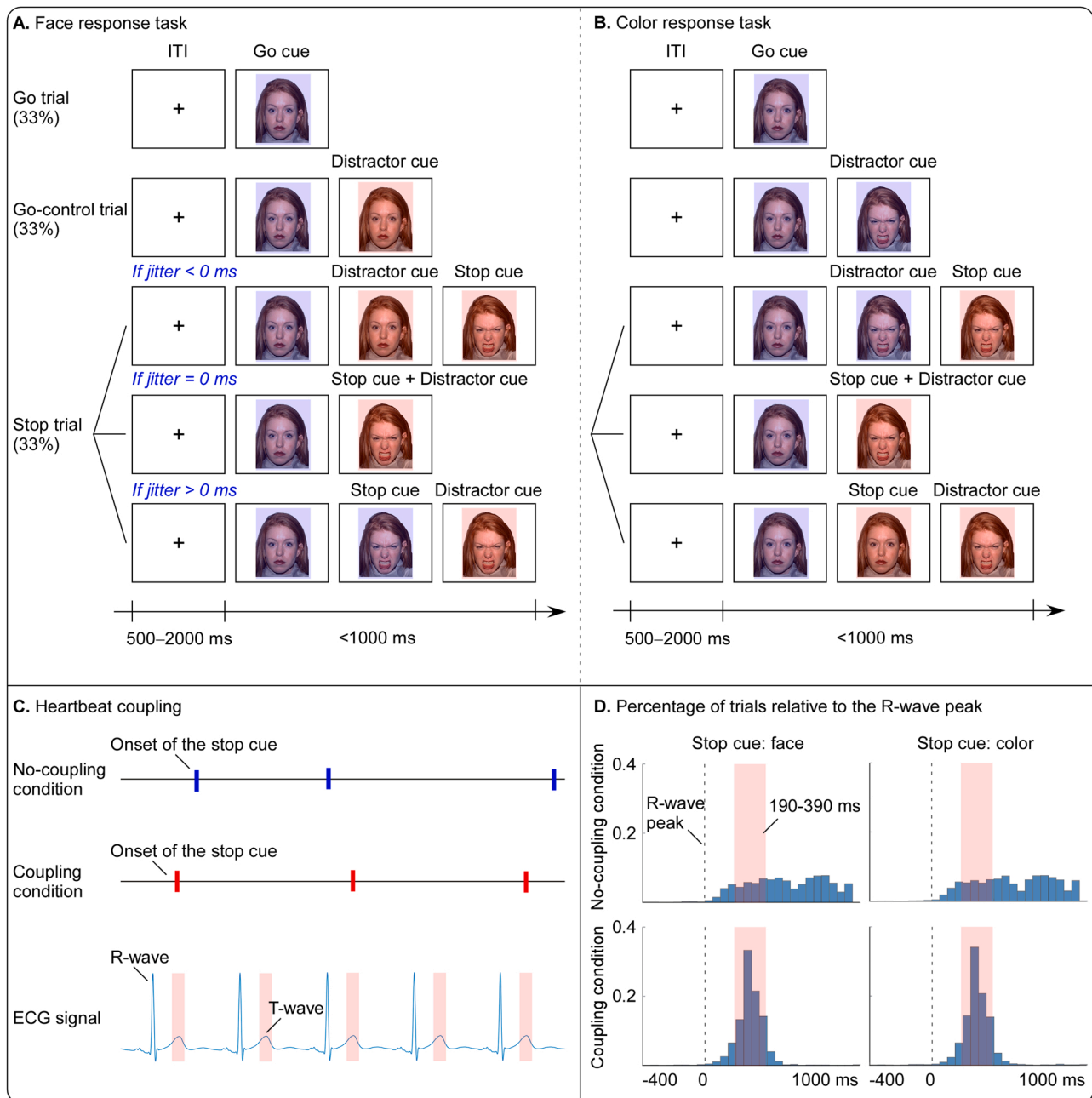


Fig. 1. Schema of the stop-signal tasks.

expression change (from neutral to angry) served as the stop cue. The jitter between the distractor cue and the stop cue was set to  $-100$ – $100$  ms. (B) Time course and trial structure of the color response task. Participants were asked to pay attention to the mask color and ignore the facial expression. The blue mask was the go cue. A facial expression change (from neutral to angry) served as the distractor cue. A color change (from blue to red) served as the stop cue. (C) Intended onset timing of the stop cue with respect to the ECG signal. In the no-coupling condition, the onset of the stop cue was intended to be  $120$ – $900$  ms after the R-wave peak, while in the coupling condition, the onset of the stop cue was intended to be  $290$  ms after the R-wave peak (around the T wave). (D) Actual onset timing of the stop cue relative to the R-wave peak. Data are expressed as the percentage of trials in  $50$ -ms time bins. In the no-coupling condition, the onsets of stop cues were evenly distributed within the cardiac cycle, while in the coupling condition, the onsets of stop cues were within  $200$  ms of the intended timing

at  $290$  ms after the R-wave peak in over  $80\%$  of the stop trials. ITI: inter-trial interval.

#### 2.4. Stimulus timing and heartbeat coupling

To maintain successful stopping at a rate of about  $0.50$  in the stop trials, the delay between the presentation of the go cue and the stop cue, i.e., the stop-signal delay (SSD), was adjusted individually on a trial-by-trial basis. Specifically, the SSD was reduced by  $50$  ms after an incorrect response commission and increased by  $50$  ms after a correctly withheld response. The starting SSD in each block was  $200$  ms, and the SSD was restricted to a range of  $100$ – $800$  ms. In addition, the stop cue and the distractor cue were jittered between  $-100$  and  $100$  ms. In this way, the distractor cue could appear earlier, later, or even simultaneously to the stop cue. Notably, to avoid a situation where the distractor cue appeared at the same time or too shortly after the go cue, the jitter was adjusted to

– 50–50 ms when the SSD was 100 ms. A trial ended when the duration of the trial reached 1000 ms, or when participants successfully responded after the appearance of all possible cues (i.e., the go cue, the distractor cue, and/or the stop cue) in a given trial. A central fixation cross was presented during the inter-trial interval, the duration of which was 500–2000 ms.

The synchronization between stimuli and the ECG signal was realized by interfacing ECG R-wave peaks with the tasks in the Presentation software. Specifically, Presentation received real-time pulses representing R-wave peaks and logged their timings during the whole experiment. According to the expected temporal relationships among the R-wave peak, stop cue, go cue, and/or distractor cue in a trial, the algorithm implemented in Presentation can calculate and set the onset timings of the upcoming stop cue, go cue, and/or distractor cue, once it receives a pulse 500 ms after the onset of the inter-trial interval (detailed calculation methods are illustrated in [Supplementary Figure 1](#)). Notably, the same calculation methods were applied in go-control trials and in stop trials even though there was no stop cue presented in go-control trials. In this way, we ensured identical and thus comparable onset timings of the go cue and the distractor cue (relative to the R-wave peaks) in go-control trials and in the corresponding stop trials. In other words, the only difference between the stop trials and the go-control trials was the appearance of the stop cue. By this means, we aimed to reduce the predictability of the go cue and distractor cue as potential subliminal signals for the trial type. That is, participants could not predict whether the ongoing trial would require response inhibition based on the temporal relationship between the heartbeat and the go cue or distractor cue.

## 2.5. ECG recording and processing

Continuous ECG was recorded using three electrodes placed below the left clavicle (reference electrode), the right clavicle (ground electrode), and the left pectoral muscle (active electrode) respectively. ECG was digitized at a sampling rate of 1000 Hz, with an online high-pass filter at 0.1 Hz, and an online low-pass filter at 1000 Hz. Signal acquisition and amplification were implemented using the BrainVision Recorder software (Brain Products, Inc.), and online detection of the ECG R-wave peaks was achieved using the BrainVision RecView software (Brain Products, Inc.). R-wave peaks were defined as the first decreasing voltage sample after exceeding a constant threshold, which was individually set by the experimenter after visually inspecting the 2.5-min resting-state ECG data. Each detection of the R-wave peak added a marker to the online ECG signal and sent a pulse to the PC controlling the tasks. During the tasks, the pulse-related markers were visually inspected by the experimenter to ensure that R-wave peaks were detected with high precision.

ECG data were offline filtered between 1 and 40 Hz. For the heartbeat tracking task, the actual number of heartbeats was calculated using the Pan-Tompkins algorithm (Pan & Tompkins, 1985; Sedghamiz, 2014) implemented in Matlab. For the resting-state ECG data, the root mean square of successive differences (RMSSD), a widely used index of heart rate variability (HRV), were calculated using the RHRV package (Rodríguez-Liñares, Vila, Mendez, Lado, & Olivieri, 2008) implemented in R. For the ECG data during the stop-signal tasks, the timings of the R-wave peak, T-wave peak, T-wave onset, and T-wave offset in each stop trial were identified using the NeuroKit2 toolbox (Makowski et al., 2021) implemented in Python.

## 2.6. EEG recording and processing

Continuous EEG was recorded using 65 active electrodes (actiCAP, Brain Products, Inc.) and one additional ground electrode, positioned according to the international 10–20 system. EEG was digitized at a sampling rate of 1000 Hz, with an online high-pass filter at 0.1 Hz, and an online low-pass filter at 1000 Hz. The online reference was placed at

electrode FCz. All impedances were kept below 20 k $\Omega$ .

EEG data were preprocessed using MATLAB toolbox FieldTrip (Oostenveld, Fries, Maris, & Schoffelen, 2011). For three participants, one or two bad electrodes were excluded and subsequently replaced via interpolation. EEG data were re-referenced to the common average, filtered between 0.1 and 40 Hz, and down-sampled to 500 Hz. Then, EEG epochs were extracted between –100 and 1600 ms around the onset of the stop cue. Independent component analysis was conducted to identify stereotypical components reflecting eye movements, blinks, and the cardiac field artifact (CFA) which is produced by the movement of the heart muscle and is the main source of contamination of the HEP. The eye-related artifactual components were manually identified and removed based on scalp topography and time course (average of 2.31 components per participant), while CFA-related components were identified using a custom algorithm. Specifically, we first redefined EEG trials around the ECG R-wave peaks. Then, we computed the coherence of the time-frequency data between each independent component and the ECG signal, and selected four components with the highest coherence. Finally, we decided which of the four components should be removed (average of 2.03 components per participant) based on additional characteristics which were commonly associated with CFA, e.g., a bimodal topography, a frequency peak around 5 Hz, and a rhythmically repeating time course (Viola et al., 2009).

For the ERP evoked by the stop cue, epochs were further segmented into periods ranging from –100–600 ms relative to the stop cue, and baseline corrected using the 100-ms interval prior to the onset of the stop cue. Artefact correction (–150 to 150  $\mu$ V) led to an average trial rejection of 0.36%. A current-source-density transformation (Perrin, Pernier, Bertrand, & Echallier, 1989; Tenke & Kayser, 2012) was applied to reduce potentially remaining contamination of other components (order of splines: 4; maximum degree of Legendre polynomials: 10; regularization parameter: 1 e-5). Consistent with previous studies (Beltran, Muneton-Ayala, & de Vega, 2018; Raud, Westerhausen, Doolley, & Huster, 2020), a salient P3 component was identified after the stop cue (see Fig. 2). Following established approaches (Dimoska et al., 2006), peak latencies and amplitudes of P3 components were extracted from single-participant average waveforms for each condition (within 250–500 ms, measured at FC1, FCz, FC2, C1, Cz, and C2). Group-level scalp topographies at the peak latencies were computed by spline interpolation.

For the HEP, epochs were further segmented into periods ranging from –100–600 ms relative to the first R-wave peak detected after the stop cue and before the next go cue, with baseline correction using the 100-ms interval prior to the R-wave peak. Artefact correction (–150 to 150  $\mu$ V) led to an average trial rejection of 0.53%. A current-source-density transformation was also applied to reduce residual CFA and potential contamination from other components. Consistent with previous studies (Marshall et al., 2019), a salient HEP was observed after the R-wave peak (see Fig. 3). A permutation-based, data-driven approach was used to determine the morphology (latency and topography) of the HEP (Marshall, Gentsch, Jelincic, & Schütz-Bosbach, 2017; Marshall, Gentsch, Schröder, et al., 2018). According to our hypothesis and the significant main effect of heartbeat coupling at the behavioral level, we identified neural phenomena that differed for the main effect of heartbeat coupling for this analysis. Specifically, a nonparametric cluster-based permutation *t*-test was applied using the FieldTrip toolbox (Oostenveld et al., 2011) to compare HEP amplitudes in the no-coupling and the coupling condition for all electrodes and for the time window from 0 to 600 ms after the R-wave peak (dependent *t*-test; cluster-defining threshold  $p = .05$ , two-tailed; iterations = 5000). This analysis revealed a significant positive cluster over fronto-centro-parietal electrodes (FC3, FC1, FCz, FC2, FC4, C3, C1, Cz, C2, C4, CP3, CP1, CPz, CP2, CP4, P1, Pz, P2, P4, and P6; ~120–600 ms;  $p < .001$ ). We extracted mean amplitudes of HEPs from single-participant average waveforms for each condition over this cluster for the subsequent analysis. Group-level scalp topographies

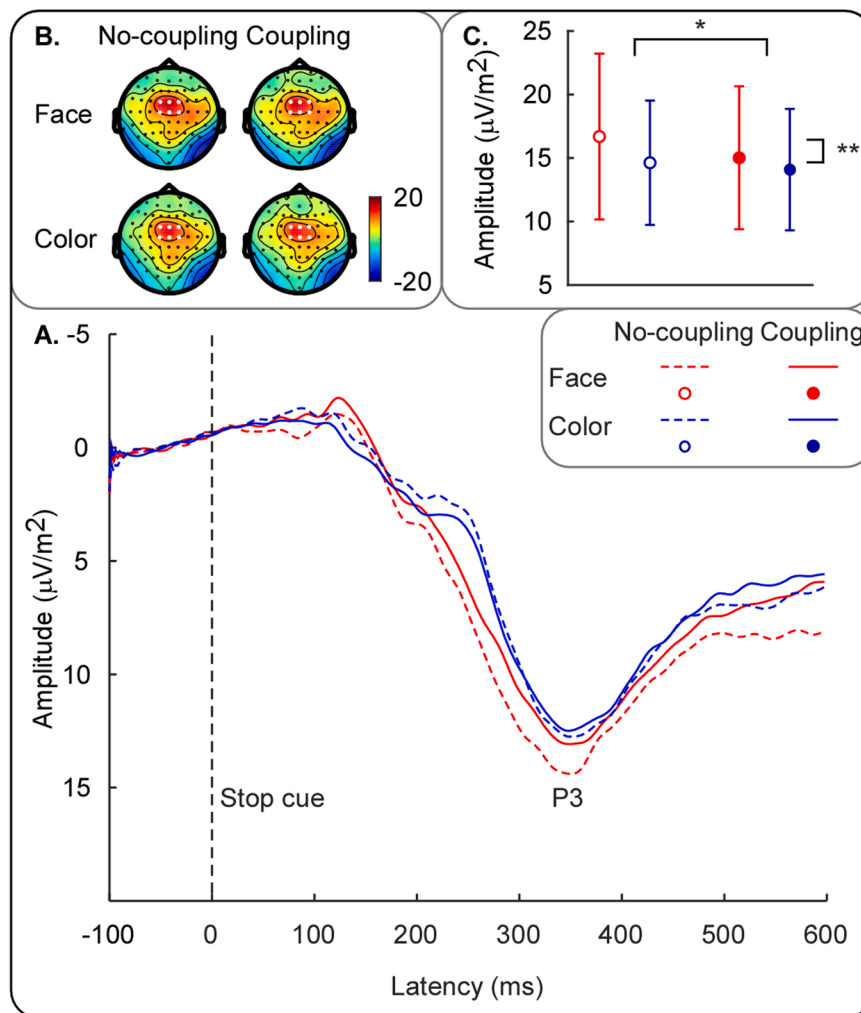


Fig. 2. P3 components evoked by stop signals.

within 120–600 ms were averaged and computed by spline interpolation. We selected the same electrodes and time window when comparing the HEP amplitudes during the resting state, during the inter-trial intervals, and during the task.

## 2.7. Statistical analysis

### 2.7.1. Control analysis

We checked the precision of the synchronization between stimuli and the ECG signal in stop trials for each condition. Specifically, descriptive statistics are separately provided for (1) the percentage of trials presenting the stop cue or distractor cue 190–390 ms after the R-wave peak, (2) the means of the interval between the R-wave peak and the stop cue or distractor cue, and (3) the standard deviations of the interval between the R-wave peak and the stop cue or distractor cue in different conditions (see Table S1). Note that we chose the time window of 190–390 ms because it was impossible to present the stimuli exactly at 290 ms after the R-wave peak in the stop-signal task. Similar analyses were performed in previous research adopting stop-signal task designs (Rae et al., 2018). For the no-coupling condition, stop cue and distractor cue were presented 190–390 ms after the R-wave peak in a minority of trials (~23%), while for the two couple-to-systole conditions (i.e., the ‘couple the stop cue to systole’ condition and the ‘couple the distractor cue to systole’ condition), either stop cue or distractor cue was presented 190–390 ms after the R-wave peak in a majority of trials (~89%). This suggested that the synchronization between stimuli and the ECG signal

in no-coupling condition was different from those in couple-to-systole conditions. However, the synchronization between stimuli and the ECG signal was similar in the two couple-to-systole conditions. Specifically, in the ‘couple the stop cue to systole’ condition, the onset of the stop cue was presented 190–390 ms after the R-wave peak in about 89% of the trials, and the onset of the distractor cue was presented 190–390 ms after the R-wave peak in about 71% of the trials. Similarly, in the ‘couple the distractor cue to systole’ condition, the onset of the stop cue was presented 190–390 ms after the R-wave peak in about 74% of the trials, and the onset of the distractor cue was presented 190–390 ms after the R-wave peak in about 90% of the trials. This similarity in synchronization resulted from the short jitter between the stop cue and the distractor cue (–100 to 100 ms). The fact that both the stop cue and the distractor cue were presented 190–390 ms after the R-wave peak in most trials of either systole alignment conditions made it difficult to disentangle the cardiac cycle effect from the stop or distractor cue respectively.

Therefore, we combined both conditions subsequently and analyzed them as one single condition (the coupling condition). Thus, the experimental design of the present study was refined as a 2 (heartbeat coupling: no-coupling vs. coupling)  $\times$  2 (target type: face vs. color) within-subject design. The aforementioned descriptive statistics about the precision of the synchronization between stimuli and the ECG signal were reanalyzed based on this design (see Table 1). In addition, to confirm that no-coupling condition and coupling condition were different in the synchronization between stimuli and the ECG signal,

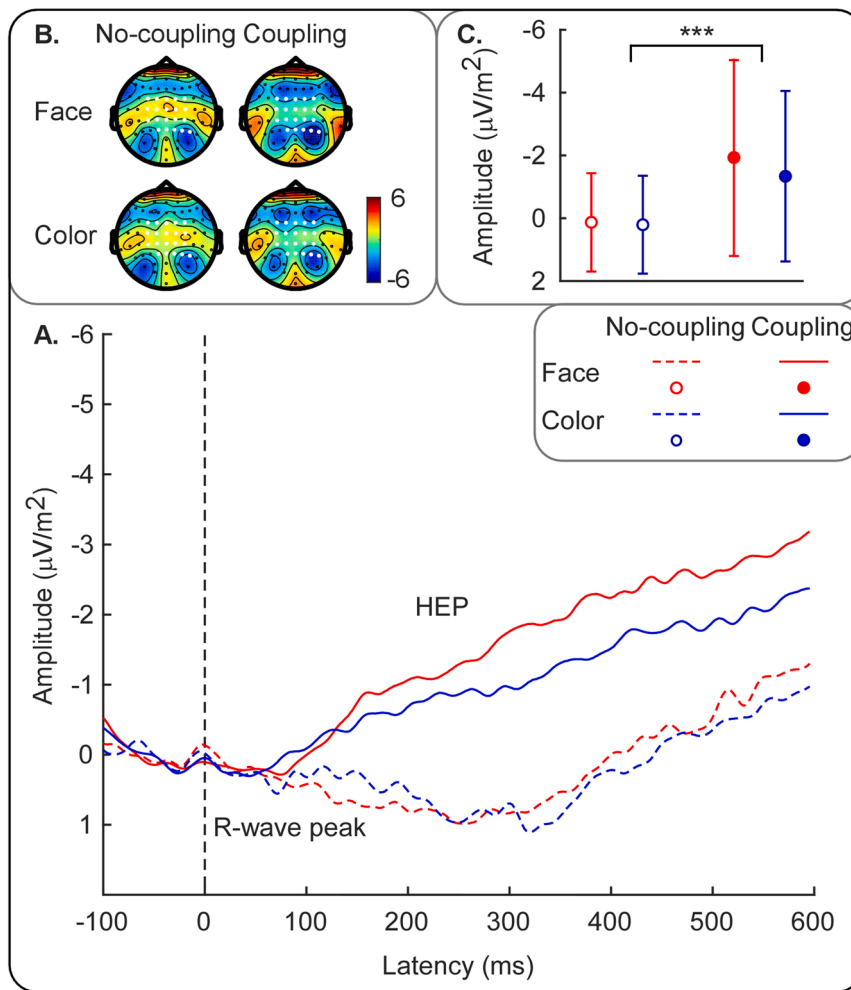


Fig. 3. Heartbeat evoked potentials (HEPs) in different task conditions.

Table 1

Percentage of trials presenting the stop cue or distractor cue 190–390 ms after the R-wave peak as well as means and standard deviations of the interval (ms) between the R-wave peak and the stop cue or distractor cue in different conditions.

	No-coupling condition		Coupling condition	
	Face as target	Color as target	Face as target	Color as target
<b>Percentage of trials</b>				
Stop cue	0.23 ± 0.04	0.23 ± 0.06	0.81 ± 0.07	0.82 ± 0.08
Distractor cue	0.23 ± 0.05	0.23 ± 0.05	0.81 ± 0.06	0.81 ± 0.07
<b>Means</b>				
Stop cue	520.07	518.94	293.60	296.36
	± 27.62	± 29.68	± 10.74	± 10.38
Distractor cue	519.23	522.31	293.28	297.28
	± 27.43	± 31.52	± 11.25	± 10.49
<b>Standard deviations</b>				
Stop cue	247.95	255.35	106.61	108.69
	± 18.59	± 20.47	± 43.09	± 49.57
Distractor cue	259.40	261.35	106.64	109.34
	± 19.55	± 22.56	± 43.18	± 49.22

two-way repeated-measures analyses of variances (ANOVAs) were conducted separately in the percentage of trials presenting the stop cue or distractor cue 190–390 ms after the R-wave peak. The results showed a significant main effect of heartbeat coupling in the percentage of trials

presenting the stop cue 190–390 ms after the R-wave peak ( $F(1,35) = 2386.79, p < .001, \eta_p^2 = 0.986$ ) and in the percentage of trials presenting the distractor cue 190–390 ms after the R-wave peak ( $F(1,35) = 2951.60, p < 0.001, \eta_p^2 = 0.988$ ). Specifically, compared with the no-coupling condition (stop cue:  $0.23 \pm 0.04$ ; distractor cue:  $0.23 \pm 0.04$ ), the coupling condition included a significantly higher percentage of trials presenting the stop cue ( $0.82 \pm 0.07$ ) and distractor cue ( $0.81 \pm 0.07$ ) 190–390 ms after the R-wave peak. These results indicated that the reclassification of the variable levels in heartbeat coupling was reasonable. The subsequent primary analysis was based on this  $2 \times 2$  design.

To further validate the no-coupling and coupling conditions, we calculated (1) the percentage of trials presenting the stop cue or distractor cue at the T wave, i.e., from the T-wave onset to the T-wave offset, (2) the means of the interval between the T-wave peak and the stop cue or distractor cue, and (3) the standard deviations of the interval between the T-wave peak and the stop cue or distractor cue in different conditions (see Table 2). Results of two-way ANOVAs showed a significant main effect of heartbeat coupling in the percentage of trials presenting the stop cue at the T wave ( $F(1,35) = 387.31, p < 0.001, \eta_p^2 = 0.917$ ) and in the percentage of trials presenting the distractor cue at the T wave ( $F(1,35) = 453.87, p < 0.001, \eta_p^2 = .928$ ). Specifically, compared with the no-coupling condition (stop cue:  $0.17 \pm 0.04$ ; distractor cue:  $0.16 \pm 0.04$ ), the coupling condition included a significantly higher percentage of trials presenting the stop cue ( $0.54 \pm 0.11$ ) and distractor cue ( $0.53 \pm 0.11$ ) at the T wave. These results validated the intended synchronization between the stimuli and the ECG T wave in the

**Table 2**

Percentage of trials presenting the stop cue or distractor cue at the T wave (from the T-wave onset to the T-wave offset) as well as means and standard deviations of the interval (ms) between the T-wave peak and the stop cue or distractor cue in different conditions.

	No-coupling condition		Coupling condition	
	Face as target	Color as target	Face as target	Color as target
<b>Percentage of trials</b>				
Stop cue	0.16 ± 0.05	0.18 ± 0.05	0.53 ± 0.12	0.54 ± 0.12
Distractor cue	0.16 ± 0.04	0.17 ± 0.05	0.54 ± 0.11	0.53 ± 0.13
<b>Means</b>				
Stop cue	278.16 ± 39.27	275.74 ± 46.10	51.07 ± 29.60	53.17 ± 31.27
Distractor cue	277.28 ± 40.38	279.15 ± 47.50	50.73 ± 28.79	54.13 ± 31.76
<b>Standard deviations</b>				
Stop cue	252.17 ± 18.29	261.59 ± 22.45	118.11 ± 39.48	122.39 ± 45.97
Distractor cue	263.22 ± 19.14	267.54 ± 24.77	118.57 ± 39.23	123.43 ± 45.43

coupling condition.

**2.7.2. Primary analysis**

First, separate two-way repeated-measures ANOVAs were conducted to analyze behavioral data and ERP data. Behavioral data included: (1) accuracy in go trials, go-control trials, and stop trials; (2) RTs in correct go trials, in correct go-control trials and in incorrect stop trials; (3) mean SSDs; (4) SSRTs calculated by subtracting the mean SSD from the go RT distribution percentile corresponding to the probability of unsuccessful stopping. ERP data included stop-signal P3 peak amplitudes and latencies as well as HEP amplitudes. Post hoc pairwise comparisons were performed when there was a significant interaction effect.

Second, to investigate whether interoceptive accuracy (indexed by heartbeat tracking scores) and resting HRV (indexed by RMSSD) relate to response inhibition, we conducted a series of Pearson correlation analyses between these two variables and all measures of response inhibition, including SSRTs and stop-signal P3 amplitudes in each condition. We corrected *p* values for multiple comparisons using a false discovery rate procedure (Benjamini & Hochberg, 1995).

Third, a one-way repeated-measures ANOVA was performed to compare the HEP amplitudes during the resting state, during the inter-trial intervals, and during the task. Post hoc pairwise comparisons (Bonferroni-corrected) were performed when there was a significant effect.

All analyses were carried out using SPSS 22.0 (IBM Corp.), and the statistical significance level was set at .05. All reported *p* values were Greenhouse-Geisser corrected, where necessary. The effect size in ANOVAs was estimated by partial eta-squared ( $\eta_p^2$ ).

**Table 3**

Means and standard deviations of behavioral data and ERP data in different conditions.

	No-coupling condition		Coupling condition	
	Face as target	Color as target	Face as target	Color as target
Go accuracy	0.87 ± 0.13	0.83 ± 0.17	0.87 ± 0.13	0.86 ± 0.13
Go-control accuracy	0.91 ± 0.11	0.90 ± 0.13	0.90 ± 0.12	0.92 ± 0.09
Stop accuracy	0.55 ± 0.04	0.54 ± 0.06	0.55 ± 0.04	0.53 ± 0.05
Correct go RT (ms)	656.64 ± 123.21	651.84 ± 126.00	663.50 ± 120.66	649.81 ± 120.29
Correct go-control RT (ms)	665.78 ± 121.11	656.01 ± 125.77	660.45 ± 109.16	644.42 ± 113.44
Incorrect stop RT (ms)	602.59 ± 143.53	583.26 ± 144.51	591.02 ± 136.31	567.45 ± 127.15
SSD (ms)	436.54 ± 133.79	421.05 ± 154.23	429.08 ± 125.81	406.10 ± 125.17
SSRT (ms)	207.69 ± 57.81	217.07 ± 72.65	224.43 ± 61.29	231.85 ± 55.45
Stop-signal P3 amplitude ( $\mu\text{V}/\text{m}^2$ )	16.80 ± 6.54	14.72 ± 4.91	15.12 ± 5.64	14.19 ± 4.79
Stop-signal P3 latency (ms)	356.89 ± 58.65	365.00 ± 38.67	368.36 ± 55.17	356.06 ± 33.95
HEP amplitude ( $\mu\text{V}/\text{m}^2$ )	0.14 ± 1.57	0.22 ± 1.56	-1.93 ± 3.15	-1.33 ± 2.72

**3. Results**

**3.1. Behavioral data**

Means and standard deviations of behavioral data in different conditions are summarized in Table 3. Results of the two-way repeated-measures ANOVAs are summarized in Table 4.

Two-way repeated-measures ANOVAs showed a significant main effect of heartbeat coupling for SSRTs ( $F(1,35) = 5.28, p = 0.028, \eta_p^2 = 0.131$ ). SSRTs were prolonged in the coupling condition ( $228.14 \pm 53.35$  ms), i.e., when the stop signal was coupled to the systole, compared with the no-coupling condition ( $212.38 \pm 54.30$  ms), i.e., when the stop signal was presented randomly within the cardiac cycle. However, the main effect of target type and the interaction effect between heartbeat coupling and target type in SSRTs were not significant (both  $p > 0.05$ ). In addition, neither main effects nor interaction effects between heartbeat coupling and target type in go accuracy, go-control accuracy, stop accuracy, correct go RTs, correct go-control RTs, incorrect stop RTs and SSDs were significant (all  $p > 0.05$ ).

**3.2. ERP data**

Means and standard deviations of ERP data in different conditions are also summarized in Table 3. Results of the two-way repeated-measures ANOVAs are summarized in Table 4.

**3.2.1. Stop-signal P3 component**

Grand-average waveforms and scalp topographies of the P3 components elicited by the stop signals are showed in Fig. 2.

For stop-signal P3 peak amplitudes, two-way repeated-measures ANOVA showed significant main effects of heartbeat coupling ( $F(1,35) = 7.41, p = 0.010, \eta_p^2 = 0.175$ ) and target type ( $F(1,35) = 8.24, p = 0.007, \eta_p^2 = 0.191$ ). P3 amplitudes decreased in the coupling condition ( $14.66 \pm 4.92 \mu\text{V}/\text{m}^2$ ), compared to the no-coupling condition ( $15.76 \pm 5.43 \mu\text{V}/\text{m}^2$ ). In addition, stop-signal P3 peak amplitudes decreased when participants responded to the mask color ( $14.46 \pm 4.54 \mu\text{V}/\text{m}^2$ ), compared with responding to the facial expression ( $15.96 \pm 5.92 \mu\text{V}/\text{m}^2$ ). The interaction effect was not significant ( $p > 0.05$ ).

For stop-signal P3 peak latencies, two-way repeated-measures ANOVA showed neither significant main effects nor significant interaction effect between heartbeat coupling and target type (all  $p > 0.05$ ).

(A) Grand-average waveforms of the P3 components elicited by stop signals, i.e., an angry facial expression (red lines) or a red mask (blue lines), presented at systole (solid lines) or presented randomly within the cardiac cycle (dashed lines). (B) Grand-average scalp topographies (time window: 250–500 ms after the stop cue). The fronto-central electrodes (FC1, FCz, FC2, C1, Cz, and C2) used to evaluate P3 amplitudes are marked using enlarged white dots. (C) Compared to when the stop signal was presented randomly within cardiac cycle (i.e., no-coupling condition), P3 amplitudes decreased when the stop signal

**Table 4**

F values of the two-way repeated-measures ANOVAs with two within-subject factors (heartbeat coupling: no-coupling or coupling; target type: face or color).

ANOVA	Go accuracy	Go-control accuracy	Stop accuracy	Correctgo RT	Correctgo-control RT	Incorrectstop RT	SSD	SSRT	Stop-signal P3 latency	Stop-signal P3 amplitude	HEP amplitude
Heartbeat coupling	1.33	0.37	0.33	0.18	2.64	3.38	2.01	5.28	0.07	7.41 <sup>a</sup>	19.05 <sup>b</sup>
Target type	2.15	< 0.01	2.23	0.50	0.89	2.06	1.54	1.25	0.12	8.24 <sup>c</sup>	1.19
Heartbeat coupling × Target type	2.40	1.97	1.01	0.47	0.22	0.09	0.19	0.02	4.08	2.76	1.34

<sup>a</sup> :  $p < 0.05$ ;  
<sup>b</sup> :  $p < 0.001$ .  
<sup>c</sup> :  $p < 0.01$ .

was coupled to the systole (i.e., coupling condition). Additionally, compared with responding to the change of the facial expression (i.e., face condition), P3 amplitudes decreased when participants responded to the change of the color (i.e., color condition). Data are expressed as  $M \pm SD$ . \*:  $p < 0.05$ ; \*\*:  $p < 0.01$ .

**3.2.2. Heartbeat evoked potential**

Grand-average waveforms and scalp topographies of HEPs in different task conditions are shown in Fig. 3.

Two-way repeated-measures ANOVA showed a significant main effect of heartbeat coupling for HEP amplitudes ( $F(1,35) = 19.05$ ,  $p < 0.001$ ,  $\eta_p^2 = 0.352$ ), highlighting increased HEP amplitudes in the coupling condition ( $-1.63 \pm 2.67 \mu V/m^2$ ) compared with the no-coupling condition ( $0.18 \pm 1.17 \mu V/m^2$ ). Neither the main effect of target type nor the interaction effect between heartbeat coupling and

target type was significant (both  $p > 0.05$ ).

Grand-average waveforms of the HEPs when the stop signal was an angry facial expression (red lines) or a red mask (blue lines) presented at systole (solid lines) or presented randomly within the cardiac cycle (dashed lines). (B) Grand-average scalp topographies (time window: 120–600 ms after the R-wave peak). The fronto-centro-parietal electrodes (FC3, FC1, FCz, FC2, FC4, C3, C1, Cz, C2, C4, CP3, CP1, CPz, CP2, CP4, P1, Pz, P2, P4, and P6) used to evaluate HEP amplitudes are marked using enlarged white dots. (C) Compared to when the stop signal was presented randomly within cardiac cycle (i.e., no-coupling condition), HEP amplitudes increased when the stop signal was coupled to systole (i.e., coupling condition). Data are expressed as  $M \pm SD$ . \*\*\*:  $p < 0.001$ .

Neither Interoceptive Accuracy nor Heart Rate Variability Correlated with Response Inhibition.

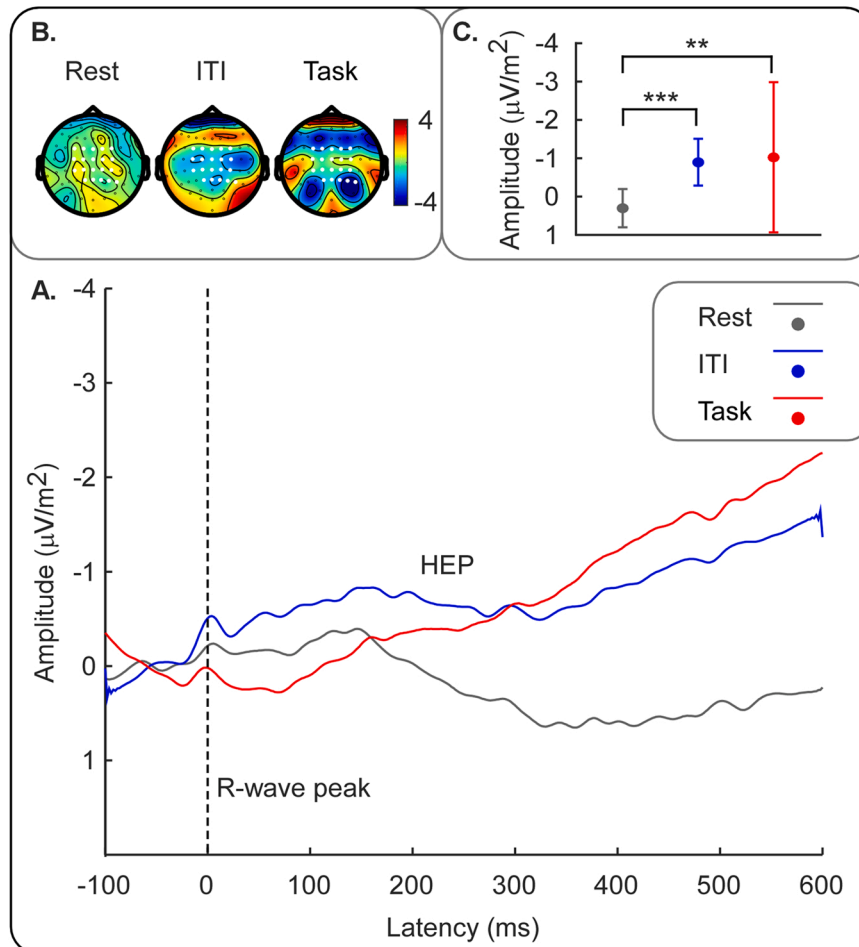


**Fig. 4.** Heartbeat evoked potentials (HEPs) during the resting state, during the inter-trial intervals, and during the task.

The heartbeat tracking score ( $0.61 \pm 0.20$ ) and the resting HRV (RMSSD:  $55.84 \pm 28.71$ ) in the current sample corresponded to previously reported samples of young adults (Marshall et al., 2019; Rae et al., 2020).

Pearson correlation analyses revealed that neither the heartbeat tracking score nor the resting HRV significantly correlated with SSRTs or stop-signal P3 amplitudes in any condition (all  $p > 0.05$ ; see Table S2).

Heartbeat Evoked Potentials Increased During the Task and During the Inter-Trial Intervals Compared to the Resting State.

Grand-average waveforms and scalp topographies of the HEPs during the resting state, during the inter-trial intervals, and during the task are shown in Fig. 4.

One-way repeated-measures ANOVA showed a significant effect ( $F(1.19, 41.68) = 14.08, p < 0.001, \eta_p^2 = 0.287$ ). Post hoc pairwise comparisons showed that HEP amplitudes were smaller during the resting state ( $0.31 \pm 0.50 \mu\text{V}/\text{m}^2$ ), compared to the HEP amplitudes during the intertrial intervals ( $-0.89 \pm 0.61 \mu\text{V}/\text{m}^2, p < .001$ ) and during the task ( $-1.02 \pm 1.96 \mu\text{V}/\text{m}^2, p = 0.001$ ), respectively. However, the HEP amplitudes during the intertrial intervals and during the task were not significantly different ( $p > 0.05$ ).

(A) Grand-average waveforms of the HEPs during the resting state (grey line), during the inter-trial intervals (blue line), and during the task (red line). (B) Grand-average scalp topographies (time window: 120–600 ms after the R-wave peak). The fronto-centro-parietal electrodes (FC3, FC1, FCz, FC2, FC4, C3, C1, Cz, C2, C4, CP3, CP1, CPz, CP2, CP4, P1, Pz, P2, P4, and P6) used to evaluate HEP amplitudes are marked using enlarged white dots. Note that the electrodes and time window were chosen to match those used in Fig. 3. (C) HEP amplitudes were smaller during the resting state compared to the HEP amplitudes during the intertrial intervals and during the task, respectively. However, the HEP amplitudes during the intertrial intervals and during the task were not significantly different. ITI: inter-trial interval. Data are expressed as  $M \pm SD$ . \*\*:  $p < 0.01$ ; \*\*\*:  $p < 0.001$ .

#### 4. Discussion

By pairing stop-signal tasks with ECG and EEG recordings, the current study aimed to clarify the cardiac cycle effect upon response inhibition at both peripheral and central levels. There are three main findings. First, we observed prolonged SSRTs and reduced stop-signal P3 peak amplitudes when the stop signal was presented during the cardiac systole, compared to when the stop signal was presented randomly within the cardiac cycle (i.e., no-coupling condition). This result indicates that response inhibition is disrupted by the alignment of the action-relevant signals to the cardiac systole. Systole alignment of the stop signal also resulted in increased HEP amplitudes, reflecting elevated cortical processing of the cardiac signals. Third, the before-mentioned effects occurred not only in a task assigning an angry facial expression as the stop signal but also in a task assigning a red mask as the stop signal, suggesting that the emotional significance of the stop signal did not influence the cardiac cycle effect on response inhibition. Taken together, these results demonstrate that cardiac signals can have an impeding effect on response inhibition and its neurophysiological signature.

Consistent with a previous study using a go/no-go paradigm (Makowski et al., 2020), the present study demonstrates that response inhibition was disrupted at systole using a stop-signal paradigm. Specifically, stop signals presented at systole resulted in prolonged SSRTs and reduced stop-signal P3 peak amplitudes, reflecting lower response inhibition efficiency (Huster et al., 2020; Verbruggen et al., 2019). Similarly, Larra, Finke, Wascher, and Schachinger (2020) found that, in a sensorimotor conflict task, participants reacted faster to response compatible stimuli but slower to incompatible stimuli at systole compared to diastole. Considering that processing response incompatible stimuli had much higher demands for cognitive control compared to processing response compatible stimuli, these results indicate that the

recruitment of high-level cognitive control leads to an inhibitory effect of cardiac activity at systole on action regulation. We thus argue that the disrupted response inhibition at systole in the present study may be attributed to the inhibitory effect of systolic cardiac signals on cognitive (motor) control processes. This view coincides with the known inhibitory effect of arterial baroreceptor firing on the activity of cortical regions such as the dorsolateral prefrontal cortex which is engaged in cognitive control (Niendam et al., 2012; Pramme, Schaechinger, & Frings, 2015; Simmonds, Pekar, & Mostofsky, 2008). Notably, we cannot exclude the possibility that systolic cardiac signals also inhibited perceptual processes of the stop signal, given that spontaneous internal activity such as systolic cardiac signals has been found to block external sensory detection (Al et al., 2020; Dehaene & Changeux, 2005; Salomon et al., 2018). In a broader context, the suppression of behavior relies on a cascade of subprocesses, including both low-level perceptual processes such as signal detection and high-level cognitive control processes (Raud et al., 2020). How these subprocesses are modulated by the cardiac cycle is an interesting potential topic for future research. Additionally, the present study demonstrates that neither interoceptive accuracy nor resting HRV was related to response inhibition, which is consistent with previous studies (Rae et al., 2020; Rae et al., 2018). This observation suggests that the individual difference in these dimensions did not influence participants' performance in our stop-signal task.

Interestingly and contrary to our findings, one previous study reported a facilitation effect of systolic cardiac signals on response inhibition in a stop-signal task (Rae et al., 2018). The discrepancies in results may be due to the different types of stop signals used. Specifically, in our study, the stop signal only included visual stimuli, while in the previous study, in addition to a color change of the original visual stimulus, the stop signal was accompanied by a concurrent auditory tone. This simultaneous presentation of visual and auditory stimuli may have facilitated participants' responses to the stop signal. This phenomenon, i.e., a concurrent stimulus of a different sensory modality speeds up the reaction to the imperative stimulus, is known as the accessory stimulus effect (Jepma, Wagenmakers, Band, & Nieuwenhuis, 2009). This effect has repeatedly been observed not only in simple and choice RT tasks (Bernstein, 1970; Stoffels, Van der Molen, & Keuss, 1985) but also in tasks involving higher-order cognitive control such as the Simon task (Fischer, Plessow, & Kiesel, 2010). Moreover, a recent study found that the cardiac cycle did not influence the accessory stimulus effect, and the cardiac cycle modulated RTs only when accessory stimuli were absent (Yang et al., 2017). We therefore argue that, in Rae et al. (2018)'s study, the real effect of the cardiac cycle on response inhibition may be overshadowed in the presence of the accessory stimulus effect. This explanation also converges with the view that the cardiac cycle effect is rather small and sensitive to other cognitive processes (Makowski et al., 2020). While this subtle difference in stop signals may contribute to the discrepancies in cardiac cycle effect on response inhibition, it also underlines the need for further exploration.

The second main finding is that impaired response inhibition at systole was accompanied by increased cortical representations of cardiac signals, manifesting as increased HEP amplitudes. The modulations of HEP amplitudes are considered to reflect attentional shifts between external stimuli and internal bodily states (Garcia-Cordero et al., 2017; Petzschner et al., 2019). Higher HEP amplitudes correlate with more attention to cardiac interoceptive information. Therefore, our finding indicates that participants paid more attention to internal cardiac signals when the stop signal was presented at systole compared with the no-coupling condition. Due to the limitations of attentional and representational resources (Franconeri, Alvarez, & Cavanagh, 2013), the more resources internal cardiac signals occupy, the fewer resources the external stop signal could use, thereby reducing response inhibition efficiency in the stop-signal task. From this perspective, our finding suggests that systolic cardiac signals disrupt response inhibition, potentially via an attentional trade-off mechanism that primes interoceptive attention over exteroceptive focus. Relatedly, Rae et al. (2020) found

that people with better interoceptive sensitivity tended to withhold actions and respond slower, while those with poorer interoceptive sensitivity tended to execute actions and respond faster when they saw the visual cue signaling a voluntary choice to make or withhold action. Given that stronger attention to internal states correlates with better interoceptive sensitivity (Ainley, Tajadura-Jiménez, Fotopoulou, & Tsakiris, 2012), these findings suggest that people with more attentional resources allocated to interoceptive information had fewer urges to move the body and had prolonged RTs, reflecting an attention competition between interoceptive processes and voluntary action responses. This also converges with the attentional trade-off mechanism.

A recent study found that participants had smaller HEP amplitudes when they engaged in a somatosensory task compared to a resting-state condition, which is considered to support the attentional trade-off mechanism (Al et al. 2021). Interestingly, the present study found that participants exhibited higher HEP amplitudes when they engaged in a stop-signal task (regardless of whether the component was measured directly after a withheld response or during the inter-trial intervals) compared to in a resting-state condition. Moreover, the HEP amplitudes during the inter-trial intervals were comparable to those during the period right after withholding the response. Given that there was neither a behavioral response nor an external stimulus during the inter-trial intervals, we argue that the increases in HEP amplitudes in the stop-signal task compared to the resting-state condition cannot be attributed to movement-related or stimulus-related processing. One possible explanation for this difference would be the increase of overall attentional resources in the stop-signal task compared to the eyes-opened resting-state condition. In other words, the total amount of attentional resources allocated to interoceptive and exteroceptive processing may be much higher when participants engaged in the stop-signal task than when they were resting with their eyes open. This point was validated by previous neuroimaging evidence that response inhibition produced strong activations in the ventral attention network, including the left supplementary area, precentral gyrus, and superior parietal gyrus (Zhang, Geng, & Lee, 2017). Therefore, we argue that this finding could not be considered as an objection for the proposed attentional trade-off mechanism. Notably, in the previous study (Al et al., 2021), HEP analyses only included trials where the somatosensory stimulation occurred at least 400 ms after the preceding R-wave peak. The total recruitment of attentional resources during this selected period in the somatosensory task may therefore not differ from the resting-state condition in Al and colleagues' task. Therefore, our explanation (i.e., the modulation of overall attentional resources) may be not applicable for their finding. Future studies should take the potential modulation of overall attentional resources into closer consideration when comparing interoceptive attention in different conditions.

Our third main finding is that the emotional attribute of the stop signal did not interact with the cardiac cycle effect on response inhibition. Previous studies taking the emotional attribute into account usually adopted facial expressions with different emotional categories as the materials and compared cardiac cycle effects on the processing of non-emotional (i.e., neutral) and emotional (e.g., fear) facial expressions (Garfinkel et al., 2014; Gray et al., 2012). However, restricted by the nature of the stop-signal paradigm, we cannot simply use non-emotional and emotional facial expressions as the stop signals to compare the corresponding cardiac cycle effects. Specifically, we should keep the emotional attributes of the go cues identical (i.e., non-emotional), and vary the emotional attributes of the stop cues (i.e., non-emotional or emotional) in different conditions. To address this issue, we took the color change (from blue to red) as the non-emotional stop signals while the facial expression change (from neutral to angry) as the emotional stop signals in the present study. To the best of our knowledge, the current study was the first to directly compare the cardiac cycle effects on the processing of simple, non-emotional stimuli and complex, emotional stimuli. Our result suggests that the cardiac cycle has similar effects on response inhibition regardless of the stop signal being simple

and non-emotional, or complex and emotional.

Previous work has reported cardiac cycle effects on the perception of simple and non-emotional stimuli, and the perception of complex and emotional stimuli, separately. Fearful or disgusted facial expressions were judged as more intense when presented at systole, while the intensity ratings of sad, happy, and neutral facial expressions were not influenced by the cardiac cycle (Garfinkel et al., 2014; Gray et al., 2012). This suggested that the cardiac cycle tended to affect the perception of facial expressions with threatening or aversive information. Given that angry facial expressions are generally perceived as threatening signals (Davis et al., 2011), the cardiac cycle may impact the perception of angry facial expressions in the present study. Cardiac cycle effects have also been repeatedly reported in the perception of simple, non-emotional visual stimuli such as abstract shapes or colors (Makowski et al., 2020; Pramme et al., 2014). Therefore, the cardiac cycle may also influence the perception of mask colors in the present study. Our finding implies that the cardiac cycle effect on simple and non-emotional stimuli is comparable with that on complex and emotional stimuli when attentional resources are intense.

Some limitations of the present study should be noted. First, our original experimental design included a separate factor to explore whether the systole needs to be coupled to the target cue or the distractor cue to produce an effect on response inhibition. However, due to the similar synchronization procedures between the stimuli and the ECG signal (see *Control Analysis*), we were unable to disentangle the conditions in which either the stop cue or distractor cue was aligned to the systole. We therefore combined the data in the two conditions and simplified the design accordingly. To address this conflation, future studies could consider increasing the temporal jitter between the occurrence of the stop cue and the distractor cue. This setting would ensure that in the target alignment condition the stop cue reliably appears during the systole in the majority of trials, while at the same time the distractor cue occurs at systole on few occasions, and vice versa for the distractor alignment condition. Second, a few trials in the no-coupling condition fell within the "coupling" period (i.e., around the T wave), which contaminated the no-coupling condition. However, we did not reclassify these trials into the coupling condition, because then we would have been unable to obtain reliable SSRT estimates based on the reclassified trials. In line with previous literature, in each condition, the estimation of SSRT uses the RTs in the go trials, the SSDs in the stop trials, and the accuracy rate in the stop trials (see e.g., Verbruggen et al., 2019). Although the existence of these "contaminated" trials weakened the difference between the no-coupling and coupling conditions, we observed impaired response inhibition in the coupling condition compared to the no-coupling condition. It is reasonable to speculate that the "uncontaminated" cardiac cycle effect on response inhibition is even more pronounced than the present study revealed.

In conclusion, response inhibition is disrupted at systole, as reflected by prolonged SSRTs, reduced stop-signal P3 peak amplitudes, and increased HEP amplitudes. We explain this heart-brain interaction within the framework of spontaneous shifts of attention between exteroception and interoception. Our findings highlight the role of interoceptive signals for other cognitive processes such as inhibitory control and hereby contribute to a more holistic understanding of action regulation and the development of interventions for patients with atypical interoception.

#### CRediT authorship contribution statement

Qiaoyue Ren, Amanda C. Marshall, and Simone Schütz-Bosbach designed the study. Qiaoyue Ren and Jakob Kaiser acquired and analysed the data. Qiaoyue Ren, Amanda C. Marshall, and Simone Schütz-Bosbach wrote the paper.

## Funding

This work was supported by Deutsche Forschungsgemeinschaft [SCHU 2471/5-1 to S.S.-B.] and China Scholarship Council [grant number 202004910347 to Q.R.]. The authors have no conflicts of interest to disclose.

## Data Availability Statement

The datasets generated for this study are available on request to the corresponding author.

## Acknowledgments

We thank Madalina Buciuman and Roman Belenya for their assistance in data collection.

## Appendix A. Supporting information

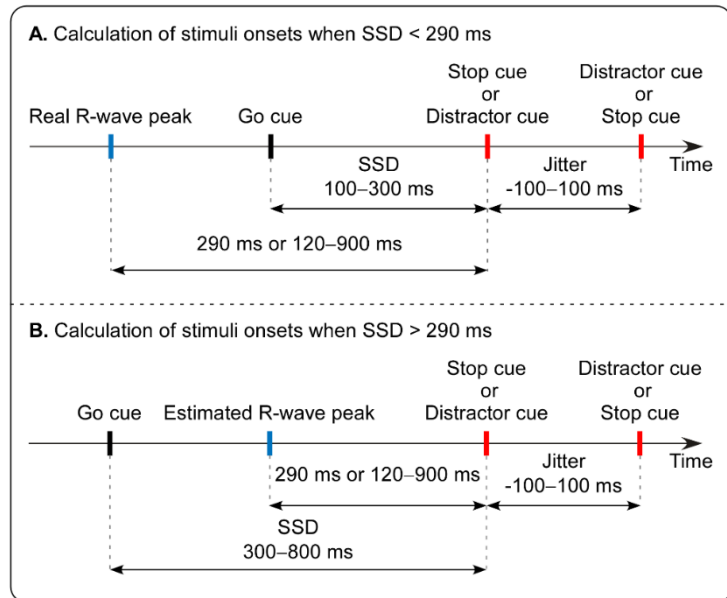
Supplementary data associated with this article can be found in the online version at [doi:10.1016/j.biopsycho.2022.108323](https://doi.org/10.1016/j.biopsycho.2022.108323).

## References

- Adelhofer, N., Schreier, M. L., & Beste, C. (2020). Cardiac cycle gated cognitive-emotional control in superior frontal cortices. *NeuroImage*, 222, Article 117275. <https://doi.org/10.1016/j.neuroimage.2020.117275>
- Ainley, V., Tajadura-Jiménez, A., Fotopoulou, A., & Tsakiris, M. (2012). Looking into myself: the effect of self-focused attention on interoceptive sensitivity. *Psychophysiology*, 49(11), 1504–1508. <https://doi.org/10.1111/j.1469-8986.2012.01468.x>
- Al, E., Iliopoulos, F., Forschack, N., Nierhaus, T., Grund, M., Motyka, P., & Villringer, A. (2020). Heart-brain interactions shape somatosensory perception and evoked potentials. *The Proceedings of the National Academy of Sciences*, 117(19), 10575–10584. <https://doi.org/10.1073/pnas.1915629117>
- Al, E., Iliopoulos, F., Nikulin, V. V., & Villringer, A. (2021). Heartbeat and somatosensory perception. *NeuroImage*, 238, Article 118247. <https://doi.org/10.1016/j.neuroimage.2021.118247>
- Azzalini, D., Rebollo, I., & Tallon-Baudry, C. (2019). Visceral signals shape brain dynamics and cognition. *Trends in Cognitive Sciences*, 23(6), 488–509. <https://doi.org/10.1016/j.tics.2019.03.007>
- Baiano, C., Santangelo, G., Senese, V. P., Di Mauro, G., Lauro, G., Piacenti, M., & Conson, M. (2021). Linking perception of bodily states and cognitive control: the role of interoception in impulsive behaviour. *Experimental Brain Research*, 239(3), 857–865. <https://doi.org/10.1007/s00221-020-06022-3>
- Band, G. P., van der Molen, M. W., & Logan, G. D. (2003). Horse-race model simulations of the stop-signal procedure. *Acta Psychologica*, 112(2), 105–142. [https://doi.org/10.1016/s0001-6918\(02\)00079-3](https://doi.org/10.1016/s0001-6918(02)00079-3)
- Beltran, D., Muneton-Ayala, M., & de Vega, M. (2018). Sentential negation modulates inhibition in a stop-signal task. Evidence from behavioral and ERP data. *Neuropsychologia*, 112, 10–18. <https://doi.org/10.1016/j.neuropsychologia.2018.03.004>
- Benjamini, Y., & Hochberg, Y. (1995). Controlling the false discovery rate: a practical and powerful approach to multiple testing. *Journal of the Royal Statistical Society: Series B (Statistical Methodology)*, 57(1), 289–300. <https://doi.org/10.1111/j.2517-6161.1995.tb02031.x>
- Bernstein, I. H. (1970). Can we see and hear at the same time?: Some recent studies of intersensory facilitation of reaction time. *Acta Psychologica*, 33, 21–35. [https://doi.org/10.1016/0001-6918\(70\)90119-8](https://doi.org/10.1016/0001-6918(70)90119-8)
- Birren, J. E., Cardon, P. V., & Phillips, S. L. (1963). Reaction time as a function of the cardiac cycle in young adults. *Science*, 140(3563), 195–196. <https://doi.org/10.1126/science.140.3563.195-a>
- Bonaz, B., Lane, R. D., Oshinsky, M. L., Kenny, P. J., Sinha, R., Mayer, E. A., & Critchley, H. D. (2021). Diseases, disorders, and comorbidities of interoception. *Trends in Neurosciences*, 44(1), 39–51. <https://doi.org/10.1016/j.tins.2020.09.009>
- Coll, M.-P., Hobson, H., Bird, G., & Murphy, J. (2021). Systematic review and meta-analysis of the relationship between the heartbeat-evoked potential and interoception. *Neuroscience & Biobehavioral Reviews*, 122, 190–200. <https://doi.org/10.1016/j.neubiorev.2020.12.012>
- Craig, A. D. (2002). How do you feel? Interoception: the sense of the physiological condition of the body. *Nature Reviews Neuroscience*, 3(8), 655–666. <https://doi.org/10.1038/nrn894>
- Critchley, H. D., & Garfinkel, S. N. (2018). The influence of physiological signals on cognition. *Current Opinion in Behavioral Sciences*, 19, 13–18. <https://doi.org/10.1016/j.cobeha.2017.08.014>
- Critchley, H. D., & Harrison, N. A. (2013). Visceral influences on brain and behavior. *Neuron*, 77(4), 624–638. <https://doi.org/10.1016/j.neuron.2013.02.008>
- Davis, F. C., Somerville, L. H., Ruberry, E. J., Berry, A. B. L., Shin, L. M., & Whalen, P. J. (2011). A tale of two negatives: differential memory modulation by threat-related facial expressions. *Emotion*, 11(3), 647–655. <https://doi.org/10.1037/a0021625>
- Dehaene, S., & Changeux, J. P. (2005). Ongoing spontaneous activity controls access to consciousness: a neuronal model for inattention blindness. *PLOS Biology*, 3(5), Article e141. <https://doi.org/10.1371/journal.pbio.0030141>
- Dimoska, A., Johnstone, S. J., & Barry, R. J. (2006). The auditory-evoked N2 and P3 components in the stop-signal task: indices of inhibition, response-conflict or error-detection? *Brain and Cognition*, 62(2), 98–112. <https://doi.org/10.1016/j.bandc.2006.03.011>
- Edwards, L., Inui, K., Ring, C., Wang, X., & Kakigi, R. (2008). Pain-related evoked potentials are modulated across the cardiac cycle. *Pain*, 137(3), 488–494. <https://doi.org/10.1016/j.pain.2007.10.010>
- Edwards, L., Ring, C., McIntyre, D., Winer, J. B., & Martin, U. (2009). Sensory detection thresholds are modulated across the cardiac cycle: evidence that cutaneous sensibility is greatest for systolic stimulation. *Psychophysiology*, 46(2), 252–256. <https://doi.org/10.1111/j.1469-8986.2008.00769.x>
- Fischer, R., Plessow, F., & Kiesel, A. (2010). Auditory warning signals affect mechanisms of response selection: evidence from a Simon task. *Exp. Psychol.*, 57(2), 89–97. <https://doi.org/10.1027/1618-3169/a000012>
- Franconeri, S. L., Alvarez, G. A., & Cavanagh, P. (2013). Flexible cognitive resources: competitive content maps for attention and memory. *Trends in Cognitive Sciences*, 17(3), 134–141. <https://doi.org/10.1016/j.tics.2013.01.010>
- Galvez-Pol, A., McConnell, R., & Kilner, J. M. (2020). Active sampling in visual search is coupled to the cardiac cycle. *Cognition*, 196, Article 104149. <https://doi.org/10.1016/j.cognition.2019.104149>
- Garcia-Cordero, I., Esteves, S., Mikulan, E. P., Hesse, E., Baglivo, F. H., Silva, W., & Sedenlo, L. (2017). Attention, in and out: scalp-level and intracranial EEG correlates of interoception and exteroception. *Frontiers in Neuroscience*, 11, 411. <https://doi.org/10.3389/fnins.2017.00411>
- Garfinkel, S. N., & Critchley, H. D. (2016). Threat and the body: how the heart supports fear processing. *Trends in Cognitive Sciences*, 20(1), 34–46. <https://doi.org/10.1016/j.tics.2015.10.005>
- Garfinkel, S. N., Minati, L., Gray, M. A., Seth, A. K., Dolan, R. J., & Critchley, H. D. (2014). Fear from the heart: sensitivity to fear stimuli depends on individual heartbeats. *Journal of Neuroscience*, 34(19), 6573–6582. <https://doi.org/10.1523/JNEUROSCI.3507-13.2014>
- Gentsch, A., Sel, A., Marshall, A. C., & Schütz-Bosbach, S. (2019). Affective interoceptive inference: evidence from heart-beat evoked brain potentials. *Human Brain Mapping*, 40(1), 20–33. <https://doi.org/10.1002/hbm.24352>
- Gray, M. A., Beacher, F. D., Minati, L., Nagai, Y., Kemp, A. H., Harrison, N. A., & Critchley, H. D. (2012). Emotional appraisal is influenced by cardiac afferent information. *Emotion*, 12(1), 180–191. <https://doi.org/10.1037/a0025083>
- Gray, M. A., Rylander, K., Harrison, N. A., Wallin, B. G., & Critchley, H. D. (2009). Following one's heart: cardiac rhythms gate central initiation of sympathetic reflexes. *Journal of Neuroscience*, 29(6), 1817–1825. <https://doi.org/10.1523/jneurosci.3363-08.2009>
- Hughes, M. E., Fulham, W. R., Johnston, P. J., & Michie, P. T. (2012). Stop-signal response inhibition in schizophrenia: behavioural, event-related potential and functional neuroimaging data. *Biological Psychology*, 89(1), 220–231. <https://doi.org/10.1016/j.biopsycho.2011.10.013>
- Huster, R. J., Messel, M. S., Thunberg, C., & Raud, L. (2020). The P300 as marker of inhibitory control—fact or fiction? *Cortex*, 132, 334–348. <https://doi.org/10.1016/j.cortex.2020.05.021>
- Jepma, M., Wagenmakers, E. J., Band, G. P., & Nieuwenhuis, S. (2009). The effects of accessory stimuli on information processing: evidence from electrophysiology and a diffusion model analysis. *Journal of Cognitive Neuroscience*, 21(5), 847–864. <https://doi.org/10.1162/jocn.2009.21063>
- Johnstone, S. J., Barry, R. J., & Clarke, A. R. (2007). Behavioural and ERP indices of response inhibition during a stop-signal task in children with two subtypes of Attention-Deficit Hyperactivity Disorder. *International Journal of Psychophysiology*, 66(1), 37–47. <https://doi.org/10.1016/j.ijpsycho.2007.05.011>
- Khalsa, S. S., Adolphs, R., Cameron, O. G., Critchley, H. D., Davenport, P. W., Feinstein, J. S., & Interoception Summit, P. (2018). Interoception and mental health: a roadmap. *Biological Psychiatry: Cognitive Neuroscience and Neuroimaging*, 3(6), 501–513. <https://doi.org/10.1016/j.bpsc.2017.12.004>
- Kok, A., Ramautaur, J. R., De Ruiter, M. B., Band, G. P., & Ridderinkhof, K. R. (2004). ERP components associated with successful and unsuccessful stopping in a stop-signal task. *Psychophysiology*, 41(1), 9–20. <https://doi.org/10.1046/j.1469-8986.2003.00127.x>
- Larra, M. F., Finke, J. B., Wascher, E., & Schachinger, H. (2020). Disentangling sensorimotor and cognitive cardioafferent effects: a cardiac-cycle-time study on spatial stimulus-response compatibility. *Scientific Reports*, 10, 4059. <https://doi.org/10.1038/s41598-020-61068-1>
- Logan, G. D., & Cowan, W. B. (1984). On the ability to inhibit thought and action: a theory of an act of control. *Psychological Review*, 91(3), 295–327. <https://doi.org/10.1037/0033-295X.91.3.295>
- Makowski, D., Pham, T., Lau, Z. J., Brammer, J. C., Lespinasse, F., Pham, H., & Chen, S. A. (2021). NeuroKit2: a Python toolbox for neurophysiological signal processing. *Behavior Research Methods*, 53, 1689–1696. <https://doi.org/10.3758/s13428-020-01516-y>
- Makowski, D., Sperduti, M., Blonde, P., Nicolas, S., & Piolino, P. (2020). The heart of cognitive control: cardiac phase modulates processing speed and inhibition. *Psychophysiology*, 57(3), Article e13490. <https://doi.org/10.1111/psyp.13490>

- Marshall, A. C., Gentsch, A., Blum, A. L., Broering, C., & Schütz-Bosbach, S. (2019). I feel what I do: relating interoceptive processes and reward-related behavior. *NeuroImage*, *191*, 315–324. <https://doi.org/10.1016/j.neuroimage.2019.02.032>
- Marshall, A. C., Gentsch, A., Jelencic, V., & Schütz-Bosbach, S. (2017). Exteroceptive expectations modulate interoceptive processing: repetition-suppression effects for visual and heartbeat evoked potentials. *Scientific Reports*, *7*, 16525. <https://doi.org/10.1038/s41598-017-16595-9>
- Marshall, A. C., Gentsch, A., Schröder, L., & Schütz-Bosbach, S. (2018). Cardiac interoceptive learning is modulated by emotional valence perceived from facial expressions. *Social Cognitive and Affective Neuroscience*, *13*(7), 677–686. <https://doi.org/10.1093/scan/nsy042>
- Marshall, A. C., Gentsch, A., & Schütz-Bosbach, S. (2018). The interaction between interoceptive and action states within a framework of predictive coding. *Frontiers in Psychology*, *9*, 180. <https://doi.org/10.3389/fpsyg.2018.00180>
- Marshall, A. C., Gentsch, A., & Schütz-Bosbach, S. (2020). Interoceptive cardiac expectations to emotional stimuli predict visual perception. *Emotion*, *20*(7), 1113–1126. <https://doi.org/10.1037/em00006631>
- McIntyre, D., Ring, C., Edwards, L., & Carroll, D. (2008). Simple reaction time as a function of the phase of the cardiac cycle in young adults at risk for hypertension. *Psychophysiology*, *45*(2), 333–336. <https://doi.org/10.1111/j.1469-8986.2007.00619.x>
- McIntyre, D., Ring, C., Hamer, M., & Carroll, D. (2007). Effects of arterial and cardiopulmonary baroreceptor activation on simple and choice reaction times. *Psychophysiology*, *44*(6), 874–879. <https://doi.org/10.1111/j.1469-8986.2007.00547.x>
- Niendam, T. A., Laird, A. R., Ray, K. L., Dean, Y. M., Glahn, D. C., & Carter, C. S. (2012). Meta-analytic evidence for a superordinate cognitive control network subserving diverse executive functions. *Cognitive, Affective, & Behavioral Neuroscience*, *12*(2), 241–268. <https://doi.org/10.3758/s13415-011-0083-5>
- Oostenveld, R., Fries, P., Maris, E., & Schoffelen, J. M. (2011). FieldTrip: open source software for advanced analysis of MEG, EEG, and invasive electrophysiological data. *Computational Intelligence and Neuroscience*, *2011*, Article 156869. <https://doi.org/10.1155/2011/156869>
- Pan, J., & Tompkins, W. J. (1985). A real-time QRS detection algorithm. *IEEE Transactions on Biomedical Engineering*, *BME-32*(3), 230–236. <https://doi.org/10.1109/TBME.1985.325532>
- Perrin, F., Pernier, J., Bertrand, O., & Echallier, J. F. (1989). Spherical splines for scalp potential and current density mapping. *Electroencephalography and Clinical Neurophysiology*, *72*(2), 184–187. [https://doi.org/10.1016/0013-4694\(89\)90180-6](https://doi.org/10.1016/0013-4694(89)90180-6)
- Petzschner, F. H., Weber, L. A., Wellstein, K. V., Paolini, G., Do, C. T., & Stephan, K. E. (2019). Focus of attention modulates the heartbeat evoked potential. *NeuroImage*, *186*, 595–606. <https://doi.org/10.1016/j.neuroimage.2018.11.037>
- Pollatos, O., & Schandry, R. (2004). Accuracy of heartbeat perception is reflected in the amplitude of the heartbeat-evoked brain potential. *Psychophysiology*, *41*, 476–482. <https://doi.org/10.1111/1469-8986.2004.00170.x>
- Pramme, L., Larra, M. F., Schachinger, H., & Frings, C. (2014). Cardiac cycle time effects on mask inhibition. *Biological Psychology*, *100*, 115–121. <https://doi.org/10.1016/j.biopsycho.2014.05.008>
- Pramme, L., Larra, M. F., Schachinger, H., & Frings, C. (2016). Cardiac cycle time effects on selection efficiency in vision. *Psychophysiology*, *53*(11), 1702–1711. <https://doi.org/10.1111/psyp.12728>
- Pramme, L., Schachinger, H., & Frings, C. (2015). Baroreceptor activity impacts upon controlled but not automatic distractor processing. *Biological Psychology*, *110*, 75–84. <https://doi.org/10.1016/j.biopsycho.2015.06.006>
- Rae, C. L., Ahmad, A., Larsson, D. E. O., Silva, M., Praag, C. D. G. V., Garfinkel, S. N., & Critchley, H. D. (2020). Impact of cardiac interoception cues and confidence on voluntary decisions to make or withhold action in an intentional inhibition task. *Scientific Reports*, *10*, 4184. <https://doi.org/10.1038/s41598-020-60405-8>
- Rae, C. L., Botan, V. E., Gould van Praag, C. D., Herman, A. M., Nyssonson, J. A. K., Watson, D. R., & Critchley, H. D. (2018). Response inhibition on the stop signal task improves during cardiac contraction. *Scientific Reports*, *8*, 9136. <https://doi.org/10.1038/s41598-018-27513-y>
- Raud, L., Westerhausen, R., Dooley, N., & Huster, R. J. (2020). Differences in unity: the go/no-go and stop signal tasks rely on different mechanisms. *NeuroImage*, *210*, Article 116582. <https://doi.org/10.1016/j.neuroimage.2020.116582>
- Rodríguez-Liñares, L., Vila, X., Mendez, A., Lado, M., & Olivieri, D., 2008, RHRV: an R-based software package for heart rate variability analysis of ECG recordings. Paper presented at the 3rd Iberian conference in systems and information technologies (CISTI 2008).
- Saari, M. J., & Pappas, B. A. (1976). Cardiac cycle phase and movement and reaction times. *Perceptual and Motor Skills*, *42*(3), 767–770. <https://doi.org/10.2466/pms.1976.42.3.767>
- Salomon, R., Ronchi, R., Donz, J., Bello-Ruiz, J., Herbelin, B., Favre, N., & Blanke, O. (2018). Insula mediates heartbeat related effects on visual consciousness. *Cortex*, *101*, 87–95. <https://doi.org/10.1016/j.cortex.2018.01.005>
- Schandry, R., & Montoya, P. (1996). Event-related brain potentials and the processing of cardiac activity. *Biological Psychology*, *42*(1–2), 75–85. [https://doi.org/10.1016/0301-0511\(95\)05147-3](https://doi.org/10.1016/0301-0511(95)05147-3)
- Schulz, A., van Dyck, Z., Lutz, A. P. C., Rost, S., & Vogeley, C. (2017). Gastric modulation of startle eye blink. *Biological Psychology*, *127*, 25–33. <https://doi.org/10.1016/j.biopsycho.2017.05.004>
- Sedghamiz, H. (2014). Matlab implementation of Pan Tompkins ECG QRS detector. Code Available at the File Exchange Site of MathWorks.
- Seth, A. K., & Friston, K. J. (2016). Active interoceptive inference and the emotional brain. *Philosophical Transactions of the Royal Society B*, *371*. <https://doi.org/10.1098/rstb.2016.0007>
- Simmonds, D. J., Pekar, J. J., & Mostofsky, S. H. (2008). Meta-analysis of go/no-go tasks demonstrating that fMRI activation associated with response inhibition is task-dependent. *Neuropsychologia*, *46*(1), 224–232. <https://doi.org/10.1016/j.neuropsychologia.2007.07.015>
- Stoffels, E. J., Van der Molen, M. W., & Keuss, P. J. (1985). Intersensory facilitation and inhibition: immediate arousal and location effects of auditory noise on visual choice reaction time. *Acta Psychologica*, *58*(1), 45–62. [https://doi.org/10.1016/0001-6918\(85\)90033-2](https://doi.org/10.1016/0001-6918(85)90033-2)
- Tenke, C. E., & Kayser, J. (2012). Generator localization by current source density (CSD): implications of volume conduction and field closure at intracranial and scalp resolutions. *Clinical Neurophysiology*, *123*(12), 2328–2345. <https://doi.org/10.1016/j.clinph.2012.06.005>
- Thayer, J. F., Hansen, A. L., Saus-Rose, E., & Johnsen, B. H. (2009). Heart rate variability, prefrontal neural function, and cognitive performance: the neurovisceral integration perspective on self-regulation, adaptation, and health. *Annals of Behavioral Medicine*, *37*, 141–153. <https://doi.org/10.1007/s12160-009-9101-z>
- Tottenham, N., Tanaka, J. W., Leon, A. C., McCarry, T., Nurse, M., Hare, T. A., & Nelson, C. (2009). The NimStim set of facial expressions: judgments from untrained research participants. *Psychiatry Research*, *168*(3), 242–249. <https://doi.org/10.1016/j.psychres.2008.05.006>
- Verbruggen, F., Aron, A. R., Band, G. P., Beste, C., Bissett, P. G., Brockett, A. T., & Boehler, C. N. (2019). A consensus guide to capturing the ability to inhibit actions and impulsive behaviors in the stop-signal task. *Elife*, *8*, Article e46323. <https://doi.org/10.7554/eLife.46323>
- Villena-González, M., Moënné-Loccoz, C., Lagos, R. A., Alliende, L. M., Billeke, P., Aboitiz, F., & Cosmelli, D. (2017). Attending to the heart is associated with posterior alpha band increase and a reduction in sensitivity to concurrent visual stimuli. *Psychophysiology*, *54*(10), 1483–1497. <https://doi.org/10.1111/psyp.12894>
- Viola, F. C., Thorne, J., Edmonds, B., Schneider, T., Eichele, T., & Debener, S. (2009). Semi-automatic identification of independent components representing EEG artifact. *Clinical Neurophysiology*, *120*(5), 868–877. <https://doi.org/10.1016/j.clinph.2009.01.015>
- Wessel, J. R., & Aron, A. R. (2015). It's not too late: the onset of the frontocentral P3 indexes successful response inhibition in the stop-signal paradigm. *Psychophysiology*, *52*(4), 472–480. <https://doi.org/10.1111/psyp.12374>
- Yang, X., Jennings, J. R., & Friedman, B. H. (2017). Exteroceptive stimuli override interoceptive state in reaction time control. *Psychophysiology*, *54*(12), 1940–1950. <https://doi.org/10.1111/psyp.12958>
- Zhang, R., Geng, X., & Lee, T. M. (2017). Large-scale functional neural network correlates of response inhibition: an fMRI meta-analysis. *Brain Structure and Function*, *222*(9), 3973–3990. <https://doi.org/10.1007/s00429-017-1443-x>

## Supplementary Materials



**Supplementary Figure 1.** Illustration of the online algorithm to calculate the stimuli onsets using the timing of the R-wave peak. **(A)** If the predetermined stop-signal delay (SSD) in this trial was not longer than 290 ms (i.e., the interval between the go cue and the stop cue was not longer than the interval between the R-wave peak and the stop cue), the R-wave peak used to couple the stop cue should precede the go cue; Thus, the onset of the stop cue could be directly set to 290 ms after the R-wave peak detected during the inter-trial interval; **(B)** If the SSD was longer than 290 ms (i.e., the interval between the go cue and the stop cue was more than the interval between the R-wave peak and the stop cue), the R-wave peak used to couple the stop cue should appear after the go cue in this trial; in this case, we first estimated the timing of the

next R-wave peak and then used this information to couple the stop cue accordingly. To estimate the timing of the next R-wave peak as accurately as possible, a median inter-beat interval was obtained based on the timings of the previous six R-wave peaks and then used to estimate the timing of the next R-wave peak. The onset of the stop cue should be set to 290 ms after this estimated R-wave peak. Next, the onset timing of the go cue (i.e., subtracting SSD from the onset timing of the stop cue) and distractor cue (i.e., subtracting jitter from the onset timing of stop cue) could be calculated accordingly. In stop trials aiming to couple the stop cue or the distractor cue to systole, the interval between the pulse and the stop cue or distractor cue was set as 290 ms. In the stop trials aiming to couple neither the stop cue nor the distractor cue to systole, the interval between the pulse and the stop cue was randomly set within 120–900 ms.

**Supplementary Table 1.** Percentage of trials presenting the stop cue or distractor cue at systole (190–390 ms after the R-wave peak) as well as means and standard deviations of the interval between the R-wave peak and the stop cue or distractor cue in different conditions based on the original experimental design.

	No-coupling		Couple distractor cue to systole		Couple stop cue to systole	
	Face as target	Color as target	Face as target	Color as target	Face as target	Color as target
<b><i>Percentage of trials</i></b>						
Stop cue	0.23 ± 0.04	0.23 ± 0.06	0.73 ± 0.07	0.75 ± 0.08	0.89 ± 0.10	0.89 ± 0.10
Distractor cue	0.23 ± 0.05	0.23 ± 0.05	0.90 ± 0.07	0.90 ± 0.08	0.71 ± 0.08	0.71 ± 0.09
<b><i>Means</i></b>						
Stop cue	520.07 ± 27.62	518.94 ± 29.68	290.23 ± 13.00	296.46 ± 12.99	296.96 ± 14.51	296.27 ± 12.49
Distractor cue	519.23 ± 27.43	522.31 ± 31.52	290.65 ± 11.34	296.45 ± 10.49	295.90 ± 16.80	298.10 ± 15.80
<b><i>Standard deviations</i></b>						
Stop cue	247.95 ± 18.59	255.35 ± 20.47	116.31 ± 40.48	115.96 ± 49.23	89.07 ± 58.26	92.94 ± 64.61
Distractor cue	259.40 ± 19.55	261.35 ± 22.56	90.56 ± 49.99	89.54 ± 57.80	116.05 ± 48.47	121.07 ± 53.26



## **2.4 Study IV: Ready to Go: Higher Sense of Agency Enhances Action Readiness and Reduces Response Inhibition**

**This article was published in *Cognition*:**

Ren, Q., Gentsch, A., Kaiser, J., & Schütz-Bosbach, S. (2023). Ready to go: Higher sense of agency enhances action readiness and reduces response inhibition. *Cognition*, 237, 105456. <https://doi.org/10.1016/j.cognition.2023.105456>

Copyright © 2023 The Authors. Published by Elsevier B.V. This is an open access article under the CC BY license (<http://creativecommons.org/licenses/by/4.0/>). The main manuscript and supplements here are the published version.

### **Contributions:**

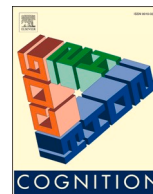
Qiaoyue Ren: Conceptualization, Methodology, Investigation, Data curation, Formal analysis, Visualization, Writing – original draft.

Antje Gentsch: Conceptualization, Methodology, Writing – review & editing.

Jakob Kaiser: Conceptualization, Methodology, Writing – review & editing.

Simone Schütz-Bosbach: Conceptualization, Methodology, Writing – review & editing, Supervision, Funding acquisition.





## Ready to go: Higher sense of agency enhances action readiness and reduces response inhibition

Qiaoyue Ren, Antje Gentsch, Jakob Kaiser, Simone Schütz-Bosbach\*

General and Experimental Psychology Unit, Department of Psychology, LMU Munich, Germany

### ARTICLE INFO

#### Keywords:

Sense of agency  
Action readiness  
Response inhibition  
Cognitive control  
Emotional valence  
Go/no-go

### ABSTRACT

Sense of agency is the subjective feeling of being in control of one's actions and their effects. Many studies have elucidated the cognitive and sensorimotor processes that drive this experience. However, less is known about how sense of agency influences flexible cognitive and motor control. Here, we investigated the effect of sense of agency on subsequent action regulation using a modified Go/No-Go task. In Experiment 1, we modulated participants' sense of agency by varying the occurrence of action outcomes (present vs. absent) both locally on a trial-by-trial basis and globally in terms of the overall probability of action outcomes within a block of trials (high vs. low). Importantly, we investigated how this manipulation influenced participants' responses to subsequent Go, No-Go, or Free-Choice cues. When participants' previous action led to an outcome (i.e., a happy face) compared with no outcome, they responded more accurately and faster to Go cues, reacted less accurately to No-Go cues, as well as made go decisions more frequently and faster to Free-Choice cues. These effects were even stronger when action outcomes occurred more frequently overall in a given block or in several previous trials. Experiment 2 further demonstrated that the effects of action outcome manipulation on subsequent action regulation were independent of the emotional valence of the action outcome (i.e., a happy or an angry face). Our results suggest that a higher sense of agency as induced by the presence of action outcomes enhanced action readiness and suppressed response inhibition. These findings highlight the impact of the control felt on the control used in action regulation, thereby providing new insights into the functional significance of the sense of agency on human behavior.

### 1. Introduction

Sense of agency refers to the subjective feeling of controlling one's own actions and their effects (Haggard, 2017; Haggard & Eitam, 2015). Abundant empirical and theoretical studies have revealed the cognitive and sensorimotor processes that drive and modulate sense of agency, including voluntary motor commands, action preparation, selection between action alternatives, and predictable sensory feedback (Haggard, 2017; Malik, Galang, & Finger, 2022). However, research on the opposite direction, i.e., whether and how sense of agency modulates upcoming actions and flexible behavior, is still sparse. Determining how sense of agency potentially affects our readiness to act would be an important step in finding out how our subjective states influence our objective ability to perform goal-directed actions.

Prior studies that aimed to investigate the effects of sense of agency on other cognitive processes typically manipulate the presence and/or the predictability of perceivable action effects to indirectly manipulate

participants' sense of agency or feeling of control (Eitam, Kennedy, & Tory Higgins, 2013; Gentsch & Schütz-Bosbach, 2015; Hemed, Bakbani-Elkayam, Teodorescu, Yona, & Eitam, 2020; Hemed, Karsh, Mark-Tavger, & Eitam, 2022; Karsh, Eitam, Mark, & Higgins, 2016; Penton, Wang, Coll, Catmur, & Bird, 2018). The modulation effects of these factors on the sense of agency have been well documented. The comparator model, the probably most widely accepted theory of the sense of agency, states that a sensory prediction is generated from an efference copy of a motor command, and is compared with the actual sensory feedback; a sense of agency arises if they match and diminishes if they mismatch (Blakemore, Wolpert, & Frith, 1998, 2002; Frith, Blakemore, & Wolpert, 2000). According to this model, being able to produce intended or predicted effects is thought to induce a high sense of agency; conversely, not being able to produce predicted effects is thought to be associated with little or no sense of agency. In addition, having a higher probability of producing action outcomes is generally considered to increase sense of agency; in contrast, having a lower

\* Corresponding author at: Department of Psychology, LMU Munich, Leopoldstr. 13, Munich D-80802, Germany.  
E-mail address: [S.Schuetz-Bosbach@psy.lmu.de](mailto:S.Schuetz-Bosbach@psy.lmu.de) (S. Schütz-Bosbach).

<https://doi.org/10.1016/j.cognition.2023.105456>

Received 23 September 2022; Received in revised form 1 March 2023; Accepted 2 April 2023

Available online 8 April 2023

0010-0277/© 2023 The Authors. Published by Elsevier B.V. This is an open access article under the CC BY license (<http://creativecommons.org/licenses/by/4.0/>).

probability of producing action outcomes is considered to reduce sense of agency. These hypotheses have been supported by many empirical studies using implicit (sensorimotor) and/or explicit measurements (judgements) of agency (Caspar, Desantis, Dienes, Cleeremans, & Haggard, 2016; Ebert & Wegner, 2010; Karsh et al., 2016; Penton et al., 2018; Sato & Yasuda, 2005; Villa, Tidoni, Porciello, & Aglioti, 2021).

Previous relevant studies have largely focused on the effect of sense of agency on action selection (i.e., which action to execute) and the efficiency of action execution (Wen & Imamizu, 2022). For example, participants responded faster when their response was consistently followed by an immediate effect, compared to when no such effect appeared or when it was followed by a time-lagged (300 or 600 ms) effect (Eitam et al., 2013). Moreover, buttons that had a high probability of causing a visual outcome were more likely to be selected and were pressed faster than buttons associated with no chance of causing a perceivable effect, even though these action outcomes were task-irrelevant and valence-neutral (Karsh & Eitam, 2015). Recent studies further found that this facilitation effect was sensitive to the effectiveness of the motor response, that is, how likely the response was to evoke a perceivable effect (Hemed et al., 2020; Tanaka, Watanabe, & Tanaka, 2021). These findings suggest that actions associated with a strong sense of agency or control are preferred and are executed more fluently. More importantly, Hemed et al. (2022) revealed the different effects of sensorimotor and judgement-based aspects of agency on different aspects of responding. Specifically, evaluations of a response's effectiveness were suggested to be driven by at least two different processes: one is based on a sensorimotor (implicit) process and the confirmation of sensorimotor prediction that reinforces response execution (as measured by response speed); the other relies on a conceptual (explicit) judgement of agency and seems to affect response selection (as measured by response frequency).

While fluent action execution is an important part of goal-directed actions, humans need also be able to suppress automatic action tendencies when they are not consistent with their current goals or not appropriate in a given situation. However, it is currently unknown whether sense of agency influences the ability to suppress unwanted or inappropriate actions (i.e., subsequent response inhibition). Response inhibition is considered a hallmark of executive function and cognitive control, and it supports flexible and goal-directed behavior in ever-changing environments (Bari & Robbins, 2013; Chambers, Garavan, & Bellgrove, 2009). Previous studies have shown the sense of agency to be modulated under high-level physical effort or cognitive load, although the results are inconclusive. Specifically, when a current trial required a high level of effort, such as an incongruent or error trial, the sense of agency in that trial decreased (Sidarus & Haggard, 2016; Vastano, Pozzo, & Brass, 2017; Wang, Damen, & Aarts, 2018). However, another study found the opposite effect (Van den Bussche, Alves, Murray, & Hughes, 2020). Additionally, it has been shown that the exertion of more effort in the previous trial led to a higher sense of agency in the current trial (Di Costa, Théro, Chambon, & Haggard, 2018; Wang et al., 2018). In contexts requiring high effort (e.g., across a block of trials), some studies found a decrease in the sense of agency (Hon, Poh, & Soon, 2013; Howard, Edwards, & Bayliss, 2016; Potts & Carlson, 2019) while others observed an increase in the sense of agency (Demanet, Muhle-Karbe, Lynn, Blotenberg, & Brass, 2013). These findings on the one hand imply a close relationship between the feeling of being in control and the engagement of cognitive control but on the other hand also suggest a functional distinction. The present study aimed to explore the effect of sense of agency on subsequent action readiness and response inhibition, which might advance our understanding of how the subjective control feeling modulates the actual control engagement in action regulation and in this way, may provide new insights into the functional significance of the sense of agency in goal-directed behavior.

To this end, we adopted a modified Go/No-Go task in which a pair of two trials included two action stimuli. The Go/No-Go paradigm is a widely-used paradigm for measuring action regulation, particularly

response inhibition (e.g., Wessel, 2018). In our task, the first action stimulus was always a Go cue (i.e., the inducement trial), while the second action stimulus was a Go, a No-Go, or a Free-Choice cue (i.e., the test trial). Participants were instructed to perform speeded keypress actions to a Go cue, withhold responses to a No-Go cue, or make free choices whether to execute or inhibit a keypress when presented with a Free-Choice cue. Similar to previous studies (Eitam et al., 2013; Hemed et al., 2020), we manipulated participants' sense of agency in the inducement trials by having them perform actions that did or did not result in visual effects. This allowed us to test the immediate effect of the "local" outcome presence on participants' performance in the next trial (i.e., the test trial). We also manipulated the likelihood (high vs. low) of obtaining action outcomes at the block level, to further explore the longer-lasting effect of "global" outcome frequency. We used positively valenced stimuli (i.e., happy face) as action outcomes since several previous studies suggest that positive compared to neutral outcomes might be particularly effective in inducing a high sense of agency (for review, see Kaiser, Buciuman, Gigl, Gentsch, & Schütz-Bosbach, 2021).

We had three hypotheses. First, we expected that the presence of an action outcome in the inducement trial would enhance action readiness in the following test trial, resulting in faster and more accurate responses to Go cues (Kaiser & Schütz-Bosbach, 2019). Similar effects have been observed in previous studies using different paradigms and neutral action outcomes (Eitam et al., 2013; Hemed et al., 2022; Karsh & Eitam, 2015). Second, we hypothesized a detrimental effect of outcome presence on subsequent response inhibition, given that an increase in readiness to act can coincide with a decrease in the ability to inhibit action (Albayay, Castiello, & Parma, 2019; van Peer, Gladwin, & Nieuwenhuys, 2019). External signals and internal decisions have been both found to affect response inhibition (Parkinson & Haggard, 2014). Successful action suppression during No-Go trials was assumed to reflect externally generated inhibition, while a lower frequency of choosing to act and slower reaction times during Free-Choice trials indicate stronger internally generated inhibition (i.e., intentional inhibition; Parkinson & Haggard, 2014). Participants' responses to Free-Choice trials also reflect their "bias" for either action execution or inhibitory tendency. We predicted that the presence of an action outcome would lead to lower accuracy rates during subsequent No-Go trials as well as a higher likelihood of choosing to act and faster choices during subsequent Free-Choice trials, indicating an influence on both types of response inhibition. Last but not least, inspired by the finding that not only the immediate context (i.e., outcome occurrence on trial n-1) but also the more distant context (e.g., number of outcome occurrences on trial n-4 through n-2) influenced participants' response speed (Hemed et al., 2020), we hypothesized that the global outcome frequency in a given block or several previous trials would further modulate the effect caused by the local outcome presence.

## 2. Experiment 1

### 2.1. Methods

#### 2.1.1. Participants

Twenty-seven healthy participants (15 females; mean age: 26.04 ± 3.48 years; range: 19–35 years), with normal or corrected-to-normal vision, were recruited for Experiment 1. Large effect sizes were observed in reaction times between the "no action effect" and the "immediate action effect" condition in related previous studies (Hemed et al., 2022; Karsh et al., 2016). A post-hoc power analysis for Experiment 1, conducted using the MorePower software (Campbell & Thompson, 2012), indicates that a sample of 27 is adequate for detecting a large ( $\eta_p^2 = 0.25$ ) effect in a 2 × 2 within-subjects design with a power of 0.80 and  $\alpha$  of 0.05. All participants provided written informed consent and received financial compensation for their participation. The procedures were approved by the local ethics committee at the Department of Psychology of LMU Munich in accordance with the Declaration of

Helsinki.

2.1.2. Materials and apparatus

A set of 42 colored photographs from the validated NimStim database (Tottenham et al., 2009) was used as action outcomes in this experiment. These photographs show happy facial expressions of 42 actors (18 females, 24 males). Go cues (i.e., a black rectangle), No-Go cues (i.e., a black rectangle with a grey cross), Free-Choice cues (i.e., a grey rectangle with black borders), as well as the photos as action outcomes were presented in the same size of 400 × 514 pixels (width × height) with a grey background on a 24-in. monitor (refresh rate: 60 Hz; resolution: 1920 × 1080 pixels) at a viewing distance of approximately 65 cm. The experiment was implemented using the Presentation software (Neurobehavioral Systems, Inc.).

2.1.3. Design and procedure

A pair of two trials included two action stimuli (see Fig. 1). Unbeknownst to the participants, the first action stimulus was always a Go cue (i.e., the **inducement trial**), while the second action stimulus was a Go, a No-Go, or a Free-Choice cue (i.e., the **test trial**), presented with equal probability (i.e., 33.33%). Participants were instructed to (1) press the “down arrow” key using their right index finger as quickly as possible in response to the Go cue; (2) withhold the keypress action in response to the No-Go cue; (3) make a free, spontaneous decision regarding whether to press the key or inhibit the keypress action in response to the Free-Choice cue. Each action stimulus remained on the screen until the participant pressed the button or the stimulus had been presented for 350 ms. An error message was presented for 800 ms if the action response was incorrect (i.e., did not press the key in Go trials or pressed the key in No-Go trials). Such message never appeared in Free-Choice trials, since both pressing the key and not pressing the key were “correct” responses. A central fixation dot was presented for 1300–1700 ms during the inter-stimulus interval.

This experiment adopted a 2 (Outcome Presence: present vs. absent) × 2 (Outcome Probability: high vs. low) within-subjects design (see the table in Fig. 1). The factor “Outcome Presence” was manipulated at the trial-by-trial level. Specifically, for each inducement trial, either a happy face (800 ms) or no visual stimulus at all was presented after participants’ keypress action. Thus, participants either had the experience that their action led to a positive effect, or they experienced that their action did not lead to any perceivable outcome. The factor “Outcome Probability” was manipulated at the block level. For each block, participants either had a high (75%) or a low (25%) probability of receiving action outcomes overall. Participants were explicitly informed about the respective outcome probability at the beginning of each block. Specifically, there were two different types of blocks, either having 75% of inducement trials with action outcomes and 25% of inducement trials without action outcomes, or having 25% of inducement trials with action outcomes and 75% of inducement trials without action outcomes. Please note that, unbeknownst to the participants, if a happy face was presented on the inducement trial, participants would also receive a happy face as the outcome of the keypress action in response to the Go cue or the Free-Choice cue during the following test trial (i.e., in case participants chose to act). In this way, we kept the test trial similar to the inducement trial, and thus excluded the possibility that participants treated the inducement trial and the test trial differently and separately over the course of the experiment.

There were 12 blocks for each block type, and 48 pairs of trials for each block. Please note that only when participants made a correct keypress action during the inducement trial, the subsequent test trial would appear, and in this way represented a complete action repetition sequence comprised of a pair of inducement and test trials, which then entered data analysis. Furthermore, only when a correct response was made on the inducement trial was the trial “counted” during data collection. In other words, a block was completed only when participants made correct responses in 48 inducement trials (unbeknownst to

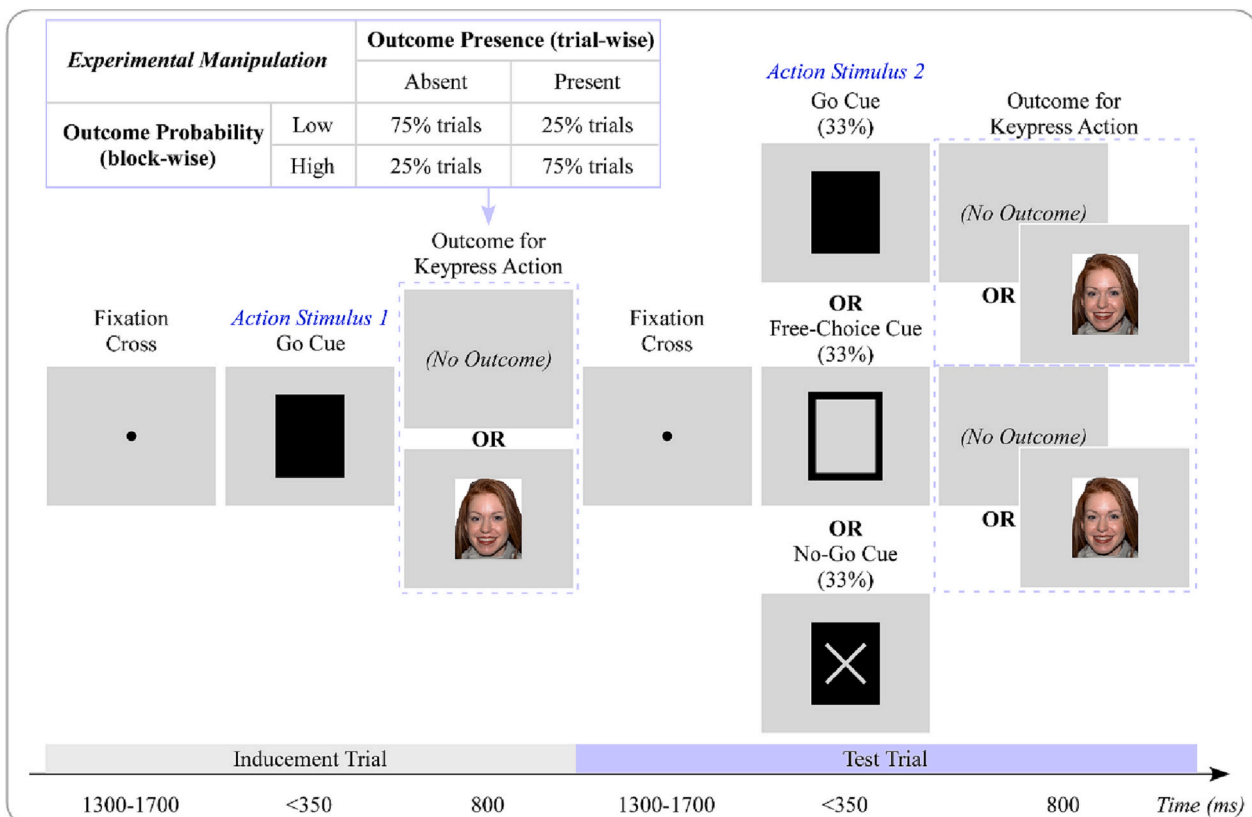


Fig. 1. Schema of the modified Go/No-Go task in Experiment 1 and Control Experiment.

the participants). Therefore, after deleting the “uncounted” inducement trials (i.e., trials with incorrect responses), always 48 pairs of trials in each block entered further analysis. This step resulted in the exclusion of  $8.43 \pm 6.25\%$  of trials (Mean  $\pm$  SD; range: 1.29–24.26% of trials) on average per participant. The uneven proportion of trials with or without action outcomes in each block (e.g., 75% trials vs. 25% trials in blocks having a high probability of obtaining action outcomes) resulted in the unbalanced number of trials in the four different experimental conditions based on the factors “Outcome Presence” and “Outcome Probability”. The Go, No-Go, and Free-Choice trials accounted for 33.33% of the test trials per condition, respectively.

To become familiar with the experimental procedures, participants completed two practice sessions (one for each block type; each including 12 pairs of trials) before the actual experiment started. All blocks and trial types were presented in random order. Participants received visual feedback on their accuracy rate and mean reaction time in Go trials as well as the accuracy rate in No-Go trials after each block during the self-paced inter-block rest.

#### 2.1.4. Manipulation check

As a manipulation check for the sense of agency, we conducted a control experiment that used the same design as Experiment 1 but included explicit judgements of agency (sample size: 22; 13 females; mean age:  $25.14 \pm 2.97$  years; range: 22–33 years; with normal or corrected-to-normal vision). Specifically, participants were required to rate how much control they felt over the face on a visual analogue scale (i.e., 0-no control to 100-total control) at the end of a subset of inducement trials (1/4 trials per block; randomly selected; followed by Go, No-Go, or Free-Choice test trials with equal probability) and also at the end of each block. In total, participants rated their sense of agency for 72 inducement trials in each of the four conditions, and also for 12 blocks with high probability of getting action outcomes and 12 blocks with low probability of getting action outcomes.

#### 2.1.5. Statistical analysis

**2.1.5.1. Behavioral performance in experiment 1.** Descriptive statistics are provided for reaction times in Go trials and Free-Choice trials, accuracy rates in Go trials and No-Go trials, as well as response rates (i.e., the relative frequency at which participants chose to press the button) in Free-Choice trials (see Supplementary Table 1). Notably, only test trials were analyzed since inducement trials were used to manipulate participants' sense of agency only. For the analysis of reaction times in Go trials, incorrect trials (i.e., did not press the key in test trials) were removed ( $15.02 \pm 8.83\%$  of trials on average per participant). For the analysis of reaction times in Free-Go trials, trials without keypress response were removed ( $35.61 \pm 15.40\%$  of trials on average per participant). None of the participants always chose not to act or always chose to act in Free-Choice trials (minimum response rate: 0.10; maximal response rate: 0.96; see Supplementary Table 2). Separate two-way repeated measures analysis of variances (ANOVA) with two within-subjects factors (Outcome Presence and Outcome Probability) were conducted on these dependent variables. Data were averaged for each of the four conditions, yielding a single value per condition for each participant, which then entered the ANOVA analysis. The number of trials per condition for each analysis is summarized in Supplementary Table 3. Additionally, a three-way repeated measures ANOVA including a third within-subjects factor (Trial Type: Go vs. No-Go trials) was performed on accuracy rates, in order to explore the effect of sense of agency on motor tendency (i.e., a preference for go or no-go responses). Partial eta-squared ( $\eta_p^2$ ) was calculated to reflect the effect size of the  $F$ -tests. Post-hoc pairwise comparisons were conducted and the Holm correction method was applied for multiple comparisons when there was a significant interaction between factors. Unlike the  $p$ -value in frequentist hypothesis testing, the Bayes Factors (e.g., the  $BF_{10}$  value) in

Bayesian hypothesis testing can indicate how much more likely the alternative hypothesis is than the null hypothesis (Wagenmakers et al., 2018). Therefore, we also reported  $BF_{10}$  values from the corresponding Bayesian repeated measures ANOVAs. A  $BF_{10}$  between 1.00 and 3.00 indicates anecdotal evidence, a  $BF_{10}$  between 3.00 and 10.00 indicates moderate evidence, and a  $BF_{10} > 10.00$  indicates strong evidence for the alternative hypothesis; in contrast, a  $BF_{10}$  between 0.33 and 1.00 indicates anecdotal evidence, a  $BF_{10}$  between 0.10 and 0.33 indicates moderate evidence, and a  $BF_{10}$  smaller than 0.10 indicates strong evidence for the null hypothesis (Wagenmakers et al., 2018). All analyses were performed in the JASP software (version 0.17.0.0; JASP Team, 2023).

In addition, following the analyses by Hemed et al. (2020), we performed a second set of analyses based on a 2 (Outcome Presence: present vs. absent)  $\times$  2 (Previous Outcome Frequency: 3–4 times vs 0 times) within-subjects design. The factor “Previous Outcome Frequency” refers to the number of times the positive outcome had occurred in the previous two pairs of trials. Notably, the number of times the positive outcome had occurred in the previous two pairs of trials can be 0, 1, 2, 3, or 4; whereas, we selected two extreme cases only for comparison (3–4 times vs. 0 times), in order to show the potential effect more clearly. In addition, we binned the trials with 3 and 4 outcome events in the previous two pairs of trials together due to the limited trial number. Descriptive statistics for all dependent variables are summarized in Supplementary Table 4. Separate two-way repeated measures ANOVAs with two within-subjects factors (Outcome Presence and Previous Outcome Frequency) were conducted on the dependent variables, and a three-way repeated measures ANOVA including a third within-subjects factor (Trial Type: Go vs. No-Go trials) was performed on accuracy rates. The number of trials per condition for each analysis is summarized in Supplementary Table 5.

**2.1.5.2. Agency ratings in control experiment.** Two-way repeated measures ANOVAs with two within-subjects factors (Outcome Presence and Outcome Probability or Outcome Presence and Previous Outcome Frequency) were conducted on agency ratings obtained at the end of inducement trials. A paired samples  $t$ -test was conducted on agency ratings obtained at the end of each block. The effect size was estimated by Cohen's  $d$ .

## 2.2. Results

### 2.2.1. Behavioral performance in experiment 1

**2.2.1.1. Results based on the factors “outcome presence” and “outcome probability”.** For reaction times in Go trials, the two-way repeated measures ANOVA showed significant main effects of Outcome Presence,  $F(1,26) = 68.46, p < .001, \eta_p^2 = 0.73, BF_{10} > 10^9$ , and Outcome Probability,  $F(1,26) = 28.77, p < .001, \eta_p^2 = 0.53, BF_{10} > 10^5$ . There was also a significant interaction between Outcome Presence and Outcome Probability,  $F(1,26) = 22.56, p < .001, \eta_p^2 = 0.47, BF_{10} > 10^4$ . Further analyses showed that, participants responded faster to Go cues when their previous action led to a positive outcome compared with no outcome (both  $ps < 0.001$ ). This effect was stronger in blocks having a high probability of obtaining positive outcomes compared with blocks having a low probability of obtaining positive outcomes (see Fig. 2A).

For reaction times in Free-Choice trials, the two-way repeated measures ANOVA showed significant main effects of Outcome Presence,  $F(1,26) = 53.46, p < .001, \eta_p^2 = 0.67, BF_{10} > 10^6$ , and Outcome Probability,  $F(1,26) = 23.87, p < .001, \eta_p^2 = 0.48, BF_{10} > 10^3$ . There was also a significant interaction between Outcome Presence and Outcome Probability,  $F(1,26) = 13.78, p < .001, \eta_p^2 = 0.35, BF_{10} > 10^2$ . Further analyses showed that, participants responded faster to Free-Choice cues when their previous action led to a positive outcome compared with no outcome (both  $ps < 0.001$ ). This effect was stronger in blocks having a

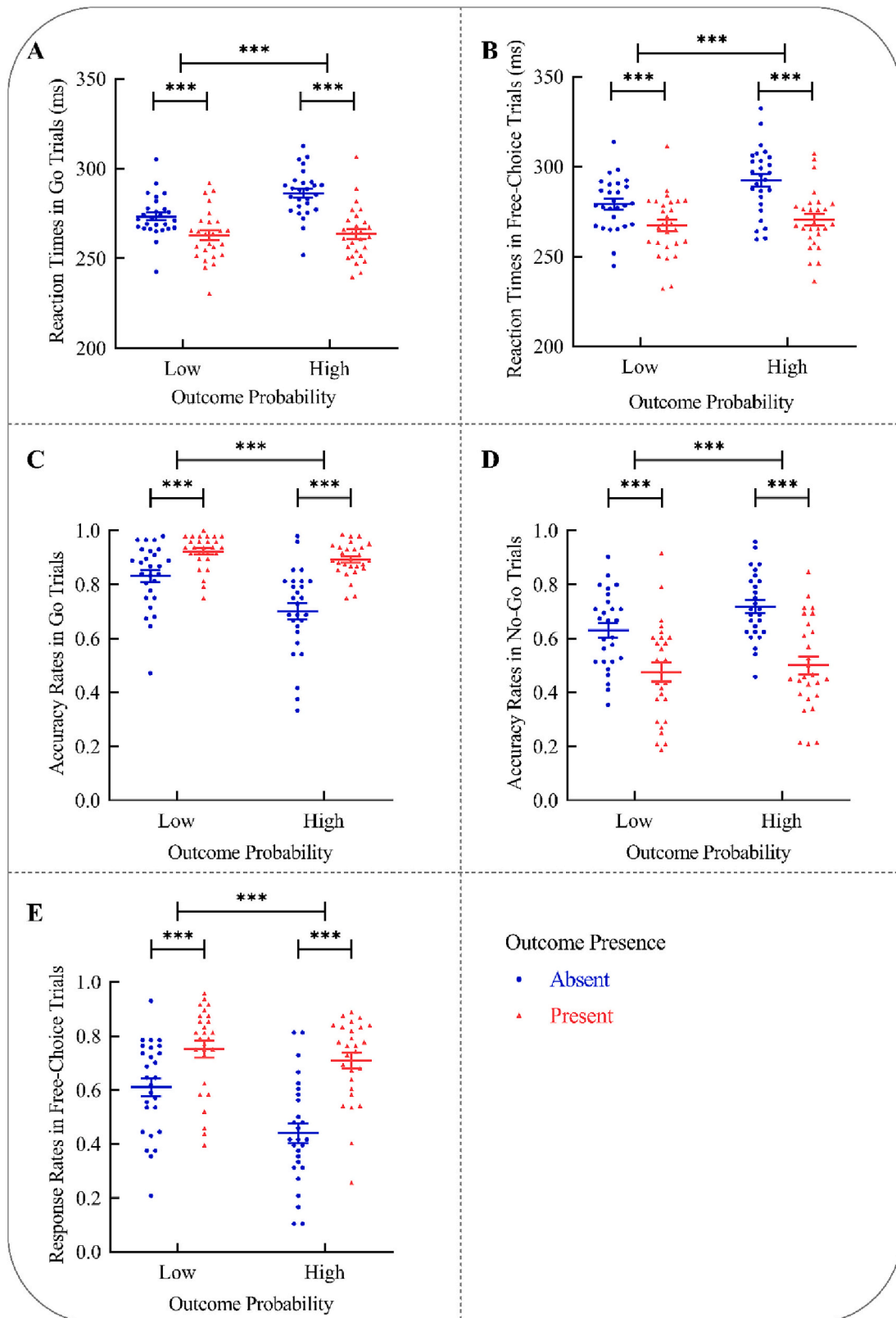


**Fig. 2.** Results of Experiment 1 based on the factors “Outcome Presence” and “Outcome Probability”. (A) Reaction times in Go trials, (B) reaction times in Free-Choice trials, (C) accuracy rates in Go trials, (D) accuracy rates in No-Go trials, and (E) response rates in Free-Go trials in different conditions. Data are expressed as Mean ± SEM. \*\*\*:  $p < .001$ .

high probability of obtaining positive outcomes compared with blocks having a low probability of obtaining positive outcomes (see Fig. 2B).

For accuracy rates in Go trials, the two-way repeated measures ANOVA showed significant main effects of Outcome Presence,  $F(1,26) = 55.53, p < .001, \eta_p^2 = 0.68, BF_{10} > 10^{10}$ , and Outcome Probability,  $F(1,26) = 66.94, p < .001, \eta_p^2 = 0.72, BF_{10} > 10^9$ . There was also a significant interaction between Outcome Presence and Outcome Probability,  $F(1,26) = 43.60, p < .001, \eta_p^2 = 0.63, BF_{10} > 10^5$ . Further analyses showed that, participants responded more accurately to Go cues when their previous action led to a positive outcome compared with no outcome (both  $ps < 0.001$ ). This effect was stronger in blocks having a high probability of obtaining positive outcomes compared with blocks having a low probability of obtaining positive outcomes (see Fig. 2C).

For accuracy rates in No-Go trials, the two-way repeated measures ANOVA showed significant main effects of Outcome Presence,  $F(1,26) = 122.40, p < .001, \eta_p^2 = 0.83, BF_{10} > 10^9$ , and Outcome Probability,  $F(1,26) = 14.10, p < .001, \eta_p^2 = 0.35, BF_{10} > 10^2$ . There was also a significant interaction between Outcome Presence and Outcome Probability,  $F(1,26) = 7.51, p = .011, \eta_p^2 = 0.22, BF_{10} = 25.21$ . Further analyses showed that, participants responded less accurately to No-Go cues when their previous action led to a positive outcome compared with no outcome (both  $ps < 0.001$ ). This effect was stronger in blocks having a high probability of obtaining positive outcomes compared with blocks having a low probability of obtaining positive outcomes (see Fig. 2D).

Moreover, the analysis of accuracy rates in both Go and No-Go trials, using a three-way repeated measures ANOVA, showed a significant interaction between Outcome Presence, Outcome Probability, and Trial Type,  $F(1,26) = 29.23, p < .001, \eta_p^2 = 0.53, BF_{10} > 10^7$ . As we were interested in the performance differences between Go and No-Go trials in each experimental condition, we further analyzed the interaction by focusing on the effect of Trial Type for each level of the other two factors (i.e., Outcome Presence and Outcome Probability). The results showed that, (1) in blocks having a high probability of obtaining positive outcomes, participants' accuracy rates were significantly higher in Go trials compared with No-Go trials when their previous action led to a positive outcome ( $p < .001$ ); however, participants' accuracy rates did not differ significantly between Go trials and No-Go trials when their previous action led to no outcome ( $p = .560$ ); (2) in blocks having a low probability of obtaining positive outcomes, participants' accuracy rates were significantly higher in Go trials compared with No-Go trials when their previous action led to a positive outcome ( $p < .001$ ) but also when their previous action led to no outcome ( $p < .001$ ; see Supplementary Fig. 1A).

For response rates (i.e., the relative frequency at which participants chose to press the button) in Free-Choice trials, the two-way repeated measures ANOVA showed significant main effects of Outcome Presence,  $F(1,26) = 111.94, p < .001, \eta_p^2 = 0.81, BF_{10} > 10^{11}$ , and Outcome Probability,  $F(1,26) = 30.77, p < .001, \eta_p^2 = 0.54, BF_{10} > 10^6$ . There was also a significant interaction between Outcome Presence and Outcome Probability,  $F(1,26) = 32.97, p < .001, \eta_p^2 = 0.56, BF_{10} > 10^4$ . Further analyses showed that, participants responded more frequently to Free-Choice cues when their previous action led to a positive outcome compared with no outcome (both  $ps < 0.001$ ). This effect was stronger in blocks having a high probability of obtaining positive outcomes compared with blocks having a low probability of obtaining positive outcomes (see Fig. 2E).

In summary, when participants' previous action led to a positive outcome compared with no outcome, they responded faster and more accurately to Go cues, responded less accurately to No-Go cues, as well as responded faster and more frequently to Free-Choice cues. These effects were stronger when the global probability of getting positive outcomes in a given block was high compared with low. In addition, participants had higher accuracy rates in Go trials compared with No-Go trials (i.e., a preference for go over no-go responses) when their previous action led to a positive outcome or when their previous action

unsurprisingly did not lead to any outcome. In contrast, participants had comparable accuracy rates in Go and No-Go trials (i.e., no obvious preference for go over no-go responses) when the global probability of getting positive outcomes in a given block was high but their previous action surprisingly did not lead to any outcome.

**2.2.1.2. Results based on the factors "outcome presence" and "Previous Outcome Frequency"**. For reaction times in Go trials, the two-way repeated measures ANOVA showed significant main effects of Outcome Presence,  $F(1,26) = 48.22, p < .001, \eta_p^2 = 0.65, BF_{10} > 10^7$ , and Previous Outcome Frequency,  $F(1,26) = 14.43, p < .001, \eta_p^2 = 0.36, BF_{10} > 10^3$ . There was also a significant interaction between Outcome Presence and Previous Outcome Frequency,  $F(1,26) = 18.61, p < .001, \eta_p^2 = 0.42, BF_{10} > 10^3$ . Further analyses showed that, participants responded faster to Go cues when their previous action led to a positive outcome compared with no outcome (both  $ps < 0.01$ ). This effect was stronger when positive outcomes had occurred three to four times compared with zero times in the previous two pairs of trials (see Fig. 3A).

For reaction times in Free-Choice trials, the two-way repeated measures ANOVA showed significant main effects of Outcome Presence,  $F(1,26) = 32.67, p < .001, \eta_p^2 = 0.56, BF_{10} > 10^6$ , and Previous Outcome Frequency,  $F(1,26) = 29.45, p < .001, \eta_p^2 = 0.53, BF_{10} > 10^5$ . There was also a significant interaction between Outcome Presence and Previous Outcome Frequency,  $F(1,26) = 23.25, p < .001, \eta_p^2 = 0.47, BF_{10} > 10^4$ . Further analyses showed that, participants responded faster to Free-Choice cues when their previous action led to a positive outcome compared with no outcome (both  $ps < 0.05$ ). This effect was stronger when positive outcomes had occurred three to four times compared with zero times in the previous two pairs of trials (see Fig. 3B).

For accuracy rates in Go trials, the two-way repeated measures ANOVA showed significant main effects of Outcome Presence,  $F(1,26) = 46.49, p < .001, \eta_p^2 = 0.64, BF_{10} > 10^9$ , and Previous Outcome Frequency,  $F(1,26) = 17.25, p < .001, \eta_p^2 = 0.40, BF_{10} > 10^7$ . There was also a significant interaction between Outcome Presence and Previous Outcome Frequency,  $F(1,26) = 40.73, p < .001, \eta_p^2 = 0.61, BF_{10} > 10^6$ . Further analyses showed that, if positive outcomes had occurred three to four times in the previous two pairs of trials, participants responded more accurately to Go cues when their previous action led to a positive outcome compared with no outcome ( $p < .001$ ). Whereas, if positive outcomes had occurred zero times in the previous two pairs of trials, their accuracy rates in Go trials did not differ significantly when their previous action led to a positive outcome compared with no outcome ( $p = .148$ ; see Fig. 3C).

For accuracy rates in No-Go trials, the two-way repeated measures ANOVA showed significant main effects of Outcome Presence,  $F(1,26) = 160.71, p < .001, \eta_p^2 = 0.86, BF_{10} > 10^{13}$ , and Previous Outcome Frequency,  $F(1,26) = 16.75, p < .001, \eta_p^2 = 0.39, BF_{10} > 10^5$ . There was also a significant interaction between Outcome Presence and Previous Outcome Frequency,  $F(1,26) = 23.67, p < .001, \eta_p^2 = 0.48, BF_{10} > 10^5$ . Further analyses showed that, participants responded less accurately to No-Go cues when their previous action led to a positive outcome compared with no outcome (both  $ps < 0.001$ ). This effect was stronger when positive outcomes had occurred three to four times compared with zero times in the previous two pairs of trials (see Fig. 3D).

Moreover, the analysis of accuracy rates in both Go and No-Go trials, using a three-way repeated measures ANOVA, showed a significant interaction between Outcome Presence, Previous Outcome Frequency, and Trial Type,  $F(1,26) = 45.48, p < .001, \eta_p^2 = 0.64, BF_{10} > 10^{13}$ . As we were interested in the performance differences between Go and No-Go trials in each experimental condition, we further analyzed the interaction by focusing on the effect of Trial Type for each level of the other two factors (i.e., Outcome Presence and Previous Outcome Frequency). The results showed that, (1) when positive outcomes had occurred three to four times in the previous two pairs of trials, participants' accuracy rates were significantly higher in Go trials compared with No-Go trials when

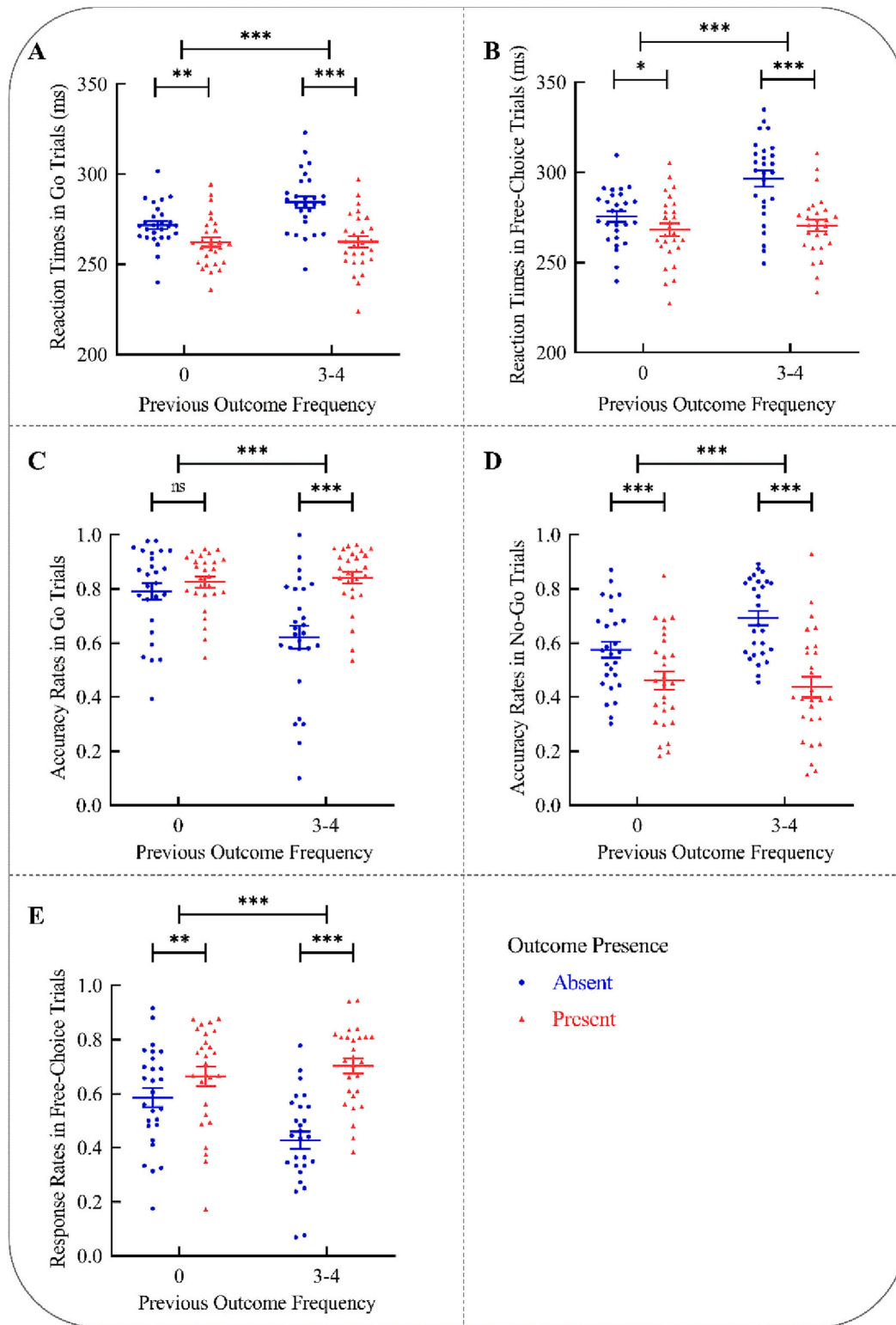


**Fig. 3.** Results of Experiment 1 based on the factors “Outcome Presence” and “Previous Outcome Frequency”. (A) Reaction times in Go trials, (B) reaction times in Free-Choice trials, (C) accuracy rates in Go trials, (D) accuracy rates in No-Go trials, and (E) response rates in Free-Go trials in different conditions. Data are expressed as Mean ± SEM. ns: not significant; \*:  $p < .05$ ; \*\*:  $p < .01$ ; \*\*\*:  $p < .001$ .

their previous action led to a positive outcome ( $p < .001$ ); however, participants' accuracy rates were significantly lower in Go trials compared with No-Go trials when their previous action led to no outcome ( $p = .043$ ); (2) when positive outcomes had occurred zero times in the previous two pairs of trials, participants' accuracy rates were

significantly higher in Go trials compared with No-Go trials when their previous action led to a positive outcome ( $p < .001$ ) but also when their previous action led to no outcome ( $p < .001$ ; see Supplementary Fig. 1B).

For response rates (i.e., the relative frequency at which participants chose to press the button) in Free-Choice trials, the two-way repeated

measures ANOVA showed significant main effects of Outcome Presence,  $F(1,26) = 62.08, p < .001, \eta_p^2 = 0.71, BF_{10} > 10^9$ , and Previous Outcome Frequency,  $F(1,26) = 11.13, p = .003, \eta_p^2 = 0.30, BF_{10} > 10^5$ . There was also a significant interaction between Outcome Presence and Previous Outcome Frequency,  $F(1,26) = 29.01, p < .001, \eta_p^2 = 0.53, BF_{10} > 10^5$ . Further analyses showed that, participants responded more frequently to Free-Choice cues when their previous action led to a positive outcome compared with no outcome (both  $ps < 0.01$ ). This effect was stronger when positive outcomes had occurred three to four times compared with zero times in the previous two pairs of trials (see Fig. 3E).

In summary, when participants' previous action led to a positive outcome compared with no outcome, they responded faster and more accurately to Go cues, responded less accurately to No-Go cues, as well as responded faster and more frequently to Free-Choice cues. These effects were stronger when positive outcomes had occurred three to four times compared with zero times in the previous two pairs of trials. In addition, participants had higher accuracy rates in Go trials compared with No-Go trials (i.e., a preference for go over no-go responses) when their previous action led to a positive outcome or when their previous action unsurprisingly did not lead to any outcome. In contrast, participants had lower accuracy rates in Go trials compared with No-Go trials (i.e., a preference for no-go over go responses) when positive outcomes had occurred three to four times in the previous two pairs of trials but their previous action surprisingly did not lead to any outcome.

2.2.2. Agency ratings in control experiment

2.2.2.1. Results based on the factors “outcome presence” and “outcome probability”. For agency ratings obtained at the end of inducement trials, the two-way repeated measures ANOVA showed significant main effects of Outcome Presence,  $F(1,21) = 21.35, p < .001, \eta_p^2 = 0.50, BF_{10} > 10^2$ , and Outcome Probability,  $F(1,21) = 20.30, p < .001, \eta_p^2 = 0.49, BF_{10} = 95.71$ . Participants reported higher agency ratings when their previous action led to a positive outcome compared with no outcome. Participants also reported higher agency ratings when they had a high compared with low probability of obtaining action outcomes in a given block (see Fig. 4A). However, the interaction between Outcome Presence and Outcome Probability was not significant,  $F(1,21) = 0.07, p = .788, \eta_p^2 < 0.01, BF_{10} = 1.02$ .

For agency ratings obtained at the end of each block, the paired samples *t*-test showed that participants reported higher agency ratings for blocks having a high probability of obtaining action outcomes compared with blocks having a low probability of obtaining action outcomes,  $t(21) = 4.79, p < .001, \text{Cohen's } d = 1.02, BF_{10} > 10^2$  (see Fig. 4B).

In summary, participants had a higher sense of agency (i.e., feeling more in control) when their previous action led to a positive outcome compared with no outcome and also when the global outcome probability in a given block was high compared with low.

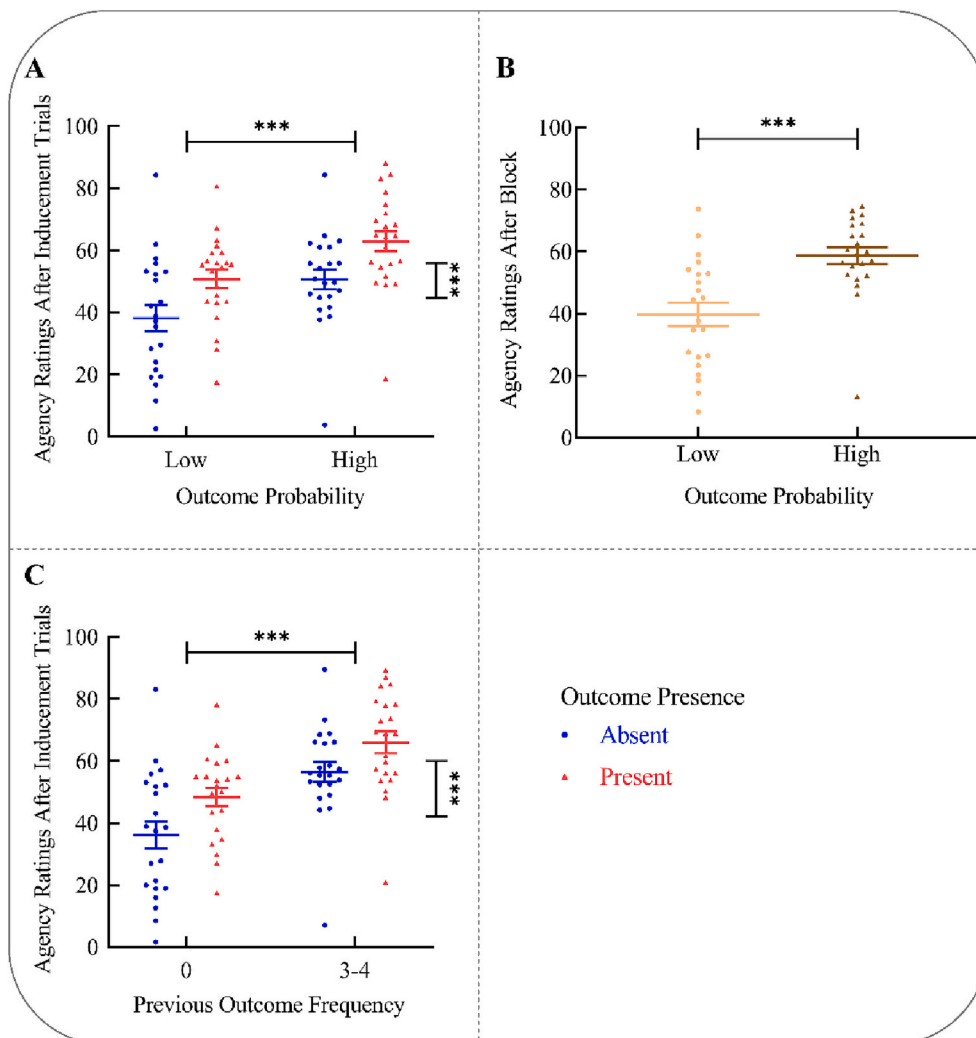


Fig. 4. Results of Agency Ratings in Control Experiment. (A) Agency ratings obtained at the end of inducement trials in different conditions based on the factors “Outcome Presence” and “Outcome Probability”. (B) Agency ratings obtained at the end of block in different types of blocks. (C) Agency ratings obtained at the end of inducement trials in different conditions based on the factors “Outcome Presence” and “Previous Outcome Frequency”. Data are expressed as Mean  $\pm$  SEM. \*\*\*:  $p < .001$ .

**2.2.2.2. Results based on the factors “outcome presence” and “Previous Outcome Frequency”.** For agency ratings obtained at the end of inducement trials, the two-way repeated measures ANOVA showed significant main effects of Outcome Presence,  $F(1,21) = 20.34, p < .001, \eta_p^2 = 0.49, BF_{10} > 10^2$ , and Previous Outcome Frequency,  $F(1,21) = 29.14, p < .001, \eta_p^2 = 0.58, BF_{10} > 10^2$ . Participants reported higher agency ratings when their previous action led to a positive outcome compared with no outcome. Participants also reported higher agency ratings when positive outcomes had occurred three to four times compared with zero times in the previous two pairs of trials (see Fig. 4C). However, the interaction between Outcome Presence and Previous Outcome Frequency was not significant,  $F(1,21) = 3.34, p = .082, \eta_p^2 = 0.14, BF_{10} = 2.94$ .

In summary, participants had a higher sense of agency (i.e., feeling more in control) when their previous action led to a positive outcome compared with no outcome and also when their action had resulted in positive outcomes frequently in several previous trials.

### 2.3. Discussion

Results of agency ratings in Control Experiment suggest that our experimental manipulation affected participants' sense of agency as intended. Specifically, participants had a higher sense of agency (i.e., feeling more in control) when their previous action led to a positive outcome (i.e., a happy face) compared with no outcome and also when positive action outcomes occurred frequently in a given block or in several previous trials. In other words, both the “local” occurrence of an action outcome and the “global” high probability of getting action outcomes led to an enhancement of the sense of agency. These effects are in line with previous literature. For example, higher feeling of control was reported when participants' action was always followed by a visual effect compared with no effect (Karsh et al., 2016) and also when the likelihood of an outcome following an action was increased (Penton et al., 2018).

Importantly, results of behavioral performance in Experiment 1 indicate that the “local” occurrence of a positive outcome following an action influenced participants' subsequent motor responses, manifested by higher accuracy rates and faster reaction times to Go cues, lower accuracy rates to No-Go cues, as well as higher response rates and faster reaction times to Free-Choice cues. In other words, the “local” outcome occurrence enhanced action readiness and suppressed response inhibition. Furthermore, these effects were stronger when positive action outcomes occurred frequently in a given block or in several previous trials, suggesting a modulation effect of the “global” outcome probability.

Together our results of behavioral performance and agency ratings both suggest that the sense of agency does play a functional role in action regulation. Specifically, the immediate, trial-by-trial enhancement of sense of agency caused by the “local” presence of an outcome led to an enhancement of action readiness and at the same time reduced response inhibition in subsequent trials. These effects were further amplified by a more longer-lasting enhancement of the sense of agency as induced by the “global” outcome frequency in a given block or in several previous trials. Under the assumption that No-Go and Free-Choice responses are reflective of internally and externally generated inhibition respectively (Parkinson & Haggard, 2014), our results indicate that when participants felt more in control over the keypress action, they not only performed worse at canceling the prepotent keypress action that is inappropriate for No-Go cues but also consciously preferred to repeat this keypress response when the Free-Choice cue appears. In addition, participants were more accurate in performing keypress actions than withholding them (i.e., a preference for go over no-go responses) in conditions with “local” outcome presence, and this tendency for motor execution was enhanced by the “global” outcome frequency in a given block or in several previous trials. This finding thus suggests an increased readiness for action at the cost of inhibitory control when

sense of agency was relatively high. In contrast, participants did not have an obvious preference for go or no-go responses (based on the factor “Outcome Probability”) or even had a preference for no-go over go responses (based on factors “Previous Outcome Frequency”), in the condition with high “global” outcome frequency but surprising outcome absence at the “local” level. This finding may indicate that a reduced sense of agency shifts participants' tendency from preparedness for action towards increased inhibitory control or general passivity.

Overall, these effects may also be explained by motivational factors related to the positively valenced action outcomes used in Experiment 1. In other words, the prospect of a positive outcome on a given trial might have induced the strong readiness for action, whereas the absence of a (rewarding) positive outcome led to the opposite effects. Therefore, in a second experiment, we further investigated the potential role of the emotional valence of action outcomes on our findings. To this end, we used the same design as in Experiment 1 but added a new condition in which the action outcome was comprised of a negatively valenced stimulus (i.e., an angry face). In the interest of limiting the overall length of the experiment, we presented Go and No-Go cues only in this version, and thus, did not include Free-Choice cues. If the presence of a positive outcome and the presence of a negative outcome (compared with no outcome) both resulted in similar effects on subsequent action regulation, it can be speculated that the effectiveness of the motor action in terms of producing a perceivable effect per se is a driving factor of our results. Otherwise, the outcome valence might be the key determinant of the observed effects.

## 3. Experiment 2

### 3.1. Methods

#### 3.1.1. Participants

A group of 30 healthy participants was recruited for Experiment 2. None of these participants took part in Experiment 1. Two participants were excluded from data analysis, because data collection was either not completed or data analysis revealed extreme values in behavioral performance ( $> 3$  standard deviations from sample mean), leaving a final sample of 28 (18 females; mean age:  $27.07 \pm 7.30$  years; range: 18–48 years). A post-hoc power analysis for Experiment 2, conducted using the MorePower software (Campbell & Thompson, 2012), indicates that a sample of 28 is adequate for detecting a large ( $\eta_p^2 = 0.16$ ) effect of the 3-level within-subjects factor with a power of 0.80 and  $\alpha$  of 0.05. Other experimental requirements were identical to Experiment 1.

#### 3.1.2. Materials and apparatus

In addition to the photographs of happy facial expressions used in Experiment 1, another set of 42 colored photographs showing angry facial expressions was selected from the same database (Tottenham et al., 2009). The action stimuli (the Go cue and the No-Go cue) and the apparatus were identical to Experiment 1.

#### 3.1.3. Design and procedure

This experiment adopted a 3 (Outcome Presence: absent vs. present positive vs. present negative)  $\times$  3 (Outcome Probability: high probability of no outcome vs. high probability of positive outcome vs. high probability of negative outcome) within-subjects design (see Fig. 5). The factor “Outcome Presence” was manipulated at the trial-by-trial level. Specifically, for each inducement trial, either a happy face, a negative face, or no visual stimulus at all was presented after participants' keypress action. The factor “Outcome Probability” was manipulated at the block level. Specifically, there were three different types of blocks (4 blocks for each block type, and 48 pairs of trials for each block), randomly presented. In each of the three block types, one of the possible action outcomes (positive/negative/no outcomes) was more likely to occur (50% of inducement trials), while the other two types of action outcomes were less likely to occur (25% of inducement trials each).

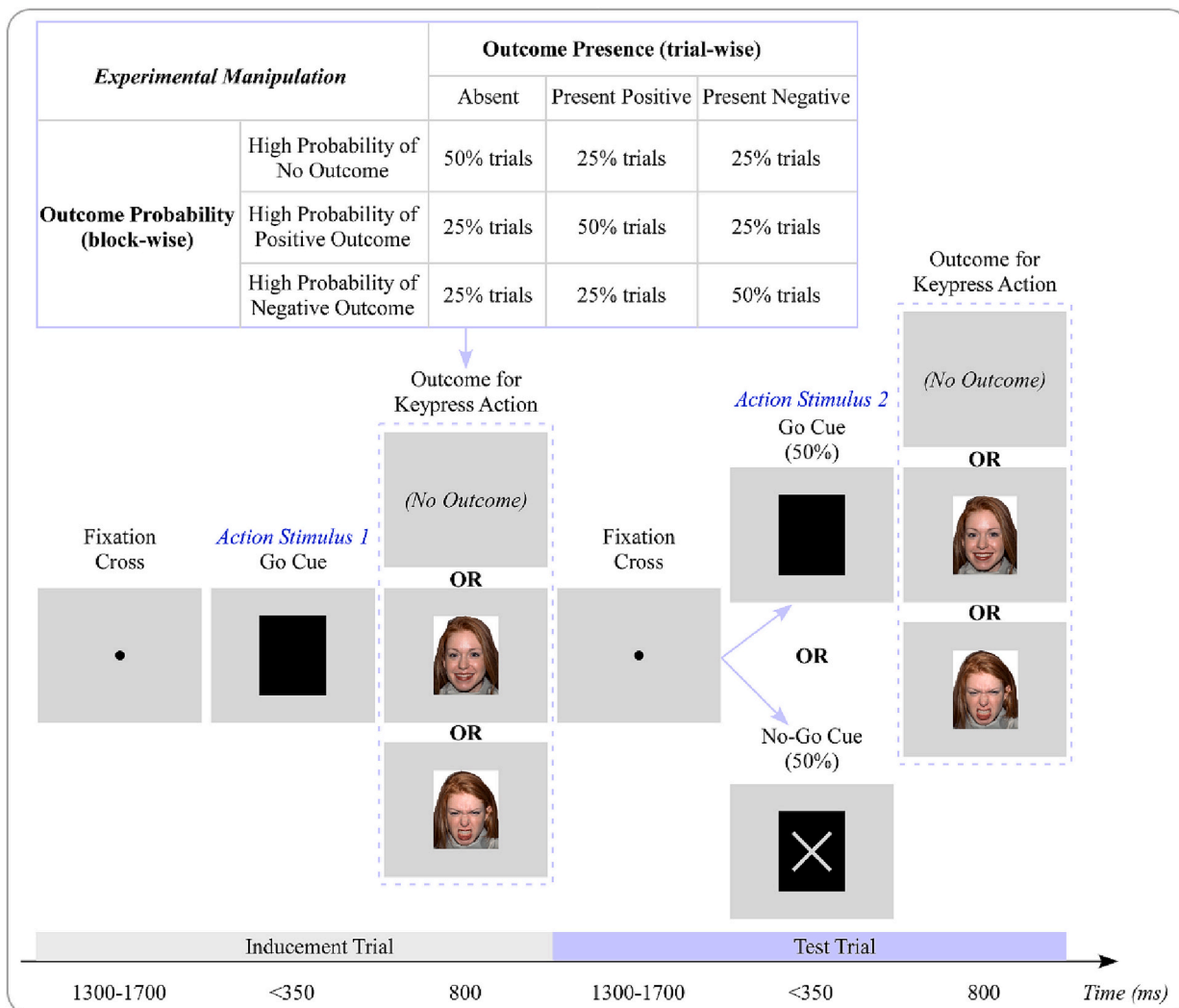


Fig. 5. Schema of the modified Go/No-Go task in Experiment 2. Experiment 2 used the same design as Experiment 1 but with the exception that a new condition was added in which the action outcome was an angry face and that only Go and No-Go cues were included.

Consistent with Experiment 1, only when a correct response was made on the inducement trial was the trial “counted” during data collection. This step resulted in the exclusion of  $11.81 \pm 6.66\%$  of trials (Mean  $\pm$  SD; range: 1.37–25.29% of trials) on average per participant. The uneven proportion of trials with positive, negative or no outcomes in each block (e.g., 50% trials vs. 25% trials vs. 25% trials in blocks having a high probability of obtaining positive outcomes) resulted in the unbalanced number of trials in the nine different experimental conditions based on the factors “Outcome Presence” and “Outcome Probability”. The Go and No-Go trials accounted for 50% of the test trials per condition, respectively. To become familiar with the experimental procedures, participants completed three practice sessions (one for each block type; each including 8 pairs of trials) before the actual experiment started. Other experimental procedures were identical to Experiment 1.

### 3.1.4. Statistical analysis

Descriptive statistics are provided for reaction times in Go trials as well as accuracy rates in Go trials and No-Go trials (see Supplementary Table 6 and 7). For the analysis of reaction times in Go trials, incorrect trials were removed ( $24.58 \pm 11.07\%$  of trials on average per participant). Consistent with Experiment 1, two sets of two-way repeated measures ANOVAs were conducted, either based on the factors “Outcome Presence” and “Outcome Probability” or the factors “Outcome Presence” and “Previous Outcome Frequency”. The factor “Previous Outcome

Frequency” refers to the number of times the type of outcome in the inducement trial had occurred in the previous two pairs of trials (2–4 times vs. 0 times). We binned the trials with 2, 3, and 4 outcome events in the previous two pairs of trials together due to the limited trial number. The number of trials per condition for each analysis is summarized in Supplementary Table 8 and 9. Additionally, three-way repeated measures ANOVAs including a third within-subjects factor (Trial Type: Go vs. No-Go trials) were performed on accuracy rates, in order to explore the effect of sense of agency on the motor tendency. The Greenhouse-Geisser correction was applied in case of violations of the sphericity assumption. For the sake of brevity, the uncorrected degrees of freedom were reported. Other statistical procedures were identical to Experiment 1.

## 3.2. Results

### 3.2.1. Results based on the factors “outcome presence” and “outcome probability”

For reaction times in Go trials, the two-way repeated measures ANOVA showed a significant main effect of Outcome Presence,  $F(2,54) = 72.87, p < .001, \eta_p^2 = 0.73, BF_{10} > 10^{13}$ . Further analyses showed that, participants responded faster to Go cues when their previous action led to a positive or negative outcome compared with no outcome (both  $ps < 0.001$ ), while their reaction times in Go trials did not differ significantly when their previous action led to a positive outcome compared with a

negative outcome ( $p = .657$ ; see Fig. 6A). The main effect of Outcome Probability was not significant,  $F(2,54) = 1.12, p = .323, \eta_p^2 = 0.04$ . The  $BF_{10}$  was 0.17, indicating moderate evidence for no main effect of Outcome Probability. The interaction between Outcome Presence and Outcome Probability was not significant,  $F(4,108) = 0.44, p = .780, \eta_p^2 = 0.02$ . The  $BF_{10}$  was 0.03, indicating strong evidence for no interaction effect.

For accuracy rates in Go trials, the two-way repeated measures ANOVA showed a significant main effect of Outcome Presence,  $F(2,54) = 99.68, p < .001, \eta_p^2 = 0.79, BF_{10} > 10^{15}$ . The main effect of Outcome Probability was not significant,  $F(2,54) = 2.33, p = .107, \eta_p^2 = 0.08, BF_{10} = 1.50$ . However, there was a significant interaction between Outcome Presence and Outcome Probability,  $F(4,108) = 3.55, p = .017, \eta_p^2 = 0.12, BF_{10} = 5.77$ . Further analyses showed that, in any of the three types of

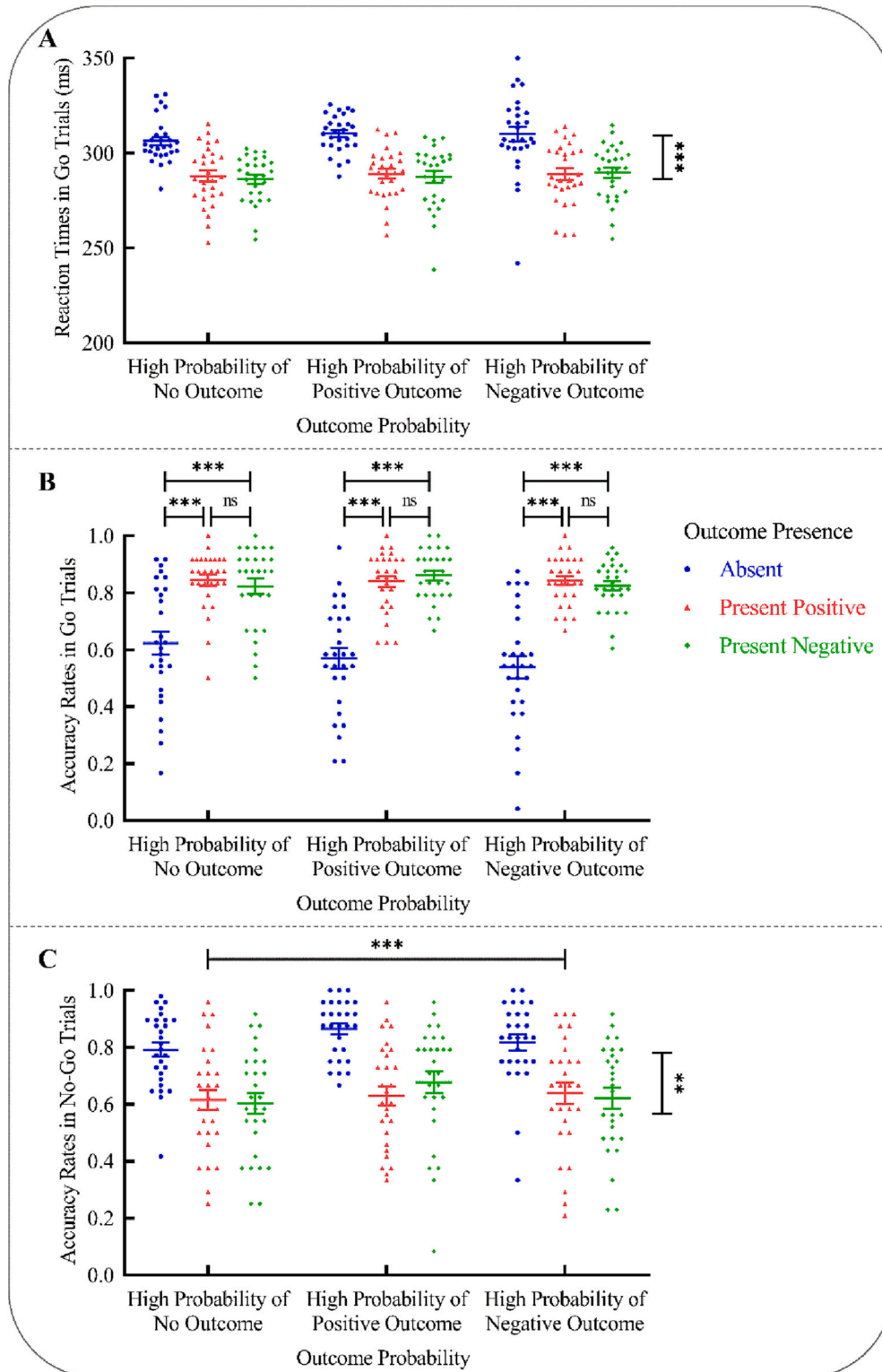


**Fig. 6.** Results of Experiment 2 based on the factors “Outcome Presence” and “Outcome Probability”. (A) Reaction times in Go trials, (B) accuracy rates in Go trials, and (C) accuracy rates in No-Go trials in different conditions. Data are expressed as Mean  $\pm$  SEM. Ns: not significant; \*\*:  $p < .01$ ; \*\*\*:  $p < .001$ .

blocks (i.e., having a high probability of obtaining positive/negative/no outcomes), participants responded more accurately to Go cues when their previous action led to a positive or negative outcome compared with no outcome (all  $p$ s < 0.001). Whereas, in none of the three types of blocks, participants' accuracy rates in Go trials differ significantly when their previous action led to a positive outcome compared with a negative outcome (all  $p$ s > 0.05; see Fig. 6B).

For accuracy rates in No-Go trials, the two-way repeated measures ANOVA showed a significant main effect of Outcome Presence,  $F(2,54) = 61.56, p < .001, \eta_p^2 = 0.70, BF_{10} > 10^{11}$ . Further analyses showed that, participants responded less accurately in No-Go trials when their previous action led to a positive or negative outcome compared with no outcome (both  $p$ s < 0.001), while their accuracy rates in No-Go trials did not differ significantly when their previous action led to a positive outcome compared with a negative outcome ( $p = .760$ ; see Fig. 6C). There was also a significant main effect of Outcome Probability,  $F(2,54) = 6.28, p = .004, \eta_p^2 = 0.19, BF_{10} = 4.83$ . Further analyses showed that, participants responded more accurately in No-Go trials in blocks having a high probability of obtaining positive outcomes, when compared with blocks having a high probability of obtaining no outcome ( $p < .001$ ), and when compared with blocks having a high probability of obtaining negative outcomes ( $p = .045$ ). Participants' accuracy rates in No-Go trials did not differ significantly in blocks having a high probability of obtaining negative outcomes compared with blocks having a high probability of obtaining no outcome ( $p = .147$ ). However, the interaction between Outcome Presence and Outcome Probability was not significant,  $F(4,108) = 1.62, p = .175, \eta_p^2 = 0.06, BF_{10} = 0.95$ .

Moreover, the analysis of accuracy rates in both Go and No-Go trials, using a three-way repeated measures ANOVA, showed that the interaction between Outcome Presence, Outcome Probability, and Trial Type was not significant,  $F(4,108) = 1.86, p = .123, \eta_p^2 = 0.06$ . However, the  $BF_{10}$  was 6.62, indicating moderate evidence for the interaction effect. As we were interested in the performance differences between Go and No-Go trials in each experimental condition, we further analyzed the interaction by focusing on the effect of Trial Type for each level of the other two factors (i.e., Outcome Presence and Outcome Probability). The results showed that, in any of the three types of blocks (i.e., having a high probability of obtaining positive/negative/no outcomes), (1) participants' accuracy rates were significantly higher in Go trials compared with No-Go trials when their previous action led to a positive or negative outcome (all  $p$ s < 0.001); (2) in contrast, participants' accuracy rates were significantly lower in Go trials compared with No-Go trials when their previous action led to no outcome (all  $p$ s < 0.001; see Supplementary Fig. 2A).

In summary, when participants' previous action led to an outcome (positive or negative) compared with no outcome, they responded faster and more accurately to Go cues, as well as responded less accurately to No-Go cues. However, their reaction times in Go trials, as well as accuracy rates in Go trials and No-Go trials, did not differ significantly when their previous action led to a positive outcome compared with a negative outcome. In addition, participants had higher accuracy rates in Go trials compared with No-Go trials (i.e., a preference for go over no-go responses) when their previous action led to an outcome, irrespective of the emotional valence (i.e., positive or negative). In contrast, participants had lower accuracy rates in Go trials compared with No-Go trials (i.e., a preference for no-go over go responses) when their previous action led to no outcome.

### 3.2.2. Results based on the factors "outcome presence" and "Previous Outcome Frequency"

For reaction times in Go trials, the two-way repeated measures ANOVA showed significant main effects of Outcome Presence,  $F(2,54) = 67.51, p < .001, \eta_p^2 = 0.71, BF_{10} > 10^{15}$ , and Previous Outcome Frequency,  $F(1,27) = 23.32, p < .001, \eta_p^2 = 0.46, BF_{10} > 10^5$ . There was also a significant interaction between Outcome Presence and Previous Outcome Frequency,  $F(2,54) = 12.32, p < .001, \eta_p^2 = 0.31, BF_{10} > 10^4$ .

Further analyses showed that, regardless of the frequency of the same type of outcome in the previous two pairs of trials (i.e., two to four times or zero times), participants responded faster to Go cues when their previous action led to a positive or a negative outcome compared with no outcome (all  $p$ s < 0.001); whereas, their reaction times in Go trials did not differ significantly when their previous action led to a positive outcome compared with a negative outcome (both  $p$ s > 0.05; see Fig. 7A).

For accuracy rates in Go trials, the two-way repeated measures ANOVA showed significant main effects of Outcome Presence,  $F(2,54) = 57.08, p < .001, \eta_p^2 = 0.68, BF_{10} > 10^{15}$ , and Previous Outcome Frequency,  $F(1,27) = 34.45, p < .001, \eta_p^2 = 0.56, BF_{10} > 10^{10}$ . There was also a significant interaction between Outcome Presence and Previous Outcome Frequency,  $F(2,54) = 29.58, p < .001, \eta_p^2 = 0.52, BF_{10} > 10^8$ . Further analyses showed that, regardless of the frequency of the same type of outcome in the previous two pairs of trials (i.e., two to four times or zero

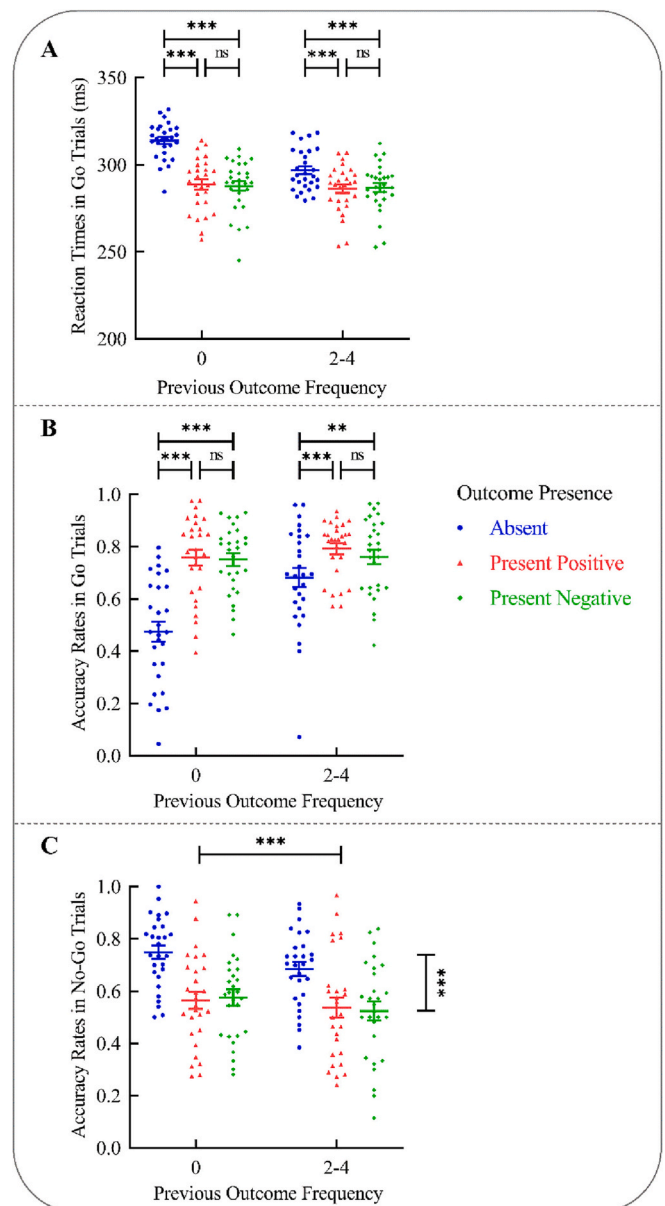


**Fig. 7.** Results of Experiment 2 based on the factors "Outcome Presence" and "Previous Outcome Frequency". (A) Reaction times in Go trials, (B) accuracy rates in Go trials, and (C) accuracy rates in No-Go trials in different conditions. Data are expressed as Mean  $\pm$  SEM. ns: not significant; \*\*  $p < .01$ ; \*\*\*  $p < .001$ .

times), participants responded more accurately to Go cues when their previous action led to a positive or a negative outcome compared with no outcome (all  $ps < 0.01$ ); whereas, their accuracy rates in Go trials did not differ significantly when their previous action led to a positive outcome compared with a negative outcome (both  $ps > 0.05$ ; see Fig. 7B).

For accuracy rates in No-Go trials, the two-way repeated measures ANOVA showed a significant main effect of Outcome Presence,  $F(2,54) = 48.49$ ,  $p < .001$ ,  $\eta_p^2 = 0.64$ ,  $BF_{10} > 10^9$ . Further analyses showed that, participants responded less accurately in No-Go trials when their previous action led to a positive or negative outcome compared with no outcome (both  $ps < 0.001$ ); whereas, their accuracy rates in No-Go trials did not differ significantly when their previous action led to a positive outcome compared with a negative outcome ( $p = .959$ ). There was also a significant main effect of Previous Outcome Frequency,  $F(1,27) = 17.42$ ,  $p < .001$ ,  $\eta_p^2 = 0.39$ ,  $BF_{10} = 16.54$ . Further analyses showed that, participants responded less accurately in No-Go trials when the same type of outcome had occurred two to four times compared with zero times in the previous two pairs of trials ( $p < .001$ ; see Fig. 7C). However, the interaction between Outcome Presence and Previous Outcome Frequency was not significant,  $F(2,54) = 0.80$ ,  $p = .453$ ,  $\eta_p^2 = 0.03$ ,  $BF_{10} = 0.84$ .

Moreover, the analysis of accuracy rates in both Go and No-Go trials, using a three-way repeated measures ANOVA, showed a significant interaction between Outcome Presence, Previous Outcome Frequency, and Trial Type,  $F(2,54) = 17.56$ ,  $p < .001$ ,  $\eta_p^2 = 0.39$ ,  $BF_{10} > 10^8$ . As we were interested in the performance differences between Go and No-Go trials in each experimental condition, we further analyzed the interaction by focusing on the effect of Trial Type for each level of the other two factors (i.e., Outcome Presence and Previous Outcome Frequency). The results showed that, (1) regardless of the frequency of the same type of outcome in the previous two pairs of trials (i.e., two to four times or zero times), when participants' previous action led to a positive or negative outcome, their accuracy rates were significantly higher in Go trials compared with No-Go trials (all  $ps < 0.001$ ); (2) in contrast, when participants' previous action did not lead to any outcome and the same type of outcome had occurred two to four times (i.e., outcomes never occurred) in the previous two pairs of trials, their accuracy rates did not differ significantly between Go trials and No-Go trials ( $p = .949$ ); (3) furthermore, when participants' previous action did not lead to any outcome but the same type of outcome had occurred zero times (i.e., outcomes had occurred two to four times) in the previous two pairs of trials, their accuracy rates were significantly lower in Go trials compared with No-Go trials ( $p < .001$ ; see Supplementary Fig. 2B).

In summary, when participants' previous action led to an outcome (positive or negative) compared with no outcome, they responded faster and more accurately to Go cues, as well as responded less accurately to No-Go cues. However, their reaction times in Go trials, as well as accuracy rates in Go trials and No-Go trials, did not differ significantly when their previous action led to a positive outcome compared with a negative outcome. In addition, participants had higher accuracy rates in Go trials compared with No-Go trials (i.e., a preference for go over no-go responses) when their previous action led to an outcome, irrespective of the emotional valence (i.e., positive or negative). In contrast, participants had comparable accuracy rates in Go and No-Go trials (i.e., no obvious preference for go over no-go responses) when action outcomes had never occurred in the previous two pairs of trials and their previous action unsurprisingly did not lead to any outcome. Furthermore, participants had lower accuracy rates in Go trials compared with No-Go trials (i.e., a preference for no-go over go responses) when outcomes had occurred two to four times in the previous two pairs of trials but their previous action surprisingly did not lead to any outcome.

### 3.3. Discussion

Consistent with Experiment 1, results in Experiment 2 indicate that the “local” outcome presence led to an enhancement of action readiness and at the same time reduced response inhibition, manifested by higher

accuracy rates and faster reaction times to Go cues as well as lower accuracy rates to No-Go cues. In addition, when participants' previous keypress action led to an outcome, they were more accurate in repeating that action than withholding it (i.e., a preference for go over no-go responses); in contrast, when participants' previous action did not result in any perceivable outcome, they had no obvious preference for go or no-go responses or even had a preference for no-go over go responses. This also supports our previous finding indicating that a reduced sense of agency might have shifted participants' tendency from preparedness for action towards increased inhibitory control or general passivity. Importantly, participants' performance did not differ significantly when their previous action led to a positive outcome compared with a negative outcome. That is, participants' action readiness and response inhibition were not modulated by the emotional valence of action outcomes, indicating that our findings are not driven by the rewarding properties of the outcome per se.

Interestingly, the modulation of our results by the “global” outcome frequency in Experiment 2 was much less prominent than in Experiment 1. For instance, in Experiment 1, the facilitation effect of “local” outcome presence on reaction times in Go trials was stronger in blocks having a high probability of getting positive outcomes (i.e., a significant interaction effect), while such facilitation effect did not differ significantly among different types of blocks in Experiment 2 (i.e., no interaction effect). This is probably because the “global” context (i.e., the relative frequency of a particular type of outcome) within a given block in Experiment 2 (50% vs. 25% vs. 25%) was less obvious than in Experiment 1 (75% vs. 25%). The longer-lasting enhancement of the sense of agency caused by the “global” outcome frequency might be much weaker in Experiment 2 than Experiment 1, and thus had less impact on participants' subsequent motor responses.

## 4. General discussion

Using a modified Go/No-Go task, the present study investigated the influence of sense of agency on subsequent action regulation. In Experiment 1, we manipulated participants' sense of agency by varying the presence of a visual outcome (i.e., a happy face) at the trial-by-trial level and the overall outcome probability at the block level (high vs. low) for a given motor action, and measured participants' responses to the subsequent Go, No-Go, or Free-Choice cue. Additionally, we conducted a control experiment including subjective judgements of agency as a manipulation check. As predicted, the immediate enhancement of sense of agency caused by the “local” outcome presence enhanced participants' readiness to act while at the same time suppressed their ability to cancel a prepotent action when required to do so. In addition, these effects were further amplified by a longer-lasting enhancement of the sense of agency caused by the “global” outcome probability in a given block or in several previous trials. In Experiment 2, we further manipulated the emotional valence of the action outcome (i.e., a happy or an angry face), and found no difference of positive versus negative outcomes on subsequent action regulation but similar effects.

One of our main findings is that participants' readiness or preparedness to perform a keypress action varies as a function of the sense of agency over that action. Both experiments demonstrate that participants responded more accurately and faster to the subsequent Go cue that signals a keypress action when the previous keypress action produced a visible effect. In addition, the control experiment confirmed that participants felt a higher sense of agency when their action led to a visible effect compared with no effect. These results support that the feeling of control over the motor action is updated on a short, trial-to-trial timescale and can have an instant impact on the following motor responses (Hemed et al., 2020). Our finding is also in line with previous empirical work showing that actions followed by predictable perceptual changes are reinforced. For example, two-month-old infants moved their limb more frequently when their movement caused a movement of the mobile tethered to that particular limb (Watanabe & Taga, 2006, 2011).

Similarly, for adult participants, a motor response that leads to a perceptual change in the environment increases the speed and the frequency of that response (Hemed et al., 2020; Karsh et al., 2020; Tanaka et al., 2021). Moreover, the reliability of action outcomes has been found to boost the readiness potential, reflecting enhanced neural activities prior to the action (Wen et al., 2018). Together, it is reasonable to conclude that feeling in control over a specific action appears to reinforce that action and in this way increases the tendency to repeat it, while feeling out of control over one action discourages repetition of that action. Consistently, the comparison results of accuracy rates in Go and No-Go trials reveal that participants' motor tendency was shifted from readiness to action towards increased inhibitory control when their sense of agency decreased. Specifically, participants exhibited a preference for go over no-go responses in conditions with "local" outcome occurrence. In contrast, no obvious preference between go and no-go responses or even a preference for no-go over go responses was observed in the condition with high outcome frequency at the block level (i.e., global) but surprising outcome absence at the trial level (i.e., local).

The present study provides, to the best of our knowledge, the first evidence that a higher sense of agency results in reduced response inhibition. Specifically, when participants felt more in control over the keypress action as induced by the occurrence of a perceivable outcome, they responded less accurately to the subsequent No-Go cue that required canceling the prepotent keypress action. Given that response inhibition is regarded as one of the central components of cognitive control (Botvinick & Braver, 2015), our finding suggests that inhibitory control deployed over one specific action increases as the feeling of control over that action decreases. This interpretation is in line with the proposal that using cognitive control needs to be distinguished from the feeling of being in control, i.e., the sense of agency (Potts & Carlson, 2019). Additionally, losing control of an already controlled visual object has been found to attract attention (Wen & Haggard, 2018). Our finding extends this earlier report by suggesting that detecting diminished control may also act as a trigger to executive function/cognitive control that aims to reassert control. Effectively controlling the environment is a psychological and biological imperative for survival (Leotti, Iyengar, & Ochsner, 2010); therefore, our observation of the sense of agency as input for adaptive adjustment of cognitive control highlights its critical role in human survival.

Importantly, results in Experiment 1 indicate that a sense of agency modulates not only the response inhibition triggered by external No-Go cues but also the response inhibition generated from internal decisions (also known as intentional inhibition). Specifically, after experiencing that the keypress action did not produce any visible effect, participants were less likely to choose to perform that action again in response to Free-Choice cues; and even when they chose to press the button, the reaction times were slower. These results indicate that participants tend to cancel the about-to-be-executed action when feeling out of control. It has been shown that subliminal masked prime presented prior to the Free-Choice cue can influence participants' decision to act or inhibit, suggesting a modulation effect of unconscious processing on intentional inhibitory control (Parkinson & Haggard, 2014). In Experiment 1, although the action-outcome contingency can be consciously perceived, it was neither explicitly associated with the sense of agency or the feeling of control nor did it provide any information about participants' performance. In other words, the sense of agency was task-irrelevant and thus most probably processed implicitly. Therefore, our results support that the free decisions to act or not to act can be influenced by implicit processing regarding our degree of control over the external environment.

Notably, there might be a link between the long reaction times in Go/Free-Choice trials and higher accuracy rates in No-Go trials in the condition with high "global" outcome probability but surprising "local" outcome absence. That is, when the previous keypress action surprisingly did not produce any outcome, participants might hesitate to press

the key again. Such hesitation could be associated with no action in the subsequent phase, resulting in a low response accuracy for the Go cue and a high response accuracy for the No-Go cue. In other words, the putative "better" response inhibition might be a result of a general response slowing or down-regulation of motor preparation, which is another side of the same coin. Dissociating the effects of sense of agency on action readiness and response inhibition, disentangling the precise nature of the underlying inhibitory mechanisms, as well as testing the specific time course of these processes would be worthwhile endeavors for future studies.

Interestingly, the effects of the "local" outcome presence on subsequent action regulation are modulated by the "global" outcome probability. Specifically, results in Experiment 1 showed that the enhancement of action readiness and the suppression of response inhibition after obtaining action outcomes compared with no outcome were amplified when participants had a high probability of obtaining action outcomes in a given block and also when action outcomes occurred frequently in several previous trials. Notably, this modulation effect was much less prominent in Experiment 2, probably because the longer-lasting enhancement of the sense of agency induced in Experiment 2 was not as strong as that in Experiment 1 due to the relative frequency rates of the different outcomes. The modulating effect of the global context has also been reported by Hemed et al. (2020), who found that reaction times on trial  $n$  was sensitive to the outcome presence on trial  $n-1$  and the magnitude of this effect was modulated by the outcome frequency in trial  $n-4$  to  $n-2$ . This finding suggests that participants' action regulation is sensitive to both the immediate, local context and the more distant, global context regarding the effectiveness of an action (i.e., whether the action can lead to an effect and how reliable it is). This is also consistent with the recent view that the brain carefully monitors one's control over external objects and is highly sensitive to any change in the degree of control (Wen et al., 2021; Wen & Haggard, 2018).

The observed effects of the sense of agency on response inhibition and action readiness could be explained within a larger framework of "motivation from control". This framework posits that the sense of agency, i.e., the feeling of control over external objects, is a form of internal reward and serves as an important source of motivation (Nafcha, Higgins, & Eitam, 2016). This view has been supported by accumulative behavioral and neuroimaging evidence. For example, a high probability of obtaining action outcomes, which contributes to an increase in the sense of agency, facilitates the likelihood and speed of an action being selected (Karsh et al., 2020; Penton et al., 2018). In addition, high action-effect contingency (Behne, Scheich, & Brechmann, 2008) and high perceived control (Lorenz et al., 2015; Tricomi, Delgado, & Fiez, 2004) are associated with increased activity in brain areas (e.g., striatum) involved in reward processing. From this perspective, the enhanced action readiness and reduced inhibitory tendency after feeling more in control in the present study may reflect a rise in motivation. Moreover, the "motivation from control" framework emphasizes the degree of control the organism has over the environment but not the value (desired or undesired) of the outcome (Nafcha et al., 2016). In other words, anything that happens after a motor response, no matter whether it is positive, negative or neutral, can be judged as feedback about successful control and hence can motivate action. Notably, the value of the outcome is another important source of motivation, known as "motivation from outcome". It can generally trump the "motivation from control", if the outcome itself provides information about the relation between the current state and the desired goal (Nafcha et al., 2016). However, participants' task goal (i.e., more accurate and faster responses) was independent of the emotional valence of action outcomes in the present study; therefore, "motivation from control" probably played a dominant role. This may explain why the emotional valence of action outcomes did not modulate participants' action regulation in the present study. From the participants' view, both the happy and the angry face presented immediately after their keypress response indicated that they were effective in controlling the environment and hence seemed to

trigger comparable degrees of motivation for future actions.

One limitation of the present study should be noted. The present study cannot isolate the relative contributions of the conceptual (explicit) judgement of agency and sensorimotor (implicit) predictability to the effects of the present study. Our control experiment showed that participants reported higher agency ratings (i.e., feeling more in control) when their previous action led to an outcome compared with no outcome and also when action outcomes occurred relatively frequently in a given block or in several previous trials. Thus, it is reasonable to speculate that higher-level aspects of the sense of agency (explicit judgement of agency) impacted our results. However, our results cannot be fully explained by changes in the explicit judgement of agency as we observed similar effects across the two main experiments in absence of any explicit judgements. More importantly, Hemed et al. (2022) have elegantly shown that fulfilled sensorimotor prediction facilitated response speed (i.e., action efficiency), while conceptual judgement in contrast mainly affected response frequency in terms of which action to choose (i.e., response selection). Therefore, it is highly likely that conceptual and sensorimotor aspects of the sense of agency both contributed to our results. Further studies are needed to disentangle the relative contributions of these factors on action regulation, for example by replacing the no-effect condition with a sensory-unpredictable condition (Hemed et al., 2020).

In conclusion, a higher sense of agency in the current trial, as induced by the presence of an outcome for a given action, facilitated action readiness but at the same time disrupted response inhibition in a subsequent trial. These effects were further amplified by a longer-lasting enhancement of the sense of agency as induced by high outcome frequency in a given block or in several previous trials. Furthermore, these effects were independent of the emotional valence of the keypress outcome. We explain these effects within the framework of motivation from control. Our findings highlight the impact of the control felt on the control used in action regulation and hereby provide new insights into the functional significance of the sense of agency on human behavior.

## Funding

This work was supported by Deutsche Forschungsgemeinschaft [GE 30841-1 to A.G. and SCHU 24716-1 to S-S-B.] and China Scholarship Council [grant number 202004910347 to Q.R.].

## CRedit authorship contribution statement

**Qiaoyue Ren:** Conceptualization, Methodology, Investigation, Data curation, Formal analysis, Visualization, Writing – original draft. **Antje Gentsch:** Conceptualization, Methodology, Writing – review & editing. **Jakob Kaiser:** Conceptualization, Methodology, Writing – review & editing. **Simone Schütz-Bosbach:** Conceptualization, Methodology, Writing – review & editing, Supervision, Funding acquisition.

## Declaration of Competing Interest

None.

## Data availability

Raw data and analysis files are available via Open Science Framework: [https://osf.io/z2qdh/?view\\_only=a6a049aa8e0c46beac4e4d30eba648245](https://osf.io/z2qdh/?view_only=a6a049aa8e0c46beac4e4d30eba648245)

## Acknowledgments

We thank Pritha Sen and Maximilian Lange for their assistance in data collection.

## Appendix A. Supplementary data

Supplementary data to this article can be found online at <https://doi.org/10.1016/j.cognition.2023.105456>.

## References

- Albayay, J., Castiello, U., & Parma, V. (2019). Task-irrelevant odours affect both response inhibition and response readiness in fast-paced go/no-go task: The case of valence. *Scientific Reports*, 9(1), 19329. <https://doi.org/10.1038/s41598-019-55977-z>
- Bari, A., & Robbins, T. W. (2013). Inhibition and impulsivity: Behavioral and neural basis of response control. *Progress in Neurobiology*, 108, 44–79. <https://doi.org/10.1016/j.pneurobio.2013.06.005>
- Behne, N., Scheich, H., & Brechmann, A. (2008). The left dorsal striatum is involved in the processing of neutral feedback. *NeuroReport*, 19(15), 1497–1500. <https://doi.org/10.1097/WNR.0b013e32830fe98c>
- Blakemore, S.-J., Wolpert, D. M., & Frith, C. D. (1998). Central cancellation of self-produced tickle sensation. *Nature Neuroscience*, 1(7), 635–640. <https://doi.org/10.1038/2870>
- Blakemore, S.-J., Wolpert, D. M., & Frith, C. D. (2002). Abnormalities in the awareness of action. *Trends in Cognitive Sciences*, 6(6), 237–242. [https://doi.org/10.1016/S1364-6613\(02\)01907-1](https://doi.org/10.1016/S1364-6613(02)01907-1)
- Botvinick, M., & Braver, T. (2015). Motivation and cognitive control: From behavior to neural mechanism. *Annual Review of Psychology*, 66(1), 83–113. <https://doi.org/10.1146/annurev-psych-010814-015044>
- Campbell, J. I. D., & Thompson, V. A. (2012). MorePower 6.0 for ANOVA with relational confidence intervals and Bayesian analysis. *Behavior Research Methods*, 44(4), 1255–1265. <https://doi.org/10.3758/s13428-012-0186-0>
- Caspar, E. A., Desantis, A., Dienes, Z., Cleeremans, A., & Haggard, P. (2016). The sense of agency as tracking control. *PLoS One*, 11(10), Article e0163892. <https://doi.org/10.1371/journal.pone.0163892>
- Chambers, C. D., Garavan, H., & Bellgrove, M. A. (2009). Insights into the neural basis of response inhibition from cognitive and clinical neuroscience. *Neuroscience & Biobehavioral Reviews*, 33(5), 631–646. <https://doi.org/10.1016/j.neubiorev.2008.08.016>
- Demant, J., Muhle-Karbe, P. S., Lynn, M. T., Blotenberg, I., & Brass, M. (2013). Power to the will: How exerting physical effort boosts the sense of agency. *Cognition*, 129(3), 574–578. <https://doi.org/10.1016/j.cognition.2013.08.020>
- Di Costa, S., Théro, H., Chambon, V., & Haggard, P. (2018). Try and try again: Post-error boost of an implicit measure of agency. *Quarterly Journal of Experimental Psychology*, 71(7), 1584–1595. <https://doi.org/10.1080/17470218.2017.1350871>
- Ebert, J. P., & Wegner, D. M. (2010). Time warp: Authorship shapes the perceived timing of actions and events. *Consciousness and Cognition*, 19(1), 481–489. <https://doi.org/10.1016/j.concog.2009.10.002>
- Eitam, B., Kennedy, P. M., & Tory Higgins, E. (2013). Motivation from control. *Experimental Brain Research*, 229(3), 475–484. <https://doi.org/10.1007/s00221-012-3370-7>
- Frith, C. D., Blakemore, S.-J., & Wolpert, D. M. (2000). Abnormalities in the awareness and control of action. *Philosophical Transactions of the Royal Society of London. Series B: Biological Sciences*, 355(1404), 1771–1788. <https://doi.org/10.1098/rstb.2000.0734>
- Gentsch, A., & Schütz-Bosbach, S. (2015). Agency and outcome prediction. In P. Haggard, & B. Eitam (Eds.), *The sense of agency* (pp. 217–231). Oxford University Press. <https://doi.org/10.1093/acprof:oso/9780190267278.003.0009>
- Haggard, P. (2017). Sense of agency in the human brain. *Nature Reviews Neuroscience*, 18, 196–207. <https://doi.org/10.1038/nrn.2017.14>
- Haggard, P., & Eitam, B. (Eds.). (2015). *The sense of agency*. Oxford University Press.
- Hemed, E., Bakbani-Elkayam, S., Teodorescu, A. R., Yona, L., & Eitam, B. (2020). Evaluation of an action's effectiveness by the motor system in a dynamic environment. *Journal of Experimental Psychology: General*, 149(5), 935–948. <https://doi.org/10.1037/xge0000692>
- Hemed, E., Karsh, N., Mark-Tavger, I., & Eitam, B. (2022). Motivation(s) from control: Response-effect contingency and confirmation of sensorimotor predictions reinforce different levels of selection. *Experimental Brain Research*, 240(5), 1471–1497. <https://doi.org/10.1007/s00221-022-06345-3>
- Hon, N., Poh, J.-H., & Soon, C.-S. (2013). Preoccupied minds feel less control: Sense of agency is modulated by cognitive load. *Consciousness and Cognition*, 22(2), 556–561. <https://doi.org/10.1016/j.concog.2013.03.004>
- Howard, E. E., Edwards, S. G., & Bayliss, A. P. (2016). Physical and mental effort disrupts the implicit sense of agency. *Cognition*, 157, 114–125. <https://doi.org/10.1016/j.cognition.2016.08.018>
- JASP Team. (2023). *JASP (Version 0.17.0.0) [Computer software]*.
- Kaiser, J., Buciuman, M., Gigl, S., Gentsch, A., & Schütz-Bosbach, S. (2021). The interplay between affective processing and sense of agency during action regulation: A review. *Frontiers in Psychology*, 12, Article 716220. <https://doi.org/10.3389/fpsyg.2021.716220>
- Kaiser, J., & Schütz-Bosbach, S. (2019). Proactive control without midfrontal control signals? The role of midfrontal oscillations in preparatory conflict adjustments. *Biological Psychology*, 148, Article 107747. <https://doi.org/10.1016/j.biopsycho.2019.107747>
- Karsh, N., & Eitam, B. (2015). I control therefore I do: Judgments of agency influence action selection. *Cognition*, 138, 122–131. <https://doi.org/10.1016/j.cognition.2015.02.002>

- Karsh, N., Eitam, B., Mark, I., & Higgins, E. T. (2016). Bootstrapping agency: How control-relevant information affects motivation. *Journal of Experimental Psychology: General*, 145(10), 1333–1350. <https://doi.org/10.1037/xge0000212>
- Karsh, N., Hemed, E., Nafcha, O., Elkayam, S. B., Custers, R., & Eitam, B. (2020). The differential impact of a response's effectiveness and its monetary value on response-selection. *Scientific Reports*, 10(1), 3405. <https://doi.org/10.1038/s41598-020-60385-9>
- Leotti, L. A., Iyengar, S. S., & Ochsner, K. N. (2010). Born to choose: The origins and value of the need for control. *Trends in Cognitive Sciences*, 14(10), 457–463. <https://doi.org/10.1016/j.tics.2010.08.001>
- Lorenz, R. C., Gleich, T., Kühn, S., Pöhlend, L., Pelz, P., Wüstenberg, T., ... Beck, A. (2015). Subjective illusion of control modulates striatal reward anticipation in adolescence. *NeuroImage*, 117, 250–257. <https://doi.org/10.1016/j.neuroimage.2015.05.024>
- Malik, R. A., Galang, C. M., & Finger, E. (2022). The sense of agency for brain disorders: A comprehensive review and proposed framework. *Neuroscience & Biobehavioral Reviews*, 139, Article 104759. <https://doi.org/10.1016/j.neubiorev.2022.104759>
- Nafcha, O., Higgins, E. T., & Eitam, B. (2016). Control feedback as the motivational force behind habitual behavior. *Progress in Brain Research*, 229, 49–68. <https://doi.org/10.1016/bs.pbr.2016.06.008>
- Parkinson, J., & Haggard, P. (2014). Subliminal priming of intentional inhibition. *Cognition*, 130(2), 255–265. <https://doi.org/10.1016/j.cognition.2013.11.005>
- Van den Bussche, E., Alves, M., Murray, Y. P. J., & Hughes, G. (2020). The effect of cognitive effort on the sense of agency. *PLoS One*, 15(8), Article e0236809. <https://doi.org/10.1371/journal.pone.0236809>
- van Peer, J. M., Gladwin, T. E., & Nieuwenhuys, A. (2019). Effects of threat and sleep deprivation on action tendencies and response inhibition. *Emotion*, 19, 1425–1436. <https://doi.org/10.1037/emo0000533>
- Penton, T., Wang, X., Coll, M.-P., Catmur, C., & Bird, G. (2018). The influence of action–outcome contingency on motivation from control. *Experimental Brain Research*, 236(12), 3239–3249. <https://doi.org/10.1007/s00221-018-5374-4>
- Potts, C. A., & Carlson, R. A. (2019). Control used and control felt: Two sides of the agency coin. *Attention, Perception, & Psychophysics*, 81(7), 2304–2319. <https://doi.org/10.3758/s13414-019-01771-y>
- Sato, A., & Yasuda, A. (2005). Illusion of sense of self-agency: Discrepancy between the predicted and actual sensory consequences of actions modulates the sense of self-agency, but not the sense of self-ownership. *Cognition*, 94(3), 241–255. <https://doi.org/10.1016/j.cognition.2004.04.003>
- Sidarus, N., & Haggard, P. (2016). Difficult action decisions reduce the sense of agency: A study using the Eriksen flanker task. *Acta Psychologica*, 166, 1–11. <https://doi.org/10.1016/j.actpsy.2016.03.003>
- Tanaka, T., Watanabe, K., & Tanaka, K. (2021). Immediate action effects motivate actions based on the stimulus–response relationship. *Experimental Brain Research*, 239(1), 67–78. <https://doi.org/10.1007/s00221-020-05955-z>
- Tottenham, N., Tanaka, J. W., Leon, A. C., McCarry, T., Nurse, M., Hare, T. A., ... Nelson, C. (2009). The NimStim set of facial expressions: Judgments from untrained research participants. *Psychiatry Research*, 168(3), 242–249. <https://doi.org/10.1016/j.psychres.2008.05.006>
- Tricomi, E. M., Delgado, M. R., & Fiez, J. A. (2004). Modulation of caudate activity by action contingency. *Neuron*, 41(2), 281–292. [https://doi.org/10.1016/S0896-6273\(03\)00848-1](https://doi.org/10.1016/S0896-6273(03)00848-1)
- Vastano, R., Pozzo, T., & Brass, M. (2017). The action congruency effect on the feelings of agency. *Consciousness and Cognition*, 51, 212–222. <https://doi.org/10.1016/j.concog.2017.04.002>
- Villa, R., Tidoni, E., Porciello, G., & Aglioti, S. M. (2021). Freedom to act enhances the sense of agency, while movement and goal-related prediction errors reduce it. *Psychological Research*, 85(3), 987–1004. <https://doi.org/10.1007/s00426-020-01319-y>
- Wagenmakers, E.-J., Love, J., Marsman, M., Jamil, T., Ly, A., Verhagen, J., ... Morey, R. D. (2018). Bayesian inference for psychology. Part II: Example applications with JASP. *Psychonomic Bulletin & Review*, 25(1), 58–76. <https://doi.org/10.3758/s13423-017-1323-7>
- Wagenmakers, E.-J., Marsman, M., Jamil, T., Ly, A., Verhagen, J., Love, J., ... Morey, R. D. (2018). Bayesian inference for psychology. Part I: Theoretical advantages and practical ramifications. *Psychonomic Bulletin & Review*, 25(1), 35–57. <https://doi.org/10.3758/s13423-017-1343-3>
- Wang, Y., Damen, T. G. E., & Aarts, H. (2018). An examination of the sequential trial effect on experiences of agency in the Simon task. *Consciousness and Cognition*, 66, 17–25. <https://doi.org/10.1016/j.concog.2018.10.005>
- Watanabe, H., & Taga, G. (2006). General to specific development of movement patterns and memory for contingency between actions and events in young infants. *Infant Behavior and Development*, 29(3), 402–422. <https://doi.org/10.1016/j.infbeh.2006.02.001>
- Watanabe, H., & Taga, G. (2011). Initial-state dependency of learning in young infants. *Human Movement Science*, 30(1), 125–142. <https://doi.org/10.1016/j.humov.2010.07.003>
- Wen, W., & Haggard, P. (2018). Control changes the way we look at the world. *Journal of Cognitive Neuroscience*, 30(4), 603–619. [https://doi.org/10.1162/jocn\\_a.01226](https://doi.org/10.1162/jocn_a.01226)
- Wen, W., & Imamizu, H. (2022). The sense of agency in perception, behaviour and human–machine interactions. *Nature Reviews Psychology*, 1(4), 211–222. <https://doi.org/10.1038/s44159-022-00030-6>
- Wen, W., Ishii, H., Ohata, R., Yamashita, A., Asama, H., & Imamizu, H. (2021). Perception and control: Individual difference in the sense of agency is associated with learnability in sensorimotor adaptation. *Scientific Reports*, 11(1), 20542. <https://doi.org/10.1038/s41598-021-99969-4>
- Wen, W., Minohara, R., Hamasaki, S., Maeda, T., An, Q., Tamura, Y., Yamakawa, H., Yamashita, A., & Asama, H. (2018). The readiness potential reflects the reliability of action consequence. *Scientific Reports*, 8, 11865. <https://doi.org/10.1038/s41598-018-30410-z>
- Wessel, J. R. (2018). Prepotent motor activity and inhibitory control demands in different variants of the go/no-go paradigm. *Psychophysiology*, 55(3), Article e12871. <https://doi.org/10.1111/psyp.12871>

### Supplementary Materials

**Supplementary Table 1.** Means and standard deviations of reaction times and accuracy rates (or response rates) in different conditions of Experiment 1 based on the factors “Outcome Presence” and “Outcome Probability”.

<b>Outcome Presence:</b>	<i>Absent</i>		<i>Present</i>	
<b>Outcome Probability:</b>	<i>Low</i>	<i>High</i>	<i>Low</i>	<i>High</i>
<i>Reaction Times (ms)</i>				
Go Trials	273.40 ± 11.56	286.40 ± 12.95	262.79 ± 14.13	263.66 ± 14.79
Free-Choice Trials	279.04 ± 14.81	292.23 ± 18.60	267.38 ± 17.12	270.48 ± 16.76
<i>Accuracy Rates</i>				
Go Trials	0.83 ± 0.12	0.70 ± 0.16	0.92 ± 0.06	0.89 ± 0.06
No-Go Trials	0.63 ± 0.14	0.72 ± 0.12	0.48 ± 0.19	0.50 ± 0.17
<i>Response Rates</i>				
Free-Choice Trials	0.61 ± 0.17	0.44 ± 0.19	0.75 ± 0.16	0.71 ± 0.16

**Supplementary Table 2.** Response rates in Free-Go trials in different conditions of Experiment 1.

<b>Outcome Presence</b>	<b>Outcome Probability</b>	Mean	SD	Minimum	Maximum
<i>Absent</i>	<i>Low</i>	0.61	0.17	0.21	0.93
<i>Absent</i>	<i>High</i>	0.44	0.19	0.10	0.81
<i>Present</i>	<i>Low</i>	0.75	0.16	0.40	0.96
<i>Present</i>	<i>High</i>	0.71	0.16	0.26	0.89

**Supplementary Table 3.** The number of trials in different conditions of Experiment 1 based on the factors “Outcome Presence” and “Outcome Probability” for each analysis.

<b>Outcome Presence:</b>	<i>Absent</i>		<i>Present</i>	
<b>Outcome Probability:</b>	<i>Low</i>	<i>High</i>	<i>Low</i>	<i>High</i>
<i>Analysis of Reaction Times</i>				
Go Trials	119.78 ± 17.13	33.67 ± 7.68	44.30 ± 3.00	128.59 ± 8.88
Free-Choice Trials	87.89 ± 24.71	21.15 ± 9.22	36.07 ± 7.67	102.15 ± 22.35
<i>Analysis of Accuracy Rates</i>				
Go Trials	144	48	48	144
No-Go Trials	144	48	48	144
<i>Analysis of Response Rates</i>				
Free-Choice Trials	144	48	48	144

**Supplementary Table 4.** Means and standard deviations of reaction times and accuracy rates (or response rates) in different conditions of Experiment 1 based on the factors “Outcome Presence” and “Previous Outcome Frequency”.

<b>Outcome Presence:</b>	<i>Absent</i>		<i>Present</i>	
	<i>0</i>	<i>3-4</i>	<i>0</i>	<i>3-4</i>
<b><i>Reaction Times (ms)</i></b>				
Go Trials	271.83 ± 11.78	284.56 ± 16.46	262.29 ± 14.02	262.40 ± 16.06
Free-Choice Trials	275.58 ± 15.37	296.54 ± 22.80	268.07 ± 18.70	270.50 ± 17.01
<b><i>Accuracy Rates</i></b>				
Go Trials	0.79 ± 0.16	0.62 ± 0.22	0.83 ± 0.11	0.84 ± 0.12
No-Go Trials	0.58 ± 0.16	0.69 ± 0.14	0.46 ± 0.18	0.44 ± 0.20
<b><i>Response Rates</i></b>				
Free-Choice Trials	0.59 ± 0.18	0.43 ± 0.17	0.66 ± 0.19	0.70 ± 0.15

**Supplementary Table 5.** The number of trials in different conditions of Experiment 1 based on the factors “Outcome Presence” and “Previous Outcome Frequency” for each analysis.

<b>Outcome Presence:</b>	<i>Absent</i>		<i>Present</i>	
<b>Previous Outcome Frequency:</b>	<i>0</i>	<i>3-4</i>	<i>0</i>	<i>3-4</i>
<i>Analysis of Reaction Times</i>				
Go Trials	72.30 ± 9.02	15.11 ± 6.52	37.19 ± 5.01	46.74 ± 12.07
Free-Choice Trials	53.89 ± 15.39	11.70 ± 5.81	31.70 ± 8.79	39.48 ± 12.07
<i>Analysis of Accuracy Rates</i>				
Go Trials	93.85 ± 15.36	23.44 ± 4.74	46.11 ± 10.77	54.70 ± 8.45
No-Go Trials	89.78 ± 11.61	26.15 ± 4.97	46.00 ± 8.79	57.00 ± 7.52
<i>Analysis of Response Rates</i>				
Free-Choice Trials	93.52 ± 14.47	26.56 ± 4.18	53.59 ± 40.98	55.30 ± 8.43

**Supplementary Table 6.** Means and standard deviations of reaction times and accuracy rates in different conditions of Experiment 2 based on the factors “Outcome Presence” and “Outcome Probability”.

<b>Outcome Presence:</b>	<i>Absent</i>			<i>Present Positive</i>			<i>Present Negative</i>		
<b>Outcome Probability:</b>	<i>High Probability of No Outcome</i>	<i>High Probability of Positive Outcome</i>	<i>High Probability of Negative Outcome</i>	<i>High Probability of No Outcome</i>	<i>High Probability of Positive Outcome</i>	<i>High Probability of Negative Outcome</i>	<i>High Probability of No Outcome</i>	<i>High Probability of Positive Outcome</i>	<i>High Probability of Negative Outcome</i>
<b>Reaction Times (ms)</b>									
Go Trials	306.37 ± 11.56	310.26 ± 9.74	310.55 ± 22.17	287.91 ± 15.54	289.07 ± 13.27	288.90 ± 16.19	286.17 ± 12.33	287.45 ± 16.26	289.58 ± 14.75
<b>Accuracy Rates</b>									
Go Trials	0.62 ± 0.21	0.57 ± 0.19	0.54 ± 0.21	0.85 ± 0.10	0.84 ± 0.11	0.84 ± 0.09	0.82 ± 0.14	0.86 ± 0.09	0.82 ± 0.09
No-Go Trials	0.79 ± 0.13	0.87 ± 0.10	0.82 ± 0.15	0.62 ± 0.19	0.63 ± 0.18	0.64 ± 0.20	0.60 ± 0.19	0.68 ± 0.21	0.62 ± 0.19

**Supplementary Table 7.** Means and standard deviations of reaction times and accuracy rates in different conditions of Experiment 2 based on the factors “Outcome Presence” and “Previous Outcome Frequency”.

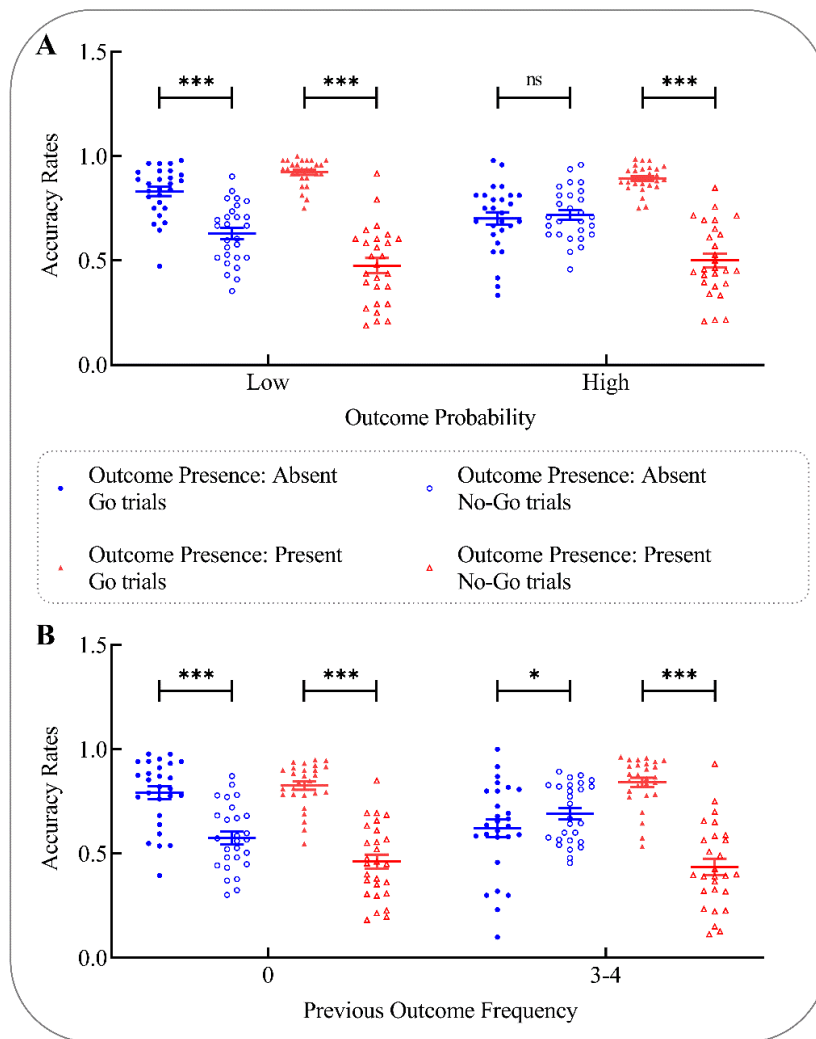
<b>Outcome Presence:</b>	<i>Absent</i>		<i>Present Positive</i>		<i>Present Negative</i>	
<b>Previous Outcome Frequency: 0</b>	<i>2-4</i>	<i>0</i>	<i>2-4</i>	<i>0</i>	<i>2-4</i>	<i>2-4</i>
<b><i>Reaction Times (ms)</i></b>						
Go Trials	313.90 ± 10.42	296.83 ± 11.91	288.76 ± 15.08	286.29 ± 13.45	287.81 ± 14.83	286.96 ± 13.89
<b><i>Accuracy Rates</i></b>						
Go Trials	0.48 ± 0.21	0.68 ± 0.20	0.76 ± 0.16	0.79 ± 0.11	0.75 ± 0.13	0.76 ± 0.15
No-Go Trials	0.75 ± 0.14	0.69 ± 0.14	0.57 ± 0.18	0.54 ± 0.20	0.58 ± 0.17	0.52 ± 0.19

**Supplementary Table 8.** The number of trials in different conditions of Experiment 2 based on the factors “Outcome Presence” and “Outcome Probability” for each analysis.

<b>Outcome Presence:</b>	<i>Absent</i>			<i>Present Positive</i>			<i>Present Negative</i>		
	<i>High Probability of No Outcome</i>	<i>High Probability of Positive Outcome</i>	<i>High Probability of Negative Outcome</i>	<i>High Probability of No Outcome</i>	<i>High Probability of Positive Outcome</i>	<i>High Probability of Negative Outcome</i>	<i>High Probability of No Outcome</i>	<i>High Probability of Positive Outcome</i>	<i>High Probability of Negative Outcome</i>
<b>Analysis of Reaction Times</b>									
Go Trials	29.89 ± 10.09	13.68 ± 4.57	12.89 ± 4.95	20.29 ± 2.49	40.29 ± 5.13	20.21 ± 2.06	19.75 ± 3.40	20.64 ± 2.16	39.57 ± 4.13
<b>Analysis of Accuracy Rates</b>									
Go Trials	48	24	24	24	48	24	24	24	48
No-Go Trials	48	24	24	24	48	24	24	24	48

**Supplementary Table 9.** The number of trials in different conditions of Experiment 2 based on the factors “Outcome Presence” and “Previous Outcome Frequency” for each analysis.

<b>Outcome Presence:</b>	<i>Absent</i>		<i>Present Positive</i>		<i>Present Negative</i>	
<b>Previous Outcome Frequency: 0</b>	<i>2-4</i>	<i>0</i>	<i>2-4</i>	<i>0</i>	<i>2-4</i>	<i>0</i>
<i>Analysis of Reaction Times</i>						
Go Trials	23.82 ± 8.92	16.36 ± 6.85	37.54 ± 3.84	22.39 ± 4.71	38.25 ± 4.63	21.54 ± 6.29
<i>Analysis of Accuracy Rates</i>						
Go Trials	52.71 ± 8.24	23.25 ± 6.53	51.79 ± 12.66	28.21 ± 3.99	52.21 ± 9.65	27.89 ± 4.07
No-Go Trials	49.86 ± 9.04	25.61 ± 5.99	49.00 ± 8.28	32.11 ± 4.96	49.89 ± 10.08	30.68 ± 5.47

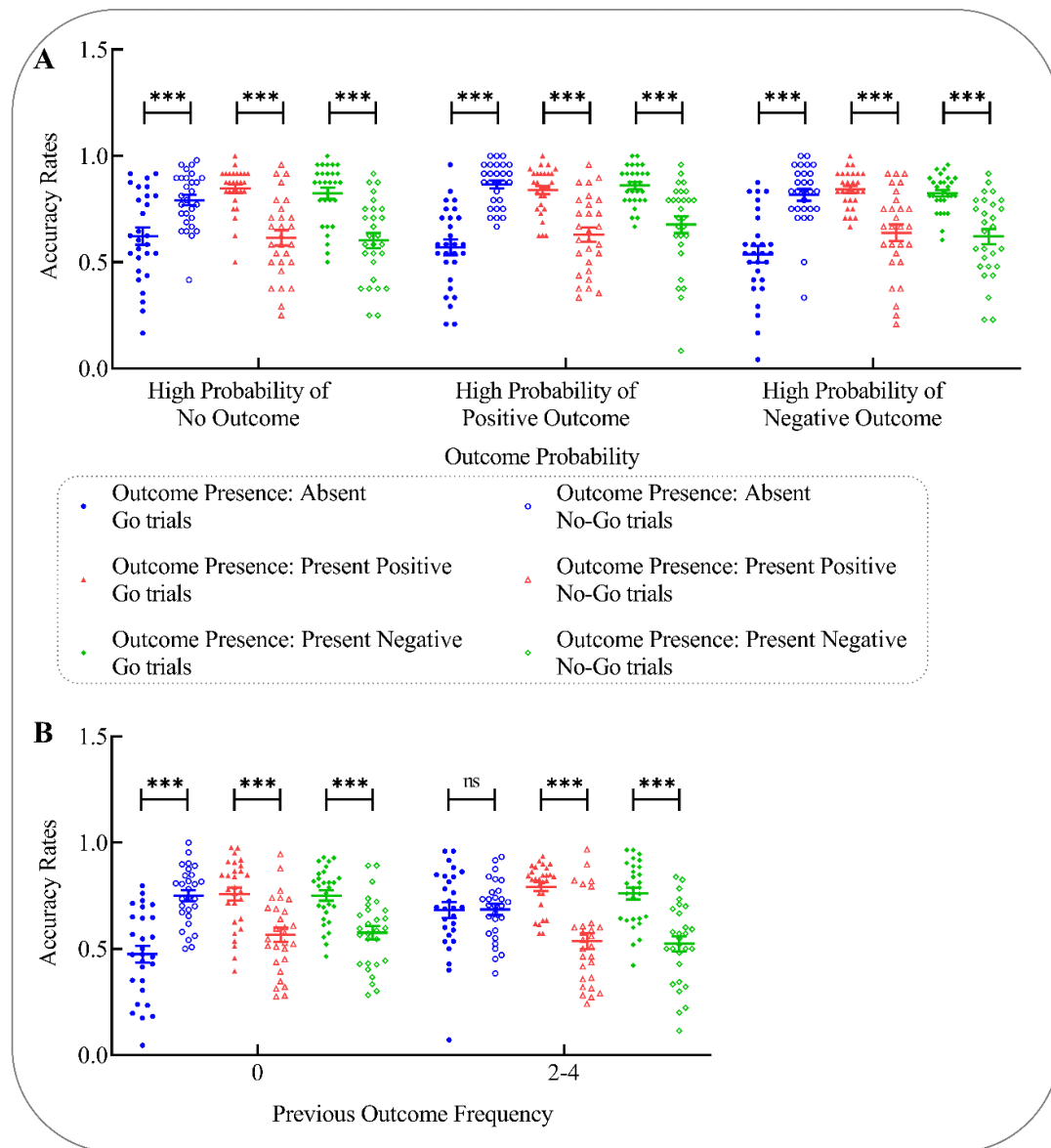


**Supplementary**

**Figure 1.**

Comparison of accuracy rates in Go and No-Go trials in Experiment 1. **(A)** Results based on the factors “Outcome Presence” and “Outcome Probability”. Participants had a preference for go over no-go responses when their previous action led to a positive outcome

or when their previous action unsurprisingly did not lead to any outcome. In contrast, participants had no obvious preference for go over no-go responses when the global probability of getting positive outcomes in a given block was high but their previous action surprisingly did not lead to any outcome. **(B)** Results based on the factors “Outcome Presence” and “Previous Outcome Frequency”. Participants had a preference for go over no-go responses when their previous action led to a positive outcome or when their previous action unsurprisingly did not lead to any outcome. In contrast, participants had a preference for no-go over go responses when positive outcomes had occurred three to four times in the previous two pairs of trials but their previous action surprisingly did not lead to any outcome. Data are expressed as  $M \pm SEM$ . ns: not significant; \*:  $p < .05$ ; \*\*\*:  $p < .001$ .



**Supplementary Figure 2.** Comparison of accuracy rates in Go and No-Go trials in Experiment 2. **(A)** Results based on the factors “Outcome Presence” and “Outcome Probability”. Participants had a preference for go over no-go responses when their previous action led to an outcome, irrespective of the emotional valence (i.e., positive or negative). In contrast, participants had a preference for no-go over go responses when their previous action led to no outcome. **(B)** Results based on the factors “Outcome Presence” and “Previous Outcome Frequency”. Participants had a preference for go over no-go responses when their previous action led to an outcome, irrespective of the emotional valence (i.e., positive or negative). In contrast,

participants had no obvious preference for go over no-go responses when action outcomes had never occurred in the previous two pairs of trials and their previous action unsurprisingly did not lead to any outcome. Furthermore, participants had a preference for no-go over go responses when outcomes had occurred two to four times in the previous two pairs of trials but their previous action surprisingly did not lead to any outcome. Data are expressed as  $M \pm SEM$ . ns: not significant; \*\*\*:  $p < .001$ .

## **2.5 Study V: Prepared to Stop: How Sense of Agency in a Preceding Trial Modulates Inhibitory Control in the Current Trial**

**This article was published in *Cerebral Cortex*:**

Ren, Q., Kaiser, J., Gentsch, A., & Schütz-Bosbach, S. (2023). Prepared to stop: How sense of agency in a preceding trial modulates inhibitory control in the current trial. *Cerebral Cortex*, 33(13), 8565–8580. <https://doi.org/10.1093/cercor/bhad141>

Copyright © The Author(s) 2023. Published by Oxford University Press. All rights reserved. This article was included in this dissertation with permission. The main manuscript and supplements here are the published version.

### **Contributions:**

Qiaoyue Ren: Conceptualization, Data curation, Formal analysis, Investigation, Methodology, Visualization, Writing – original draft.

Jakob Kaiser: Conceptualization, Methodology, Writing – review & editing.

Antje Gentsch: Conceptualization, Methodology, Writing – review & editing.

Simone Schütz-Bosbach: Conceptualization, Methodology, Supervision, Writing – review & editing.



# Prepared to stop: how sense of agency in a preceding trial modulates inhibitory control in the current trial

Qiaoyue Ren, Jakob Kaiser, Antje Gentsch, Simone Schütz-Bosbach\*

General and Experimental Psychology Unit, Department of Psychology, LMU, Munich 80802, Germany

\*Corresponding author: Department of Psychology, LMU Munich, Leopoldstr. 13, D-80802 Munich, Germany. Email: S.Schuetz-Bosbach@psy.lmu.de

Feeling in control of actions and events can enhance motivation for further actions. How this sense of agency (SoA) in fact influences flexible motor control remains poorly understood. Here, we investigated the effect of SoA on subsequent response inhibition in a modified go/no-go task with EEG recordings. We manipulated participants' SoA by varying the presence, predictability, and emotional valence of a visual outcome for a given motor action. When participants unexpectedly did not receive any visible outcome following their action on trial  $n - 1$ , they exhibited slower responses and lower hit rates to the go signal but higher rates of successful inhibition to the no-go signal on trial  $n$ , regardless of the emotional valence of the expected action outcome. Furthermore, enhanced inhibitory tendencies were accompanied by reduced N2 and P3 amplitudes, midfrontal theta power, and theta synchronization between midfrontal and medial to parietal areas, indicating that less top-down control is required for successful response inhibition on trial  $n$  after experiencing low SoA on trial  $n - 1$ . These findings suggest that feeling less in control in a preceding trial makes it easier to implement inhibitory control in the current trial, thereby providing new insights into the role of SoA in goal-directed behavior.

**Key words:** cognitive control; EEG; prediction error; response inhibition; sense of agency.

## Introduction

When our voluntary actions produce predictable effects in the external environment, it may induce a subjective feeling of control over those actions and their effects. This experience is called the sense of agency (SoA; Haggard 2017). Recently, several empirical studies have reported that actions associated with a stronger feeling of control were selected more frequently and were executed more rapidly (Eitam et al. 2013; Karsh and Eitam 2015; Karsh et al. 2016, 2020; Penton et al. 2018; Wen and Haggard 2018; Hemed et al. 2020; see review: Wen and Imamizu 2022), suggesting that a higher SoA can reinforce the given motor action. In addition to action selection and execution, response inhibition also plays a vital role in goal-directed behavior (Chambers et al. 2009). Response inhibition is the ability to suppress unwanted or inappropriate actions (Verbruggen and Logan 2008). However, how SoA influences subsequent response inhibition remains poorly understood. Addressing this gap would contribute to a better understanding of how our subjective states influence our objective ability to regulate behavior flexibly in a rapidly changing environment.

Response inhibition is considered a hallmark of cognitive and motor control (Chambers et al. 2009; Bari and Robbins 2013). Existing behavioral evidence implies that the actual engagement of control and the feeling of control are functionally distinct but interact with each other. For example, physical effort or cognitive load has been shown to influence participants' SoA on that same trial, with most studies finding a lower SoA in trials requiring a high level of effort (Sidarus and Haggard 2016; Vastano et al. 2017; Wang et al. 2018; but see Van den Bussche et al. 2020 for an opposite effect). Similar effects have also been found in contexts requiring high effort (e.g. across a block of trials): most studies have observed a decrease in the SoA after participants

completing a high-demand compared with low-demand block (Hon et al. 2013; Howard et al. 2016; Potts and Carlson 2019; but see Demanet et al. 2013 for an opposite effect). Moreover, our recent work demonstrates that when participants felt less in control as induced by the absence of a visible effect following their preceding action (as measured by explicit judgments of agency), they responded less accurately and slower to go signal, reacted more accurately to no-go signal, as well as made go decisions less frequently and slower to free-choice signal on the next trial. These effects were even stronger when action outcomes occurred more frequently in a given block or in several previous trials (Ren et al. 2023). These findings provide preliminary evidence that a reduced SoA on trial  $n - 1$  leads to an enhanced intention to inhibit upcoming actions on trial  $n$ .

The current study aimed to clarify the effect of SoA on subsequent response inhibition, and intended to specify the underlying brain mechanisms in particular. To this end, we adopted a modified go/no-go task with simultaneous EEG recordings. In this task, a pair of 2 trials included 2 action stimuli. The first action stimulus was always a go signal (i.e. the inducement trial), whereas the second action stimulus was a go or a no-go signal (i.e. the test trial). In the inducement trial, we manipulated participants' SoA indirectly by varying the presence and the predictability of perceivable outcomes for their actions. This approach has a theoretical and empirical justification: according to the comparator model of agency, our brain predicts the sensory consequence of the action we plan and execute, and then compares it with the actual sensory feedback received from the sensory system and the external world. SoA emerges if the compared signals are congruent and diminishes if they are incongruent (Blakemore et al. 1998, 2002; Frith et al. 2000). In other words, a prediction error between the predicted and actual action effect can reduce the

SoA. In line with this theory, converging empirical studies reveal that participants experienced a decreased SoA if the actual action outcome (e.g. an auditory or visual event presented immediately after their action) violated their expectation (Sato and Yasuda 2005; Ebert and Wegner 2010; Caspar et al. 2016; Majchrowicz and Wierzchoń 2018; Villa et al. 2021). Therefore, we assumed that being able to produce predictable action effects can induce a high SoA. In contrast, not being able to produce intended effects can induce a low SoA. Notably, the present study adopted facial stimuli as action outcomes since several previous studies suggest that emotional facial stimuli (i.e. social reward) compared with simple neutral stimuli might be particularly effective in inducing a high SoA (see review: Kaiser et al. 2021).

The test trial following the inducement trial allowed us to test how our manipulation of SoA in a preceding behavioral episode influenced participants' behavioral and electrophysiological responses to the subsequent action stimulus. At the behavioral level, we focused on participants' reaction times (RTs) and accuracy rates (ACCs) in response to go signals, as well as their ACCs in response to no-go signals. Faster and more accurate responses in go trials are thought to indicate action readiness or motor preparedness (Kaiser and Schütz-Bosbach 2019), whereas successful action cancellation in no-go trials is known to reflect response inhibition (Zhang et al. 2015; Raud et al. 2020). We hypothesized that the absence of an action outcome in the inducement trial would reduce action readiness but enhance response inhibition in the following test trial, manifested as slower and less accurate responses to go signals but more accurate responses to no-go signals. This effect was expected to be more pronounced when the prediction error was high compared with low. Similar effects have been observed in previous behavioral studies using different paradigms and/or neutral action outcomes (Eitam et al. 2013; Karsh and Eitam 2015; Hemed et al. 2022; Ren et al. 2023). At the electrophysiological level, we assessed the N2 and P3 components evoked by no-go signals. The no-go N2 and P3 components are the most common event-related potentials (ERPs) reflecting subprocesses of inhibitory control (Falkenstein et al. 1999). The N2 component is usually detected between 200 and 300 ms after the presentation of the no-go signal over the frontocentral region and is believed to reflect conflict monitoring (Lavric et al. 2004; Smith et al. 2008; Beste et al. 2010). The P3 component is generally observed between 300 and 600 ms after the presentation of the no-go signal in the central area and is considered to reflect the inhibitory process itself or an evaluation of the response inhibition process (Huster et al. 2011; Chmielewski and Beste 2015, 2019; Wessel and Aron 2015). Our hypothesis in behavioral performance (see above) was that experiencing unexpected outcome absence on trial  $n - 1$  would result in enhanced inhibitory tendencies on trial  $n$ . As a further prediction, we expected that encountering a no-go signal as the upcoming action stimulus on trial  $n$  would result in less cognitive conflict for participants, as they would be less motivated to repeat the keypress action after experiencing unexpected outcome absence on trial  $n - 1$ . In this case, it would have been also easier for participants to implement inhibitory processes in response to the no-go signal on trial  $n$ . Therefore, we predicted that smaller N2 and P3 amplitudes would be observed (as neurophysiological correlates of inhibitory processes; Huster et al. 2013; Chmielewski and Beste 2019) during no-go trials following outcome absence compared with outcome presence for a preceding action, and these effects might be further amplified when the prediction error was high compared with low.

In addition to the no-go N2 and P3 components, we also measured the midfrontal theta (4–7 Hz) power after no-go signals and its synchronization with other brain areas to gain additional insights into the neural mechanisms underlying the effect on inhibitory control. Conflict-related increases in midfrontal theta power have been observed in a wide range of different experimental paradigms (Derosiere et al. 2018; Vissers et al. 2018; Cooper et al. 2019; Kaiser et al. 2019; Kaiser and Schütz-Bosbach 2019). A recent study conducted in our lab has shown that midfrontal theta oscillations during reactive control primarily reflect motor conflicts, rather than attentional conflicts (Kaiser and Schütz-Bosbach 2020). In line with our hypotheses for behavioral and ERP responses, we hypothesized that the absence of an action outcome in the inducement trial would reduce motor conflicts caused by no-go signals and facilitate motor-related adjustments in subsequent test trials, which would be indexed by a reduced midfrontal theta enhancement during no-go trials, and this effect would be more pronounced when the prediction error was high. Importantly, in contrast to ERP analysis, oscillatory measures allow to investigate task-related changes in interbrain connectivity. The neural synchronization of oscillatory waves across brain areas is assumed to facilitate intercommunication between different brain areas (Fries 2005; Klimesch et al. 2007). More specifically, it has been suggested that theta synchronization between midfrontal and other domain-specific brain areas is reflective of the information exchange necessary for exerting cognitive and motor control to overcome conflicts (van Driel et al. 2012; Cooper et al. 2015; Duprez et al. 2020; Kaiser and Schütz-Bosbach 2020). Thus, neural theta synchronization represents a potential functional mechanism to implement goal-directed adaptation of neural processes, such as sudden changes in motor activation during the inhibition of motor actions (Beste et al. 2023). We expected to observe a decrease in theta synchronization during no-go trials following unexpected outcome absence, as there would be less conflict to overcome for successful motor inhibition. This is in line with our theoretical assumption that unexpected outcome absence reduces motor readiness, making the implementation of motor inhibition less effortful.

Last but not least, to exclude the possibility that the potential effects in the current study were driven by motivational factors related to the outcome valence (i.e. seeking positive outcomes and avoiding negative outcomes), we conducted 2 versions of the task—the positive outcome task and the negative outcome task—adopting happy or angry faces as visual action outcomes, respectively. If similar effects are observed in both tasks (e.g. having positive or negative action outcomes compared with no outcomes undermines subsequent inhibitory control), we can conclude that the effectiveness of the motor action in terms of producing a perceivable effect plays a dominant role in the effect of SoA on subsequent action regulation. Conversely, if opposite effects are observed across the 2 tasks (e.g. having positive action outcomes compared with no outcomes undermines subsequent inhibitory control, whereas having negative action outcomes compared with no outcomes facilitates subsequent inhibitory control), it can be speculated that the outcome valence (positive or negative) is the key determinant of the observed empirical effects.

## Materials and methods

### Participants

Fifty-four healthy participants took part in the present study, with half of them (14 females; mean age:  $26.93 \pm 0.64$  years;

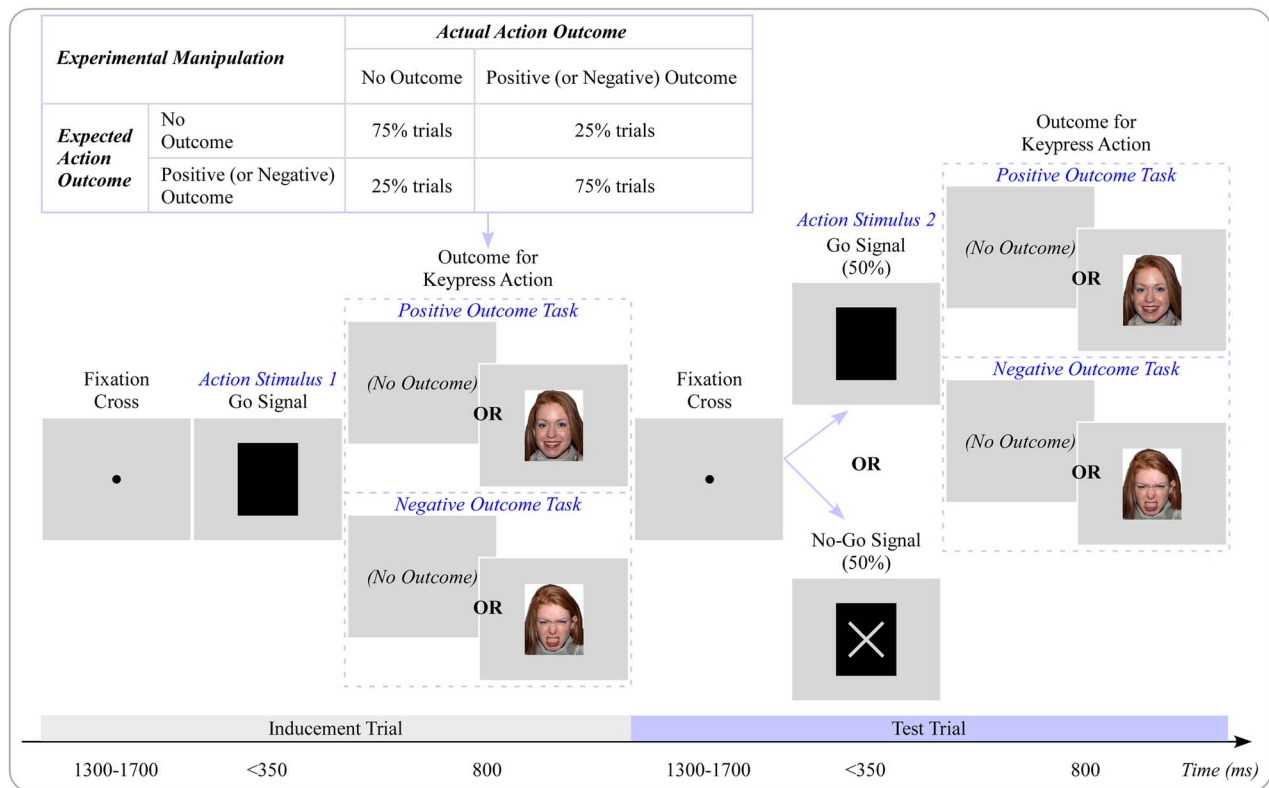


**Fig. 1.** Schema of the modified go/no-go task. A pair of 2 trials included 2 action stimuli. The first action stimulus was always a go signal (i.e. the inducement trial), whereas the second action stimulus was either a go or a no-go signal (i.e. the test trial). The instruction at the beginning of each block indicated that the probability of receiving either no action outcome or a visual outcome (positive outcome task: a happy face; negative outcome task: an angry face) was high. In a specific trial, participants would have a low prediction error if the actual action outcome confirmed their expectation and a high prediction error if the actual action outcome violated their expectation.

range: 22–35 years) participating in the positive outcome task, and the other half (15 females; mean age:  $25.93 \pm 0.68$  years; range: 20–35 years) participating in the negative outcome task. All participants had normal or corrected-to-normal vision, and none had a history of neurological or psychiatric disorders. The study was approved by the local ethics committee at the Department of Psychology of LMU Munich in accordance with the Declaration of Helsinki. All participants provided written informed consent and received financial compensation (9 euros per hour) for their participation. Given that large effect sizes ( $\eta_p^2 \geq 0.56$ ) were observed for the main effect of Outcome Presence in a related study (Ren et al. 2023), we estimated the required sample size in the present study also considering a large effect size. A power analysis using the MorePower software (Campbell and Thompson 2012) revealed that our sample size ensured a power of 0.80 to detect 3-way or 2-way interactions or a main effect of at least  $\eta_p^2 = 0.14$ .

## Materials and apparatus

A set of 84 colored photographs, showing either happy or angry faces of 42 actors (18 females and 24 males), were selected from the validated NimStim database (Tottenham et al. 2009). Go signals (i.e. a black rectangle), no-go signals (i.e. a black rectangle with a gray cross), and the photographs were presented in the same size of  $400 \times 514$  pixels (width  $\times$  height) with a gray background on the screen (24 inches; refresh rate: 60 Hz; resolution:  $1920 \times 1080$  pixels). Participants were seated  $\sim 65$  cm from the screen. The tasks were performed using the Presentation software (Neurobehavioral Systems, Inc.).

## Design and procedure

Both tasks in the present study employed a within-subjects design with 2 factors: outcome presence (absent vs. present) and prediction error (low vs. high). The positive outcome task used happy faces as action outcomes, whereas the negative outcome task used angry faces as action outcomes. Notably, data collection for the 2 tasks was done separately. That is, participants were not randomly assigned to one of the 2 tasks within the same data collection. Since both tasks were identical apart from the emotional valence of the action outcome, and no participant took part in both tasks, we combined the data of the 2 tasks for analysis, including “task” (positive vs. negative outcome task) as a between-subject factor.

An overview of the trial structure is shown in Fig. 1. Each pair of trials included 2 action stimuli. Unbeknownst to the participants, the first action stimulus was always a go signal (i.e. “the inducement trial”). In contrast, the second action stimulus was either a go or a no-go signal (i.e. “the test trial”), with equal probability (50%). Participants were instructed to press the “down arrow” key using their right index finger as quickly as possible in response to the go signal but withhold the keypress action in response to the no-go signal. Each action stimulus remained on the screen until the participant pressed the button or the stimulus had been presented for 350 ms. If the action response was correct, it was immediately followed by an action outcome (if there was one) for a duration of 800 ms. If the action response was incorrect, it was followed by an error message for a duration of 800 ms. A central fixation dot was presented for 1,300–1,700 ms during the interstimulus interval.

We manipulated outcome presence and prediction error in the inducement trial, and measured participants' responses to the go or no-go signal in the following test trial. Specifically, to manipulate outcome presence, either a visual outcome (positive outcome task: a happy face; negative outcome task: an angry face) or no visual stimulus was presented after participants' keypress action in the inducement trial. Thus, participants felt either that their action led to a visual outcome, or that their action did not result in any visible effect. To manipulate participants' prediction error between the actual and the expected action outcome, at the beginning of each block, we explicitly informed them whether their correct keypress action had a high or low probability of producing a visual effect (positive outcome task: a happy face; negative outcome task: an angry face) in that block. Therefore, there were 2 types of blocks: high- and low-probability blocks. In high-probability blocks, participants' action led to a visual outcome in 75% of all inducement trials. In low-probability blocks, participants' action produced a visual outcome only in 25% of all inducement trials. During high-probability blocks, participants experienced low prediction error if their action resulted in a visual effect, but high prediction error if no visible outcome followed their action. Conversely, during low-probability blocks, participants experienced low prediction error if their action did not have any visible effect, but high prediction error if their action produced a visual effect. Notably, participants were not informed that if a visual outcome was presented during the inducement trial, they would also receive a visual outcome when they pressed the key in response to the go signal in the following test trial. This was done to ensure that the go signals in both types of trials, inducement and test trials, were similar in nature, with participants having an opportunity to receive a visual outcome after taking action, and thus excluded the possibility of participants treating the 2 types of trials differently.

To get familiar with the experimental procedure, participants completed 2 practice sessions (one for each block type; each including 12 pairs of trials) before the task started. The formal task consisted of 12 high-probability blocks and 12 low-probability blocks. Each block had 48 pairs of trials. Altogether, in each task, there were 432 pairs of trials for the outcome absent—low prediction error condition, 144 pairs of trials for the outcome absent—high prediction error condition, 432 pairs of trials for the outcome present—low prediction error condition, and 144 pairs of trials for the outcome present—high prediction error condition. Notably, only when participants made a correct keypress action in the inducement trial would the subsequent test trial appear, forming a complete action repetition sequence consisting of a pair of inducement and test trials, which were then included in the data analysis. It is also worth noting that participants were not informed that some trials were inducement trials containing go trials only, whereas the others were test trials containing a no-go signal in half of the trials. Therefore, their subjective estimation about the relative proportion of no-go vs. go trials was most likely determined by the inducement and test trials jointly. As a result, participants most likely perceived a significantly lower number of no-go trials compared with go trials within each block, with a perceived ratio of ~25% no-go trials (test trials only) to 75% go trials (inducement + test trials). All blocks and trials were presented in random order. Participants received visual feedback on their ACC and mean RT in go trials and ACC in no-go trials after each block during the self-paced inter-block rest. Each task lasted ~2 h, and an additional 40 min was required for EEG preparation.

## EEG recording and preprocessing

During the task the EEG was recorded from 65 active electrodes (BrainProducts, ActiSnap) and one additional ground electrode, placed according to the international extended 10–20 system. The FCz electrode functioned as the online reference. The sampling rate was 1,000 Hz. The online bandpass filter was 0.1–1,000 Hz. All impedances were kept below 20 k $\Omega$ . Signal acquisition was implemented using the BrainVision Recorder software (Brain Products, Inc.).

Offline EEG data were preprocessed using FieldTrip (Oostenveld et al. 2011), an open-source toolbox running in MATLAB (Mathworks Inc., Natick, MA). First, we manually inspected the raw data to remove bad channels (1 channel for 7 participants and 3 channels for 1 participant). Then, EEG data were re-referenced to the average of all electrodes, filtered using a 40-Hz low-pass filter, and down-sampled to 500 Hz. Next, we performed independent component (IC) analysis on the continuous EEG data. ICs representing eye movements and eye blinks were identified by visual inspection of their time course and scalp topography. A mean of 2.89 ICs per participant was rejected, and artifact-free EEG data were obtained by back-projecting the remaining non-artifactual components onto the scalp electrodes. Last, each bad channel deleted in the first step was interpolated using the average of its neighboring channels using the function `ft_channelrepair`.

## EEG analysis

Since the main goal of the present study was to explore how high or low SoA in a preceding behavioral episode impacted subsequent response inhibition, our analysis focused on participants' electrophysiological responses to the no-go signal in the test trial.

For ERP analysis, we segmented the continuous EEG data into periods ranging from –100 to 600 ms relative to the onset of the no-go signal. We then conducted a baseline correction using the period from –100 to 0 ms prior to the presentation of the no-go signal. Next, the epochs contaminated by artifacts (e.g. muscle activity) were automatically rejected based on a threshold of  $\pm 150 \mu\text{V}$  in all EEG channels. Furthermore, only trials with correct responses were included in further EEG analysis. The number of trials remaining per condition is summarized in [Supplementary Table 1](#). We created averaged epochs for each participant and condition, and determined the time windows and electrodes for the quantification of the N2 and P3 components via visual inspection of the scalp topography. To validate that the most important electrodes were chosen for data quantification, we utilized a statistical method described in Mückschel et al. (2014). Specifically, we calculated the mean amplitude for each ERP component in its respective time window for every electrode, and then compared each value to the average of all other electrodes (excluding the compared electrode). We applied Bonferroni-Holm correction for multiple comparisons, and selected electrodes that showed significantly larger amplitudes (negative for N2 and positive for P3) compared with the average of remaining electrodes. These electrodes were identical to the electrodes selected via visual inspection. N2 and P2 amplitudes were quantified relative to baseline for each participant and condition. N2 amplitude was quantified as the negative peak at frontocentral electrodes (AFz, AF3, AF4, Fz, F1–F5, FCz, FC1–FC6, Cz, and C5) between 200 and 300 ms after the onset of the no-go signal. P3 amplitude was quantified as the positive peak at central electrodes (FCz, FC1–FC4, Cz, C1–C4, C6, CPz, CP1–CP4, CP6, Pz, and P1–P4) between 300 and 600 ms after the onset of

the no-go signal. These time windows and electrodes are typically analyzed in go/no-go paradigms (see review: Huster et al. 2013).

We also calculated the time-frequency data time-locked to the no-go signal. First, we segmented the continuous EEG data into periods ranging from  $-1,100$  to  $1,800$  ms relative to the onset of the no-go signal. Second, we filtered the EEG epochs using a Laplacian spatial filter (order of splines: 4; maximum degree of Legendre polynomials: 14; regularization parameter:  $1 \text{ e-}5$ ). This step increases the spatial specificity for the results of time-frequency and connectivity analysis (see below; Cohen 2015). Third, we decomposed the filtered data sets into their time-frequency representations using Morlet wavelets from 2 to 20 Hz in steps of 1 Hz (Kaiser and Schütz-Bosbach 2020). The number of wavelet cycles increased from 3 to 6 in linearly spaced steps to have a good balance between time and frequency resolution. Last, we further segmented the time-frequency data into periods ranging from  $-300$  to  $1,000$  ms relative to the onset of the no-go signal, with baseline correction via decibel conversion using the first 200-ms period. This baseline interval was chosen to avoid the adverse influence of spectral estimates biased by windowing poststimulus activity and padding values (Hu and Zhang 2019; Zhang et al. 2020). Consistent with previous studies (Kaiser et al. 2019; Kaiser and Schütz-Bosbach 2019), a salient theta power enhancement was observed at midfrontal electrodes (FCz, FC1, and FC2) after the no-go signal.

To explore the interconnectivity between the midfrontal and other brain regions, we further calculated the phase synchronization between midfrontal electrodes (FCz, FC1, and FC2) and all other electrodes in the theta range (4–7 Hz) time-locked to the no-go signal. First, we calculated the debiased weighted phase lag index (WPLI; Vinck et al. 2011) between the midfrontal seed electrodes and all other electrodes in the time window from  $-300$  to  $1,000$  ms relative to the onset of the no-go signal. WPLI values for each seed electrode itself were set to 0. The WPLI was used to estimate the phase synchronization because, compared with other synchronization measures, it is less susceptible to the influence of volume conduction, which can artificially inflate connectivity estimates (Bastos and Schoffelen 2016). Second, the resulting synchronization values were baseline corrected using the first 200-ms period. Therefore, higher WPLI values at any electrode indicate an increase in synchronization between that electrode and the midfrontal region. Similar to previous research (Kaiser and Schütz-Bosbach 2020), salient synchronizations between the midfrontal and some other cortical areas in the theta range were observed after the no-go signal.

However, we did not have clear predictions regarding the morphology (time windows and/or electrodes) of the effect on midfrontal theta power and synchronization. Therefore, to identify spatio-temporal clusters of condition differences in midfrontal oscillation power, we applied a nonparametric cluster-based permutation test in the time window from 0 to 600 ms relative to the stimulus onset and in frequencies from 2 to 20 Hz. Additionally, to identify spatio-temporal clusters of condition differences in midfrontal theta synchronization, we applied a nonparametric cluster-based permutation test in the time window from 0 to 600 ms relative to the stimulus onset and over all electrodes. This method has been frequently used in previous related studies (e.g. Cooper et al. 2019; Kaiser and Schütz-Bosbach 2020). We quantified the midfrontal theta power and synchronization for each participant and condition over the respective cluster that revealed a significant interaction or main effect in the permutation test.

Nonparametric cluster-based permutation tests were performed using the FieldTrip toolbox (Oostenveld et al. 2011).

Permutation analysis allows for statistical tests over whole time-frequency maps, whereas still controlling for multiple comparisons (Maris and Oostenveld 2007). More specifically, for each permutation test used in the present study, the adjacent spatio-spectro-temporal points for which  $F$ -values exceed a threshold were clustered (cluster-defining threshold  $P=0.05$ , 2-tailed; iterations=5,000). Then, the cluster-level statistics were calculated by taking the sum of the  $F$ -values of all points within each cluster. Lastly, the observed cluster-level statistic was compared against the permutation distribution in order to test the null hypothesis of no difference across conditions (2-tailed test). Clusters with  $P < 0.05$  were considered significant. Notably, we ensured that the midfrontal theta power during the baseline was comparable across conditions (see [Supplementary Analysis and Results](#)), which helps exclude the possibility that the effects observed in the midfrontal theta power and synchronization after the no-go signal were driven by any differences during the baseline.

## Statistical analysis

The behavioral data in the present study included RTs and ACCs in go trials, as well as ACCs in no-go trials. The ERP data included N2 and P3 amplitudes evoked by no-go signals. The time-frequency data included the midfrontal theta power and synchronization elicited by no-go signals. Notably, all of these data were collected during test trials.

To analyze the effects of our manipulation on trial  $n - 1$  on participants' responses on trial  $n$ , we performed separate mixed-design 3-way analysis of variances (ANOVA) with 2 within-subjects factors (outcome presence: absent vs. present; prediction error: low vs. high) and 1 between-subjects factor (task: positive vs. negative outcome task) for each of the aforementioned behavioral data, ERP data, and time-frequency data. In cases where a significant 3-way interaction was observed, we conducted 2 kinds of post hoc analyses: (i) to further explore the effects of outcome presence and prediction error on participants' performance, we conducted post hoc 2-way ANOVAs separately for the positive and negative outcome tasks, and post hoc pairwise comparisons were conducted when a significant 2-way interaction was observed. (ii) To further explore performance differences between the 2 tasks in each sub-condition, we broke down the 3-way interaction by focusing on the effect of task for each level of the other 2 factors (i.e. outcome presence and prediction error). However, performance differences between the 2 tasks were not further explored when neither the 3-way or 2-way interaction between task and other factors nor the main effect of task was significant.

In addition, to explore the effect of our manipulation on trial  $n - 1$  on participants' motor tendency (i.e. a preference for go or no-go responses) on trial  $n$ , we performed a mixed-design 4-way ANOVA on ACCs in both go and no-go trials. This included a fourth within-subject factor (trial type: go vs. no-go trials) in addition to the aforementioned 3 factors (outcome presence, prediction error, and task). In cases where a significant 4-way interaction was observed, we broke down the interaction by focusing on the effect of trial type for each level of the other 3 factors. That is, we compared ACCs between go and no-go trials in each sub-condition. If participants had higher ACCs in go trials compared with no-go trials, it indicated a preference for go over no-go responses, whereas a higher ACC in no-go trials indicated a preference for no-go over go responses. Partial eta-squared ( $\eta_p^2$ ) was calculated as effect size. All analyses were performed using the JASP software (version 0.17.0.0; JASP Team 2023).

**Table 1.** Statistical comparisons of behavioral and neural responses during positive and negative outcome tasks.

	Go RTs	Go ACCs	No-go ACCs	No-go N2 amplitudes	No-go P3 amplitudes	No-go theta power	No-go theta synchronization (cluster 1)	No-go theta synchronization (cluster 2)
Outcome presence	$F = 125.04^c$	$F = 80.60^c$	$F = 124.70^c$	$F = 16.73^c$	$F = 29.98^c$	$F = 11.84^b$	$F = 16.63^c$	$F = 17.53^c$
Prediction error	$F = 53.94^c$	$F = 41.34^c$	$F = 1.65$	$F = 0.02$	$F = 1.06$	$F = 21.59^c$	$F = 16.45^c$	$F = 6.79^a$
Task	$F = 2.75$	$F = 0.27$	$F = 0.81$	$F = 3.39$	$F = 3.09$	$F = 0.03$	$F = 0.18$	$F = 0.12$
Outcome presence $\times$ prediction error	$F = 88.21^c$	$F = 133.05^c$	$F = 42.40^c$	$F = 0.01$	$F = 17.53^c$	$F = 18.91^c$	$F = 23.28^c$	$F = 26.33^c$
Outcome presence $\times$ task	$F = 0.82$	$F = 1.68$	$F = 2.16$	$F = 0.91$	$F = 0.10$	$F = 0.03$	$F = 0.06$	$F = 0.19$
Prediction error $\times$ task	$F = 1.12$	$F = 0.13$	$F = 0.10$	$F = 0.07$	$F = 0.04$	$F = 0.04$	$F = 5.38^a$	$F = 1.61$
Outcome presence $\times$ prediction error $\times$ task	$F = 4.05^a$	$F = 4.41^a$	$F = 1.93$	$F < 0.01$	$F = 0.79$	$F = 0.03$	$F = 0.02$	$F = 2.07$

<sup>a</sup> $P < 0.05$ <sup>b</sup> $P < 0.01$ <sup>c</sup> $P < 0.001$ .

## Manipulation check

To verify our manipulation of varying the SoA in inducement trials, we compared the amplitudes of feedback-related negativity (FRN) across conditions. First, continuous EEG data were segmented into periods ranging from  $-100$  to  $600$  ms relative to the keypress responses in inducement trials and baseline corrected using the period from  $-100$  to  $0$  ms. Then, epochs contaminated by artifacts were automatically rejected based on a threshold of  $\pm 150 \mu\text{V}$  in all EEG channels. Next, we created difference waveforms between outcome-present and outcome-absent conditions for each participant and level of prediction error (high or low). Consistent with previous studies (see review: Krigolson 2018), FRN amplitude was quantified as the mean amplitude at FCz between  $250$  and  $350$  ms after the keypress response.

FRN amplitudes were compared across conditions using a mixed-design 2-way ANOVA with 1 within-subjects factor (prediction error) and 1 between-subjects factor (task). The analysis showed a significant main effect of prediction error ( $F_{1,52} = 24.00$ ,  $P < 0.001$ ,  $\eta_p^2 = 0.32$ ; see Supplementary Fig. 1), indicating that high prediction error resulted in larger FRN amplitudes in inducement trials compared with low prediction error. However, neither the main effect of task nor the interaction between task and prediction error was significant (both  $P_s > 0.05$ ). Previous research has shown that FRN amplitudes vary with prediction error (Talmi et al. 2013) and predict lower judgments of agency (Sidarus et al. 2017). Therefore, this result confirms the effectiveness of our manipulation in varying the SoA in inducement trials.

## Results

### Behavioral results

Behavioral responses (including RTs and ACCs in go trials, as well as ACCs in no-go trials) were compared using a mixed-design 3-way ANOVA with 2 within-subjects factors (outcome presence and prediction error) and 3 between-subjects factor (Task). Relevant statistics are summarized in Table 1.

#### Go trials

The analysis of RTs in go trials, using a mixed-design 3-way ANOVA, showed a significant 3-way interaction between outcome presence, prediction error, and task ( $F_{1,52} = 4.05$ ,  $P = 0.049$ ,  $\eta_p^2 = 0.07$ ). To further explore the effects of outcome presence and prediction error on participants' performance, we conducted

post hoc 2-way ANOVAs separately for the positive and negative outcome tasks. These analyses revealed significant interactions between outcome presence and prediction error (positive outcome task:  $F_{1,26} = 65.73$ ,  $P < 0.001$ ,  $\eta_p^2 = 0.72$ ; negative outcome task:  $F_{1,26} = 26.95$ ,  $P < 0.001$ ,  $\eta_p^2 = 0.51$ ). Post hoc pairwise comparisons showed that, regardless of the prediction error, the absence of a positive or negative outcome, compared with its presence in inducement trials, led to slower RTs in subsequent go trials (all  $P_s < 0.001$ ). Furthermore, this effect was more pronounced when the prediction error was high, compared with when it was low (see Fig. 2A). That is, during both tasks, when participants unexpectedly did not receive any visible outcome following their action in inducement trials, they responded slower in the subsequent go trials.

Additionally, to explore performance differences between the 2 tasks in each sub-condition, we also broke down the 3-way interaction by focusing on the effect of task for each level of the other 2 factors (i.e. outcome presence and prediction error). The results showed that RTs in go trials were significantly slower during the positive outcome task than the negative outcome task in the no outcome—high prediction error condition ( $P = 0.043$ ). However, there were no significant differences in go RTs between tasks in the other 3 conditions (all  $P_s > 0.05$ ; see Fig. 2B). That is, in the context of expecting positive outcomes compared with expecting negative outcomes, participants responded slower in the subsequent go trials when they unexpectedly did not receive any visible outcome following their action in inducement trials.

The analysis of ACCs in go trials, using a mixed-design 3-way ANOVA, also showed a significant 3-way interaction between outcome presence, prediction error, and task ( $F_{1,52} = 4.41$ ,  $P = 0.041$ ,  $\eta_p^2 = 0.08$ ,  $BF_{10} = 1.79$ ). To further explore the effects of outcome presence and prediction error on participants' performance, we conducted post hoc 2-way ANOVAs separately for the positive and negative outcome tasks. These analyses revealed significant interactions between outcome presence and prediction error (positive outcome task:  $F_{1,26} = 124.96$ ,  $P < 0.001$ ,  $\eta_p^2 = 0.83$ ; negative outcome task:  $F_{1,26} = 35.43$ ,  $P < 0.001$ ,  $\eta_p^2 = 0.58$ ). Post hoc pairwise comparisons showed that, regardless of the prediction error, the absence of a positive or negative outcome, compared with its presence in inducement trials, led to lower ACCs in subsequent go trials (all  $P_s < 0.001$ ). Furthermore, this effect was more pronounced when the prediction error was high, compared with when it was low (see Fig. 2C). That is, during both tasks, when participants unexpectedly did not receive any visible outcome

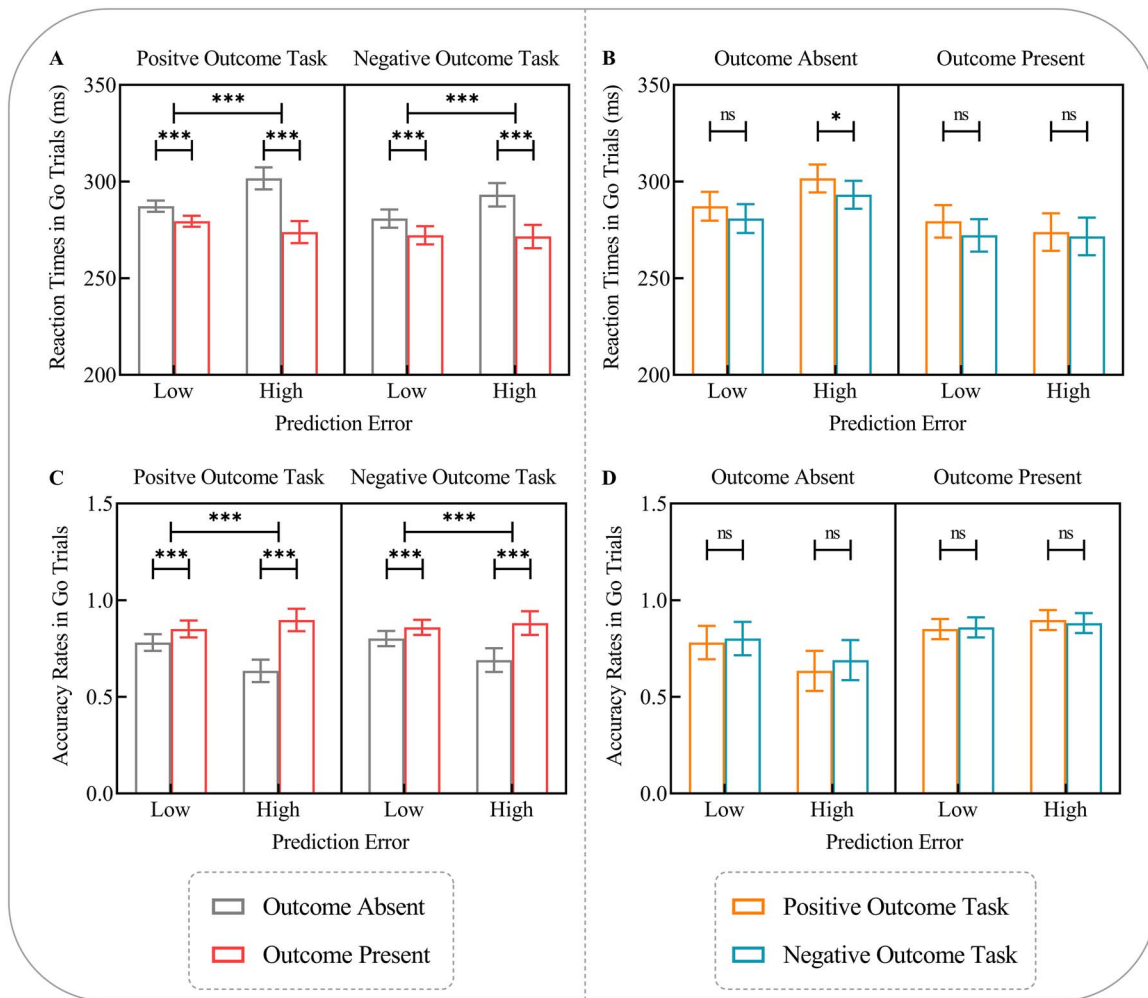


**Fig. 2.** RTs and ACCs in go trials. During both positive and negative outcome tasks, the unexpected absence of an action outcome resulted in (A) slower RTs and (C) lower ACCs in subsequent go trials. Compared with the unexpected absence of a negative outcome, the unexpected absence of a positive outcome resulted in (B) slower RTs in subsequent go trials, whereas (D) there was no significant difference in go ACCs between the two tasks. Data are expressed as mean  $\pm$  CI. Note that, in (A) and (C), the CI refers to the 95% confidence interval of the pairwise difference between the 2 compared sub-conditions; in (B) and (D), the CI refers to the 95% confidence interval of the difference between the 2 independent means. ns: not significant; \* $P < 0.05$ ; \*\*\* $P < 0.001$ .

following their action in inducement trials, they responded less accurately in the subsequent go trials.

Additionally, to explore performance differences between the 2 tasks in each sub-condition, we also broke down the 3-way interaction by focusing on the effect of task for each level of the other 2 factors (i.e. outcome presence and prediction error). The results showed no significant differences in go ACCs between tasks across all 4 conditions (all  $P$ s  $> 0.05$ ; see Fig. 2D).

In summary, results of RTs and ACCs in go trials showed that when participants unexpectedly did not receive any visible outcome following their action on trial  $n - 1$ , they responded slower and less accurately to the go signal on trial  $n$ . This suggests that the unexpected outcome absence in the preceding trial reduces participants' readiness to act in the current trial. This effect was observed in both tasks but was stronger when the emotional valence of the expected outcome was positive compared with negative.

### No-go trials

The analysis of ACCs in no-go trials, using a mixed-design 3-way ANOVA, found no significant 3-way interaction between outcome presence, prediction error, and task ( $P > 0.05$ ). However, it revealed

a significant 2-way interaction between outcome presence and prediction error ( $F_{1,52} = 42.40$ ,  $P < 0.001$ ,  $\eta_p^2 = 0.45$ ). Post hoc pairwise comparisons showed that, regardless of the prediction error, the absence of an action outcome, compared with its presence in inducement trials, resulted in higher ACCs in subsequent no-go trials (both  $P$ s  $< 0.001$ ). Furthermore, this effect was more pronounced when the prediction error was high, compared to when it was low (see Fig. 3).

In summary, results of ACCs in no-go trials showed that when participants unexpectedly did not receive any visible outcome following their action on trial  $n - 1$ , they responded more accurately to the no-go signal on trial  $n$ . This suggests that, regardless of the emotional valence of the expected outcome, the unexpected outcome absence in the preceding trial enhances participants' ability to suppress prepotent but inappropriate action in the current trial.

### Comparisons between go and no-go trials

To explore the effect of our manipulation on trial  $n - 1$  on participants' motor tendency on trial  $n$ , we performed a mixed-design 4-way ANOVA on ACCs in both go and no-go trials. The analysis showed a significant 4-way interaction between outcome

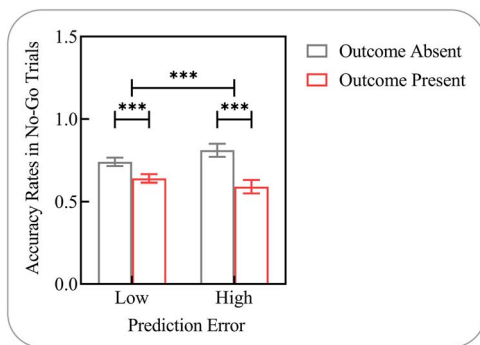


**Fig. 3.** ACCs in no-go trials. The unexpected absence of an action outcome resulted in higher ACCs in subsequent no-go trials. Data are expressed as mean  $\pm$  CI. Note that the CI refers to the 95% confidence interval of the pairwise difference between the 2 compared sub-conditions. \*\*\* $P < 0.001$ .

presence, prediction error, trial type, and task ( $F_{1,52} = 4.39$ ,  $P = 0.041$ ,  $\eta_p^2 = 0.08$ ). To further explore performance differences between go and no-go trials in each sub-condition, we broke down the interaction by focusing on the effect of trial type for each level of the other 3 factors. The results showed that when an action outcome was present in inducement trials, ACCs in subsequent go trials were significantly higher than those in no-go trials (all  $P$ s  $< 0.001$ ). However, in the absence of an action outcome in inducement trials, ACCs did not significantly differ between go and no-go trials ( $P$ s  $> 0.50$ ), or were even significantly lower in go trials compared with no-go trials ( $P < 0.001$ ; see Fig. 4).

In summary, the results of comparing ACCs between go and no-go trials showed that participants had a preference for go over no-go responses on trial  $n$  when they received a positive or negative outcome following their action on trial  $n - 1$ . However, when they did not receive any visible outcome on trial  $n - 1$ , there was no obvious preference for go over no-go responses, or even a preference for no-go over go responses on trial  $n$ . These findings suggest that, regardless of the emotional valence of the expected outcome, outcome absence in the preceding trial may shift participants' motor tendency from action to inaction or inhibition in the current trial.

## ERP results

ERP responses (including N2 and P3 amplitudes in no-go trials) were compared using a mixed-design 3-way ANOVA with 2 within-subjects factors (outcome presence and prediction error) and 1 between-subjects factor (task). Relevant statistics are summarized in Table 1.

The analysis of N2 amplitudes evoked by no-go signals, using a mixed-design 3-way ANOVA, did not find any significant 3-way (or 2-way) interactions between outcome presence, prediction error, and task (all  $P$ s  $> 0.05$ ). However, it revealed a significant main effect of outcome presence ( $F_{1,52} = 16.73$ ,  $P < 0.001$ ,  $\eta_p^2 = 0.24$ ), which indicated that the absence of an action outcome, compared with its presence in inducement trials, resulted in smaller N2 amplitudes in subsequent no-go trials (see Fig. 5A).

The analysis of P3 amplitudes evoked by no-go signals, using a mixed-design 3-way ANOVA, found no significant 3-way interaction between outcome presence, prediction error, and task ( $P > 0.05$ ). However, it revealed a significant 2-way interaction between outcome presence and prediction error ( $F_{1,52} = 17.53$ ,  $P < 0.001$ ,  $\eta_p^2 = 0.25$ ). Post hoc pairwise comparisons showed that, when the prediction error was high, the absence of an action outcome in inducement trials resulted in smaller P3 amplitudes

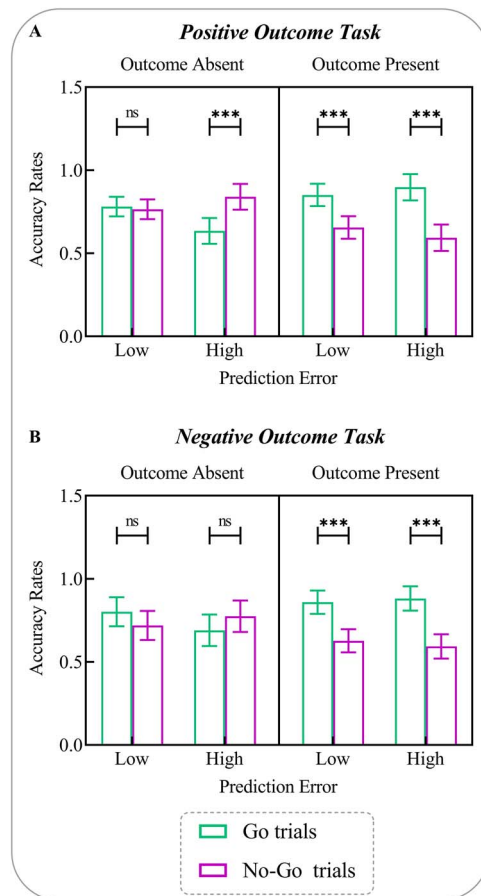


**Fig. 4.** Comparison of ACCs between go and no-go trials. During both (A) positive and (B) negative outcome tasks, the presence of an action outcome was associated with higher ACCs in subsequent go trials compared with no-go trials, whereas this effect was either absent or reversed in conditions without action outcomes. Data are expressed as mean  $\pm$  CI. Note that the CI refers to the 95% confidence interval of the pairwise difference between the 2 compared sub-conditions. ns: not significant; \*\*\* $P < 0.001$ .

in subsequent no-go trials, compared with its presence ( $P < 0.001$ ). However, when the prediction error was low, there was no significant difference in P3 amplitudes between the outcome presence and outcome absence conditions ( $P = 0.167$ ; see Fig. 5B).

In summary, results of ERP amplitudes evoked by no-go signals showed that, compared with receiving a positive or negative outcome, when participants did not receive any visible outcome following their action on trial  $n - 1$ , the no-go signal on trial  $n$  evoked smaller N2 amplitudes. This finding suggests that there are lower cognitive demands for conflict monitoring when participants attempt to cancel prepotent but inappropriate keypress actions in the current trial, after experiencing outcome absence, compared with outcome presence, in the preceding trial. In addition, when participants unexpectedly did not receive any visible outcome following their action on trial  $n - 1$ , the no-go signal on trial  $n$  evoked smaller P3 amplitudes. This finding suggests that the unexpected outcome absence in the preceding trial leads to a reduction in the recruitment of cognitive resources required for implementing inhibitory control in the current trial.

## Time-frequency results

We employed permutation analysis to identify clusters of interest in the time-frequency responses (including midfrontal theta

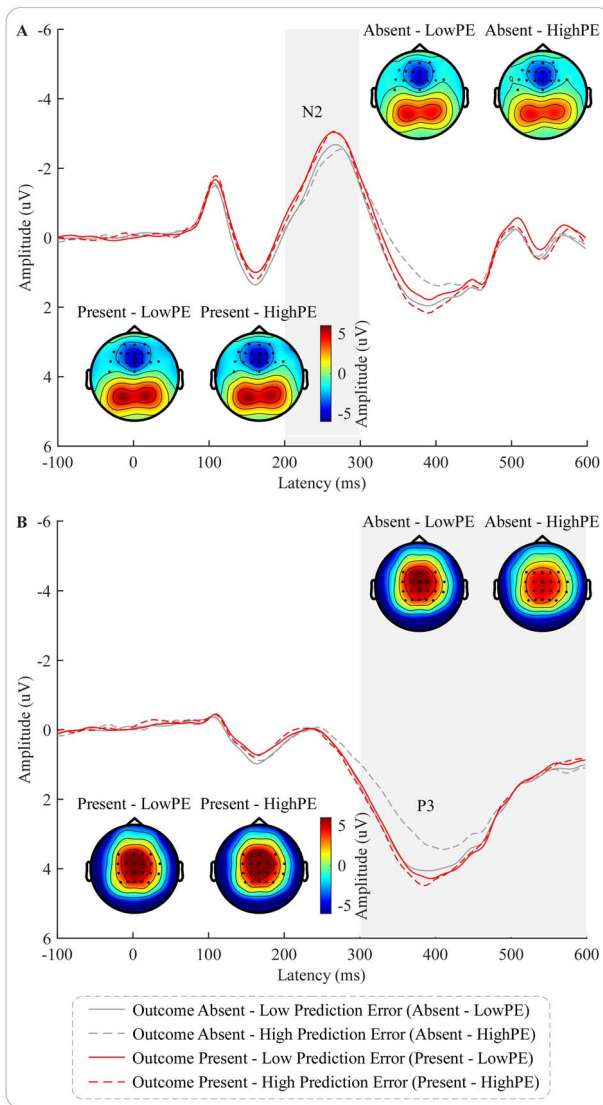


**Fig. 5.** N2 and P3 in no-go trials. (A) The absence of an action outcome resulted in smaller N2 amplitudes in subsequent no-go trials. (B) The unexpected absence of an action outcome resulted in smaller P3 amplitudes in subsequent no-go trials. The scalp topography plots show the topography at the peak of the N2 and P3 components within the time windows marked using gray rectangles in waveforms. The electrodes used to extract N2 and P3 amplitudes are marked using black dots in the scalp topography plots.

power and synchronization in no-go trials). The data from these clusters were then compared using a mixed-design 3-way ANOVA with 2 within-subjects factors (outcome presence and prediction error) and 1 between-subjects factor (task). Relevant statistics are summarized in Table 1.

The permutation analysis of midfrontal oscillatory power evoked by no-go signals did not yield any significant cluster for the 3-way interaction between outcome presence, prediction error, and task ( $P > 0.05$ ). However, it did uncover a significant 2-way interaction between outcome presence and prediction error in the theta and adjacent low alpha frequency ranges (frequencies: 4–10 Hz; electrodes: FCz, FC1, and FC2; time window: ~0–410 ms;  $P = 0.004$ ). Based on the theta power (frequencies: 4–7 Hz) averaged over this cluster, the mixed-design 3-way ANOVA also revealed a significant 2-way interaction between outcome presence and prediction error ( $F_{1,52} = 18.91$ ,  $P < 0.001$ ,  $\eta_p^2 = 0.27$ ). Post hoc

pairwise comparisons showed that, when the prediction error was high, the absence of an action outcome in inducement trials resulted in smaller midfrontal theta power in subsequent no-go trials, compared with its presence ( $P < 0.001$ ). However, when the prediction error was low, there was no significant difference in midfrontal theta power between the outcome presence and outcome absence conditions ( $P = 0.886$ ; see Fig. 6). That is, when participants unexpectedly did not receive any visible outcome following their action in inducement trials, there was smaller midfrontal theta enhancement in subsequent no-go trials.

The permutation analysis of the theta synchronization (frequencies: 4–7 Hz) between the midfrontal electrodes (FCz, FC1, and FC2) and all other electrodes did not yield any significant cluster for the 3-way interaction between outcome presence, prediction error, and task ( $P > 0.05$ ). However, it did uncover a significant 2-way interaction between outcome presence and prediction error over 2 clusters: one was over the parietal area (electrodes: TP9, Pz, P3, P7, Oz, P4, P8, CP3, P1, P5, PO7, POz, PO4, PO8, P6, and Iz; time window: ~160–260 ms;  $P = 0.005$ ), the other was over the medial area (electrodes: C4, T8, FC6, C6, and FC4; time window: ~140–260 ms;  $P = 0.017$ ). Based on the theta synchronization averaged over each cluster, the mixed-design 3-way ANOVAs also showed significant 2-way interactions between outcome presence and prediction error (cluster 1:  $F_{1,52} = 23.28$ ,  $P < 0.001$ ,  $\eta_p^2 = 0.31$ ; cluster 2:  $F_{1,52} = 26.33$ ,  $P < 0.001$ ,  $\eta_p^2 = 0.34$ ). Post hoc pairwise comparisons showed that, when the prediction error was high, the absence of an action outcome in inducement trials resulted in smaller midfrontal theta synchronization in subsequent no-go trials, compared with its presence (in both clusters:  $P_s < 0.001$ ). However, when the prediction error was low, there was no significant difference in midfrontal theta synchronization between the outcome presence and outcome absence conditions (in both clusters:  $P_s > 0.05$ ; see Fig. 7). That is, when participants unexpectedly did not receive any visible outcome following their action in inducement trials, there was smaller theta synchronization between the midfrontal and the medial to parietal areas in subsequent no-go trials.

In summary, results of theta power and synchronization showed that compared with receiving a positive or negative outcome, when participants did not receive any visible outcome following their action on trial  $n - 1$ , the no-go signal on trial  $n$  evoked smaller midfrontal theta enhancement as well as smaller theta synchronization between the midfrontal and the medial to parietal areas. These findings suggest that the unexpected outcome absence in the preceding trial leads to a decrease in motor conflicts triggered by no-go signals, and a reduction in information exchange between midfrontal and other brain areas that are essential for resolving conflicts in the current trial.

## Discussion

The current study explored the effect of SoA on subsequent response inhibition by performing a modified go/no-go task with EEG recordings. We manipulated participants' SoA indirectly by varying the presence and the predictability of a visual outcome (positive outcome task: a happy face; negative outcome task: an angry face) for a given motor action, and measured participants' responses to a subsequent go or no-go signal. Similar results were observed in both tasks: participants exhibited slower RTs and lower ACCs in response to go signals, as well as higher ACCs to no-go signals, when their preceding action unexpectedly did not result in any visible outcome. Additionally, ACCs were higher in go trials compared with no-go trials in conditions with

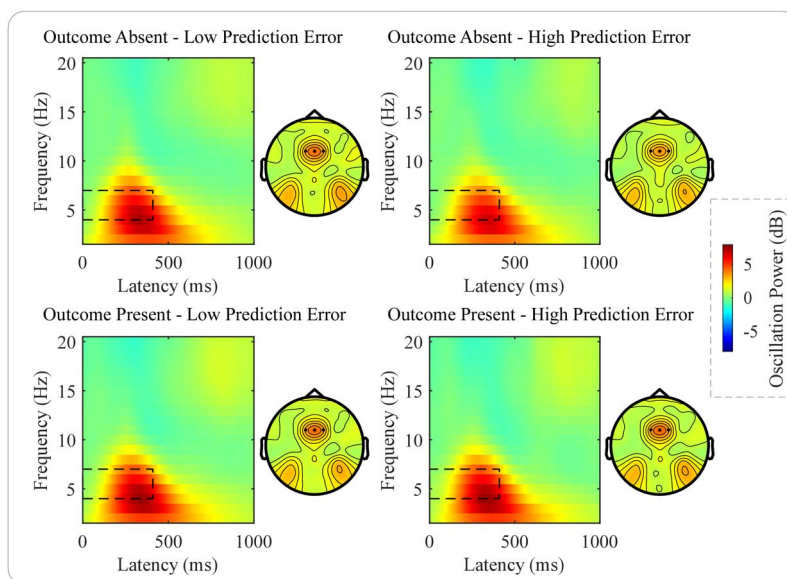


**Fig. 6.** Midfrontal theta power in no-go signals. The unexpected absence of an action outcome resulted in smaller midfrontal theta power in subsequent no-go trials. The scalp topography plots show the topography of the mean power across the frequencies and time windows marked using dashed rectangles in the time-frequency maps. The electrodes used to extract theta power are marked using black dots in the scalp topography plots.

a visual outcome following the preceding action, whereas such effect was less pronounced or even reversed in conditions without action outcomes. Moreover, the enhanced inhibitory tendencies were accompanied by reduced N2 and P3 amplitudes, reduced midfrontal theta power, as well as reduced theta synchronization between the midfrontal and the medial to parietal areas following no-go signals. These results suggest that a reduced SoA (i.e. feeling less in control) on trial  $n - 1$  can facilitate response inhibition and its neural processing (i.e. improved inhibitory control) on trial  $n$ .

Previous studies found that actions having an effect on the environment are reinforced (Eitam et al. 2013; Karsh and Eitam 2015; Hemed et al. 2020; Karsh et al. 2020). For example, participants' RTs were faster if an immediate effect consistently followed their action compared with no effect or a delayed effect (Eitam et al. 2013). Furthermore, buttons having a high probability of causing a visual effect were pressed more frequently and rapidly compared with buttons that never produced any visual effect, even though these action effects were task-irrelevant and valence-neutral (Karsh and Eitam 2015). Consistent with existing evidence, the behavioral results of the present study indicate that participants' readiness to perform a keypress action in the current trial depends on their SoA over this action and action-triggered events in the preceding trial. Specifically, participants had slower responses and lower hit rates in the following go trials when they did not receive any visible outcome for their preceding action. This effect was even more pronounced when the prediction error was high compared with when it was low. The absence of action outcomes and high prediction error has been regarded to reduce the SoA (Majchrowicz and Wierchoń 2018; Wen and Haggard 2020). Thus, our results reflect that low SoA on trial  $n - 1$  reduces action readiness on trial  $n$ .

In addition, our behavioral results suggest that low SoA on trial  $n - 1$  can facilitate response inhibition on trial  $n$ . This was manifested as higher ACCs in no-go trials when the preceding keypress action unexpectedly did not produce any visible effect. Our finding suggests that a decrease in the feeling of control over a specific action in a preceding behavioral episode can result

in improved inhibitory control over that action in the current episode. A prior study found that when participants already had a high level of control over an external object through their actions, a slight reduction in the degree of control rapidly captured their attention (Wen and Haggard 2018). Our finding extends this earlier report by showing that the detection of diminished control may also contribute to higher-order cognitive control processes that aim to reassert control over the external world.

Interestingly, we found that participants' motor tendency/action preference on trial  $n$  was also sensitive to the changes in their SoA on trial  $n - 1$ . In the current study, the relative proportion of go and no-go trials in both inducement trials and test trials created the impression that there were far fewer no-go trials than go trials (~25% no-go trials vs. 75% go trials). It has been reported that go/no-go tasks with rare no-go trials reliably elicit prepotent motor activity (Wessel 2018) and thus increase action readiness. Indeed, in conditions presenting action outcomes in inducement trials, we observed higher ACCs in go trials compared with no-go trials. This suggests that when participants' SoA in the preceding trial was relatively high, they tended to act rather than stop in the following trial. In contrast, in conditions without action outcomes, participants had comparable ACCs in go and no-go trials or even lower ACCs in go trials than in no-go trials. That is, when participants' SoA in the preceding trial was relatively low, their preference for go over no-go responses in the following trial was significantly reduced. These results indicate that a reduced SoA on trial  $n - 1$  can shift participants' motor tendency from action to inaction or inhibition on trial  $n$ .

Importantly, EEG results reveal the neural mechanisms underlying the effects mentioned above. For ERP responses, reductions in no-go N2 and P3 amplitudes accompanied the improvement in response inhibition at behavior. The N2 component has been regarded as an indicator of conflict monitoring (Donkers and van Boxtel 2004; Lavric et al. 2004; Smith et al. 2008; Beste et al. 2010). Thus, the suppression of the no-go N2 component in conditions without action outcomes compared with conditions with action outcomes may reflect lower cognitive demands for conflict

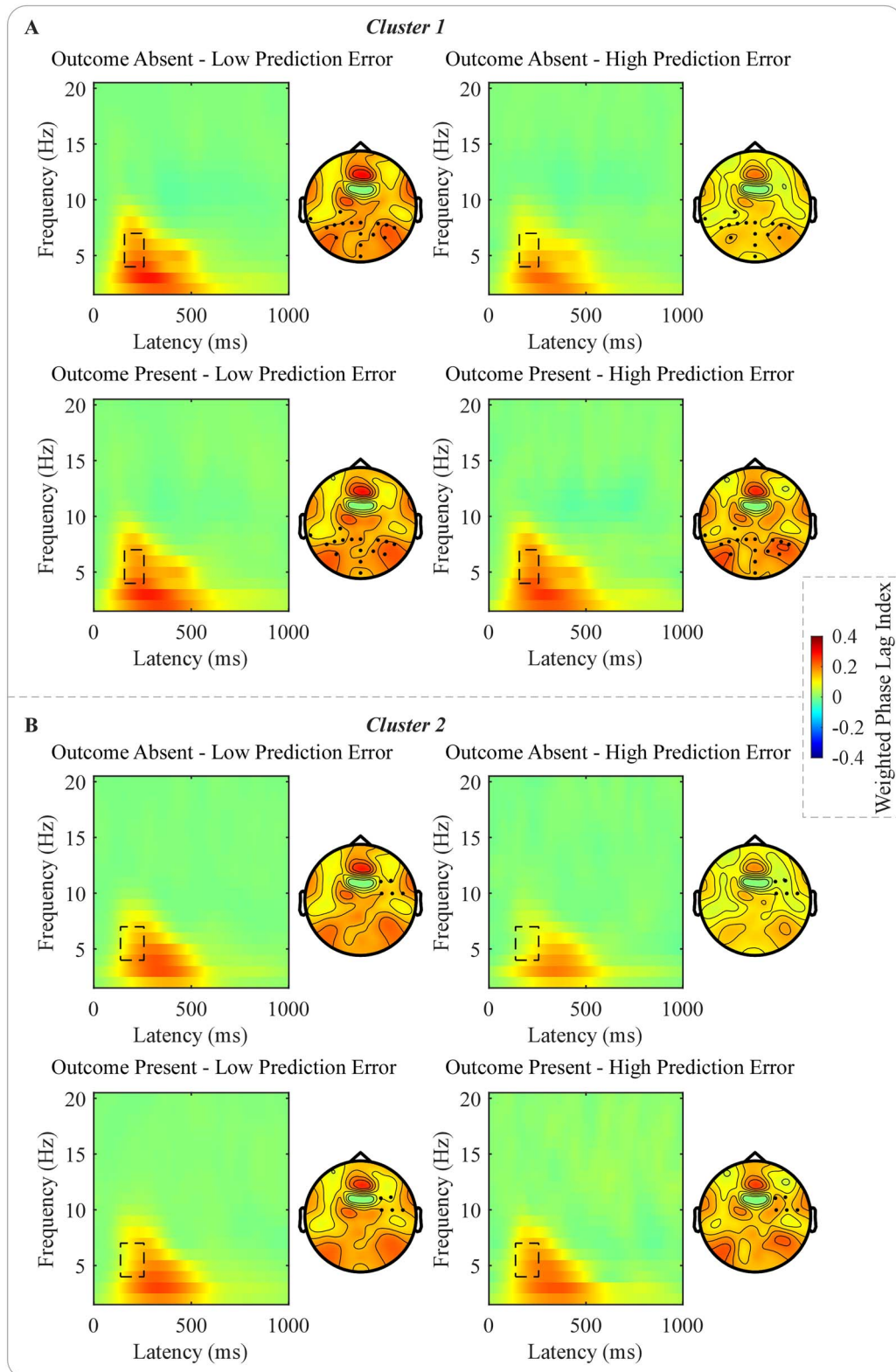


**Fig. 7.** Midfrontal theta synchronization in no-go signals. The unexpected absence of an action outcome resulted in smaller theta synchronization (A) between midfrontal and parietal area, as well as (B) between midfrontal and medial area in subsequent no-go trials. The scalp topography plots show the topography of the mean synchronization across the frequencies and time windows marked using dashed rectangles in the time-frequency maps. The electrodes used to extract theta synchronization are marked using black dots in the scalp topography plots.

monitoring in the current trial after experiencing less in control in the preceding trial. The P3 component has been suggested to reflect the implementation of inhibitory processes (Huster et al. 2011; Chmielewski and Beste 2015, 2019; Wessel and Aron 2015). Thus, our result that no-go signals evoked smaller P3 when participants' preceding action unexpectedly did not produce any visible effect may indicate that fewer cognitive resources were recruited to overcome motor conflict on trial  $n$  because of a reduced SoA on trial  $n - 1$ . Notably, in the current study, N2 amplitudes were modulated by the factor "outcome presence (absent vs. present)" but not by the factor "prediction error (low vs. high)," whereas both factors modulated P3 amplitudes. While the N2 and P3 components are often associated with cognitive and motor conflict processing, they have also been found to be influenced by more general mechanisms, such as expectation violations and updating (Wessel 2018). In the present study, the anticipated repetition of the face stimulus in go trials may lead to expectation updating which could be especially reflected in a P3 enhancement. Therefore, it is possible that the N2/P3 effects found in the present study reflect other cognitive processes, such as the processing of expectation violations, rather than only inhibitory control.

Consistent with the ERP results, we observed the smallest midfrontal theta power enhancement after no-go signals in the condition with the best response inhibition performance, i.e. in the condition with unexpected outcome absence in the preceding trial. Motor conflicts have been frequently found to increase the theta power over the midfrontal cortex (Vissers et al. 2018; Kaiser et al. 2019; Kaiser and Schütz-Bosbach 2019). Thus, our findings indicate that the occurrence of a no-go signal evoked fewer motor conflicts on trial  $n$  if participants' SoA on trial  $n - 1$  was low. Moreover, we found that theta synchronization between the midfrontal and the medial to parietal areas after no-go signals greatly decreased following a preceding trial with a low SoA. Oscillatory synchronization is assumed to reflect information exchange between task-relevant brain regions, which is one of the core neural processes in conflict resolution (Cooper et al. 2015; van de Vijver et al. 2018; Duprez et al. 2020). Thus, our finding indicates that less intercortical communication was required to achieve successful response inhibition on trial  $n$  after experiencing a low SoA on trial  $n - 1$ . The observed decrease in synchronicity in the medial region may indicate a reduction in intercommunication between the midfrontal area and the motor cortex (Kaiser and Schütz-Bosbach 2020). Additionally, the reduced synchronicity in the parietal region could suggest a temporary disruption in visual attention, as frontoparietal connectivity is frequently associated with attentional processes (Marshall et al. 2015; Ptak et al. 2017; Dixon et al. 2018). Despite the frontoparietal network being proposed to support cognitive control (Marek and Dosenbach 2018), to our best knowledge, there is a lack of literature about synchronization patterns during response inhibition. Our findings provide primary empirical evidence that frontoparietal interconnectivity plays a critical role in implementing inhibition.

The observation of similar effects in both positive and negative outcome tasks suggests that the feeling of control over external objects, rather than outcome valence, plays a dominant role in the impact of SoA on subsequent action regulation. This finding fits well with the view that the SoA is internally rewarding and thus can motivate future actions (Nafcha et al. 2016; Gozli 2019; Schwarz et al. 2022). This view received substantial support from behavioral and neuroimaging studies. For example, a high level of control over an action (e.g. encoded as being able to produce predictable perceptual changes) has been observed to facilitate

the selection of that action in human infants (Watanabe and Taga 2006; Watanabe and Taga 2011) and adults (Hemed et al. 2020, 2022; Karsh et al. 2020; Tanaka et al. 2021). Furthermore, a recent study found that participants' subjective judgments of agency based on their past experience of action-effect contingencies were associated with their future action choices in situations of higher outcome certainty. More specifically, higher agency ratings in the first part of a block predicted higher success rates in the second part of the block (Schwarz et al. 2022). Additionally, high action-effect contingency (Behne et al. 2008) and high perceived control (Tricomi et al. 2004; Lorenz et al. 2015) that contribute to positive judgments of agency have been found to increase activation in brain areas involved in reward processing (e.g. striatum). From this perspective, our findings can be attributed to a decline in the motivation to act following a low SoA in a preceding behavioral episode. More specifically, if an action failed to produce expected outcomes, participants were less motivated to repeat it and thus more primed for inaction. Therefore, they could "enact inhibition" with more ease when no-go signals arrived, but "enact action" with more difficulty when go signals appeared. This phenomenon could be explained as a general slowing down or a tendency toward more deliberate processing for upcoming action stimuli because of increased uncertainty. One could speculate that shifting motor tendency from action to inhibition on trial  $n$  after experiencing a low SoA on trial  $n - 1$  might be adaptive, as it prevents us from wasting limited resources on actions that cannot effectively control the environment.

The emotional valence of the expected action outcome did not greatly shape the observed effects probably because it did not provide any information about participants' task performance. In parallel with the aforementioned "motivation from control" view, the action outcome itself can also serve as an important source of motivation if it provides information about the relation between the current state and the desired goal, which is termed "motivation from outcome" (Nafcha et al. 2016). In the current study, participants could easily tell whether their responses were correct in a trial according to whether an error message appeared at the end of that trial. They were also explicitly informed of their ACCs and RTs after each block. This information was relevant to their task goals, i.e. more accurate and faster responses. In contrast, the outcome valence has nothing to do with judgments of their performance, and thus it was unlikely to have a substantial effect on participants' motivation to act. It should be noted that outcome valence did have some effects on our results. The suppression of action readiness (as measured by go ACCs and RTs) on trial  $n$  caused by the unexpected absence of action outcomes on trial  $n - 1$  were stronger in the context of expecting positively valenced outcomes compared with expecting negatively valenced outcomes. Previous studies using self-report measures have consistently shown that positive action outcomes increase the explicit SoA when compared with negative outcomes (see review: Kaiser et al. 2021). However, studies using implicit measures of agency (sensory attenuation or temporal binding) have produced inconclusive findings, with some studies indicating that positive compared with negative action outcomes increase implicit SoA (e.g. Gentsch et al. 2015), whereas others suggest a decrease (e.g. Majchrowicz and Wierzchoń 2018) or no influence (e.g. Moreton et al. 2017) on implicit SoA. Examining the differential impact of experiencing a negative prediction error (failing to produce expected positive outcomes) vs. a positive prediction error (failing to produce expected negative outcomes) on the SoA on trial  $n - 1$ , and its subsequent influence on action regulation on trial  $n$ , would be a valuable direction for future research. Importantly, however,

our study found that independent of valence-specific effects, both positive and negative outcomes facilitated subsequent action execution, whereas the absence of either effect hindered motor readiness. These findings support that the effectiveness of the motor action in producing a perceivable event is a key factor driving the observed effects.

Several limitations of the present study should be acknowledged. First, although we used a well-established method for manipulating the SoA by varying the presence and predictability of a visual outcome (e.g. Caspar et al. 2016; Majchrowicz and Wierchoń 2018; Villa et al. 2021), we did not include any explicit measures to assess participants' judgments of agency in inducement and test trials. Our finding that high prediction error conditions led to larger FRN confirmed the effectiveness of our manipulation of the SoA in inducement trials to some extent (Talmi et al. 2013; Sidarus et al. 2017); however, it remains unclear whether such effects on agency carry over to the upcoming response. Previous studies have suggested that experiencing unpredicted events, such as errors on trial  $n - 1$ , may lead to increased rather than decreased SoA on trial  $n$  (Di Costa et al. 2018; Majchrowicz et al. 2020). Thus, based on our current findings, we can only conclude that the SoA on trial  $n - 1$  modulates action regulation on trial  $n$ , but it remains to be investigated whether the SoA on trial  $n$  is increased and plays a more direct role in action regulation. To gain a more comprehensive understanding of how the control felt influences the control used, future studies could, for example, include self-report measures of agency in some of the inducement trials and also in some of the test trials. Second, it remains unclear whether the observed effects are specific to action (agency) or whether they reflect a more general effect of expectancy violation independent of action. Oddball stimuli have been known to recruit control, as reported in the present study, i.e. in terms of post-oddball slowing and related neurophysiological adaptations (Saunders and Jentsch 2012; Pfister et al. 2020). Further studies are needed to dissociate the effects caused by unpredicted action outcomes and unpredicted events in general, for example, by adding a control condition in which unpredicted outcomes occur in the absence of any action.

To conclude, we observed that when participants' action unexpectedly did not result in any perceivable effect on trial  $n - 1$ , it was easier for them to inhibit their action in response to no-go signals on trial  $n$ , which manifested as higher ACCs, smaller N2 and P3 amplitudes, smaller midfrontal theta power, and smaller theta synchronization between the midfrontal and the medial to parietal areas. Our findings support the theory that information regarding our control over the environment is a crucial motivator for future behavior, and highlight the impact of the control felt in a preceding behavioral episode on the control used in the subsequent action regulation, thereby shedding new light on the functional significance of the SoA in goal-directed behavior.

## Acknowledgments

We thank Elsa Sangaran and Marija Ivanovic for their assistance in data collection.

## CRedit author statement

Qiaoyue Ren (Conceptualization, Data curation, Formal analysis, Investigation, Methodology, Visualization, Writing – original draft), Jakob Kaiser (Conceptualization, Methodology, Writing – review & editing), Antje Gentsch (Conceptualization, Methodology, Writing

– review & editing), Simone Schuetz-Bosbach (Conceptualization, Methodology, Supervision, Writing – review & editing).

## Supplementary material

Supplementary material is available at *Cerebral Cortex* online.

## Funding

The Deutsche Forschungsgemeinschaft (GE 30841-1 to AG, SCHU 24716-1 to SS-B); China Scholarship Council (202004910347 to QR).

Conflict of interest statement: None declared.

## Data availability

Data and analysis files are available via Open Science Framework: [https://osf.io/2dmvf/?view\\_only=6c429ee3f0eb4155895828d7ce9c239](https://osf.io/2dmvf/?view_only=6c429ee3f0eb4155895828d7ce9c239).

## References

- Bari A, Robbins TW. Inhibition and impulsivity: behavioral and neural basis of response control. *Prog Neurobiol*. 2013;108:44–79. <https://doi.org/10.1016/j.pneurobio.2013.06.005>.
- Bastos AM, Schoffelen J-M. A tutorial review of functional connectivity analysis methods and their interpretational pitfalls. *Front Syst Neurosci*. 2016;9:175. <https://doi.org/10.3389/fnsys.2015.00175>.
- Behne N, Scheich H, Brechmann A. The left dorsal striatum is involved in the processing of neutral feedback. *Neuroreport*. 2008;19(15):1497–1500. <https://doi.org/10.1097/WNR.0b013e32830fe98c>.
- Beste C, Willemsen R, Saft C, Falkenstein M. Response inhibition subprocesses and dopaminergic pathways: basal ganglia disease effects. *Neuropsychologia*. 2010;48(2):366–373. <https://doi.org/10.1016/j.neuropsychologia.2009.09.023>.
- Beste C, Münchau A, Frings C. Towards a systematization of brain oscillatory activity in actions. *Commun Biol*. 2023;6(1):1–11. <https://doi.org/10.1038/s42003-023-04531-9>.
- Blakemore S-J, Wolpert DM, Frith CD. Central cancellation of self-produced tickle sensation. *Nat Neurosci*. 1998;1(7):635–640. <https://doi.org/10.1038/2870>.
- Blakemore S-J, Wolpert DM, Frith CD. Abnormalities in the awareness of action. *Trends Cogn Sci*. 2002;6(6):237–242. [https://doi.org/10.1016/S1364-6613\(02\)01907-1](https://doi.org/10.1016/S1364-6613(02)01907-1).
- Campbell JID, Thompson VA. MorePower 6.0 for ANOVA with relational confidence intervals and Bayesian analysis. *Behav Res Methods*. 2012;44(4):1255–1265. <https://doi.org/10.3758/s13428-012-0186-0>.
- Caspar EA, Desantis A, Dienes Z, Cleeremans A, Haggard P. The sense of agency as tracking control. *PLoS One*. 2016;11(10):e0163892. <https://doi.org/10.1371/journal.pone.0163892>.
- Chambers CD, Garavan H, Bellgrove MA. Insights into the neural basis of response inhibition from cognitive and clinical neuroscience. *Neurosci Biobehav Rev*. 2009;33(5):631–646. <https://doi.org/10.1016/j.neubiorev.2008.08.016>.
- Chmielewski WX, Beste C. Action control processes in autism spectrum disorder – insights from a neurobiological and neuroanatomical perspective. *Prog Neurobiol*. 2015;124:49–83. <https://doi.org/10.1016/j.pneurobio.2014.11.002>.
- Chmielewski WX, Beste C. Stimulus-response recoding during inhibitory control is associated with superior frontal and

- parahippocampal processes. *NeuroImage*. 2019;196:227–236. <https://doi.org/10.1016/j.neuroimage.2019.04.035>.
- Cohen MX. Effects of time lag and frequency matching on phase-based connectivity. *J Neurosci Methods*. 2015;250:137–146. <https://doi.org/10.1016/j.jneumeth.2014.09.005>.
- Cooper PS, Wong ASW, Fulham WR, Thienel R, Mansfield E, Michie PT, Karayanidis F. Theta frontoparietal connectivity associated with proactive and reactive cognitive control processes. *NeuroImage*. 2015;108:354–363. <https://doi.org/10.1016/j.neuroimage.2014.12.028>.
- Cooper PS, Karayanidis F, McKewen M, McLellan-Hall S, Wong ASW, Skippen P, Cavanagh JF. Frontal theta predicts specific cognitive control-induced behavioural changes beyond general reaction time slowing. *NeuroImage*. 2019;189:130–140. <https://doi.org/10.1016/j.neuroimage.2019.01.022>.
- Demanet J, Muhle-Karbe PS, Lynn MT, Blotenberg I, Brass M. Power to the will: how exerting physical effort boosts the sense of agency. *Cognition*. 2013;129(3):574–578. <https://doi.org/10.1016/j.cognition.2013.08.020>.
- Derosiere G, Klein P-A, Nozaradan S, Zénon A, Mouraux A, Duque J. Visuomotor correlates of conflict expectation in the context of motor decisions. *J Neurosci*. 2018;38(44):9486–9504. <https://doi.org/10.1523/JNEUROSCI.0623-18.2018>.
- Di Costa S, Théro H, Chambon V, Haggard P. Try and try again: post-error boost of an implicit measure of agency. *Q J Exp Psychol*. 2018;71(7):1584–1595. <https://doi.org/10.1080/17470218.2017.1350871>.
- Dixon ML, De La Vega A, Mills C, Andrews-Hanna J, Spreng RN, Cole MW, Christoff K. Heterogeneity within the frontoparietal control network and its relationship to the default and dorsal attention networks. *Proc Natl Acad Sci*. 2018;115(7):E1598–E1607. <https://doi.org/10.1073/pnas.1715766115>.
- Donkers FCL, van Boxtel GJM. The N2 in go/no-go tasks reflects conflict monitoring not response inhibition. *Brain Cogn*. 2004;56(2):165–176. <https://doi.org/10.1016/j.bandc.2004.04.005>.
- van Driel J, Ridderinkhof KR, Cohen MX. Not all errors are alike: theta and alpha EEG dynamics relate to differences in error-processing dynamics. *J Neurosci*. 2012;32(47):16795–16806. <https://doi.org/10.1523/JNEUROSCI.0802-12.2012>.
- Duprez J, Gulbinaite R, Cohen MX. Midfrontal theta phase coordinates behaviorally relevant brain computations during cognitive control. *NeuroImage*. 2020;207:116340. <https://doi.org/10.1016/j.neuroimage.2019.116340>.
- Ebert JP, Wegner DM. Time warp: authorship shapes the perceived timing of actions and events. *Conscious Cogn*. 2010;19(1):481–489. <https://doi.org/10.1016/j.concog.2009.10.002>.
- Eitam B, Kennedy PM, Tory HE. Motivation from control. *Exp Brain Res*. 2013;229(3):475–484. <https://doi.org/10.1007/s00221-012-3370-7>.
- Falkenstein M, Hoormann J, Hohnsbein J. ERP components in go/nogo tasks and their relation to inhibition. *Acta Psychol*. 1999;101(2):267–291. [https://doi.org/10.1016/S0001-6918\(99\)00008-6](https://doi.org/10.1016/S0001-6918(99)00008-6).
- Fries P. A mechanism for cognitive dynamics: neuronal communication through neuronal coherence. *Trends Cogn Sci*. 2005;9(10):474–480. <https://doi.org/10.1016/j.tics.2005.08.011>.
- Frith CD, Blakemore S-J, Wolpert DM. Abnormalities in the awareness and control of action. *Philos Trans R Soc Lond Ser B Biol Sci*. 2000;355(1404):1771–1788. <https://doi.org/10.1098/rstb.2000.0734>.
- Gentsch A, Weiss C, Spengler S, Synofzik M, Schütz-Bosbach S. Doing good or bad: how interactions between action and emotion expectations shape the sense of agency. *Soc Neurosci*. 2015;10(4):418–430. <https://doi.org/10.1080/17470919.2015.1006374>.
- Gozli D. *Experimental psychology and human agency*. Cham: Springer; 2019.
- Haggard P. Sense of agency in the human brain. *Nat Rev Neurosci*. 2017;18:196–207. <https://doi.org/10.1038/nrn.2017.14>.
- Hemed E, Bakbani-Elkayam S, Teodorescu AR, Yona L, Eitam B. Evaluation of an action's effectiveness by the motor system in a dynamic environment. *J Exp Psychol Gen*. 2020;149(5):935–948. <https://doi.org/10.1037/xge0000692>.
- Hemed E, Karsh N, Mark-Tavger I, Eitam B. Motivation(s) from control: response-effect contingency and confirmation of sensorimotor predictions reinforce different levels of selection. *Exp Brain Res*. 2022;240(5):1471–1497. <https://doi.org/10.1007/s00221-022-06345-3>.
- Hon N, Poh J-H, Soon C-S. Preoccupied minds feel less control: sense of agency is modulated by cognitive load. *Conscious Cogn*. 2013;22(2):556–561. <https://doi.org/10.1016/j.concog.2013.03.004>.
- Howard EE, Edwards SG, Bayliss AP. Physical and mental effort disrupts the implicit sense of agency. *Cognition*. 2016;157:114–125. <https://doi.org/10.1016/j.cognition.2016.08.018>.
- Hu L, Zhang Z. *EEG signal processing and feature extraction*. Singapore: Springer; 2019.
- Huster RJ, Eichele T, Enriquez-Geppert S, Wollbrink A, Kugel H, Konrad C, Pantev C. Multimodal imaging of functional networks and event-related potentials in performance monitoring. *NeuroImage*. 2011;56(3):1588–1597. <https://doi.org/10.1016/j.neuroimage.2011.03.039>.
- Huster RJ, Enriquez-Geppert S, Lavallee CF, Falkenstein M, Herrmann CS. Electroencephalography of response inhibition tasks: functional networks and cognitive contributions. *Int J Psychophysiol*. 2013;87(3):217–233. <https://doi.org/10.1016/j.ijpsycho.2012.08.001>.
- JASP Team. JASP (version 0.17.0.0) (computer software). 2023.
- Kaiser J, Schütz-Bosbach S. Proactive control without midfrontal control signals? The role of midfrontal oscillations in preparatory conflict adjustments. *Biol Psychol*. 2019;148:107747. <https://doi.org/10.1016/j.biopsycho.2019.107747>.
- Kaiser J, Schütz-Bosbach S. Motor interference, but not sensory interference, increases midfrontal theta activity and brain synchronization during reactive control. *J Neurosci*. 2020;41(8):1788–1801. <https://doi.org/10.1523/JNEUROSCI.1682-20.2020>.
- Kaiser J, Simon NA, Sauseng P, Schütz-Bosbach S. Midfrontal neural dynamics distinguish between general control and inhibition-specific processes in the stopping of motor actions. *Sci Rep*. 2019;9(1):13054. <https://doi.org/10.1038/s41598-019-49476-4>.
- Kaiser J, Buciuman M, Gigl S, Gentsch A, Schütz-Bosbach S. The interplay between affective processing and sense of agency during action regulation: a review. *Front Psychol*. 2021;12:716220. <https://doi.org/10.3389/fpsyg.2021.716220>.
- Karsh N, Eitam B. I control therefore I do: judgments of agency influence action selection. *Cognition*. 2015;138:122–131. <https://doi.org/10.1016/j.cognition.2015.02.002>.
- Karsh N, Eitam B, Mark I, Higgins ET. Bootstrapping agency: how control-relevant information affects motivation. *J Exp Psychol Gen*. 2016;145(10):1333–1350. <https://doi.org/10.1037/xge0000212>.
- Karsh N, Hemed E, Nafcha O, Elkayam SB, Custers R, Eitam B. The differential impact of a response's effectiveness and its monetary value on response-selection. *Sci Rep*. 2020;10(1):3405. <https://doi.org/10.1038/s41598-020-60385-9>.
- Klimesch W, Sauseng P, Hanslmayr S. EEG alpha oscillations: the inhibition-timing hypothesis. *Brain Res Rev*. 2007;53(1):63–88. <https://doi.org/10.1016/j.brainresrev.2006.06.003>.

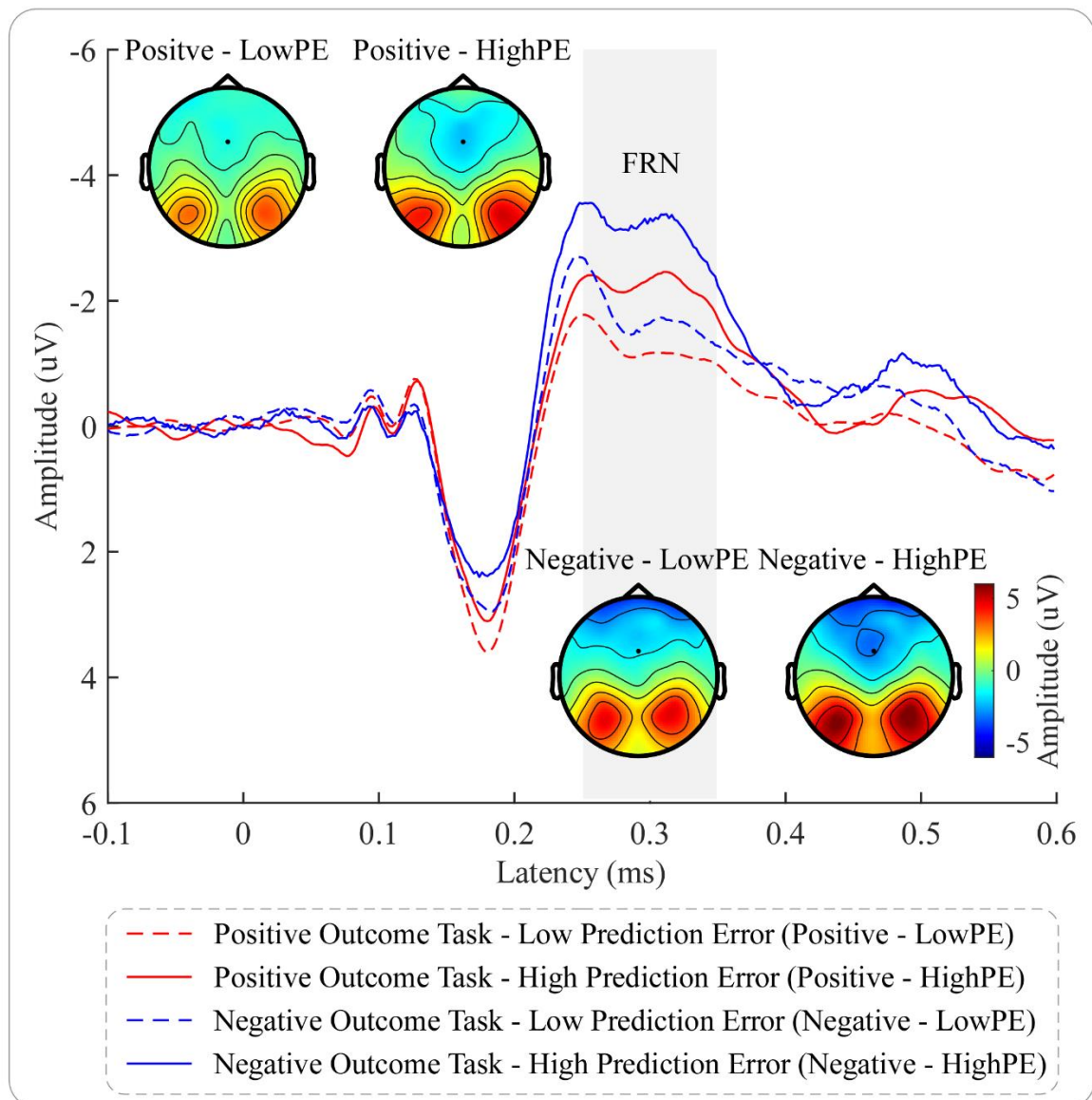
- Krigolson OE. Event-related brain potentials and the study of reward processing: methodological considerations. *Int J Psychophysiol.* 2018;132:175–183. <https://doi.org/10.1016/j.ijpsycho.2017.11.007>.
- Lavric A, Pizzagalli DA, Forstmeier S. When “go” and “nogo” are equally frequent: ERP components and cortical tomography: ERP localization when “go” and “nogo” are equally frequent. *Eur J Neurosci.* 2004;20(9):2483–2488. <https://doi.org/10.1111/j.1460-9568.2004.03683.x>.
- Lorenz RC, Gleich T, Kühn S, Pöhlend L, Pelz P, Wüstenberg T, Raufelder D, Heinz A, Beck A. Subjective illusion of control modulates striatal reward anticipation in adolescence. *NeuroImage.* 2015;117:250–257. <https://doi.org/10.1016/j.neuroimage.2015.05.024>.
- Majchrowicz B, Wierchoń M. Unexpected action outcomes produce enhanced temporal binding but diminished judgement of agency. *Conscious Cogn.* 2018;65:310–324. <https://doi.org/10.1016/j.concog.2018.09.007>.
- Majchrowicz B, Kulakova E, Di Costa S, Haggard P. Learning from informative losses boosts the sense of agency. *Q J Exp Psychol.* 2020;73(12):2272–2289. <https://doi.org/10.1177/1747021820958258>.
- Marek S, Dosenbach NUF. The frontoparietal network: function, electrophysiology, and importance of individual precision mapping. *Dialogues Clin Neurosci.* 2018;20(2):133–140. <https://doi.org/10.31887/DCNS.2018.20.2/smarek>.
- Maris E, Oostenveld R. Nonparametric statistical testing of EEG- and MEG-data. *J Neurosci Methods.* 2007;164(1):177–190. <https://doi.org/10.1016/j.jneumeth.2007.03.024>.
- Marshall TR, Bergmann TO, Jensen O. Frontoparietal structural connectivity mediates the top-down control of neuronal synchronization associated with selective attention. *PLoS Biol.* 2015;13(10):e1002272. <https://doi.org/10.1371/journal.pbio.1002272>.
- Moreton J, Callan MJ, Hughes G. How much does emotional valence of action outcomes affect temporal binding? *Conscious Cogn.* 2017;49:25–34. <https://doi.org/10.1016/j.concog.2016.12.008>.
- Mückschel M, Stock A-K, Beste C. Psychophysiological mechanisms of interindividual differences in goal activation modes during action cascading. *Cereb Cortex.* 2014;24(8):2120–2129. <https://doi.org/10.1093/cercor/bht066>.
- Nafcha O, Higgins ET, Eitam B. Control feedback as the motivational force behind habitual behavior. *Prog Brain Res.* 2016;229:49–68. <https://doi.org/10.1016/bs.pbr.2016.06.008>.
- Oostenveld R, Fries P, Maris E, Schoffelen J-M. FieldTrip: open source software for advanced analysis of MEG, EEG, and invasive electrophysiological data. *Comput Intell Neurosci.* 2011;2011:156869. <https://doi.org/10.1155/2011/156869>.
- Penton T, Wang X, Coll M-P, Catmur C, Bird G. The influence of action–outcome contingency on motivation from control. *Exp Brain Res.* 2018;236(12):3239–3249. <https://doi.org/10.1007/s00221-018-5374-4>.
- Pfister R, Weller L, Kunde W. When actions go awry: monitoring partner errors and machine malfunctions. *J Exp Psychol Gen.* 2020;149(9):1778–1787. <https://doi.org/10.1037/xge0000748>.
- Potts CA, Carlson RA. Control used and control felt: two sides of the agency coin. *Atten Percept Psychophys.* 2019;81(7):2304–2319. <https://doi.org/10.3758/s13414-019-01771-y>.
- Ptak R, Schnider A, Fellrath J. The dorsal frontoparietal network: a core system for emulated action. *Trends Cogn Sci.* 2017;21(8):589–599. <https://doi.org/10.1016/j.tics.2017.05.002>.
- Raud L, Westerhausen R, Dooley N, Huster RJ. Differences in unity: the go/no-go and stop signal tasks rely on different mechanisms. *NeuroImage.* 2020;210:116582. <https://doi.org/10.1016/j.neuroimage.2020.116582>.
- Ren Q, Gentsch A, Kaiser J, Schütz-Bosbach S. Ready to go: higher sense of agency enhances action readiness and reduces response inhibition. *Cognition.* 2023;237:105456. <https://doi.org/10.1016/j.cognition.2023.105456>.
- Sato A, Yasuda A. Illusion of sense of self-agency: discrepancy between the predicted and actual sensory consequences of actions modulates the sense of self-agency, but not the sense of self-ownership. *Cognition.* 2005;94(3):241–255. <https://doi.org/10.1016/j.cognition.2004.04.003>.
- Saunders B, Jentsch I. False external feedback modulates posterror slowing and the f-P300: implications for theories of posterror adjustment. *Psychon Bull Rev.* 2012;19(6):1210–1216. <https://doi.org/10.3758/s13423-012-0314-y>.
- Schwarz KA, Klaffehn AL, Hauke-Forman N, Muth FV, Pfister R. Never run a changing system: action-effect contingency shapes prospective agency. *Cognition.* 2022;229:105250. <https://doi.org/10.1016/j.cognition.2022.105250>.
- Sidarus N, Haggard P. Difficult action decisions reduce the sense of agency: a study using the Eriksen flanker task. *Acta Psychol.* 2016;166:1–11. <https://doi.org/10.1016/j.actpsy.2016.03.003>.
- Sidarus N, Vuorre M, Haggard P. How action selection influences the sense of agency: an ERP study. *NeuroImage.* 2017;150:1–13. <https://doi.org/10.1016/j.neuroimage.2017.02.015>.
- Smith JL, Johnstone SJ, Barry RJ. Movement-related potentials in the go/nogo task: the P3 reflects both cognitive and motor inhibition. *Clin Neurophysiol.* 2008;119(3):704–714. <https://doi.org/10.1016/j.clinph.2007.11.042>.
- Talmi D, Atkinson R, El-Deredy W. The feedback-related negativity signals salience prediction errors, not reward prediction errors. *J Neurosci.* 2013;33(19):8264–8269. <https://doi.org/10.1523/JNEUROSCI.5695-12.2013>.
- Tanaka T, Watanabe K, Tanaka K. Immediate action effects motivate actions based on the stimulus–response relationship. *Exp Brain Res.* 2021;239(1):67–78. <https://doi.org/10.1007/s00221-020-05955-z>.
- Tottenham N, Tanaka JW, Leon AC, McCarry T, Nurse M, Hare TA, Marcus DJ, Westerlund A, Casey B, Nelson C. The Nim-Stim set of facial expressions: judgments from untrained research participants. *Psychiatry Res.* 2009;168(3):242–249. <https://doi.org/10.1016/j.psychres.2008.05.006>.
- Tricomi EM, Delgado MR, Fiez JA. Modulation of caudate activity by action contingency. *Neuron.* 2004;41(2):281–292. [https://doi.org/10.1016/S0896-6273\(03\)00848-1](https://doi.org/10.1016/S0896-6273(03)00848-1).
- Van den Bussche E, Alves M, Murray YPJ, Hughes G. The effect of cognitive effort on the sense of agency. *PLoS One.* 2020;15(8):e0236809. <https://doi.org/10.1371/journal.pone.0236809>.
- Vastano R, Pozzo T, Brass M. The action congruency effect on the feelings of agency. *Conscious Cogn.* 2017;51:212–222. <https://doi.org/10.1016/j.concog.2017.04.002>.
- Verbruggen F, Logan GD. Response inhibition in the stop-signal paradigm. *Trends Cogn Sci.* 2008;12(11):418–424. <https://doi.org/10.1016/j.tics.2008.07.005>.
- van de Vijver I, van Driel J, Hillebrand A, Cohen MX. Interactions between frontal and posterior oscillatory dynamics support adjustment of stimulus processing during reinforcement learning. *NeuroImage.* 2018;181:170–181. <https://doi.org/10.1016/j.neuroimage.2018.07.014>.

- Villa R, Tidoni E, Porciello G, Aglioti SM. Freedom to act enhances the sense of agency, while movement and goal-related prediction errors reduce it. *Psychol Res*. 2021;85(3):987–1004. <https://doi.org/10.1007/s00426-020-01319-y>.
- Vinck M, Oostenveld R, van Wingerden M, Battaglia F, Pennartz CMA. An improved index of phase-synchronization for electrophysiological data in the presence of volume-conduction, noise and sample-size bias. *NeuroImage*. 2011;55(4):1548–1565. <https://doi.org/10.1016/j.neuroimage.2011.01.055>.
- Vissers ME, Ridderinkhof KR, Cohen MX, Slagter HA. Oscillatory mechanisms of response conflict elicited by color and motion direction: an individual differences approach. *J Cogn Neurosci*. 2018;30(4):468–481. [https://doi.org/10.1162/jocn\\_a\\_01222](https://doi.org/10.1162/jocn_a_01222).
- Wang Y, Damen TGE, Aarts H. An examination of the sequential trial effect on experiences of agency in the Simon task. *Conscious Cogn*. 2018;66:17–25. <https://doi.org/10.1016/j.concog.2018.10.005>.
- Watanabe H, Taga G. General to specific development of movement patterns and memory for contingency between actions and events in young infants. *Infant Behav Dev*. 2006;29(3):402–422. <https://doi.org/10.1016/j.infbeh.2006.02.001>.
- Watanabe H, Taga G. Initial-state dependency of learning in young infants. *Hum Mov Sci*. 2011;30(1):125–142. <https://doi.org/10.1016/j.humov.2010.07.003>.
- Wen W, Haggard P. Control changes the way we look at the world. *J Cogn Neurosci*. 2018;30(4):603–619. [https://doi.org/10.1162/jocn\\_a\\_01226](https://doi.org/10.1162/jocn_a_01226).
- Wen W, Haggard P. Prediction error and regularity detection underlie two dissociable mechanisms for computing the sense of agency. *Cognition*. 2020;195:104074. <https://doi.org/10.1016/j.cognition.2019.104074>.
- Wen W, Imamizu H. The sense of agency in perception, behaviour and human–machine interactions. *Nat Rev Psychol*. 2022;1(4):211–222. <https://doi.org/10.1038/s44159-022-00030-6>.
- Wessel JR. Prepotent motor activity and inhibitory control demands in different variants of the go/no-go paradigm. *Psychophysiology*. 2018;55(3):e12871. <https://doi.org/10.1111/psyp.12871>.
- Wessel JR, Aron AR. It's not too late: the onset of the fronto-central P3 indexes successful response inhibition in the stop-signal paradigm. *Psychophysiology*. 2015;52(4):472–480. <https://doi.org/10.1111/psyp.12374>.
- Zhang D, Ding H, Wang X, Qi C, Luo Y. Enhanced response inhibition in experienced fencers. *Sci Rep*. 2015;5(1):16282. <https://doi.org/10.1038/srep16282>.
- Zhang L, Li Z, Zhang F, Gu R, Peng W, Hu L. Demystifying signal processing techniques to extract task-related EEG responses for psychologists. *Brain Sci Adv*. 2020;6(3):171–188. <https://doi.org/10.26599/BSA.2020.9050018>.

## Supplementary Materials

**Supplementary Table 1.** Trial number ( $M \pm SD$ ) for each EEG analysis.

	<b>Outcome Absent</b>		<b>Outcome Present</b>	
	<b>Low</b>	<b>High</b>	<b>Low</b>	<b>High</b>
	<b>Prediction Error</b>	<b>Prediction Error</b>	<b>Prediction Error</b>	<b>Prediction Error</b>
<b><i>Positive Outcome</i></b>				
N2 and P3	109.85 $\pm$ 16.24	40.30 $\pm$ 4.63	94.11 $\pm$ 23.61	28.41 $\pm$ 9.07
Theta Power and Synchronization	108.30 $\pm$ 16.74	39.70 $\pm$ 4.86	92.74 $\pm$ 23.16	28.07 $\pm$ 8.89
<b><i>Negative Outcome</i></b>				
N2 and P3	85.30 $\pm$ 35.80	50.59 $\pm$ 30.72	92.07 $\pm$ 27.07	30.11 $\pm$ 9.66
Theta Power and Synchronization	101.44 $\pm$ 21.87	36.48 $\pm$ 6.73	88.89 $\pm$ 27.92	27.78 $\pm$ 8.65



**Supplementary Figure 1.** Feedback-related negativity (FRN) time-locked to the keypress responses in inducement trials. FRN amplitude was quantified based on difference waveforms between outcome-present and outcome-absent conditions. High compared to low prediction error resulted in larger FRN amplitudes. The electrode and time window used to extract FRN amplitudes are marked using black dots and gray rectangles, respectively.

## **Supplementary Analysis and Results**

### **1 Midfrontal theta power during the baseline before the No-Go signal**

To exclude the possibility that any differences during the baseline might have affected our results in the midfrontal theta power and synchronization evoked by the No-Go signal, we compared the midfrontal theta power during the baseline (frequencies: 4–7 Hz; electrodes: FCz, FC1, and FC2; time window: -300 – -100 ms) across conditions.

Baseline midfrontal theta power were compared across conditions using a mixed-design three-way ANOVA with two within-subjects factors (Outcome Presence and Prediction Error) and one between-subjects factor (Task). The analysis showed that none of the main effects of Outcome Presence or Prediction Error, nor any of the three-way/two-way interactions, were significant (all  $ps > .05$ ).

These results indicate that the midfrontal theta power during the baseline was comparable across conditions. Therefore, it is unlikely that the effects observed in the midfrontal theta power and synchronization were driven by differences in baseline.



### **3 General Discussion**

The present thesis includes five studies that investigated behavioral and electrophysiological mechanisms regarding (i) the impacts of cardiac signals on visual perception (Study I and Study II) and action regulation (Study III), and (ii) the impacts of the sense of agency on action regulation (Study IV and Study V). All studies underwent rigorous peer review, enhancing the research quality of this thesis. Study II is currently under review in an international peer-reviewed journal. In the following sections, I summarize the findings of these studies, discuss their contributions to the current framework, and point out potential future directions.

#### **3.1 How Do Cardiac Signals Influence Visual Perception?**

Study I found that the co-occurrence of visual information and cardiac signals makes it harder to detect the visual target among multiple visual distractors, as reflected by a slower visual search. This finding is consistent with prior evidence highlighting the inhibitory impact of systolic cardiac activity on the perception of weak and neutral external stimuli (e.g., Al et al., 2020; Al, Iliopoulos, et al., 2021; Grund et al., 2022; Motyka et al., 2019). Previous studies usually presented the target sensory stimuli at different cardiac phases (e.g., McIntyre et al., 2007; Sandman et al., 1977; Walker & Sandman, 1982), leading to results that imply a suppression effect of cardiac signals on goal-directed sensory processing. In contrast, Study I engaged participants in identifying the orientation of a target line, with a task-irrelevant attribute of the target (i.e., color change) synchronized with cardiac signals. Thus, our findings extend earlier reports, demonstrating that even visual information lacking direct relevance to the task at hand is suppressed by cardiac processing.

Moreover, Study I reveals the electrophysiological mechanisms underlying the multisensory integration of cardiac and visual processes. The concurrent processing of visual inputs and cardiac signals initially leads to a downregulation in early ERP amplitude and beta power. Then, it results in suppressing lateralized N2pc amplitude and lateralized beta power. As discussed in Study I, these findings might be explained using the attentional trade-off mechanism between exteroception and interoception (Al

et al., 2020; Kritzman et al., 2022; Marshall, Gentsch, Schröder, et al., 2018). That is, attentional and representational resources are limited and are shared between exteroceptive and interoceptive processing. During systole, strong cardiac signals are conveyed from the body to the brain, consequently utilizing a portion of the processing resources. As a result, fewer resources were available to process external signals.

Study II offers a more direct lens into the modulation of attentional resources across the cardiac cycle. Results in SSVEP responses suggest that participants directed reduced attention towards visual stimuli whose task-irrelevant attribute (i.e., direction change) consistently coincides with strong cardiac signals, and they paid more attention to the visual stimuli that consistently coincided with weak cardiac signals, compared with concurrently presented visual stimuli that shared the same spatial location but lacked synchronization with heartbeats. These findings indicate that the brain automatically allocates different levels of attention to diverse visual information upon synchronization with cardiac signals. Another important observation is that participants exhibited heightened brain responses to internal cardiac signals (reflected by a larger HEP amplitude) and diminished brain responses to the external visual target (reflected by a smaller visual N2 amplitude) when visual stimuli were synchronized with strong cardiac signals. These findings propose an automatic shift of attention from the external to the internal environment in the presence of cardiac signals.

Moreover, our findings from both Study I and Study II can find a coherent explanation within the larger framework of interoceptive predictive coding. This theoretical model posits that the brain can predict periodic bodily activities, such as heartbeats and the associated physiological fluctuations, and thus can downregulate their processing (Allen et al., 2022; Barrett & Simmons, 2015; Critchley & Garfinkel, 2018). This serves the dual purpose of preventing misinterpretation of these internal signals as external inputs and conserving limited cognitive resources (Al et al., 2020; Marshall, Gentsch, Schröder, et al., 2018). In Study I, the observed diminished visual search performance and decreased multisensory brain responses during systole can be attributed to visual information coinciding with cardiac signals being misinterpreted as "internal noise" associated with heartbeats. Consequently, these inputs receive a decreased allocation of attentional and representational resources. This interpretation can also be applied to

Study II, where varying levels of selective attention were allocated to visual stimuli coupled with different strengths of cardiac signals. In Study II, the shift of attention from the external to the internal in the condition with repeated coincidence between visual inputs and cardiac signals can be attributed to the stronger-than-expected "cardiac signals". The perceived "cardiac signals" might comprise both genuine cardiac signals and misinterpreted signals from external sources, leading to a discrepancy or prediction error between the anticipated and perceived "cardiac signals" and thus attracting a heightened level of attentional and representational resources.

Taken together, Study I and Study II provide valuable insights into the interplay between internal cardiac signals and external visual inputs, and support the attentional trade-off mechanism between exteroception and interoception and the interoceptive predictive coding framework.

### **3.2 How Do Cardiac Signals Influence Action Regulation?**

In Study III, we observed (i) disrupted response inhibition (reflected by prolonged stop-signal reaction time and reduced stop-signal P3 amplitude) and (ii) elevated cardiac processing (reflected by increased HEP amplitude) when the stop signal was presented during systole, compared to when it was presented randomly within the cardiac cycle in a stop-signal task. These findings suggest that the co-occurrence of an action-relevant external cue and cardiac signals makes it harder to cancel prepotent motor behavior.

As discussed in Study III, this phenomenon could also be explained using the attentional trade-off mechanism between exteroception and interoception (Al et al., 2020; Kritzman et al., 2022; Marshall, Gentsch, Schröder, et al., 2018). Specifically, participants might redirect their attention from the external to the internal environment in the presence of cardiac signals during systole. This reallocation of attention results in enhanced cardiac processing. In contrast, the available resources for sensorimotor responses to external visual cues are reduced. We think the disruption in response inhibition could be attributed to both inhibited perceptual processes of the visual cue and heightened action readiness. As mentioned above, the perceptual attenuation effect at systole has been well documented (e.g., Grund et al., 2022; McIntyre et al., 2007;

Motyka et al., 2019). Hence, systolic cardiac signals might reduce the perceptual processing of the visual cue that signifies action cancellation. In addition, recent research has indicated augmented motor excitability during systole (Al, Stephani, et al., 2021; Galvez-Pol et al., 2020). This finding implies that the impaired response inhibition observed during systole might not necessarily reflect a deficiency in inhibitory control ability itself, but rather could be attributed to an elevated state of action readiness.

Taken together, Study III reveals the influence of cardiac signals on response inhibition and supports the attentional trade-off mechanism between exteroception and interoception.

### **3.3 How Does Sense of Agency Influence Action Regulation?**

Study IV demonstrated that the immediate increase in the sense of agency, induced by the presence of action outcomes following a preceding action, enhanced the readiness for performing the same action. This was evident through faster and more accurate "go" responses, as well as faster and more frequent "voluntary go" responses in a modified go/no-go task. Additionally, the increased sense of agency over a preceding action made it harder to inhibit the same action, as reflected by more failures in "no-go" responses. These findings were replicated in Study V. Importantly, in both studies, these effects were observed without participants explicitly evaluating their sense of agency or the relevance of action outcomes to their task goal of achieving faster and more accurate responses. This indicates that the sense of agency primarily influences subsequent action regulation at an implicit or unconscious level.

Study IV also unveiled that the effects of outcome presence on subsequent action regulation were magnified by a longer-lasting enhancement of the sense of agency caused by a high likelihood of producing outcomes in prior actions. In contrast, despite employing similar experimental paradigms, Study V adopted an alternative viewpoint and demonstrated that the effects of outcome presence on subsequent action regulation were amplified by the discrepancy or prediction error between the predicted and actual action outcomes. Given that the appearance of action outcomes, a high probability of

producing action outcomes, and a low prediction error between expected and actual action outcomes all contribute to a stronger sense of agency (Gentsch & Schütz-Bosbach, 2015; Hemed et al., 2020; Penton et al., 2018), these findings suggest that experiencing a stronger sense of agency over an action makes it easier to repeat this action while at the same time making it harder to inhibit the same action.

Furthermore, both studies discovered that the emotional valence of the action outcome (i.e., positive or negative) had no impact on subsequent action regulation. As discussed in Study IV and Study V, this finding confirms that the observed effects on action regulation are not driven by the rewarding properties of the outcome *per se* but by the implicit monitoring of the effectiveness of the actions, i.e., whether a specific action can make changes in the environment. When an action fails to yield any perceivable effects, it signifies inefficacy and a waste of energy. Conversely, when an action can produce perceivable effects, it conveys information about our current progress toward our goal and helps regulate our behavior toward achieving that goal. Therefore, we are more motivated to perform such actions. This can prevent us from wasting limited resources on ineffective motor behavior.

With EEG, Study V further revealed the electrophysiological mechanisms that underlie the impact of the sense of agency on response inhibition. Specifically, the enhanced inhibitory tendencies after experiencing a low sense of agency over an action were accompanied by reduced N2 and P3 amplitudes, reduced midfrontal theta power, and reduced theta synchronization between midfrontal and medial-to-parietal areas. These findings indicate that less top-down control is required for successfully canceling an action linked to a reduced sense of agency.

Taken together, Study IV and Study V provide compelling evidence regarding the facilitatory effect of the sense of agency on subsequent action readiness and its inhibitory effect on subsequent response inhibition, and shed new light on how the automatic evaluation of action effectiveness dynamically shapes our ability to regulate motor actions flexibly.

### **3.4 General Conclusions**

The present thesis provides empirical evidence demonstrating that fluctuations in internal bodily signals, i.e., interoceptive signals, influence how we perceive and react to information from the outside world. This finding indicates a profound link between visceral signals and brain dynamics, highlighting the strong connection between the body and the mind. The traditional view of cognition often treats the mind and body as separate entities. The more recent theories of "embodied cognition" challenge this perspective, proposing that the mind is not just a product of the neural activity in the brain but is also shaped by the interactions between the body and the environment (Clark, 1999; Wilson & Golonka, 2013). However, these theories have mainly emphasized the importance of motor actions in shaping cognitive processes while often overlooking the short-lived nature of motor signals, which are only present when an action is planned or executed. In contrast, interoceptive signals continuously ascend from the body to the brain, albeit with fluctuations in intensity. The constant presence of interoception provides the format needed for sustained information processing and stable self-awareness. Therefore, interoceptive processing may play a fundamental role in "embodied cognition".

### **3.5 Limitations and Future Directions**

There are three research directions that would be of high interest for future investigation.

Firstly, it would be interesting to investigate the specific brain regions that play a role in the spontaneous reallocation of attention between interoception and exteroception. The present thesis employed EEG to explore the temporal dynamics of interoceptive and exteroceptive processing across the cardiac cycle, while the brain areas involved in these processes remain largely uncharted. Anatomofunctional studies in animals have revealed that interoceptive signals are relayed to diverse subcortical areas, including the hypothalamus, cerebellum, amygdala, and striatum, as well as various cortical areas, including the primary and secondary somatosensory cortices, insula, ventromedial prefrontal cortex, and cingulate motor regions (as reviewed by Azzalini et al., 2019). Furthermore, fMRI studies in humans have found distinct brain activations and

connectivity patterns when participants actively attend to external visual information versus paying attention to internal respiratory signals (Farb et al., 2013; Wang et al., 2019). Notably, the pivotal role of the insula in interoceptive attention towards inspiration has been highlighted by the studies of Farb et al. (2013) and Wang et al. (2019). Nonetheless, whether similar brain networks contribute to the spontaneous shifts of attention across the cardiac cycle is an open question.

Secondly, it would be worthwhile to investigate the effect of alternative forms of interoceptive signals on perception and action. The present thesis focuses on the effects of cardiac signals only. However, it should be noted that beyond cardiac signals, the brain constantly receives interoceptive information from various organs, including the lungs, stomach, intestines, bladder, and so on (Chen et al., 2021). Recent studies have uncovered the modulation effects of respiration on the detection of near-threshold visual (Kluger et al., 2021) and somatosensory stimuli (Grund et al., 2022), as well as on voluntary action initiation (Park et al., 2020). Future studies could further investigate the effects of respiration on the perception of suprathreshold sensory stimuli and its effect on action regulation. Concerning stomach activity, researchers have discovered a resting-state cortical network that is in sync with the gastric rhythm, a 0.05-Hz oscillation that coordinates stomach contractions that are important for digestion (Rebollo et al., 2018). More importantly, this gastric resting-state network has been found to cover all sensory and motor cortices and some transmodal regions associated with higher-order cognitive processes (Rebollo & Tallon-Baudry, 2022). These findings underscore the potential impact of brain-stomach interactions on perception, action, and cognition (Rebollo et al., 2021).

Last but not least, delving into the intricate interplay between interoception, action, and agency would also be interesting. In the present thesis, the effects of interoception on action and the effects of agency on action were investigated separately. Theoretical models such as the interoceptive predictive coding framework propose that interoceptive states, motor behavior, and agentic experience are strongly interconnected (Marshall, Gentsch, & Schütz-Bosbach, 2018; Seth et al., 2012). Preliminary empirical evidence supports the hypothesis that interoception contributes to the emergence and modulation of the sense of agency. For example, there was a positive correlation

between participants' interoceptive accuracy and the implicit measure of sense of agency; moreover, the participants with higher interoceptive accuracy demonstrated increased sense of agency during cardiac systole compared to diastole (Koreki et al., 2022). Additionally, the role of interoceptive awareness has long been recognized in the literature on action control (as reviewed by Ullsperger et al., 2010). Therefore, fluctuations in interoceptive states may serve as potential mediators of the impact of the sense of agency on subsequent action regulation, warranting in-depth investigation.

## References (General Introduction and General Discussion)

- Al, E., Iliopoulos, F., Forschack, N., Nierhaus, T., Grund, M., Motyka, P., Gaebler, M., Nikulin, V. V., & Villringer, A. (2020). Heart–brain interactions shape somatosensory perception and evoked potentials. *Proceedings of the National Academy of Sciences*, *117*(19), 10575–10584. <https://doi.org/10.1073/pnas.1915629117>
- Al, E., Iliopoulos, F., Nikulin, V. V., & Villringer, A. (2021). Heartbeat and somatosensory perception. *NeuroImage*, *238*, 118247. <https://doi.org/10.1016/j.neuroimage.2021.118247>
- Al, E., Stephani, T., Engelhardt, M., Villringer, A., & Nikulin, V. V. (2021). Cardiac activity impacts cortical motor excitability. *Research Square* [Preprint]. <https://doi.org/10.21203/rs.3.rs-1023617/v1>.
- Allen, M., Levy, A., Parr, T., & Friston, K. J. (2022). In the body’s eye: The computational anatomy of interoceptive inference. *PLOS Computational Biology*, *18*(9), e1010490. <https://doi.org/10.1371/journal.pcbi.1010490>
- Azzalini, D., Rebollo, I., & Tallon-Baudry, C. (2019). Visceral signals shape brain dynamics and cognition. *Trends in Cognitive Sciences*, *23*(6), 488–509. <https://doi.org/10.1016/j.tics.2019.03.007>
- Babo-Rebelo, M., Richter, C. G., & Tallon-Baudry, C. (2016). Neural responses to heartbeats in the default network encode the self in spontaneous thoughts. *Journal of Neuroscience*, *36*(30), 7829–7840. <https://doi.org/10.1523/JNEUROSCI.0262-16.2016>
- Barrett, L. F., & Simmons, W. K. (2015). Interoceptive predictions in the brain. *Nature Reviews Neuroscience*, *16*(7), 419–429. <https://doi.org/10.1038/nrn3950>
- Chen, W. G., Schloesser, D., Arensdorf, A. M., Simmons, J. M., Cui, C., Valentino, R., Gnadt, J. W., Nielsen, L., Hillaire-Clarke, C. St., Spruance, V., Horowitz, T. S., Vallejo, Y. F., & Langevin, H. M. (2021). The emerging science of interoception:

- Sensing, integrating, interpreting, and regulating signals within the self. *Trends in Neurosciences*, 44(1), 3–16. <https://doi.org/10.1016/j.tins.2020.10.007>
- Chen, X., Holland, P., & Galea, J. M. (2018). The effects of reward and punishment on motor skill learning. *Current Opinion in Behavioral Sciences*, 20, 83–88. <https://doi.org/10.1016/j.cobeha.2017.11.011>
- Clark, A. (1999). An embodied cognitive science? *Trends in Cognitive Sciences*, 3(9), 345–351. [https://doi.org/10.1016/S1364-6613\(99\)01361-3](https://doi.org/10.1016/S1364-6613(99)01361-3)
- Clark, A. (2013). Whatever next? Predictive brains, situated agents, and the future of cognitive science. *Behavioral and Brain Sciences*, 36(3), 181–204. <https://doi.org/10.1017/S0140525X12000477>
- Coll, M.-P., Hobson, H., Bird, G., & Murphy, J. (2021). Systematic review and meta-analysis of the relationship between the heartbeat-evoked potential and interoception. *Neuroscience & Biobehavioral Reviews*, 122, 190–200. <https://doi.org/10.1016/j.neubiorev.2020.12.012>
- Critchley, H. D., & Garfinkel, S. N. (2018). The influence of physiological signals on cognition. *Current Opinion in Behavioral Sciences*, 19, 13–18. <https://doi.org/10.1016/j.cobeha.2017.08.014>
- DeSaix, P., Betts, Gordon J., Johnson, Eddie, Johnson, Jody E., Oksana, Korol, Kruse, Dean H., Poe, Brandon, Wise, James A., & Young, Kelly A. (2013). *Anatomy & Physiology*. openStax.
- Eitam, B., Kennedy, P. M., & Tory Higgins, E. (2013). Motivation from control. *Experimental Brain Research*, 229(3), 475–484. <https://doi.org/10.1007/s00221-012-3370-7>
- Elliott, R., & Graf, V. (1972). Visual sensitivity as a function of phase of cardiac cycle. *Psychophysiology*, 9(3), 357–361. <https://doi.org/10.1111/j.1469-8986.1972.tb03219.x>

- Farb, N. A. S., Segal, Z. V., & Anderson, A. K. (2013). Attentional modulation of primary interoceptive and exteroceptive cortices. *Cerebral Cortex*, *23*(1), 114–126. <https://doi.org/10.1093/cercor/bhr385>
- Fittipaldi, S., Abrevaya, S., Fuente, A. de la, Pascariello, G. O., Hesse, E., Birba, A., Salamone, P., Hildebrandt, M., Martí, S. A., Pautassi, R. M., Huepe, D., Martorell, M. M., Yoris, A., Roca, M., García, A. M., Sedeño, L., & Ibáñez, A. (2020). A multidimensional and multi-feature framework for cardiac interoception. *NeuroImage*, *212*, 116677. <https://doi.org/10.1016/j.neuroimage.2020.116677>
- Fox, M. D., & Raichle, M. E. (2007). Spontaneous fluctuations in brain activity observed with functional magnetic resonance imaging. *Nature Reviews Neuroscience*, *8*(9), 700–711. <https://doi.org/10.1038/nrn2201>
- Friston, K. (2009). The free-energy principle: A rough guide to the brain? *Trends in Cognitive Sciences*, *13*(7), 293–301. <https://doi.org/10.1016/j.tics.2009.04.005>
- Friston, K. (2010). The free-energy principle: A unified brain theory? *Nature Reviews Neuroscience*, *11*(2), 127–138. <https://doi.org/10.1038/nrn2787>
- Friston, K. (2012). Prediction, perception and agency. *International Journal of Psychophysiology*, *83*(2), 248–252. <https://doi.org/10.1016/j.ijpsycho.2011.11.014>
- Galvez-Pol, A., McConnell, R., & Kilner, J. M. (2020). Active sampling in visual search is coupled to the cardiac cycle. *Cognition*, *196*, 104149. <https://doi.org/10.1016/j.cognition.2019.104149>
- Garfinkel, S. N. (2016). Threat and the body: How the heart supports fear processing. *Trends in Cognitive Sciences*, *20*(1), 34–46. <https://doi.org/10.1016/j.tics.2015.10.005>
- Garfinkel, S. N., Minati, L., Gray, M. A., Seth, A. K., Dolan, R. J., & Critchley, H. D. (2014). Fear from the heart: Sensitivity to fear stimuli depends on individual

- heartbeats. *Journal of Neuroscience*, 34(19), 6573–6582.  
<https://doi.org/10.1523/JNEUROSCI.3507-13.2014>
- Gentsch, A., & Schütz-Bosbach, S. (2015). Agency and outcome prediction. In P. Haggard & B. Eitam (Eds.), *The Sense of Agency* (pp. 217–231). Oxford University Press. <https://doi.org/10.1093/acprof:oso/9780190267278.003.0009>
- Gray, M. A., Taggart, P., Sutton, P. M., Groves, D., Holdright, D. R., Bradbury, D., Brull, D., & Critchley, H. D. (2007). A cortical potential reflecting cardiac function. *Proceedings of the National Academy of Sciences*, 104(16), 6818–6823.  
<https://doi.org/10.1073/pnas.0609509104>
- Grund, M., Al, E., Pabst, M., Dabbagh, A., Stephani, T., Nierhaus, T., Gaebler, M., & Villringer, A. (2022). Respiration, heartbeat, and conscious tactile perception. *Journal of Neuroscience*, 42(4), 643–656.  
<https://doi.org/10.1523/JNEUROSCI.0592-21.2021>
- Haggard, P. (2017). Sense of agency in the human brain. *Nature Reviews Neuroscience*, 18, 196–207. <https://doi.org/10.1038/nrn.2017.14>
- Haggard, P., & Eitam, B. (Eds.). (2015). *The Sense of Agency*. Oxford University Press.
- Hemed, E., Bakbani-Elkayam, S., Teodorescu, A. R., Yona, L., & Eitam, B. (2020). Evaluation of an action's effectiveness by the motor system in a dynamic environment. *Journal of Experimental Psychology: General*, 149(5), 935–948.  
<https://doi.org/10.1037/xge0000692>
- Herman, A. M., & Tsakiris, M. (2020). Feeling in control: The role of cardiac timing in the sense of agency. *Affective Science*, 1(3), 155–171.  
<https://doi.org/10.1007/s42761-020-00013-x>
- Kaiser, J., Buciuman, M., Gigl, S., Gentsch, A., & Schütz-Bosbach, S. (2021). The interplay between affective processing and sense of agency during action regulation: A review. *Frontiers in Psychology*, 12, 716220.  
<https://doi.org/10.3389/fpsyg.2021.716220>

- Karsh, N., & Eitam, B. (2015). I control therefore I do: Judgments of agency influence action selection. *Cognition*, *138*, 122–131. <https://doi.org/10.1016/j.cognition.2015.02.002>
- Karsh, N., Hemed, E., Nafcha, O., Elkayam, S. B., Custers, R., & Eitam, B. (2020). The differential impact of a response's effectiveness and its monetary value on response-selection. *Scientific Reports*, *10*(1), 3405. <https://doi.org/10.1038/s41598-020-60385-9>
- Kern, M., Aertsen, A., Schulze-Bonhage, A., & Ball, T. (2013). Heart cycle-related effects on event-related potentials, spectral power changes, and connectivity patterns in the human ECoG. *NeuroImage*, *81*, 178–190. <https://doi.org/10.1016/j.neuroimage.2013.05.042>
- Khalsa, S. S., Adolphs, R., Cameron, O. G., Critchley, H. D., Davenport, P. W., Feinstein, J. S., Feusner, J. D., Garfinkel, S. N., Lane, R. D., Mehling, W. E., Meuret, A. E., Nemeroff, C. B., Oppenheimer, S., Petzschner, F. H., Pollatos, O., Rhudy, J. L., Schramm, L. P., Simmons, W. K., Stein, M. B., ... Zucker, N. (2018). Interoception and mental health: A roadmap. *Biological Psychiatry: Cognitive Neuroscience and Neuroimaging*, *3*(6), 501–513. <https://doi.org/10.1016/j.bpsc.2017.12.004>
- Kim, C.-S., Ober, S. L., McMurtry, M. S., Finegan, B. A., Inan, O. T., Mukkamala, R., & Hahn, J.-O. (2016). Ballistocardiogram: Mechanism and potential for unobtrusive cardiovascular health monitoring. *Scientific Reports*, *6*(1), 31297. <https://doi.org/10.1038/srep31297>
- Kluger, D. S., Balestrieri, E., Busch, N. A., & Gross, J. (2021). Respiration aligns perception with neural excitability. *ELife*, *10*, e70907. <https://doi.org/10.7554/eLife.70907>
- Konttinen, N., Mets, T., Lyytinen, H., & Paananen, M. (2003). Timing of triggering in relation to the cardiac cycle in nonelite rifle shooters. *Research Quarterly for*

*Exercise and Sport*, 74(4), 395–400.  
<https://doi.org/10.1080/02701367.2003.10609110>

Koreki, A., Goeta, D., Ricciardi, L., Eilon, T., Chen, J., Critchley, H. D., Garfinkel, S. N., Edwards, M., & Yogarajah, M. (2022). The relationship between interoception and agency and its modulation by heartbeats: An exploratory study. *Scientific Reports*, 12(1), 13624. <https://doi.org/10.1038/s41598-022-16569-6>

Kritzman, L., Eidelman-Rothman, M., Keil, A., Freche, D., Sheppes, G., & Levit-Binnun, N. (2022). Steady-state visual evoked potentials differentiate between internally and externally directed attention. *NeuroImage*, 254, 119133. <https://doi.org/10.1016/j.neuroimage.2022.119133>

Kunzendorf, S., Klotzsche, F., Akbal, M., Villringer, A., Ohl, S., & Gaebler, M. (2019). Active information sampling varies across the cardiac cycle. *Psychophysiology*, 56(5), e13322. <https://doi.org/10.1111/psyp.13322>

Leganes-Fonteneau, M., Buckman, J. F., Suzuki, K., Pawlak, A., & Bates, M. E. (2021). More than meets the heart: Systolic amplification of different emotional faces is task dependent. *Cognition and Emotion*, 35(2), 400–408. <https://doi.org/10.1080/02699931.2020.1832050>

Lewthwaite, R., Chiviawosky, S., Drews, R., & Wulf, G. (2015). Choose to move: The motivational impact of autonomy support on motor learning. *Psychonomic Bulletin & Review*, 22(5), 1383–1388. <https://doi.org/10.3758/s13423-015-0814-7>

Maier, S. F., & Seligman, M. E. P. (2016). Learned helplessness at fifty: Insights from neuroscience. *Psychological Review*, 123(4), 349–367. <https://doi.org/10.1037/rev0000033>

Makowski, D., Sperduti, M., Blondé, P., Nicolas, S., & Piolino, P. (2020). The heart of cognitive control: Cardiac phase modulates processing speed and inhibition. *Psychophysiology*, 57(3), e13490. <https://doi.org/10.1111/psyp.13490>

- Marshall, A. C., Gentsch, A., Blum, A.-L., Broering, C., & Schütz-Bosbach, S. (2019). I feel what I do: Relating interoceptive processes and reward-related behavior. *NeuroImage*, *191*, 315–324. <https://doi.org/10.1016/j.neuroimage.2019.02.032>
- Marshall, A. C., Gentsch, A., Jelinčić, V., & Schütz-Bosbach, S. (2017). Exteroceptive expectations modulate interoceptive processing: Repetition-suppression effects for visual and heartbeat evoked potentials. *Scientific Reports*, *7*(1), 16525. <https://doi.org/10.1038/s41598-017-16595-9>
- Marshall, A. C., Gentsch, A., Schröder, L., & Schütz-Bosbach, S. (2018). Cardiac interoceptive learning is modulated by emotional valence perceived from facial expressions. *Social Cognitive and Affective Neuroscience*, *13*(7), 677–686. <https://doi.org/10.1093/scan/nsy042>
- Marshall, A. C., Gentsch, A., & Schütz-Bosbach, S. (2018). The interaction between interoceptive and action states within a framework of predictive coding. *Frontiers in Psychology*, *9*, 180. <https://doi.org/10.3389/fpsyg.2018.00180>
- Marshall, A. C., Gentsch, A., & Schütz-Bosbach, S. (2020). Interoceptive cardiac expectations to emotional stimuli predict visual perception. *Emotion*, *20*(7), 1113–1126. <https://doi.org/10.1037/emo0000631>
- Marshall, A. C., Gentsch-Ebrahimzadeh, A., & Schütz-Bosbach, S. (2022). From the inside out: Interoceptive feedback facilitates the integration of visceral signals for efficient sensory processing. *NeuroImage*, *251*, 119011. <https://doi.org/10.1016/j.neuroimage.2022.119011>
- Matsumiya, K. (2021). Awareness of voluntary action, rather than body ownership, improves motor control. *Scientific Reports*, *11*(1), 418. <https://doi.org/10.1038/s41598-020-79910-x>
- McIntyre, D., Ring, C., Hamer, M., & Carroll, D. (2007). Effects of arterial and cardiopulmonary baroreceptor activation on simple and choice reaction times. *Psychophysiology*, *44*(6), 874–879. <https://doi.org/10.1111/j.1469-8986.2007.00547.x>

- Motyka, P., Grund, M., Forschack, N., Al, E., Villringer, A., & Gaebler, M. (2019). Interactions between cardiac activity and conscious somatosensory perception. *Psychophysiology*, *56*(10), e13424. <https://doi.org/10.1111/psyp.13424>
- Ohl, S., Wohltat, C., Kliegl, R., Pollatos, O., & Engbert, R. (2016). Microsaccades are coupled to heartbeat. *Journal of Neuroscience*, *36*(4), 1237–1241. <https://doi.org/10.1523/JNEUROSCI.2211-15.2016>
- Palser, E. R., Glass, J., Fotopoulou, A., & Kilner, J. M. (2021). Relationship between cardiac cycle and the timing of actions during action execution and observation. *Cognition*, *217*, 104907. <https://doi.org/10.1016/j.cognition.2021.104907>
- Park, H.-D., Barnoud, C., Trang, H., Kannape, O. A., Schaller, K., & Blanke, O. (2020). Breathing is coupled with voluntary action and the cortical readiness potential. *Nature Communications*, *11*(1), 289. <https://doi.org/10.1038/s41467-019-13967-9>
- Park, H.-D., Bernasconi, F., Bello-Ruiz, J., Pfeiffer, C., Salomon, R., & Blanke, O. (2016). Transient modulations of neural responses to heartbeats covary with bodily self-consciousness. *Journal of Neuroscience*, *36*(32), 8453–8460. <https://doi.org/10.1523/JNEUROSCI.0311-16.2016>
- Park, H.-D., Bernasconi, F., Salomon, R., Tallon-Baudry, C., Spinelli, L., Seeck, M., Schaller, K., & Blanke, O. (2018). Neural sources and underlying mechanisms of neural responses to heartbeats, and their role in bodily self-consciousness: An intracranial EEG study. *Cerebral Cortex*, *28*(7), 2351–2364. <https://doi.org/10.1093/cercor/bhx136>
- Park, H.-D., & Blanke, O. (2019). Heartbeat-evoked cortical responses: Underlying mechanisms, functional roles, and methodological considerations. *NeuroImage*, *197*, 502–511. <https://doi.org/10.1016/j.neuroimage.2019.04.081>
- Park, H.-D., Correia, S., Ducorps, A., & Tallon-Baudry, C. (2014). Spontaneous fluctuations in neural responses to heartbeats predict visual detection. *Nature Neuroscience*, *17*(4), 612–618. <https://doi.org/10.1038/nn.3671>

- Park, H.-D., & Tallon-Baudry, C. (2014). The neural subjective frame: From bodily signals to perceptual consciousness. *Philosophical Transactions of the Royal Society B: Biological Sciences*, 369(1641), 20130208. <https://doi.org/10.1098/rstb.2013.0208>
- Parvizi, J., & Kastner, S. (2018). Promises and limitations of human intracranial electroencephalography. *Nature Neuroscience*, 21(4), 474–483. <https://doi.org/10.1038/s41593-018-0108-2>
- Penton, T., Wang, X., Coll, M.-P., Catmur, C., & Bird, G. (2018). The influence of action–outcome contingency on motivation from control. *Experimental Brain Research*, 236(12), 3239–3249. <https://doi.org/10.1007/s00221-018-5374-4>
- Petzschner, F. H., Weber, L. A., Wellstein, K. V., Paolini, G., Do, C. T., & Stephan, K. E. (2019). Focus of attention modulates the heartbeat evoked potential. *NeuroImage*, 186, 595–606. <https://doi.org/10.1016/j.neuroimage.2018.11.037>
- Pollatos, O., & Schandry, R. (2004). Accuracy of heartbeat perception is reflected in the amplitude of the heartbeat-evoked brain potential. *Psychophysiology*, 41(3), 476–482. <https://doi.org/10.1111/1469-8986.2004.00170.x>
- Pramme, L., Larra, M. F., Schächinger, H., & Frings, C. (2014). Cardiac cycle time effects on mask inhibition. *Biological Psychology*, 100, 115–121. <https://doi.org/10.1016/j.biopsycho.2014.05.008>
- Pramme, L., Larra, M. F., Schächinger, H., & Frings, C. (2016). Cardiac cycle time effects on selection efficiency in vision: Baroreceptor activity and visual attention. *Psychophysiology*, 53(11), 1702–1711. <https://doi.org/10.1111/psyp.12728>
- Quigley, K. S., Kanoski, S., Grill, W. M., Barrett, L. F., & Tsakiris, M. (2021). Functions of interoception: From energy regulation to experience of the self. *Trends in Neurosciences*, 44(1), 29–38. <https://doi.org/10.1016/j.tins.2020.09.008>

- Rae, C. L., Ahmad, A., Larsson, D. E. O., Silva, M., Praag, C. D. G. van, Garfinkel, S. N., & Critchley, H. D. (2020). Impact of cardiac interoception cues and confidence on voluntary decisions to make or withhold action in an intentional inhibition task. *Scientific Reports*, *10*(1), 4184. <https://doi.org/10.1038/s41598-020-60405-8>
- Rae, C. L., Botan, V. E., Gould van Praag, C. D., Herman, A. M., Nyysönen, J. A. K., Watson, D. R., Duka, T., Garfinkel, S. N., & Critchley, H. D. (2018). Response inhibition on the stop signal task improves during cardiac contraction. *Scientific Reports*, *8*(1), 9136. <https://doi.org/10.1038/s41598-018-27513-y>
- Raud, L., Westerhausen, R., Dooley, N., & Huster, R. J. (2020). Differences in unity: The go/no-go and stop signal tasks rely on different mechanisms. *NeuroImage*, *210*, 116582. <https://doi.org/10.1016/j.neuroimage.2020.116582>
- Rebollo, I., Devauchelle, A.-D., Béranger, B., & Tallon-Baudry, C. (2018). Stomach-brain synchrony reveals a novel, delayed-connectivity resting-state network in humans. *ELife*, *7*, e33321. <https://doi.org/10.7554/eLife.33321>
- Rebollo, I., & Tallon-Baudry, C. (2022). The sensory and motor components of the cortical hierarchy are coupled to the rhythm of the stomach during rest. *Journal of Neuroscience*, *42*(11), 2205–2220. <https://doi.org/10.1523/JNEUROSCI.1285-21.2021>
- Rebollo, I., Wolpert, N., & Tallon-Baudry, C. (2021). Brain–stomach coupling: Anatomy, functions, and future avenues of research. *Current Opinion in Biomedical Engineering*, *18*, 100270. <https://doi.org/10.1016/j.cobme.2021.100270>
- Rochat, P., & Striano, T. (1999). Emerging self-exploration by 2-month-old infants. *Developmental Science*, *2*(2), 206–218. <https://doi.org/10.1111/1467-7687.00069>
- Ronchi, R., Bernasconi, F., Pfeiffer, C., Bello-Ruiz, J., Kaliuzhna, M., & Blanke, O. (2017). Interoceptive signals impact visual processing: Cardiac modulation of

- visual body perception. *NeuroImage*, 158, 176–185.  
<https://doi.org/10.1016/j.neuroimage.2017.06.064>
- Salamone, P. C., Esteves, S., Sinay, V. J., García-Cordero, I., Abrevaya, S., Couto, B., Adolphi, F., Martorell, M., Petroni, A., Yoris, A., Torquati, K., Alifano, F., Legaz, A., Cassará, F. P., Bruno, D., Kemp, A. H., Herrera, E., García, A. M., Ibáñez, A., & Sedeño, L. (2018). Altered neural signatures of interoception in multiple sclerosis. *Human Brain Mapping*, 39(12), 4743–4754.  
<https://doi.org/10.1002/hbm.24319>
- Salomon, R., Ronchi, R., Dönnz, J., Bello-Ruiz, J., Herbelin, B., Faivre, N., Schaller, K., & Blanke, O. (2018). Insula mediates heartbeat related effects on visual consciousness. *Cortex*, 101, 87–95.  
<https://doi.org/10.1016/j.cortex.2018.01.005>
- Salomon, R., Ronchi, R., Dönnz, J., Bello-Ruiz, J., Herbelin, B., Martet, R., Faivre, N., Schaller, K., & Blanke, O. (2016). The insula mediates access to awareness of visual stimuli presented synchronously to the heartbeat. *Journal of Neuroscience*, 36(18), 5115–5127. <https://doi.org/10.1523/JNEUROSCI.4262-15.2016>
- Sandman, C. A., McCanne, T. R., Kaiser, D. N., & Diamond, B. (1977). Heart rate and cardiac phase influences on visual perception. *Journal of Comparative and Physiological Psychology*, 91(1), 189–202. <https://doi.org/10.1037/h0077302>
- Schandry, R., & Montoya, P. (1996). Event-related brain potentials and the processing of cardiac activity. *Biological Psychology*, 42(1), 75–85.  
[https://doi.org/10.1016/0301-0511\(95\)05147-3](https://doi.org/10.1016/0301-0511(95)05147-3)
- Schulz, A., Köster, S., Beutel, M. E., Schächinger, H., Vögele, C., Rost, S., Rauh, M., & Michal, M. (2015). Altered patterns of heartbeat-evoked potentials in depersonalization/derealization disorder: Neurophysiological evidence for impaired cortical representation of bodily signals. *Psychosomatic Medicine*, 77(5), 506–516. <https://doi.org/10.1097/PSY.0000000000000195>

- Seth, A. K., & Friston, K. J. (2016). Active interoceptive inference and the emotional brain. *Philosophical Transactions of the Royal Society B: Biological Sciences*, 371(1708), 20160007. <https://doi.org/10.1098/rstb.2016.0007>
- Seth, A. K., Suzuki, K., & Critchley, H. D. (2012). An interoceptive predictive coding model of conscious presence. *Frontiers in Psychology*, 2, 395. <https://doi.org/10.3389/fpsyg.2011.00395>
- Shao, S., Shen, K., Wilder-Smith, E. P. V., & Li, X. (2011). Effect of pain perception on the heartbeat evoked potential. *Clinical Neurophysiology*, 122(9), 1838–1845. <https://doi.org/10.1016/j.clinph.2011.02.014>
- Skora, L. I., Livermore, J. J. A., & Roelofs, K. (2022). The functional role of cardiac activity in perception and action. *Neuroscience & Biobehavioral Reviews*, 137, 104655. <https://doi.org/10.1016/j.neubiorev.2022.104655>
- Tallon-Baudry, C. (2023). Interoception: Probing internal state is inherent to perception and cognition. *Neuron*, 11(12), 1854–1857. <https://doi.org/10.1016/j.neuron.2023.04.019>
- Tanaka, T., Watanabe, K., & Tanaka, K. (2021). Immediate action effects motivate actions based on the stimulus–response relationship. *Experimental Brain Research*, 239(1), 67–78. <https://doi.org/10.1007/s00221-020-05955-z>
- Ullsperger, M., Harsay, H. A., Wessel, J. R., & Ridderinkhof, K. R. (2010). Conscious perception of errors and its relation to the anterior insula. *Brain Structure and Function*, 214(5–6), 629–643. <https://doi.org/10.1007/s00429-010-0261-1>
- van Elk, M., Lenggenhager, B., Heydrich, L., & Blanke, O. (2014). Suppression of the auditory N1-component for heartbeat-related sounds reflects interoceptive predictive coding. *Biological Psychology*, 99, 172–182. <https://doi.org/10.1016/j.biopsycho.2014.03.004>

- Walker, B. B., & Sandman, C. A. (1982). Visual evoked potentials change as heart rate and carotid pressure change. *Psychophysiology*, *19*(5), 520–527. <https://doi.org/10.1111/j.1469-8986.1982.tb02579.x>
- Wang, X., Wu, Q., Egan, L., Gu, X., Liu, P., Gu, H., Yang, Y., Luo, J., Wu, Y., Gao, Z., & Fan, J. (2019). Anterior insular cortex plays a critical role in interoceptive attention. *ELife*, *8*, e42265. <https://doi.org/10.7554/eLife.42265>
- Watanabe, H., & Taga, G. (2006). General to specific development of movement patterns and memory for contingency between actions and events in young infants. *Infant Behavior and Development*, *29*(3), 402–422. <https://doi.org/10.1016/j.infbeh.2006.02.001>
- Watanabe, H., & Taga, G. (2011). Initial-state dependency of learning in young infants. *Human Movement Science*, *30*(1), 125–142. <https://doi.org/10.1016/j.humov.2010.07.003>
- Wen, W., & Haggard, P. (2020). Prediction error and regularity detection underlie two dissociable mechanisms for computing the sense of agency. *Cognition*, *195*, 104074. <https://doi.org/10.1016/j.cognition.2019.104074>
- Wen, W., & Imamizu, H. (2022). The sense of agency in perception, behaviour and human–machine interactions. *Nature Reviews Psychology*, *1*(4), 211–222. <https://doi.org/10.1038/s44159-022-00030-6>
- Wen, W., Shibata, H., Ohata, R., Yamashita, A., Asama, H., & Imamizu, H. (2020). The active sensing of control difference. *IScience*, *23*(5), 101112. <https://doi.org/10.1016/j.isci.2020.101112>
- Wen, W., Yamashita, A., & Asama, H. (2017). Measurement of the perception of control during continuous movement using electroencephalography. *Frontiers in Human Neuroscience*, *11*, 392. <https://doi.org/10.3389/fnhum.2017.00392>
- Wilson, A., & Golonka, S. (2013). Embodied cognition is not what you think it is. *Frontiers in Psychology*, *4*, 58. <https://doi.org/10.3389/fpsyg.2013.00058>

Winston, J. S., & Rees, G. (2014). Following your heart. *Nature Neuroscience*, *17*(4), 482–483. <https://doi.org/10.1038/nn.3677>

Zadra, J. R., & Clore, G. L. (2011). Emotion and perception: The role of affective information. *WIREs Cognitive Science*, *2*(6), 676–685. <https://doi.org/10.1002/wcs.147>

## Summary

How we perceive and react to the environment is not fixed; instead, it changes dynamically. This variability can be attributed to various factors operating at conscious and subconscious levels. Interoception, the processing of internal bodily signals such as heartbeats, has been found to modulate perception and action. However, the findings are partly inconsistent, and the underlying neural mechanisms are largely unclear. Sense of agency, the feeling of control over our actions and their outcomes, has also been found to shape our actions. Nevertheless, whether and how changes in our sense of agency influence our capacity to regulate behavior flexibly are largely unknown. The present thesis investigates the effects of cardiac interoception and the sense of agency on visual perception and action regulation. It includes five studies with behavioral and electrophysiological data from healthy human participants.

### **The Influence of Cardiac Interoception on Visual Perception (Study I and Study II)**

In Study I, we investigated the perceptual effects and electrophysiological mechanisms of cardio-visual integration by coupling the color change of a visual target with participants' heartbeats in dynamically changing displays. Participants' task was to identify the orientation of the visual target. We found that (i) reaction times increased when the target change coincided with strong cardiac signals (during systole), compared to when the target change occurred at a time when cardiac signals were relatively weak (during diastole); (ii) the co-occurrence of the target change and cardiac signals modulated the ERP amplitude and the beta power in an early period (~100 ms after stimulus onset), and decreased the lateralized N2pc amplitude and the lateralized beta power in a later period (~200 ms after stimulus onset). Our results suggest that the multisensory integration of anticipated cardiac signals with a visual target negatively affects its detection among multiple visual stimuli, potentially by suppressing sensory processing and reducing attention toward the visual target.

In study II, we investigated the spontaneous shifts of attention between the internal and external environment across the cardiac cycle. Two groups of flickering dots moved continuously and changed direction dynamically within the same spatial location of the

screen. However, only the direction change of one group of dots was coupled with participants' heartbeats. Participants' task was to detect a brief color change in the moving dots. We found that (i) compared to the visual dots whose direction change occurred randomly within the cardiac cycle, the dots coincided with strong cardiac signals (during systole) induced decreased SSVEP power, while the dots that coincided with weak cardiac signals (during diastole) induced increased SSVEP phase synchronization; (ii) the coupling of visual stimuli to the systole led to a larger HEP but a smaller N2 component evoked by the color change; (iii) the increase in HEP amplitude was related to the decrease in N2 amplitude. Our results suggest cardiac signals automatically redirect attention from external to internal domains.

Both studies reveal the interplay between cardiac processing and visual processing and support the spontaneous shifts of attention between interoception and exteroception across the cardiac cycle.

### **The Influence of Cardiac Interoception on Action Regulation (Study III)**

In study III, we investigated how cardiac signals influence response inhibition in a stop-signal task by coupling the occurrence of the stop signal with participants' heartbeats. The stop signal signified the cancellation of the prepotent motor response. We observed prolonged stop-signal reaction times, reduced stop-signal P3 amplitudes, and higher HEP amplitudes when the stop signal was presented during cardiac systole, compared to presentation randomly within the cardiac cycle. Furthermore, these effects were independent of the emotional attribute of the stop signal (emotional facial expression change or non-emotional color change). Our results suggest that the co-occurrence of the action-relevant external cue and cardiac signals makes it harder to cancel the prepotent motor behavior. This effect may be attributed to inhibited perceptual processes of the visual cue, heightened readiness for action, or impaired inhibitory control ability during systole.

This study reveals the impact of cardiac signals on response inhibition and supports the attentional trade-off mechanism between interoception and exteroception.

### **The Influence of Sense of Agency on Action Regulation (Study IV and Study V)**

Both Study IV and Study V investigated the effect of the sense of agency on subsequent action regulation by adopting modified go/no-go tasks. The first experiment of Study IV modulated participants' sense of agency by varying the occurrence of action outcomes (present vs. absent) both locally on a trial-by-trial basis and globally regarding the overall probability of action outcomes within a block of trials (high vs. low). When participants' previous action led to an outcome (i.e., a happy face) compared with no outcome, they responded more accurately and faster to go cues, reacted less accurately to no-go cues, and made go decisions more frequently and faster to free-choice cues. These effects were even stronger when action outcomes occurred more frequently in a given block or several previous trials. The second experiment of Study IV further demonstrated that the effects of outcome presence on subsequent action regulation were independent of the emotional valence of the action outcome (a happy or an angry face). Taken together, Study IV provides behavioral evidence that a higher sense of agency as induced by the presence of action outcomes enhanced action readiness and suppressed response inhibition.

Study V manipulated participants' sense of agency by varying the presence, predictability, and emotional valence of a visual outcome for a given motor action. Consistent with the results of Study IV, when participants unexpectedly did not receive any visible outcome following their action, they exhibited slower responses and lower hit rates to the subsequent go signal but higher rates of successful inhibition to the subsequent no-go signal, regardless of the emotional valence of the expected action outcome. Furthermore, enhanced inhibitory tendencies were accompanied by reduced N2 and P3 amplitudes, midfrontal theta power, and theta synchronization between midfrontal and medial-to-parietal areas, indicating that less top-down control is required for successful response inhibition after experiencing a low sense of agency. These findings suggest that feeling less in control in a preceding trial makes it easier to implement inhibitory control in the current trial.

Both studies reveal the facilitatory effect of sense of agency on subsequent action readiness and its inhibitory effect on subsequent response inhibition, and they uncover how the automatic evaluation of action effectiveness shapes our ability to regulate actions flexibly.

## **General Conclusions**

Overall, the present thesis suggests that fluctuations in internal bodily signals can influence perception and action, indicating a strong link between mind and body. Additionally, the effectiveness of motor action can shape subsequent action tendencies. These findings shed new light on the theory of embodied cognition.

## **Zusammenfassung**

Die Wahrnehmung unserer Umwelt und wie wir auf sie reagieren, ist nicht festgelegt, sondern verändert sich dynamisch. Diese Variabilität lässt sich auf verschiedene Faktoren zurückführen, die auf bewusster und unbewusster Ebene wirken. Ein Faktor, der unsere Wahrnehmung und unser Handeln beeinflusst, ist die Interozeption, die Verarbeitung und Wahrnehmung innerer Körpersignale wie des Herzschlags. Bisher durchgeführte Studien berichten jedoch teilweise entgegengerichtete Effekte interozeptiver Signale auf unsere Wahrnehmung und unser Handeln und die zugrunde liegenden neuronalen Mechanismen sind weitgehend unklar. Auch das Agentivitätserleben (englisch: Sense of Agency), das Gefühl der Kontrolle über unsere Handlungen und deren Ergebnisse, beeinflusst nachweislich unsere Interaktion mit der Umwelt. Ob und wie Veränderungen des Agentivitätserlebens unsere Fähigkeit zur flexiblen Verhaltensregulation beeinflussen, ist jedoch weitgehend unbekannt. Die vorliegende Arbeit untersucht die Auswirkungen kardialer Interozeption und Agentivitätserlebens auf die visuelle Wahrnehmung und die Handlungsregulation. Sie umfasst fünf Studien mit verhaltensbiologischen und elektrophysiologischen Daten von gesunden menschlichen Studienteilnehmenden.

### **Der Einfluss kardialer Interozeption auf die visuelle Wahrnehmung (Studie I und Studie II)**

Studie I untersuchte die multisensorische Integration kardial und visueller Informationen. Zu diesem Zweck wurde die Farbveränderung eines auf einem Computerdisplay angezeigten visuellen Zielreizes mit den Herzschlägen der Versuchsteilnehmenden gekoppelt. Die Aufgabe der Teilnehmenden bestand darin, die räumliche Ausrichtung des visuellen Ziels zu identifizieren. Unsere Ergebnisse zeigten, dass (i) sich die Reaktionszeiten der Teilnehmenden verlängerten, wenn die Farbreizänderung mit starken Herzsignalen (während der Systole) relativ zu schwachen Herzsignalen (während der Diastole) einherging; (ii) das simultane Auftreten der Farbänderung des Zielreizes und der Herzsignale, die ERP-Amplitude und die Beta-Leistung in einer frühen Phase (~100 ms) nach Stimulusbeginn modulierte und die lateralisierte N2pc-Amplitude sowie die lateralisierte Beta-Leistung in einer späteren

Phase (~200 ms) nach Stimulusbeginn reduzierte. Unsere Ergebnisse indizieren, dass die multisensorische Integration erwarteter kardialer Signale mit einem visuellen Ziel dessen Erkennung unter mehreren Distraktoren negativ beeinflusst, ein Effekt der möglicherweise durch die Unterdrückung der sensorischen Verarbeitung und Verringerung der Aufmerksamkeit gegenüber dem visuellen Ziel zu erklären ist.

In Studie II untersuchten wir die durch den Herzzyklus verursachte spontane Reorientierung der Aufmerksamkeit zwischen körperinternen und körperexternen Reizen. Teilnehmende beobachteten sich auf dem Computerbildschirm schnell verändernde Punkte, die sich kontinuierlich bewegten und ihre Richtung dynamisch innerhalb derselben räumlichen Position des Bildschirms änderten. Eine Gruppe der Punkte änderte die Bewegungsrichtung synchron zum Herzschlag der Teilnehmenden. Die andere Gruppe der Punkte bewegte sich unabhängig vom Herzschlag der Teilnehmenden. Die Aufgabe der Teilnehmenden bestand darin, einen kurzen Farbwechsel in den sich bewegenden Punkten zu erkennen. Es zeigte sich, dass (i) im Vergleich zu den visuellen Punkten, deren Richtungsänderung zufällig innerhalb des Herzzyklus auftrat, die Punkte, die zeitlich mit starken Herzsignalen (während der Systole) zusammenfielen, eine verringerte SSVEP-Leistung induzierten, während die Punkte, die mit schwachen Herzsignalen (während der Diastole) zusammenfielen, eine erhöhte SSVEP-Phasensynchronisation induzierten; (ii) die Kopplung der visuellen Stimuli an die Systole zu einer größeren HEP-, aber einer kleineren N2-Komponente führte, die durch die Farbänderung hervorgerufen wurde; (iii) der Anstieg der HEP-Amplitude mit dem Rückgang der N2-Amplitude korrelierte. Unsere Ergebnisse deuten darauf hin, dass kardiale Signale zu einer automatischen Aufmerksamkeitsverschiebung von Körperexternen auf körpreinterne Reize führen.

Beide Studien zeigen das Zusammenspiel zwischen kardialer und visueller Signalverarbeitung und deuten auf eine spontane Verschiebung der Aufmerksamkeit zwischen interozeptiven und exterozeptiven Reizen während des Herzzyklus hin.

### **Der Einfluss kardialer Interozeption auf die Handlungsregulation (Studie III)**

In Studie III untersuchten wir wie kardiale Signale die Fähigkeit, eine Reaktion zu unterdrücken, bei einer Stoppsignalaufgabe beeinflussen, indem wir das Auftreten des Stoppsignals mit dem Herzschlag der Teilnehmer koppelten. Das in der Aufgabe präsentierte Stoppsignal bedeutete, dass die Teilnehmenden ihre präpotente motorische Reaktion unterbinden müssen. Wir beobachteten verlängerte Stoppsignal-Reaktionszeiten, reduzierte Stoppsignal-P3-Amplituden und erhöhte HEP-Amplituden, wenn das Stoppsignal während der Herzsysteme an Stelle eines zufälligen Zeitpunktes innerhalb des Herzzyklus präsentiert wurde. Diese Effekte waren unabhängig davon, ob das Stoppsignal emotional oder neutral war. Unsere Ergebnisse deuten darauf hin, dass das gleichzeitige Auftreten eines handlungsrelevanten externen Reizes und der Herzsysteme zu einer Erschwerung der Aufhebung präpotenter motorischer Handlung führt. Dieser Effekt könnte auf gehemmte visuelle Wahrnehmungsprozesse, eine erhöhte Handlungsbereitschaft während der Systeme, oder eine verminderte Fähigkeit, die eigenen Handlungen während der Systeme zu kontrollieren, zurückzuführen sein.

Studie III demonstriert den Einfluss kardialer Signale auf die Reaktionshemmung und zeigt, wie diese die Aufmerksamkeitsausrichtung auf körperinterne oder externe Reize beeinflussen.

### **Der Einfluss von Agentivitätserleben auf die Handlungsregulation (Studie IV und Studie V)**

Studie IV und V untersuchten den Einfluss von Agentivitätserleben auf die Fähigkeit der Handlungsregulation in modifizierten Go/No-Go-Aufgaben. Im ersten Experiment in Studie IV wurde das Agentivitätserleben der Teilnehmenden manipuliert, indem das Auftreten von Handlungsergebnissen (anwesend vs. abwesend) sowohl lokal, auf einer Trial-by-Trial-Basis, als auch global, in Bezug auf die Gesamtwahrscheinlichkeit von Handlungsergebnissen innerhalb eines Blocks von Trials (hoch vs. niedrig), variiert wurde. Unsere Ergebnisse zeigten, dass Handlungen, die ein Ergebnis zufolge hatten (z. B. ein glückliches Gesicht), zu schnelleren und akkurateren Reaktionen auf „Go“-Hinweise, weniger akkuraten Reaktionen auf „No-Go“-Hinweise und zu schnelleren und häufigeren „Go“-Entscheidungen auf „Free-choice“-Hinweise führten. Diese Effekte waren stärker, wenn Handlungen innerhalb eines Blocks oder wenn die einer

Handlung vorangegangenen Durchgänge häufiger zu dem Auftreten eines Ergebnisses führten als zum Ausbleiben dessen. Das zweite Experiment in Studie IV zeigte außerdem, dass die Auswirkungen des Vorhandenseins des Ergebnisses auf die nachfolgende Handlungsregulation unabhängig von der emotionalen Valenz des Handlungsergebnisses (ein glückliches oder ein wütendes Gesicht) waren. Zusammenfassend liefert Studie IV Verhaltensbelege dafür, dass ein höheres Agentivitätserleben, das durch die Anwesenheit von Handlungsergebnissen hervorgerufen wird, die Handlungsbereitschaft erhöht und die Reaktionshemmung unterdrückt.

In Studie V manipulierten wir das Agentivitätserleben der Teilnehmenden, indem wir das Vorhandensein, die Vorhersagbarkeit und die emotionale Valenz eines visuellen Ergebnisses für eine bestimmte motorische Handlung variierten. In Übereinstimmung mit den Ergebnissen von Studie IV zeigten die Teilnehmenden unter Abwesenheit eines erwarteten Handlungsergebnisses langsamere Reaktionszeiten und niedrigere Trefferquoten auf das nachfolgende „Go“-Signal, und höhere Raten erfolgreicher Handlungsinhibition auf das nachfolgende „No-Go“-Signal, unabhängig von der emotionalen Valenz des erwarteten Handlungsergebnisses. Die verbesserte Unterdrückung einer Reaktion ging mit reduzierten N2- und P3-Amplituden, einer verringerten Theta-Leistung im mittleren Frontalbereich und einer verringerten Theta-Synchronisation zwischen dem mittleren Frontalbereich und den medialen bis parietalen Arealen einher. Diese Ergebnisse deuten darauf hin, dass ein geringes Agentivitätserleben weniger kognitive Kontrolle für die erfolgreiche Unterdrückung einer Reaktion erfordert. Diese Ergebnisse suggerieren, dass ein geringes Agentivitätserleben, das durch das Ausbleiben eines Handlungsergebnisses erzeugt wird, die anschließende Unterdrückung motorischer Handlungen erleichtert.

Die Studien IV und V zeigen, wie situativ erschaffenes Agentivitätserleben die Handlungsbereitschaft fördert sowie die Fähigkeit, Handlungen zu unterdrücken, beeinträchtigt. Diese Ergebnisse demonstrieren, wie unsere automatische Bewertung der Handlungseffektivität die Fähigkeit zur flexiblen Handlungsregulierung beeinflusst.

## **Allgemeine Schlussfolgerungen**

Zusammenfassend deutet die vorliegende Arbeit darauf hin, dass Schwankungen interner Körpersignale unsere Wahrnehmung und unser Handeln beeinflussen können. Dies weist auf eine enge Verbindung zwischen Geist und Körper hin. Darüber hinaus kann die Effektivität einer motorischen Handlung die nachfolgende Tendenz, eine Handlung auszuführen, beeinflussen. Diese Erkenntnisse werfen ein neues Licht auf die Theorie der verkörperten Kognition.



## **Acknowledgments**

Throughout my PhD, I have had the great fortune to receive guidance and support from many wonderful people, without whom this thesis would not have been possible. First of all, I want to thank my supervisor, Prof. Dr. Simone Schütz-Bosbach, for giving me the chance to study in Germany and pursue a line of research that truly interests me. She not only always gave me prompt, insightful feedback, but also encouraged me to explore new ideas freely. She is a role model for me as a researcher and a supervisor.

Additionally, I am grateful to Dr. Amanda Marshall, Dr. Jakob Kaiser, and Dr. Antje Gentsch for generously sharing their expertise and offering insightful suggestions during our collaborations. Every discussion I had with them was inspiring and invaluable for my research.

I would also like to thank the other PhD students in our lab: Maren Giersiepen, Junhui Liu, and Zahra Rezazadeh. They have not only promoted a supportive and communicative work environment, but also shown remarkable care and kindness. I have learned a lot of soft skills from them, such as how to work and collaborate efficiently. A special acknowledgment goes to our dedicated student assistants, particularly Elsa Sangaran, for their assistance with data collection, and to other colleagues in our department, especially Gabriella Zopcsak and Dr. Artyom Zinchenko, for their help with administrative matters.

Lastly, I would like to express my gratitude towards my friends and boyfriend for giving me strength and encouragement throughout this journey and also my parents for their endless love and support throughout my life.



## **Curriculum Vitae**

To ensure data protection, the CV has been excluded from the PDF version of this thesis.



## List of Publications

### Peer-reviewed Journal Articles as First Author

- Ren, Q.**, Marshall, A. C., Kaiser, J., & Schütz-Bosbach, S. (2022). Multisensory integration of anticipated cardiac signals with visual targets affects their detection among multiple visual stimuli. *NeuroImage*, 262, 119549. <https://doi.org/10.1016/j.neuroimage.2022.119549>
- Ren, Q.**, Marshall, A. C., Kaiser, J., & Schütz-Bosbach, S. (2022). Response inhibition is disrupted by interoceptive processing at cardiac systole. *Biological Psychology*, 170, 108323. <https://doi.org/10.1016/j.biopsycho.2022.108323>
- Ren, Q.**, Gentsch, A., Kaiser, J., & Schütz-Bosbach, S. (2023). Ready to go: Higher sense of agency enhances action readiness and reduces response inhibition. *Cognition*, 237, 105456. <https://doi.org/10.1016/j.cognition.2023.105456>
- Ren, Q.**, Kaiser, J., Gentsch, A., & Schütz-Bosbach, S. (2023). Prepared to stop: How sense of agency in a preceding trial modulates inhibitory control in the current trial. *Cerebral Cortex*, 33(13), 8565–8580. <https://doi.org/10.1093/cercor/bhad141>
- Ren, Q.**, Yang, Y., Wo, Y., Lu, X., & Hu, L. (2022). Different priming effects of empathy on neural processing associated with first-hand pain and nonpain perception. *Annals of the New York Academy of Sciences*, 1509(1), 184–202. <https://doi.org/10.1111/nyas.14723>
- Ren, Q.**, Lu, X., Zhao, Q., Zhang H., & Hu, L. (2020). Can self-pain sensitivity quantify empathy for other' pain?. *Psychophysiology*, 57(10), e13637. <https://doi.org/10.1111/psyp.13637>

For a complete publication list, please refer to the link:

<https://www.scopus.com/authid/detail.uri?authorId=57211080710>

## Conference Abstracts

**Ren, Q.**, Marshall, A. C., Kaiser, J., & Schütz-Bosbach, S. (2023). Multisensory integration of cardiac signals with visual targets hinders visual search. The Annual Meeting of the Organization for Human Brain Mapping, *Montréal, Canada*

**Ren, Q.**, Kaiser, J., Gentsch, A., & Schütz-Bosbach, S. (2023) Prepared to stop: How sense of agency modulates inhibitory control. The Annual Meeting of the General Psychology Section of the German Psychological Society, *Trier, Germany*